Condition Assessment of Medium Voltage Cable Joints – Dielectric Spectroscopy of Field Grading Materials

Biran Abil

June 2017

MASTER THESIS

Department of Electric Power Engineering

Norwegian University of Science and Technology

and

Department of Electrical Engineering, Mathematics and Computer Science

Delft University of Technology

Supervisor 1: Dr. Frank Mauseth, Associate Proffesor at NTNU

Supervisor 2: Dr. Armando Rodrigo Mor, Assistant Proffesor at TU Delft

Supervisor 3: Dr. Sverre Hvidsten, Senior Researcher at SINTEF Energy Research

Project Description

Currently, the main task of non-destructive diagnostic testing is to estimate accurately the degree of aging. This knowledge is used in developing and planning of condition-based maintenance actions, which result in decreased number of unexpected failures and lower maintenance costs.

A significant part of the medium voltage cable distribution network in Norway is already older than the expected lifetime of 30 years. Cable joints have shorter lifetime than the cables themselves. Specifically, those installed in the 80s have led to significant service failures, due to overheating of the metallic connector in the joint. Additionally, the introduction of renewable energy sources such as wind turbines will increase the current loading of the existing cable network, which could give a further rise in the failure rate.

Field grading materials are usually used in cable joint and termination designs for obtaining the desired field distribution in such way to avoid local field enhancements and the possible subsequent insulation failures. Field control ability of these materials is a function of their dielectric properties. The latter will be affected by the level of applied voltage, but also temperature, aging degree and also humidity will influence the resulting field distribution.

The project work is mainly experimental. Physical, mechanical and dielectric properties of a field grading material are characterized as a function of electric field, temperature and level of aging of the material. The influence of humidity is also important and is investigated during the master work.

Preface

This master thesis is written during spring semester of 2017. It is a final assignment of a two years MSc Programme European Wind Energy Master within Electrical Power Systems study track.

The thesis is carried out at the Department of Electric Power Engineering of the Norwegian University of Science and Technology in collaboration with SINTEF Energy Research.

The project work presented is a continuation of previous master thesis research projects done in the area of medium voltage cable joints.

Trondheim, 20-06-2017

Biran Abil

Acknowledgment

The research conducted in this MSc thesis would not have been possible without the support and guidance of several individuals to whom I owe sincere gratitude and respect.

Firstly, I would like to show my profound gratitude to my supervisor Dr. Frank Mauseth at NTNU and my co-supervisor Sverre Hvidsten at SINTEF Energy Research for all the help and guidance throughout this master thesis. I highly appreciate their constant availability for discussions and support.

I would also like to thank my supervisor at TU Delft, Armando Rodrigo Mor for his insightful advices and for providing me, during my semester in TU Delft, with invaluable knowledge in the area of high voltage equipment condition assessment, which is the backbone of this master thesis.

I would like to appreciate and acknowledge the extensive help and assistance I received from Torbjørn Andersen Ve during my work in the laboratories and for providing and helping me use the needed test equipment.

I would also like to thank all my colleagues working in Vestas Wind Systems Bulgaria for supporting me in taking this important decision to join this master programme.

Last, but certainly not the least, I would like to thank and show my utmost gratitude to my mother Gyulvan and my brother Sinan. Dad, you will be always in my heart, hold my hand when I need you. I dedicate this work to them.

Biran Abil

Abstract

The electrical properties of a widely used stress control tube for medium voltage heat-shrink joints are examined in this master thesis by using non-destructive laboratory methods. They were determined by use of time domain dielectric response test while changing the DC electric field, temperature and level of humidity.

In order to determine the physical and mechanical characteristics of the material at different aging stages and conditions, both differential scanning calorimetry and tensile test measurements were performed on stress control tube samples.

Two types of test samples were prepared. For dielectric response tests, Raychem JSCR 42/16 stress control tube was shrunk on a cylindrical rod, consisting of two metal electrodes, separated by a PTFE (Teflon) insulating rod. For differential scanning calorimetry and tensile tests, the stress control tube was shrunk on a cylindrical PTFE rod only, with the same diameter as for the dielectric response tests without the presence of metal electrodes.

Tensile test measurements were performed in order to characterize and compare the mechanical properties of the stress control tube material at different aging stages.

Differential scanning calorimetry measurements were used to estimate aging degree by assessment of thermal resistivity of the material and antioxidants consumption when exposed to high temperatures for a certain period of time.

To calculate the conductivity, dielectric response measurements were performed in time domain at different voltage levels up to 20 kV and charging and discharging time duration of 10800s. They were conducted by placing the test object in a climate chamber in order to examine the influence of temperature and humidity. The measurements were performed on unaged and thermally aged heat shrinkable stress control tubes. The aging process was obtained in heat cabinets at 98°C dry air, 98°C wet air and 150°C dry air conditions.

Results from the analysis show that conductivity has not significant dependency of the electric field up to 0.2 kV/mm at different temperatures, aging degree and humidity. It was revealed that conductivity is more temperature dependent, as a significant increase was observed when the temperature was elevated at higher values. Conductivity was found out to be strongly dependent on humidity, especially when combined with high aging degree.

Abbreviations

SCT Stress control tube

DR Dielectric response

PDC Polarization depolarization currents

FGM Field grading material

DSC Differential scanning calorimetry

PTFE Polytetrafluoroethylene

TD Time domain

XLPE Cross-linked polyethylene

EDPM Ethylene propylene diene monomer

PVC Polyvinyl chloride

RH Relative Humidity

TOV Transient overvoltages

Contents

Chapter 1

Introduction

1.1 Background

Significant part of the medium voltage (12 and 24 kV) cable distribution networks in Norway have already reached their expected lifetime of 30 years. It is observed that increasing number of cable sections incorporating heat-shrink joints, especially those installed in the 80's have been subjected to overheating. The main source of the overheating is probably the too high resistance in the metallic connector. However, it seems that these joints still withstand the service conditions. On the other side, further introduction of renewable energy sources such as wind power plants will lead to increased current loading of the existing distribution cable network. This can result in overheating of additional joints that yet are not critical and to increase the overheating level in those, which are already subjected to this phenomenon.[11]

Recent experience from the Netherlands also reveals problems with compression type metallic connectors in joints used for wind park distribution network cables, even after being shortly in use (some years). Again, the major problem was proved to be the high contact resistance resulting in high temperatures.[21]

Due to the overheating, temperature of cable joints can increase significantly above 90°C during normal operating conditions. This is the reason that the properties of a heat shrink stress control tube used in these joints has been characterized at temperatures reaching up to 150°C. It has been proposed that such joints have very low electrical resistance.[11]

Cable joints and terminations being among the weakest parts of the cable network need special attention in design perspective and materials used. In general, stress control tube with field grading abilities is involved. It is used in order to minimize and avoid field enhancement, which can lead to premature failures way before the expected cable life time. The main function of such stress control tube is to provide a more uniform field distribution along the cable length, resulting in reduced probability of field concentrations. This function is based

on the dielectric properties of the stress control tube material. These properties are affected by the electric field strength, temperature, humidity and degree of thermal aging. For various reasons, the field grading tube in cable joints ages faster in result of high temperature and the presence of oxygen.

Based on that, this master thesis examines the behavior of a stress control tube that have experienced overheating of up to 150°C. Additionally, the effects of thermal aging and humidity are investigated. The aging degree is estimated by differential scanning calorimetry and tensile test, while the effects of temperature and humidity on the dielectric properties of the material are examined in a climate chamber by using dielectric response test in time domain and calculating the conductivity of the stress control tube.

In Norway, it has been observed in that a lot of medium voltage cable sections, containing one or several heat-shrink joints have a very low resistance of the insulation. This master thesis is a part of a larger project which aims to elucidate the mechanisms leading to low insulation resistance (high conductivity) in medium voltage cable joints. SINTEF Energy Research is working on developing a simple method including using an insulation tester for investigating whether joints can be the reason for the low resistance of cable section. It is proposed that this method should be used as an initial step, before applying any other additional diagnostics. A significant measurement database is developed, which will help e.g. to distinguish a service-aged low-resistance joint from heavily water treed cable insulation, avoiding misinterpretation of the cable condition. [10]

1.2 Hypothesis

This master thesis is mainly experimental and deals with a commercially available stress control tube, which is made of the same material as the one used in the cable joints installed in the 80's. The impact of varying temperature, electric field, humidity and aging degree to the dielectric properties of the stress control tube material will be examined. In order to characterize the physical and mechanical properties of the material, differential scanning calorimetry and tensile test are applied, while the master thesis work will be focused on the dielectric response time based measurements. The corresponding experimental work has been done in order to check the following hypothesis.

1. Differential Scanning Calorimetry.

i. Oxidation induction time measured decreases with increasing of the aging degree.

ii. Oxidation induction temperature decreases with increasing of the aging degree.

2. Dielectric Response.

i. Conductivity of stress control tube increases with increasing the temperature.

ii. Conductivity of stress control tube increases with increased aging degree.

iii. Conductivity of stress control tube increases as a function of increasing moisture content.

iv. Stress control tube material has no hysteresis effects.

1.3 Objectives and Approach

Accurate condition assessment is a prerequisite to perform successful maintenance and to take adequate reinvestment decisions. Dielectric response measurements for cable sections, including joints can be utilized as such an assessment tool. DR measurement results will vary with the applied voltage, the material in question, chemistry, type of fault, temperature, presence of humidity, measuring device and statistical properties. New knowledge about conditions and mechanisms affecting the stress control tube conductivity can help improve condition assessment of cable joints and distribution cable networks in general.

The main objectives in this master thesis have been to:

- Create test objects and simulate overheating due to high contact resistance in cable joints which results in deterioration of stress control tube material, caused by high temperatures at dry and high humidity conditions.

- Perform accurate time domain dielectric response measurements for test objects at voltage levels of up to 20kV (0.2 kV/mm) and at temperatures of 30°C, 90°C, 150°C. DR measurements at 95%RH and temperature of 30°C are also taken in consideration.

- Detect aging in stress control material by preforming DSC and Tensile tests.

- Compare dielectric response measurements performed at different voltages, temperatures, aging degrees and presence of humidity.

1.4 Master Thesis Structure

Chapter 1 of this thesis work includes a brief introduction and the most important motivations. Chapter 2 deals with theory, explaining different aspects of the master project. In chapter 3, an overview of the different experiments and simulations is presented. Results and discussions based on them are shown in chapter 4. Chapter 5 focuses on conclusions. Further work suggestions are presented in Chapter 6. All appendices containing detailed results, graphs, equipment data and additional information are placed at the end.

Chapter 2

Theory

2.1 Cable Joint

Cables are manufactured under strictly controlled conditions and environment. Keeping the high quality of the production process and the cable itself leads to several factors limiting the length of the cable produced. On the other hand, manufacturing cable sections with predefined length favors the subsequent transport, installing, service and repair activities. Installation of two separate cable sections is performed by connecting them with a cable joint, which provides the needed level of insulation and protection.

The insulating layers of cable sections are stripped down until the conductors are revealed and they are connected by means of screwing or crimping a metallic connector. In that way the cable sections are electrically connected. The metallic connector is further insulated and provided with a water tight layer preventing water ingress.

During cable joint installation, skilled personnel is needed, following strictly the prescribed manufacturer installation procedures. Poor workmanship such as cuts on the cable during shield cutback operation, insufficient crimping between conductors and contamination can result in enhancement of the local field stress.

Special attention should be kept during installation of the metallic connector between the cable conductors. Weak connection leads to high resistance and increased heat generation inside the cable joint. If this heat generation surpasses the heat dissipation properties of the joint the overall temperature will increase. This temperature rise will accelerate degradation of materials, resulting in unfavorable change of their mechanical and electrical properties. Thus, sufficient attention should be kept during designing, manufacturing and installing cable joints.[6]

A typical cable joint design is shown in Figure 2.1

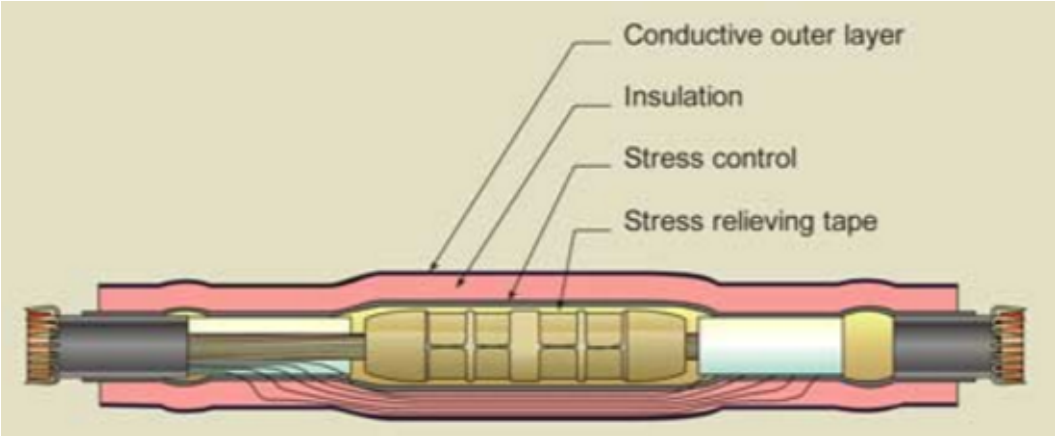

Figure 2.1: A typical cable joint design.

2.2 Stress Control Tube

Heat-shrink stress control material is a composite material comprised of polymeric materials (thermoplastics) and filler, such as conductive and semi-conductive particles. Both, polymeric material and filler can be of different types, depending of what dielectric and environment withstand properties are needed. As a thermoplastic material PVC, PTFE, EPDM rubber and Viton can be used while the filler particles can be SiC (silicon carbide), ZnO (zinc oxide) or carbon black. [19]

During manufacturing process, polymer materials are exposed to high-energy electron beam that causes cross-linking of adjacent molecules. Hydrogen atoms are removed from the polyethylene chains and carbon atoms create connections between the adjacent chains.[2] The cross-linking process is shown in Figure 2.2.

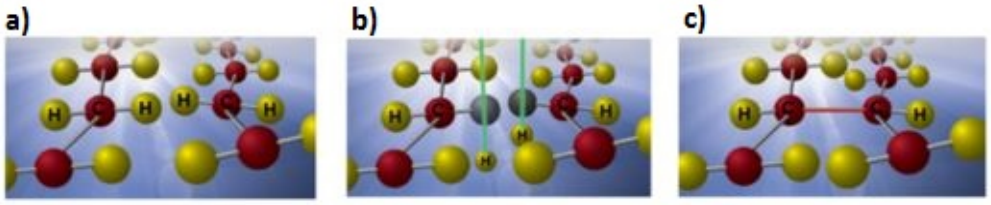

Figure 2.2: Cross-linking process: a) Unprocessed polyethylene chains, b) Hydrogen atoms removed by high-energy electron beam and c) Connections between adjacent chains [2].

As a result from cross-linking, the heat-shrinking material loses its melting property enabling it to be heated to temperatures considerably higher than the crystalline melting point without melting. At temperatures higher than this, heat shrink tubes can be expanded and

shaped in forms and sizes which will remain unchanged, while the temperature decreases below the crystalline melting point again.[2]

Heat shrink stress control tubes are supplied in this expanded form to the customers. During the installation process when the tube is heated up again, above the crystalline melting point, with a gas torch or hot air gun, the tube tends to shrink back to its original shape. As the material shrinks during installation, high pressure builds up, creating excellent sealing and electrical behavior.[2]

Installation process steps are presented in Figure 2.3.

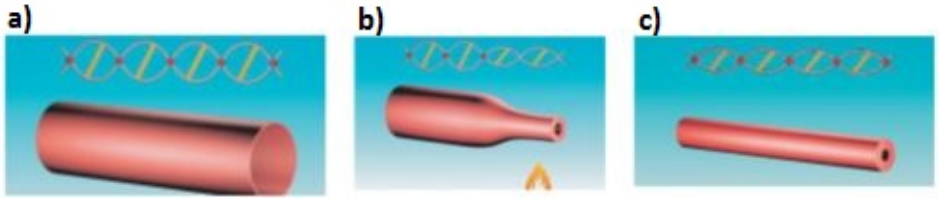

Figure 2.3: Installation process: a) After heating, expanding and cooling the crystals reappear, locking the expanded form of the tube indefinitely. This form is supplied to customers. b) The customer heats the tube, crystals are melting, allowing the cross-links to make the tube to return its original form. c) After cooling, the crystals reappear and lock the tube to its recovered form [1].

2.3 Field Grading

Field grading comprises methods of reducing local field enhancements in different devices. Also called stress control, it is an indispensable part of the insulation coordination as currently the voltage levels are continuously increasing, component sizes are decreasing and the demand for devices, incorporating several functions is becoming more and more important. A design which effectively balances features like cost, safety, low electric field and temperature is needed. An adequate field grading can be the key for obtaining such a design.[8]

Field grading methods are divided into two main groups:

i) Capacitive field grading which incorporates:

-Geometrical grading, based on the shape of the electrode parts.

-Refractive grading, using high-permittivity materials.

-Condenser grading, integrating metallic elements.

ii) Resistive field grading, using materials with specific current-field characteristics.

Nonlinear resistive field grading is proven technology, suitable for both ac and dc applications at continuously increasing system voltage levels. The fact that resistive stress control is governed by conduction currents rather than displacement currents can lead to production of considerable heat amount. On the other side the maximum field enhancements, in general, occur during very short time periods, such as impulse tests and the Joule heating can be considered as irrelevant. That establishes the requirement that stress control materials act only during those short-time excessive stress events and remain insulating with low losses during normal operation at nominal field strength. This is valid if the material conductivity has a strong field dependence which is meant by the term nonlinearity.[8]

An example of a typical conductivity-field dependency for an ideal nonlinear resistive field grading material can be seen in Figure 2.4.

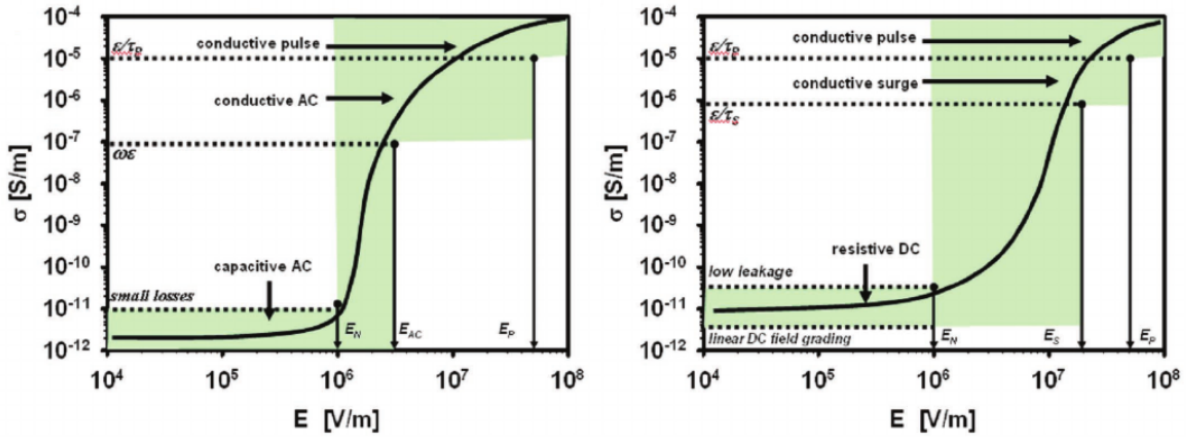

Figure 2.4: Qualitative conductivity-field dependency for an ideal nonlinear resistive field grading material used in AC and DC applications [8].

Cable joints are among the most common high voltage accessories, where stress concentrations occur. A cable in general consists of a conductor at high voltage, an insulating material and a grounded screen. During installation of a cable joint or a termination of a cable, the screen is stripped off, which results in discontinuity of the cable uniform geometry. If no additional actions are taken, this will cause an enhanced field at the region closest to the screen end, see Figure 2.5. This can result in severe failures, such as insulation breakdown or flashover.

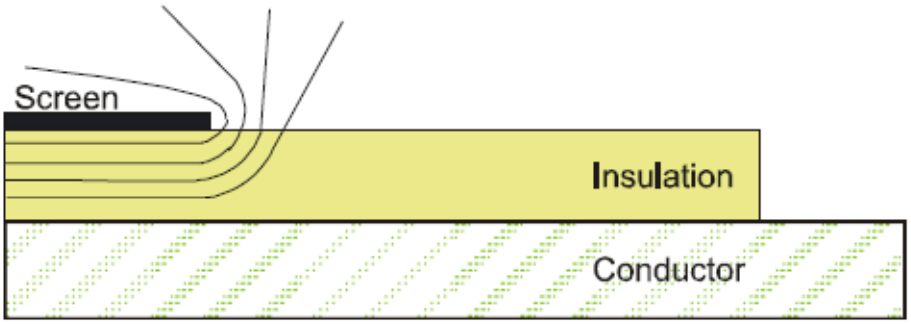

Figure 2.5: Field concentration in cable termination without field grading [19].

In cases like this a field grading material can be implemented in the cable joint design. Its electrical properties should be selected in such way, that the voltage equipotential lines achieve more even distribution in the material, spreading over larger area and thus the field strength is significantly reduced, as shown in Figure 2.6.

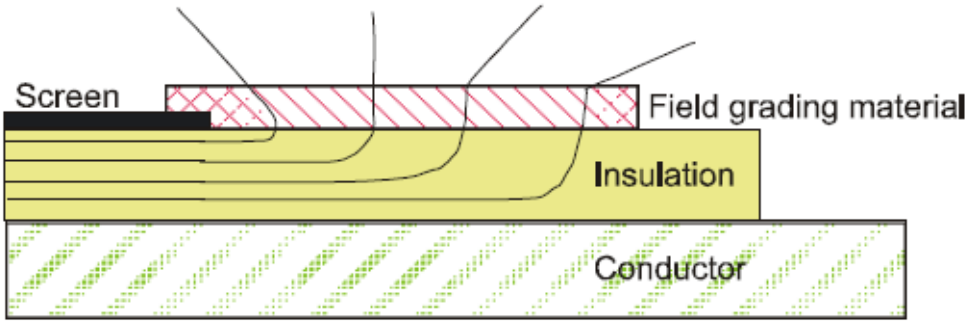

Figure 2.6: Field distribution in cable termination with field grading layer [19].

In case of resistive field grading, the electrical field strength is controlled by changing the conductivity of the material used. This type of grading can be used under dc, ac and impulse conditions, which makes it very appropriate for high voltage cable accessories use, especially considering the fact that in general it is more compact in size compared to geometrical and capacitive field grading [8]. The latter is important, because cable installation conditions often provide limited space. It should be mentioned that in case of applied ac and impulse voltages the times of application are really short, so in order resistive field grading to be achieved, the conductivity has to be significantly high, which inevitably leads to high losses.[19]

Using a stress control material with a nonlinear behavior can provide sufficient field grading under various conditions, such as impulse voltages, transient overvoltages (TOV) and

operating voltages. In case of a nonlinear resistive stress control, the conductivity of the material increases with the increasing electric field in such way, that the field is more evenly distributed which results in significantly reduced field enhancements.[19]

At the region with a critically high field concentration the material becomes conductive, space charge is formed and thus counter field is created [11]. In general, conductivity values can change from low to very high in a narrow field region. As a result the material should have the ability to change its state from highly conductive to resistive in order to minimize the losses [8] [15].

In order to explain the basic theory behind field grading properties of the stress control tube material, an equivalent circuit of a stripped cable termination is presented in Figure 2.7. Cable surface is divided in conductive ring segments, marked as black dots. K_n represents the capacitance between the rings and C the capacitance of the insulation between the ring and the conductor. When the cable is energized, current density increases as closer it is approached to the cable grounded screen since total current is a sum of the currents of the individual ring segments, where C capacitances cause the current to flow to ground through K capacitances. The voltage across capacitances K will increase in the direction to the grounded shield and the maximum field strength will increase with the ratio $\sqrt{\frac{C}{K}}$. In order to keep the field strength below critical level, the value of C should be increased or the value of K decreased. [15] [16]

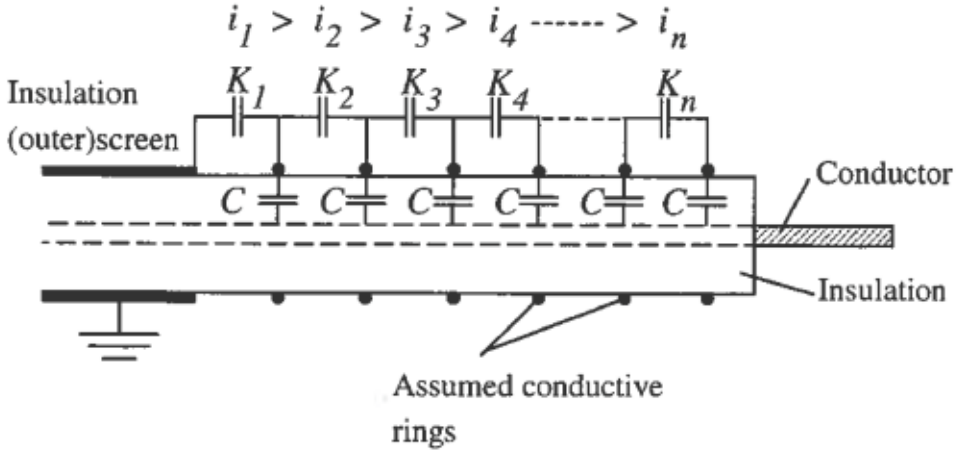

Figure 2.7: Simplified circuit for a stripped cable termination [15].

It should be mentioned that the value of C is not so easy to be decreased, as it is restricted by the potential between the conductor and the outer screen. A better option is to increase the

value of K instead. In case of resistive field grading as shown in Figure 2.8 a resistive layer is introduced. It is presented by the resistances R. As a result capacitance K is in parallel with the resistance R which gives an equivalent impedance. [15] [16]

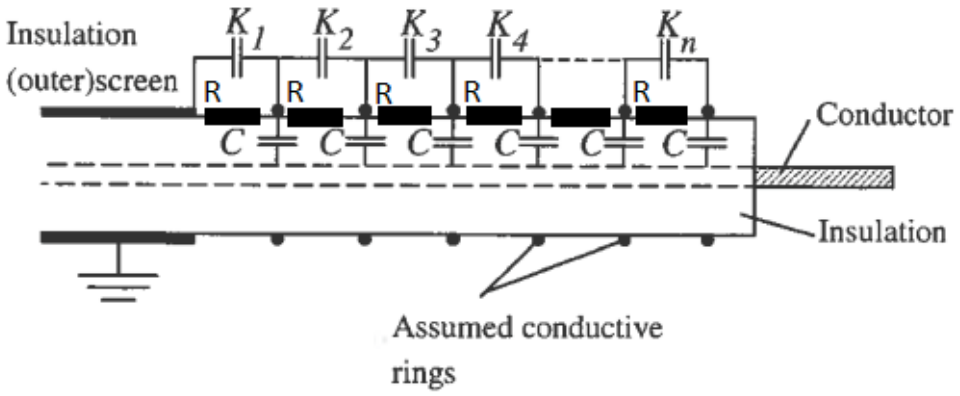

Figure 2.8: Simplified circuit for a stripped cable termination with a resistive layer applied.

The obtained field distribution behavior is presented in Figure 2.9.

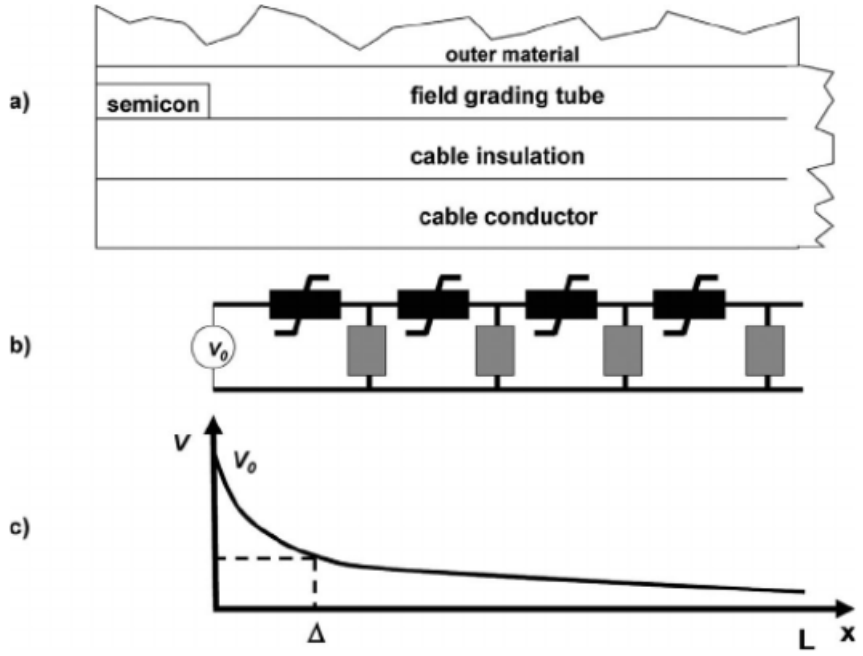

Figure 2.9: a) Sketch of a cylindrical geometry of a cable joint or termination with a field grading tube. b) Equivalent circuit with potential V_0 between cable conductor and semicon end. The field grading layer is explained with a nonlinear impedance per length (black rectangles) and an admittance to the cable conductor per length (grey rectangles). c) Axial AC voltage distribution characterized by penetration depth Δ. [8]

Penetration depth Δ is important in practice, because it gives the minimum efficient length of a stress control tube. If the tube's length is bigger, the field values become equal to the switching field (when the field grading becomes active) until distance Δ and then decrease to lower values. If the tube is shorter than Δ, it starts to act as a prolonged electrode with a dangerously enhanced field at its end.[8]

A cross section of a cable joint is shown in Figure 2.10, presenting typical field distribution, obtained by a field grading material.

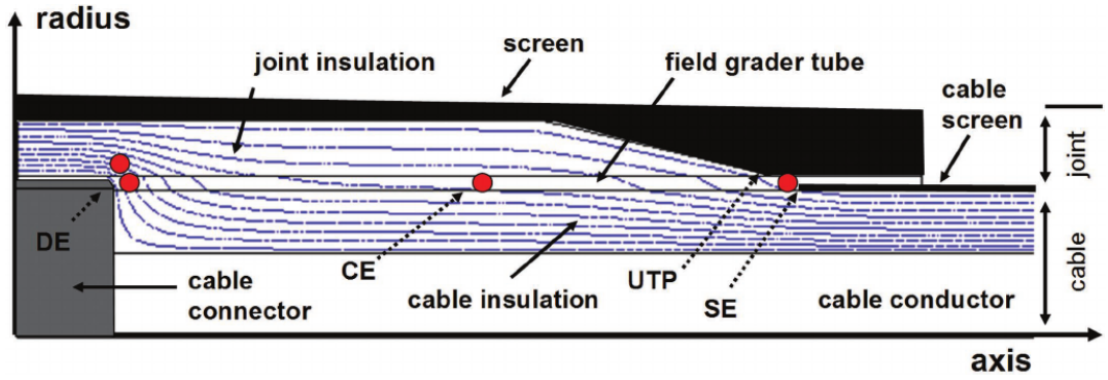

Figure 2.10: Cylindrically symmetric cable joint is presented. The cable connector and the deflector (DE - deflector edge) are on high voltage, while the cable screen is grounded. The stress control tube forms a connection between the deflector and the outer cable semicon screen, reaching behind the UTP (upper triple point) and overlaps the SE (semicon edge). Additionally, stress control tube separates the joint insulation from the cable insulation. Characteristic field points are shown as red circles. [8]

2.4 Dielectric Response

2.4.1 Polarization Mechanisms

Purely dielectric materials contain bounded charges which are randomly oriented when no electric field is applied. If the material is subjected to an electric field the dipoles start aligning themselves in the direction of the applied field. This process is called polarization and it is divided into four groups:

1. Electronic polarization

By applying an electric field, the electrons in the atom are drawn towards the positive electrode and the positive atom core towards the negative electrode. As a result, the otherwise

neutral atom temporarily becomes a dipole, slightly positive on one side and slightly negative on the other. The effect is considered as instantaneous and terminated by removing the field. [16]

2. Ionic polarization

An ionic bonded material consists of repetitive chains of positive and negative ions placed in symmetrical arrangement and because of that, no dipole effect is observed. If an electric field is applied, the positive and negative ions will be forced to go in opposite directions. This causes temporary dipoles due to shifting of the lattice structure. The effect is considered as instantaneous and vanishes when the field is removed.[16]

3. Orientation polarization

Molecules which have asymmetric distribution of electrons are permanent dipoles, like it is in the case of water. In a material consisting of randomly oriented molecules, an applied field will make them align with it. In case of liquids, dipoles have considerable freedom to move and will align with the applied field relatively fast, while in solid materials dipoles have less freedom to move which makes the process time consuming and can vary in the range of minutes to several days to complete and is referred to as relaxation mechanism.[16]

4. Interface polarization

Usually, insulation systems used for high voltage applications consist of several dielectrics. As a result, charge will be accumulated at the internal interfaces in case of DC or low frequency AC voltage. The effect is time consuming and is related to the relaxation mechanism.[16]

2.4.2 Time Dependent Polarization in Dielectric

The dipole alignment in dielectric material needs time. When electric field is applied electronic and ionic polarization mechanisms happen immediately, while orientation and interface polarization mechanisms take considerable time and they are recognized as relaxation mechanisms.[16]

If a parallel plate capacitor with dielectric material between the electrodes is present and DC voltage is applied, the dipoles align with the resulting electric field direction. Dipoles, adjacent to the electrodes are aligned in such a manner, that they will contribute to the surface

charge at the interface between the electrodes and the dielectric and some of the charges will cancel each other. That results in decreased potential between capacitor electrodes, when a dielectric is introduced between them.[16]

This effect is presented in Figure 2.11.

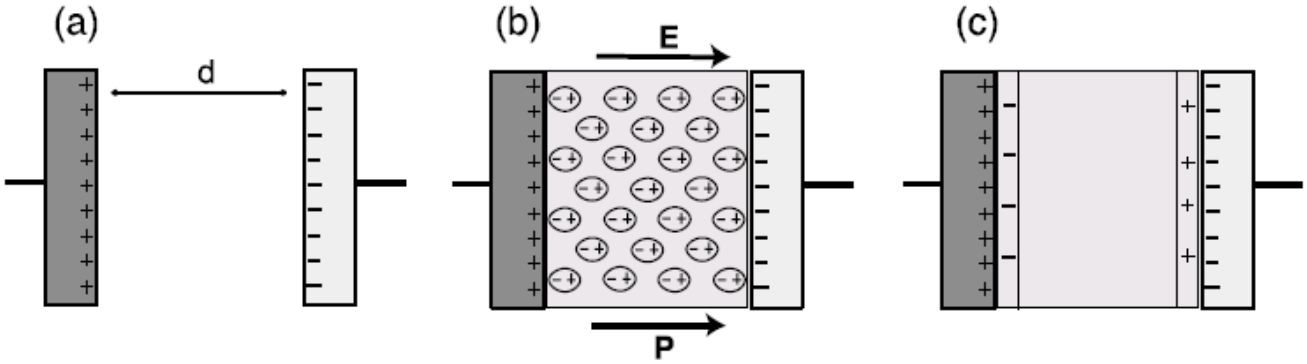

Figure 2.11: Parallel plate capacitor: a) Vacuum between electrodes. b) Dielectric between electrodes. c) Resulting net charge at the interface surface [16].

Introduction of dielectric material results in an increased flux density, which can be expressed by the sum of the vacuum flux density and $P(t)$, which denotes the polarization term. [16]

$$D(t) = \epsilon_0 E(t) + P(t) = \epsilon_0 (1 + \chi) E(t) \tag{2.1}$$

where χ represents the susceptibility of the dielectric.

Then the polarization current can be expressed as

$$I_p(t) = \left(\sigma_0 E(t) + \frac{dD(t)}{dt} \right) A \tag{2.2}$$

An equivalent circuit, as shown in Figure 2.12 can be modeled, elaborating on the current which flows through dielectric material when a DC step voltage is applied. This current is an overall contribution from momentary polarization, relaxation polarization and conduction mechanisms, which have different time dependence or time constants.[16]

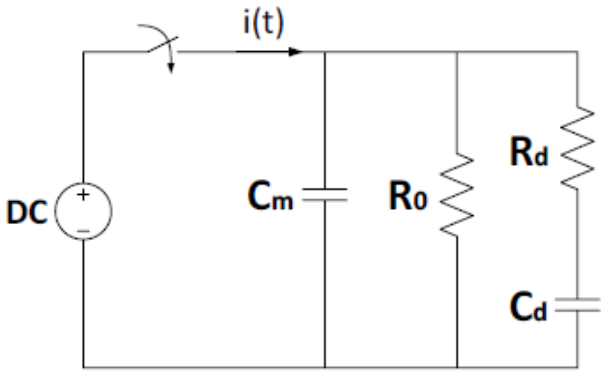

Figure 2.12: Equivalent circuit of a dielectric material subjected to DC voltage representing momentary, relaxation and conduction mechanisms.

Capacitor C_m represents the momentary polarization mechanism, which results in a high current spike right after the step voltage is applied. R_0 shows the conduction mechanism and it is related to the stationary part of the current flowing. R_d and C_d model the relaxation polarization mechanism, which is comparatively slow and highly temperature dependent. Time constants for polarization and depolarization modes can be considered as equal.[16]

The total current flowing through the dielectric material can be expressed as:

$$i(t) = \left(J_\delta(t) + \frac{P_d(\infty)}{\tau} e^{-\frac{t}{\tau}} + \sigma E \right) A \tag{2.3}$$

The momentary polarization mechanism gives current density J_δ, which is the reason for the high current spike obtained by the step voltage applied. The relaxation mechanism is related to P_d. The contribution from this mechanism decreases as the dipoles aligns with the applied electric field and the decay speed is dependent on the time constant.

After sufficiently long time, momentary and relaxation mechanisms are complete and the current stabilizes at stationary level, which represents the conductive current, as can be seen in Figure 2.13. It is related to the conductivity properties of the dielectric material involved.

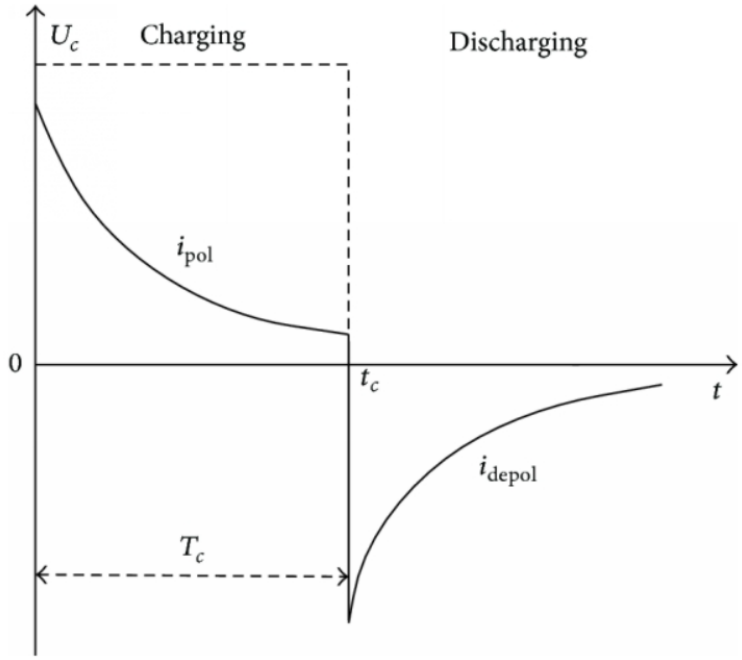

Figure 2.13: Graph representing the current for polarization and depolarization periods.

2.4.3 Time Domain Dielectric Response Analysis

Polarization and depolarization current measurements in time domain are used for examining an insulation material properties. The corresponding simplified test set-up circuit, as presented in Figure 2.14, incorporates DC voltage source, switching module controlling the mode (charging or discharging), electrometer for measuring I_{pol} and I_{depol} and the dielectric test object.

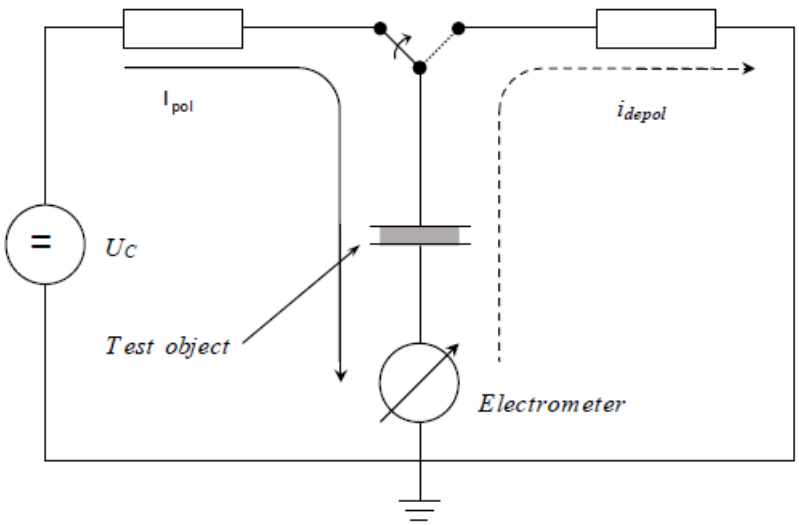

Figure 2.14: Equivalent circuit for time domain dielectric response measurements set-up.

Polarization and depolarization current behavior is presented in Figure 2.15.

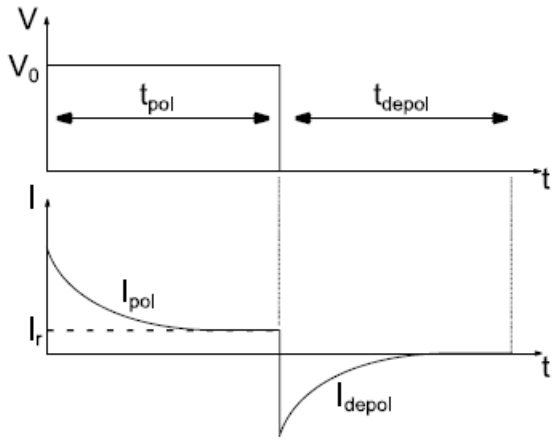

Figure 2.15: When a DC step voltage is applied, molecules start to polarize and with time I_{pol} decreases. After sufficient time, all molecules are polarized, the dielectric displacement current vanishes and only a steady state conductive current remains. When the test object is short-circuited molecules will relax to their original position. Therefore, a new current I_{depol} will flow in a direction, opposite to that of the I_{pol} [10].

When the test object is subjected to DC voltage, polarization current I_{pol} will flow through the dielectric material as a result of its conductivity and dielectric displacement. It can be expressed by

$$I_p(t) = C_0 U_0 \left(\frac{\sigma}{\epsilon_0} + f(t) \right) \tag{2.4}$$

where C_0 represents the geometric capacitance of the insulation material, U_0 is the DC voltage applied, ϵ_0 is the permittivity of vacuum, σ is material conductivity and $f(t)$ is the dielectric response function of the material. [18]

After sufficient time t_{pol}, the dipoles are fully aligned with the electric field, thus the polarization process is completed and the effect of the dielectric response function disappears. As a result, at this moment only a stationary conductive current flows through the test object.

After the time period t_{pol}, the switching module changes the test mode to discharging by short-circuiting the test object. That will make a depolarization current to flow in the opposite of the polarization current direction as the dipoles tend to align themselves in their original position. The depolarization current can be presented by

$$I_d(t) = C_0 U_0 \big[f(t) - f(t + t_c) \big] \tag{2.5}$$

where $f(t+t_c)$ expresses the remaining charge in the insulation material caused by previous voltage applications. It is important to mention that conductivity plays no role here as there is no voltage applied.

By combining equations 2.4 and 2.5, and taking into account the assumption that $f(t+t_c)$ can be disregarded because it is small, the conductivity can be expressed as in 2.6. [18]

$$\sigma \approx \frac{\epsilon_0}{C_0 U_0}\left[I_p(t) - I_d(t)\right] \tag{2.6}$$

Additionally, the following relation between the dielectric response function and the depolarization current can be expressed as

$$f(t) \approx \frac{I_d(t)}{C_0 U_0} \tag{2.7}$$

Dielectric response function is estimated when the polarization cycle is long enough for a complete relaxation of the material before the start of the depolarization current measurements, when the test object is short-circuited. The response function is used for describing the polarization mechanism and can also be used for describing the material susceptibility in frequency domain.[28]

2.5 Aging

IEC TC 63 gives a general definition of aging as: “Irreversible deleterious change to the serviceability of insulation systems. Such changes are characterized by a failure rate which increases with time”.[6]

Accelerated aging may occur, for example at increasing temperatures, exposure to UV radiation, chemicals, oxygen and water. Aging processes and rates are strongly dependent on the type of material used and the surrounding environment. Aging can often be recognized by discoloration, deformations and changes in the mechanical and physical properties of the material. Specific aging characteristics of polymer materials are that their color changes, become more brittle and change of their electrical properties is also observed.

Cable joints are usually well protected from the surrounding environment and located underground. Therefore, no radiation contributes to the aging, but instead, heat generation and chemicals access are the dominant factors in this case. As it is very expensive to make the cable joints 100% tight, water and oxygen penetration is assumed to happen with time.

Overheating in cable joints and the adjacent cable parts results in oxidation of the polymeric materials which can subsequently cause auto-oxidation and embrittlement [21] [14]. Additionally, it is possible that partial discharges to occur in micro cracks and lead to service failure. On the contrary, it is observed that polymer insulation (XLPE) with even very high level of oxidation still keeps comparatively sufficient remaining breakdown strength [21] [13]. Furthermore, in cable joints the oxidation is a diffusion limited process and research shows that the lifetime of the insulation system, even at high temperatures can be relatively long [21] [14]. Most importantly, overheating can change the stress control tube properties, because of the fact that oxidation and correspondingly formed carbonyl groups can lead to a significant increase of material conductivity [21] [13]. This is likely to cause an unfavorable field distribution and stress concentrations within the cable joint.

Oxidation process theory

When an oxidation process takes place, it is not necessarily that the oxygen is a part of the chemical reactions as other chemical elements and compounds can produce the same result. However, since the oxygen is a very reactive element and constitutes about 20,8% of the atmosphere, in most of the cases it will be the oxidant. Polymeric materials can age continuously in result of a chain reaction caused by formation of free radicals. Free radicals are molecules that have one unpaired valence electron and are denoted as R. They are formed by processes, such as thermal aging, radiation and chemical reactions. In order to be explained, the process is based on the interaction between oxygen (O_2) and polyethylene ($(C_2H_4)_nH_2$), as the free radical is due to one missing hydrogen atom ($(C_2H_4)_nH$) [23].

Initial phase:

$$Polymer \rightarrow R\bullet$$

Propagation:

$$R\bullet + O_2 \rightarrow ROO\bullet$$

$$ROO\bullet + RH \rightarrow ROOH + R\bullet$$

Termination:

$$2R\bullet \rightarrow R—R$$

$$R\bullet + ROO\bullet \rightarrow ROOR$$

$$2ROO\bullet \rightarrow ROOR + O_2$$

The initial phase of a radical in this case is a polyethylene polymer that loses one hydrogen atom as a result of energy supply in form of radiation, heat or light [23]. Propagation process explains how a chain reaction can occur. The starting radical reacts with oxygen and form a new radical $ROO\bullet$. The new radical $ROO\bullet$ then reacts with another polyethylene molecule resulting in $ROOH$ and a new radical, which can be involved in the same process, thus a chain reaction can be started. The chain reaction can be terminated when two radicals react with each other to form a new molecule, or the radical is included in the formation of new inert products.

Typical thermally induced oxidation reaction can be expressed as

$$RH + O_2 \rightarrow R\bullet + HO_2\bullet$$

where RH is a damage free polymer chain, $R\bullet$ is a polymer free radical and $HO_2\bullet$ is a hydroperoxide free radical. Polymer free radicals are formed when the molecule is subjected to some form of energy such as ionizing radiation or extensive thermal exposure. This forces an electron to be ejected. These free radicals propagate the degradation of the polymer if there is no presence of antioxidants in the material. Antioxidants are meant to react with the free radicals as inert molecules are formed and in that way acting against the degradation of the polymer.[20]

2.6 Tensile Test

One of the most common tests used for examining the mechanical properties of a given material is the tensile test, reproducing the stress-strain behavior. A test object is deformed, most often until a fracture is observed by gradually applying an increasing tensile load that is in uniaxial direction along the long axis of the test object. A standard tensile specimen used in tensile tests for polymers is presented in Figure 2.16.[7]

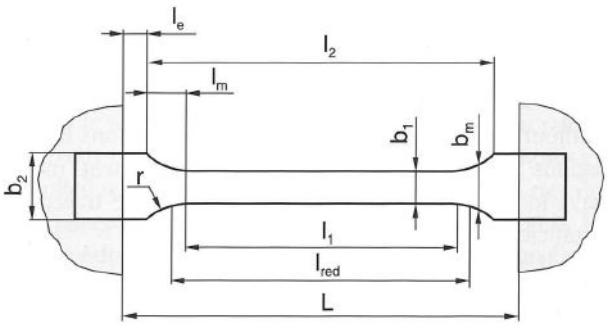

Figure 2.16: Typical test object for polymeric materials [12].

During the test, deformation is mostly restricted to the center region of the test object, which has uniform rectangular cross section along its length. The test specimen is positioned by putting both ends into the holding grips of the testing equipment. The testing machine is adjusted to elongate the test object, keeping a constant rate and measuring at the same time, both the applied load (load cell) and the corresponding extension (extensometer). The tensile test is destructive and the test specimen is permanently deformed and in general fractured.[7]

The result of this process can be represented as a stress-strain curve as shown in Figure 2.17.

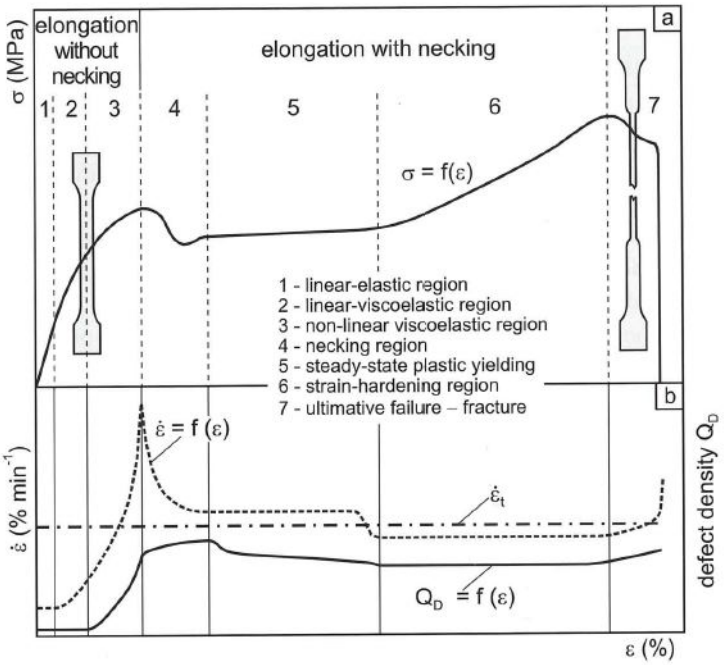

Figure 2.17: Typical stress-strain curve for a polymeric test object [12].

Different polymeric materials obtain different behavior during tensile test as can be seen in Figure 2.18.

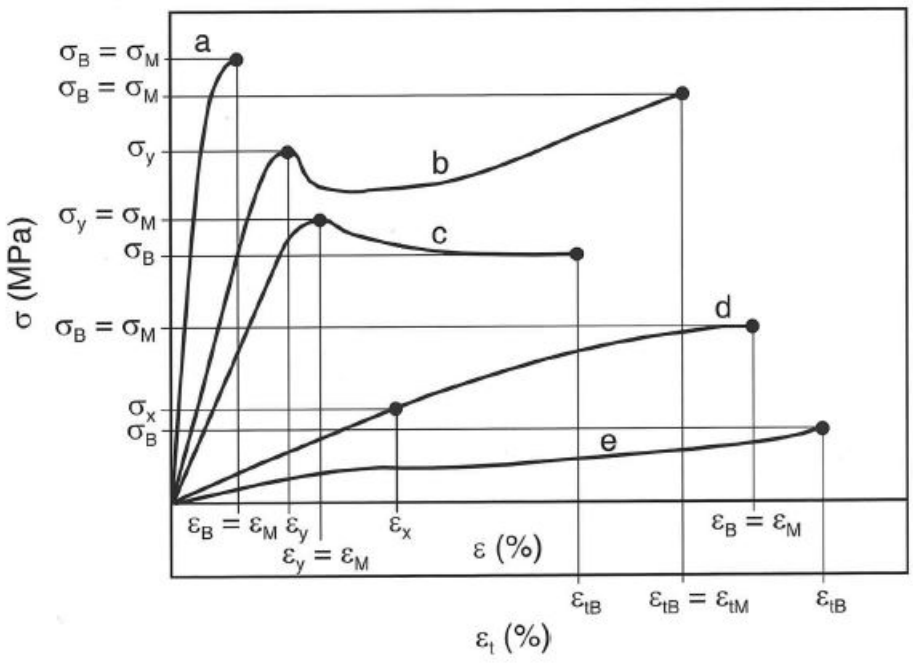

Figure 2.18: Stress-strain curves for different type of polymers : a) brittle materials; b) and c) though polymeric materials with yield point; d) though materials without yield point; e) elastomeric materials [12].

The mechanical properties of polymers, usually are very sensitive to testing speed, temperature and exposure to chemicals (such as water, oxygen, organic solvents, etc.) as it is shown in Figure 2.19.[7]

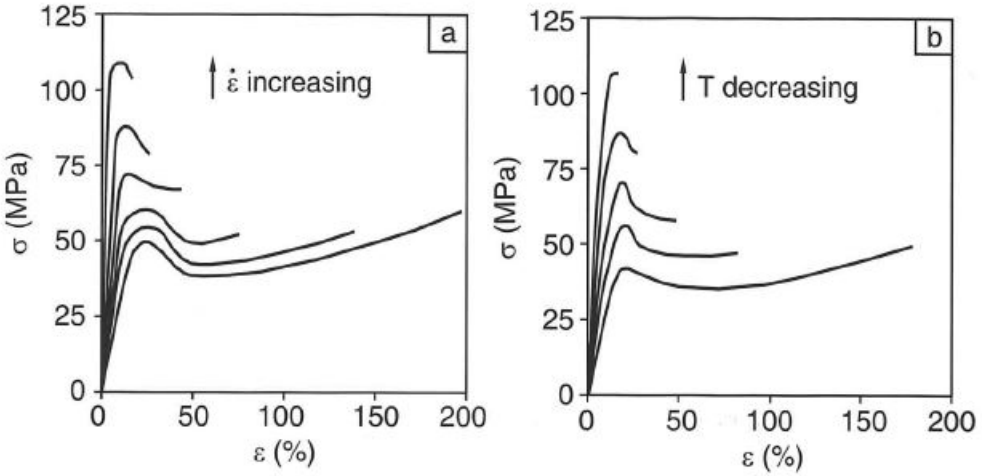

Figure 2.19: Stress-strain diagrams of a polymeric material as a function of a) strain rate (testing speed) and b) temperature. When strain rate $\dot{\epsilon}$ is increased, the percentage strain at break ϵ(%) decreases and stress at break σ is increasing as seen in a). When temperature T is decreasing, the percentage strain at break ϵ(%) decreases and stress at break σ is increasing as seen in b) [12].

Several parameters, calculated by the tensile test measurement equipment can be used when comparing the mechanical properties of different test objects.

Stress σ is represented by the external load F, acting on the initial cross-sectional area A_0 of the central part of the test object [12]. The following expression is used:

$$\sigma = \frac{F}{A_0} \tag{2.8}$$

Strain is the ratio between ΔL and L, where ΔL corresponds to the actual test object length and is a function of the test duration and L is the initial gauge length. Strain is dimensionless and it can be expressed as a percentage strain. The strain presented in Equation 2.9 is also called nominal strain.[12]

$$\epsilon_t = \frac{\Delta L}{L} \tag{2.9}$$

Strain rate or nominal strain rate can be obtained by the derivation of strain with time, where V_T is the testing speed of the measurement equipment [12]:

$$\dot{\epsilon}_t = \frac{d\epsilon_t}{dt} = \frac{1}{L}\frac{d(\Delta L)}{dt} = \frac{V_T}{L} \tag{2.10}$$

Yield stress is denoted as the first stress value at which strain increase occurs without increasing the stress [12]. It is shown in Equation 2.11.

$$\sigma_y = \frac{F_y}{A_0} \tag{2.11}$$

Tensile strength is the maximum tensile stress measured during the test period [12]. It is presented in Equation 2.12.

$$\sigma_M = \frac{F_{max}}{A_0} \tag{2.12}$$

Tensile strength at break is the stress at which the test object breaks and is expressed with Equation 2.13. [12]

$$\sigma_B = \frac{F_B}{A_0} \tag{2.13}$$

Depending on the measuring equipment the values of yield stress, tensile strength and tensile strength at break can be identical or at least very similar.[12]

2.7 Differential Scanning Calorimetry – Oxidation Induction Time and Induction Temperature

2.7.1 Oxidation Induction Time

Differential scanning calorimetry is a method which is used, when examining the thermal transitions in polymeric materials. The DSC technique used in this project work is a heat-flux type calorimetry. The principle of operation includes simultaneously heating of two crucibles, inside which the test object and a reference medium are placed. Usually, air is used as a reference.[29]

Both crucibles are placed in a common cylindrical oven and considering the thermal symmetry of the arrangement, no temperature difference is observed between the crucibles when the temperature in the oven is increased. However, if the test object changes its specific heat capacity during the temperature elevation, such a temperature difference between the test and reference crucible pans will occur. This will indicate endothermic (receiving energy) or exothermic (releasing energy) behavior of the test specimen, depending on the specific processes taking place in the material.[29]

A typical oven module for a heat-flow DSC can be seen in Figure 2.20 and a typical graph obtained during DSC measurement is presented in Figure 2.21.

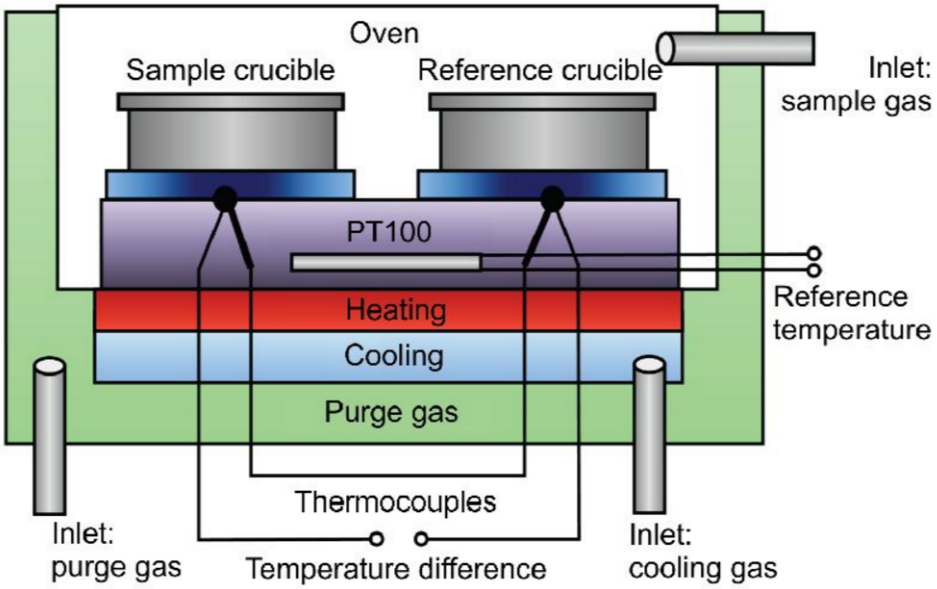

Figure 2.20: Schematic view of a DSC oven module [29].

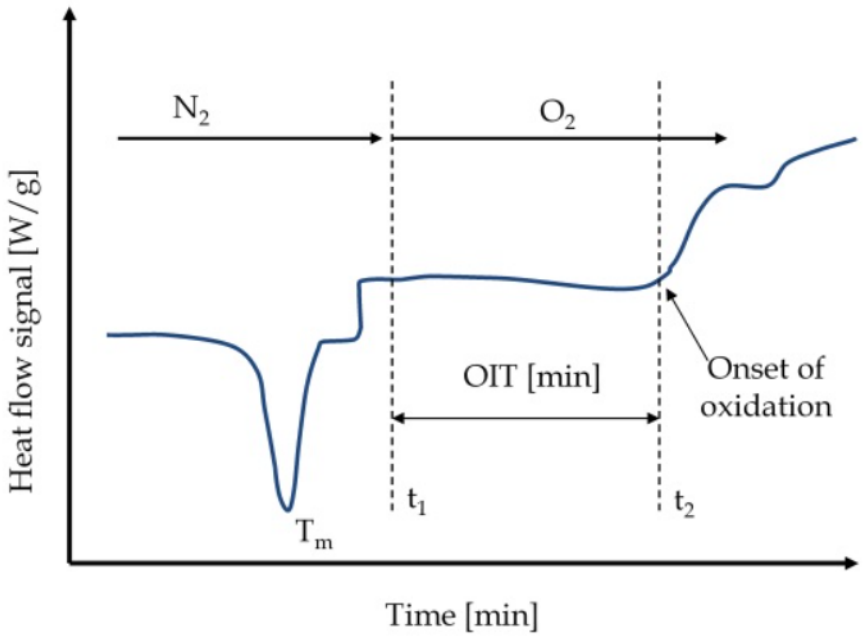

Figure 2.21: A typical DSC measurement curve [26].

DSC can be used for estimating the resistance properties of polymer materials to thermos-oxidative degradation by determining their oxidation induction time (OIT) [24].

In this master thesis project, OIT test is applied in order to evaluate the aging degree and compare the test samples subjected to different time period and conditions of thermal aging.

OIT in general is an accelerated aging test. In principle, the test and reference crucible pans are heated to a temperature above the melting one under inert nitrogen gas conditions. As can be seen in Figure 2.21, when an equilibrium state is reached and the temperature stabilizes, the inert medium is shifted to oxidizing oxygen gas. The time from shifting to oxygen until an oxidation process occurs is taken as the OIT value.[24]

OIT results for two different materials are presented in Figure 2.22.

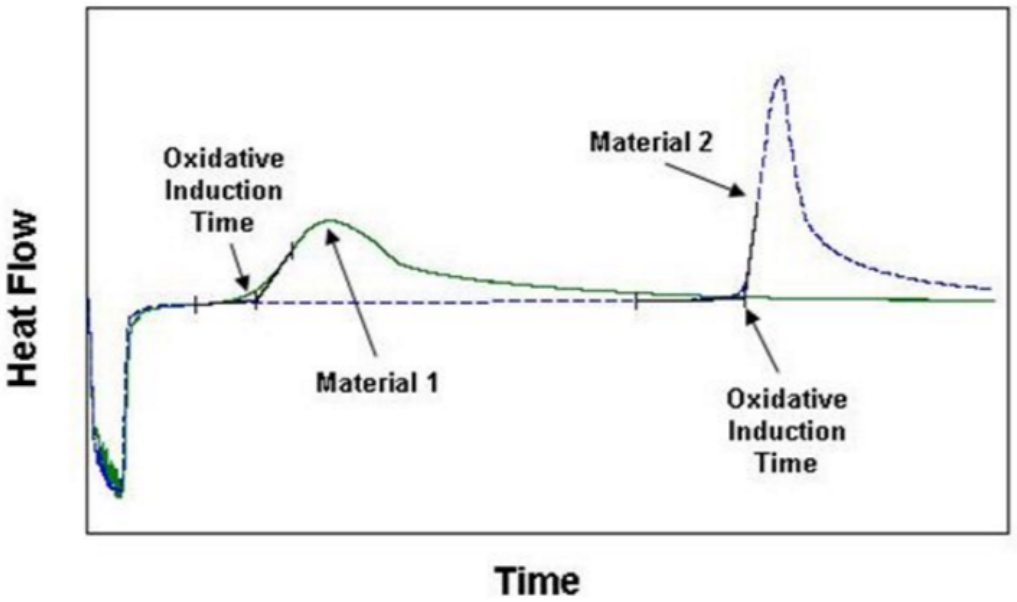

Figure 2.22: A typical OIT measurement curve. Oxidation induction time for Material 1 is shorter than the one for Material 2, which represents a lower thermal resistance. This can be due to consumed antioxidants during aging, different antioxidant types or polymeric material, etc [5].

OIT test is an appropriate technique to measure the effectiveness of the antioxidants added into the polymer material to improve its lifetime [24].

2.8 Oxidation Induction Temperature

DSC equipment is adjusted to a temperature scanning mode and the test sample is subjected to a rising temperature with a constant change rate as oxygen is used as a purge gas. Antioxidants present in the polymer material are consumed until full exhaustion, presented by a rapid oxidation of the material. The temperature at which this spike occurs is taken as the oxidation induction temperature, T_{ind}.

A typical thermogram showing an oxidation induction time measurement for an insulation material can be seen in Figure 2.23. In general, T_{ind} is characterized by a very rapid slope which leaves little margin of error.

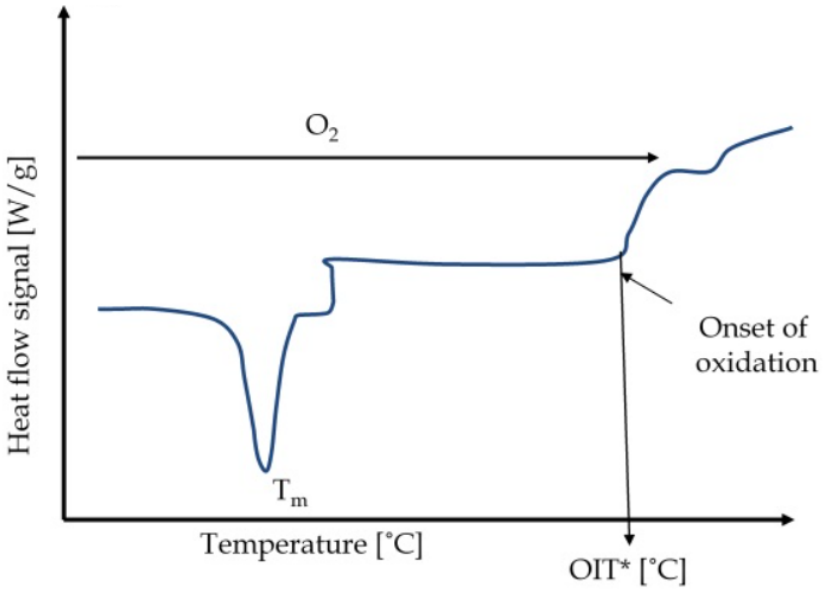

Figure 2.23: A typical T_{ind} measurement curve [26].

Chapter 3

Experimental Work

3.1 Test Object

Sufficient number of test objects were made considering the extensive number of test procedures and test conditions used in this project work. Two types of test objects were used, named Test object 1 and Test object 2. Test object 1 was used in the nondestructive dielectric response measurement tests, examining the electrical properties of the stress control tube, while Test object 2 was used in tensile and differential scanning calorimetry tests, which are destructive and performed for characterization of the deterioration level of the stress control tube material.

3.1.1 Time Domain Dielectric Response Measurements

Test object 1 consists of two cylindrical electrodes, separated by an insulating cylinder and a stress control tube shrunk over this composition. Diameters of the electrodes and the insulating cylinder are of the same size of 25 mm, which is in the recommended stress control tube shrinking range. The insulating cylinder is 100 mm in length and it is made of polytetrafluoroethylene (PTFE/Teflon). PTFE is used since it has excellent insulating properties, such as very low values of conductivity, tanδ and dielectric constant. Therefore, it does not affect the dielectric response measurements, as the measured conductivity is due only to the stress control tube material. Additionally, PTFE has very good heat resistance, as high temperatures are used during tests and the thermal aging process. Metal electrodes are made of stainless steel and are assembled with the insulating cylinder by screwing. An overview of this assembly is shown in Figure 3.1 and Figure 3.2.

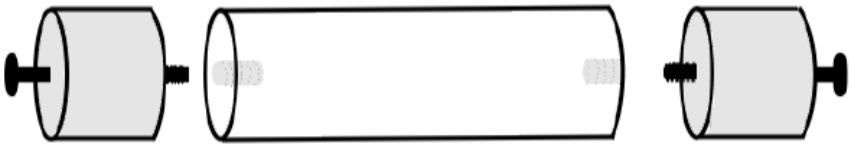

Figure 3.1: Cylinder assembly of two separate metal electrodes and an insulating cylinder.

Figure 3.2: Separate parts are assembled by screwing the electrodes into the PTFE insulation.

The stress control tube used in this project work is Raychem JSCR 42/16. Installing and shrinking of the tube was done in clean environment with a lot of attention, as unwanted impurities involved could affect the measurement results. Plastic gloves were used, while the cylinder assembly and the stress control tube were thoroughly cleaned with isopropanol and lint-free paper. After that the tube was placed on the cylinder assembly and the tube length was chosen, so that after shrinking it had considerable contact area with the electrodes. In order to perform the shrinking, a professional heat gun was used, which generates an air flow with a temperature up to 630°C. The shrinking process starts in the middle of the object going in outwards direction by using continuous circular movements of the heat gun. It was proceeded like that, in order to avoid possible air cavities and excessive local overheating, which could lead to thermal damages of the material. The final test object is presented in Figure 3.3.

Figure 3.3: Final test object after installing the Raychem stress control tube.

Test object 2, used for DSC and Tensile tests is comprising of only a PTFE cylinder of the same diameter as Test object 1 and stress control tube. The process of installing the SCT on the cylinder is the same as for the Test object 1.

3.1.2 Tensile Test

Test object type 2 is used. Stress control tube is cut along the PTFE cylinder, so that it can be folded out into a rectangular sheet. Then using a manual punch machine with a "dog bone" shaped cutter, the required number of samples were obtained. The specified stress control tube sheet provides 5 dog bone test samples, which equals the minimum number of test objects used in tensile test, required by IEC 608011-1-1 standard. The latter also specifies standardized measures and shape of test specimens as shown in Figure 3.4.

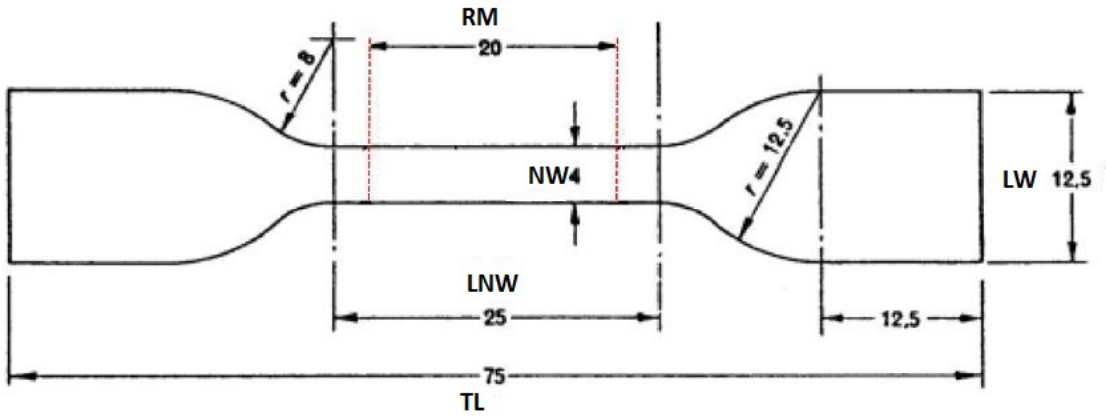

Figure 3.4: Standard shape of dog bone test sample, ready for tensile test and complying with IEC 60811-1-1. Total Length TL=75mm, Length of Narrowed Width LNW=25mm, Large Width LW=12.5mm, Narrowed Width NW=4mm. The red dotted lines indicate the location of reflector tapes for measuring length change by means of a remote laser gauge. [3]

All dimensions of the dog bone sample are constant except for the thickness, which may vary depending on production or craft related issues. In practice, it is very difficult to perform a perfect shrinkage, resulting in a constant thickness around the PTFE cylinder. Before tensile test is performed, the thickness of the center narrow part of the test sample (LNW) was measured at three places and the smaller value became the basis for the cross area of the test object. This is done, because the material's tensile strength is directly related to the sample thickness, wherein a thinner object withstand less than a corresponding thicker object, experiencing the same strain.

Length change in dog bone test sample is measured by a remote laser gauge. In order the length extension to be registered by the laser meter, two reflective tape pieces with a width of around 1 mm are placed on the dog bone sample, as indicated in Figure 3.4 with a distance of 20mm between each other. This area is specified by IEC 60811-1-1 and it is required that the fracture under tensile testing should occur in that area. Differences from the specified

distance when mounting the reflective tapes are compensated by the external laser meter.

3.1.3 Differential Scanning Calorimetry

After removing the stress control tube from The PTFE rod and using it to obtain dog-bone test samples for the tensile test, the remaining part of the material is cut into smaller pieces, used for DSC test specimens preparation. Those pieces are further shrunk with a heat gun until reaching their final shrinkage leve,l in order test specimens to keep their shape and size during DSC measurements when subjected to high temperatures. In that way, additional processes that can affect the measurements are minimized. As the crucible pans have a volume of only $40\mu L$ the fully shrunk SCT pieces were cut into smaller rectangular test specimens in order to be placed inside the crucibles. For obtaining more accurate results, temperature gradients over the test sample had to be avoided, thus the height h was kept small in comparison with the rest dimensions of the specimen. The final samples were formed by slicing the fully shrunk SCT pieces with a slicing machine and adjusting the length with a scalpel. The width of a specimen represents the actual thickness of the stress control tube. A sketch of the final test specimen is presented in Figure 3.5.

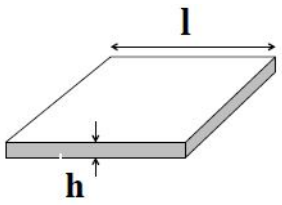

Figure 3.5: Illustration of DSC test sample. The hight is set to $h = 0,25mm$.

After preparation, the test sample is positioned in a crucible pan and a lid with three circular openings is crimped over the pan. The reference crucible is prepared the same way, but it is kept empty.

3.2 Thermal Aging

Based on the insulation material composition, cables have different working specification. XLPE insulated cables have maximum operating temperature of around 90°C and it is not unlikely that due to a poor metallic contact the temperature can rise up to and even exceed 150°C. [17]

One of the main purposes of this master project is to examine the effects of thermal aging on the stress control tube material dielectric response. Therefore, electric heat chambers are used to recreate three aging conditions for the test objects - dry air environment at 98°C, air with high relative humidity at 98°C and dry air at 150°C.

First two conditions were obtained in a common heating chamber adjusted to a constant temperature of 98°C. Test objects meant to age at dry air environment were positioned on a PTFE stands, directly placed on the chamber shelves, while the test objects aged at high relative humidity conditions were placed on PTFE stands in a sealed polyethylene box filled partially with deionized water. The box has a maximum withstand temperature of 120°C, which complies the temperature setting of the heat chamber. The test objects in the box were positioned just above the water level.

The test samples subjected to 150°C dry air were placed in a separate heat chamber, adjusted to the corresponding temperature level. They were positioned similarly to the previous case, on a PTFE stand, which was placed at the heat chamber shelf. Considering the higher temperature level, the stress control tube edges of those samples used in dielectric response measurements were protected by covering them with Viton heat shrink tube pieces with a specified minimum shrink temperature of 300°C. In that way, the stress control tube edges were prevented from possible cracking of the material, which would affect the contact between tube and electrodes of the test object. Viton tube pieces covered only a limited area of the stress control tube edge, letting the electrode contact area of the field grading tube to age sufficiently. The edges of test samples used for DSC and Tensile tests were left unprotected as the surface area of stress control samples was big enough for the corresponding test purposes.

Upon a predetermined aging programme, test samples were taken out from the heat chambers after corresponding time periods to be examined with DSC, Tensile and DR tests.

3.3 Vacuum Treatment

After taken out of the heat chambers, before being subjected to the corresponding measurements, test objects were dried in a vacuum cabinet for 3 days at 70°C and then lowering the temperature at 25°C for a day. In that way, the test samples have the same condition state before measurements, which in turn gives comparable results.

3.4 Test Procedures

Aging is a relative term and must be studied with accordance of a specified starting point or date. A method for estimating the aging degree of a given material should compare its present properties with those that the test object had at the starting point, known also as reference properties. It is usually beneficial to set the zero point for a new material with factory properties or for an object with a processed state, if the material must be processed to achieve its purpose. Those test samples at zero state are meant as reference samples.

Some material properties are better suited to compare based on what type of material is examined. Polymeric materials tend to become brittle upon thermal aging as polymer chains are shortened and the elasticity of the material is reduced. This can be determined by tensile testing, which results in reduced extension at break for an aged polymer material, giving an indication of aging degree. Extension at break was determined to be a measure of how far the aging reached, and the preferable target was the extension to be decreased to minimum the half for aged objects compared to unaged reference ones. It is difficult to define aging degree and life remaining, but it is proposed that 50% of percentage strain at break indicates life end of cross-linked polyethylene [14].

Another parameters suitable for estimating the aging degree and comparison are oxidation induction time and oxidation induction temperature of a test material. Usually, antioxidant additives are included in polymeric materials working against material aging processes. During thermal aging, antioxidants are gradually consumed, aging evolves faster and in result oxidation induction time and temperature decrease compared to that of an unaged sample. [24]

Dielectric properties of SCT are characterized in function of temperature, aging degree and

humidity by using time domain dielectric response measurements.

3.4.1 Tensile Test Procedure

Tensile testing is used for characterization of material mechanical properties. In this master project, it is used to characterize the aging degree of stress control tube, which was exposed to accelerated thermal aging, by comparing the results for reference and aged test objects.

When the basis thickness is measured and the reflectors are mounted, the test samples are ready for stretching. The larger width ends of the test specimen are positioned in the holding grips of the test equipment in a way that the test sample doesn't slip out during subjecting it to tension. The external laser sensor is adjusted so that the laser beam is centered along the dog bone object. Based on where the reflectors are mounted, the laser gauge can show a percentage value that indicates the distance between the reflectors, relative to the maximum measurement length of the gauge. Maximum measuring length is set to 500mm and the laser meter shows 4%, if the reflectors are placed at a distance of exactly 20mm.

Computer software Nexygen is used to log and process data during tensile testing. In the programme the needed sample size is selected from a list corresponding to IEC 60811-1-1 as only the specimen thickness varies, which can be manually entered in the software interface. Strain rate must also be specified and according to the standard it is 25mm/min. After adjusting the software the tensile test is started and it is waited until the test specimen breaks in the area between the reflectors. At least five samples obtained from one stress control tube sheet are subjected to test.

3.4.2 Differential Scanning Calorimetry Procedure

DSC is used for investigation of OIT (oxidation induction time) and T_{ind} (oxidation induction temperature) of test samples with different level of thermal aging. These results are used to compare and differentiate between several aging conditions and aging levels of stress control tube test samples. The DSC measurements are used as an addition to the results obtained from the Tensile tests.

The test equipment used for the measurements was Mettler Toledo High-Pressure Differential Scanning Calorimetry apparatus with nitrogen and oxygen used as an surrounding environment for the test samples.

Both crucible pans were placed in the DSC apparatus, a temperature test program was selected and started.

Oxidation Induction Time

OIT measurements are done by using the isothermal mode of the DSC equipment, as the test objects are located in nitrogen gas, while heated to the isothermal temperature. Oxygen is

purged when the needed temperature is obtained.

The OIT temperature programme used in this master project consists of four intervals:

1) Initial isothermal interval of 30 minutes at 25°C. During this period the temperature of the test sample is stabilized giving a reference line for the ongoing intervals.

2) The second section of the programme is dynamic with a heating rate of 20°C/min. The end temperature is the one at which the oxidation induction time will be estimated and it is set by the test software.

3) The third period is isothermal at a temperature equal of the end temperature of section 2). The time period which is set is inversely proportional to the test sample aging level and proportional to the test temperature. The less aged is an object, the more time it needs until the oxidation starts for one and the same test temperature and on the other hand, the higher is the test temperature, the shorter time is needed until the oxidation process starts for one and the same specimen. During this period the medium, surrounding the test and reference samples is changed from nitrogen to oxygen gas. The standard recommends minimum waiting time of three minutes before switching to oxygen. This waiting period should be noted down and used when estimating graphically the oxidation induction time from thermograms, provided by the corresponding software. OIT is considered the period between the point of switching from nitrogen to oxygen until the start of an oxidation (exothermal) process.

4) The last part of the test programme is cooling the sample back to the starting temperature of 25^oC with a cooling rate of -20°C/min. In this way the equipment is ready for testing the next specimen.

An example of a temperature test programme is shown in Figure 3.6

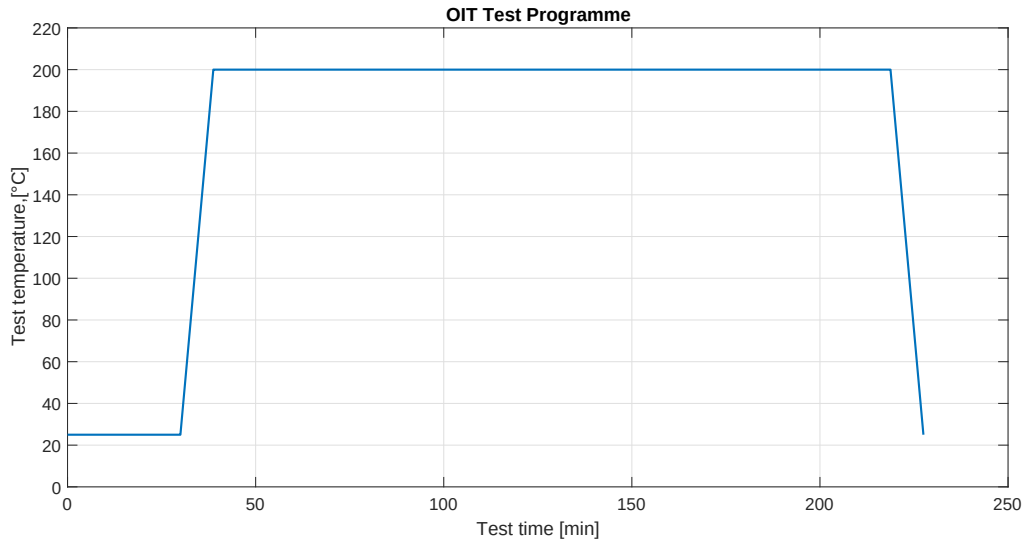

Figure 3.6: OIT test programme with an isothermal period of 180 minutes at 200°C.

Based on previous studies for oxidative behavior of materials with similar composition, the testing temperature range changes roughly in the range of 180- 240°C [20] [24]. For this master project the range was extended to 160- 300°C for better certainty of the results.

The temperature test programs, presented in Table 3.1 were used.

OIT Test Programmes			
Interval 1	Interval 2	Interval 3	Interval 4
25°C, 30min	25°C- 300°C, 20°C/min	300°C, 90min	300°C-25°C, -20°C/min
25°C, 30min	25°C- 290°C, 20°C/min	290°C, 90min	290°C-25°C, -20°C/min
25°C, 30min	25°C- 280°C, 20°C/min	280°C, 90min	280°C-25°C, -20°C/min
25°C, 30min	25°C- 260°C, 20°C/min	260°C, 90min	260°C-25°C, -20°C/min
25°C, 30min	25°C- 240°C, 20°C/min	240°C, 120min	240°C-25°C, -20°C/min
25°C, 30min	25°C- 220°C, 20°C/min	220°C, 180min	220°C-25°C, -20°C/min
25°C, 30min	25°C- 200°C, 20°C/min	200°C, 180min	200°C-25°C, -20°C/min
25°C, 30min	25°C- 180°C, 20°C/min	180°C, 180min	180°C-25°C, -20°C/min
25°C, 30min	25°C- 160°C, 20°C/min	160°C, 180min	160°C-25°C, -20°C/min

Table 3.1: Test procedure sequence for OIT measurements.

Oxidation Induction Temperature

Finding the induction temperature is another DSC technique estimating the aging degree and the thermal resistance of a given polymeric material. The test includes dynamic approach as the temperature is gradually increased with a given rate. The induction temperature is considered the one at which an oxidation process starts, when the antioxidants are entirely consumed.

The temperature programme used for defining T_{ind} consists of 2 intervals and both of them uses oxygen as a purge gas:

1) Initial isothermal interval of 10 minutes at 25°C. During this period the temperature of the test sample is stabilized, giving a reference line for the next interval.

2) The next interval is dynamic with a starting temperature of 25°C, end temperature of 400°C and a heating rate of 10°C/min.

The test program used is shown in Table 3.2 and Figure 3.7.

T_{ind} Test Programme	
Interval 1	Interval 2
25°C, 10min	25°C- 400°C, 10°C/min

Table 3.2: T_{ind} Test Programme.

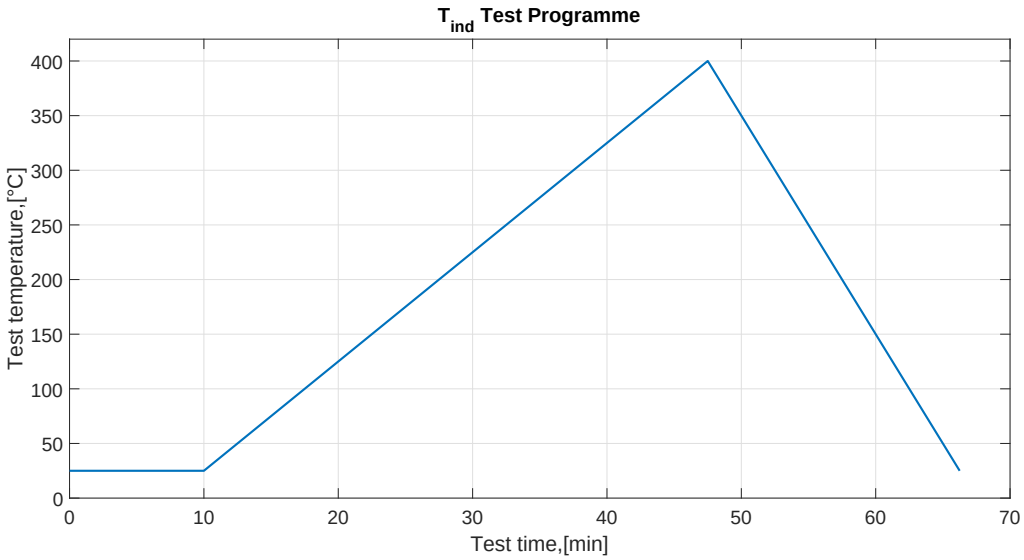

Figure 3.7: Graphically presented oxidation induction test programme.

Analysis of measured data

OIT and T_{ind} are determined graphically from a DSC thermogram by using STARe Excellent software.

The y-axis represents the differential heat flow used to maintain the reference and the test specimens at the chosen isothermal temperature. The measurement graph deviates from the base line, which is relatively horizontal, when the antioxidants are consumed and the process becomes exothermic. The OIT is estimated as the time period between the oxygen introduction and the intersection point of the exothermic slope and the baseline.

In a similar way T_{ind} is measured from the beginning of the test procedure until the intersection between the baseline and the exothermic slope. The temperature at this intersection point is assumed as T_{ind} and shows the temperature at which the antioxidants are already exhausted and a rapid oxidation of the polymer occurs.

3.4.3 Dielectric Response in Time Domain

Experimental Setup

The setup used for time domain dielectric response measurements is developed by researchers working at SINTEF Energy Research. It is presented in Figure 3.8.

Originally, this setup is suitable for both, time and frequency domain dielectric response measurements. These methods use the same principle of measuring the current through dielectric test object while voltage is applied across it. Due to the fact that measured currents are very small, in the range of $10^{-11} - 10^{-5}$, the measurement results appear to be very sensitive to the surrounding noise. Therefore, the test object is placed in a Faraday cage. The cage itself is positioned in a climate chamber, which controls the needed test temperature and relative humidity.

The equivalent test circuit, shown in Figure 3.11 is used for time domain dielectric response measurements. Polarization and depolarization currents are measured, correspondingly when a DC step voltage is applied across the test object and when the electrode connected to the HVDC source is grounded after that. Using these results, the conductivity of the material under examination can be calculated. Measurement procedure are more extensively

elaborated further in this section, presenting the operation of the test setup.

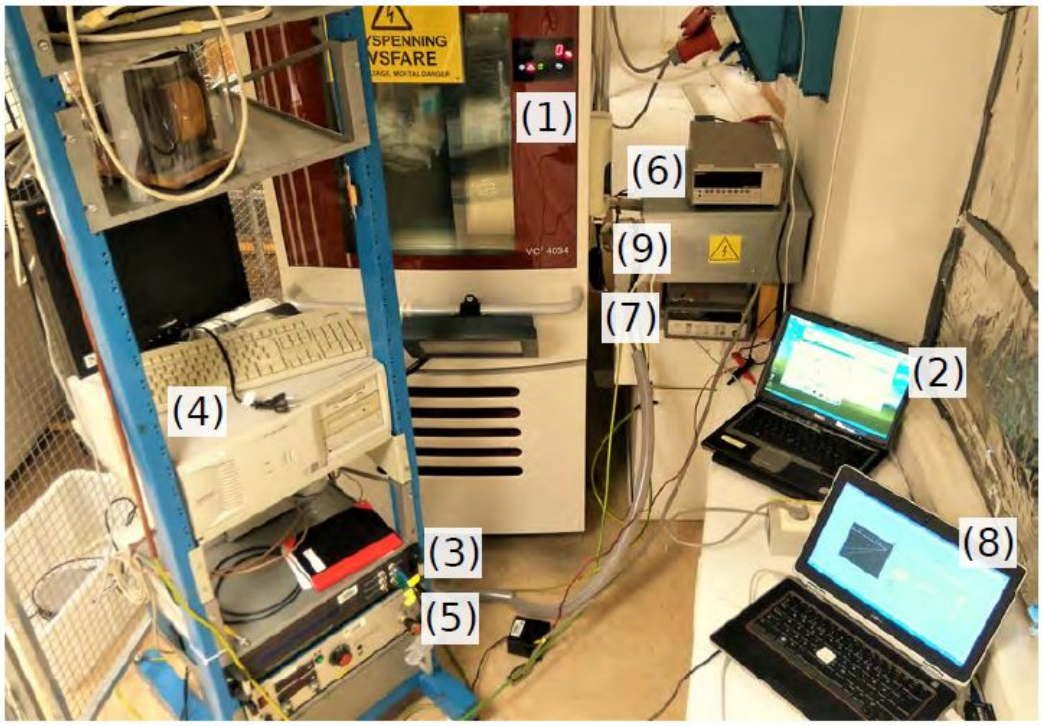

Figure 3.8: Experimental setup for measurements of dielectric response measurements of stress control tube in time domain. The test object is placed inside a climate chamber (1) maintaining constant temperature and humidity conditions, controlled by PC (2). For time domain measurements, the voltage applied across the test object is supplied by a stable HVDC source (5). The current through the test sample is measured by a picoamperemeter (6). The test and measuring procedures are automatically controlled using LabVIEW software (PC (8) and Agilent (7)), connecting and disconnecting the voltage source and picoamperemeter by means of a relays installed in box (9).

Test Object Preparation

For dielectric response measurements in time domain, Test object type 1 is used. Its assembly is explained in details in Section 3.1. As a result a test sample is obtained, consisting of a stress control tube shrunk on a PTFE rod with metallic electrodes attached at both sides. After installation, the outer diameter of the test object is 29 mm, which is in the recommended range when the stress control tube is installed in real cable joints.

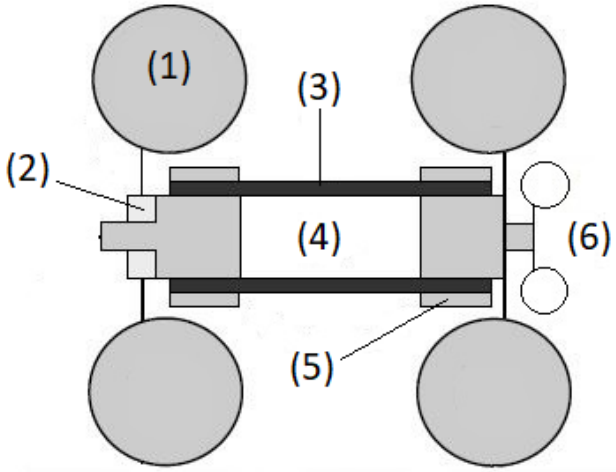

Figure 3.9: Illustration of the test object: (1) aluminum corona rings, (2) PTFE ring insulating the measuring electrode from the grounded corona ring, (3) stress control tube, (4) PTFE rod, (5) metallic clamps and (6) copper corona ring.

During measurements, one of the metal electrodes is connected to the stable HVDC source, while the other is connected to the picoamperemeter. Aluminum corona rings are attached at both electrodes in order to avoid corona discharges, see Figure 3.9. Additionally, metallic clamps are used at both ends of the test object. By applying pressure they provide good electric contact between the stress control tube and the metal electrodes. Additional copper corona ring is added where the HVDC source is connected to the metal electrode.

Measuring of Dielectric Response in Time Domain

The dielectric response in time domain of stress control tube Raychem JSCR 42/16 is estimated by measuring polarization and depolarization currents through a test object by applying a DC step voltage. A test object is prepared as described in Section 3.4.3. After that the test sample is placed inside the Faraday cage, positioned in the climate chamber, as it is presented in Figure 3.10. Inside the Faraday cage the test object is positioned vertically on an insulation cylindrical stand. The latter lays on a metal plate with conical legs, minimizing the vibrations, which can affect the measurement results. This plate is grounded by attaching it to the Faraday cage with a metal wire.

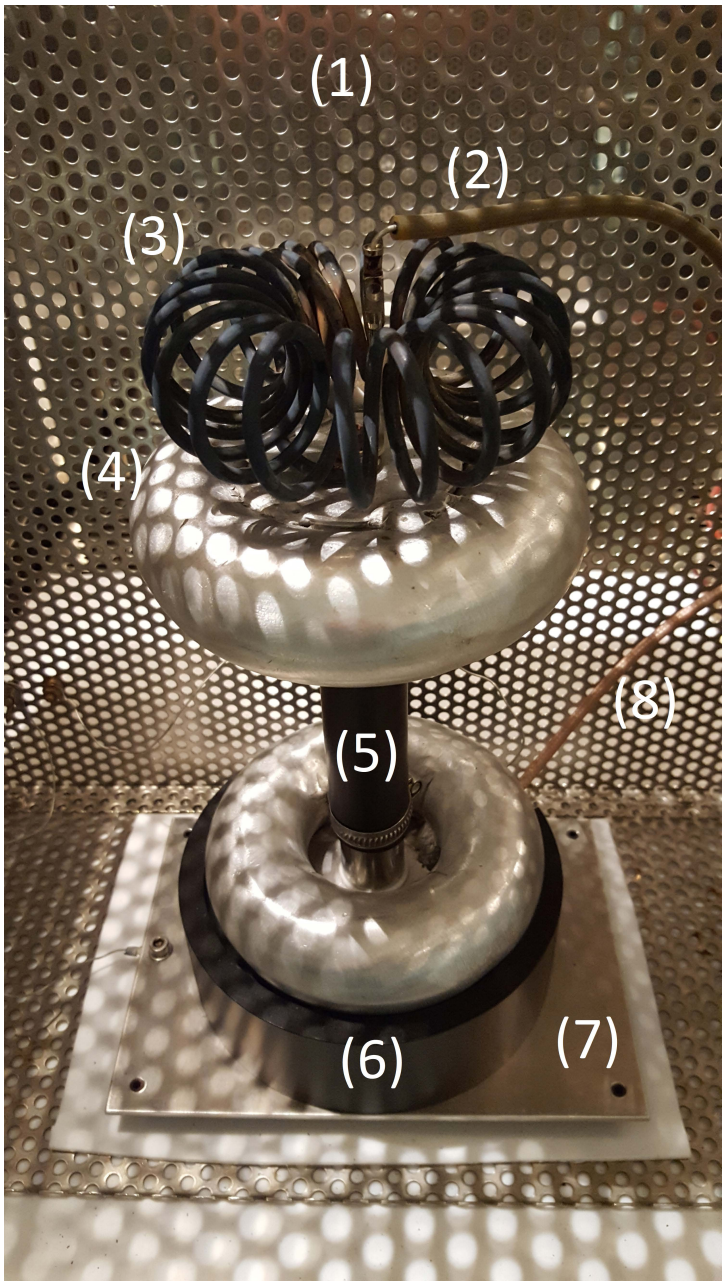

Figure 3.10: Picture of the test object: (1) Faraday cage, (2) high voltage cable, (3) copper corona ring, (4) aluminum corona rings, (5) stress control tube, (6) insulating plastic stand, (7) vibration dampening plate, (8) picoamperemeter measuring cable. The front cover of the Faraday cage is removed in order a clear picture to be taken.

After connecting all cables and adjusting the temperature and humidity levels in the climate chamber, a delay period of minimum 4 hours is considered before conducting the measurements. This allows an even and stable temperature of the test object, as well as warming up of the HVDC source and the picoamperemeter, which provides better measurement accuracy. The delay period also reduces the noise developed by the triboelectric effect, which is obtained when cables are subjected to movement, vibration or thermal expansion, as charge

generation may arise between the insulation and conductor due to friction [4].

The test setup, presented as an equivalent circuit can be seen in Figure 3.11. HVDC source is involved to ensure the stable voltage application across the test object while a picoamperemeter handles current measurements through the test object. The first stage of the test procedure is the noise level measurement as it is done for a period of 15 minutes. Secondly, a step voltage is applied for 3 hours as the polarization current is measured in that time. At last, the electrode connected to the high voltage supply is grounded and depolarization current measurements are collected for 3 hours. The HVDC source is connected and disconnected to the test circuit by means of high voltage relay. During this switching in and out, the picoamperemeter input is grounded due to the high transient currents, which can damage the apparatus. The HVDC source and the picoamperemeter are automatically controlled by LabVIEW software. The same is in charge of collecting dielectric response data and store it in text files. Then after suitable processing it can be used for calculating the conductivity of the material subjected to test. Temperature and humidity in the climate chamber are controlled by SIMPATI software installed on a separate computer.

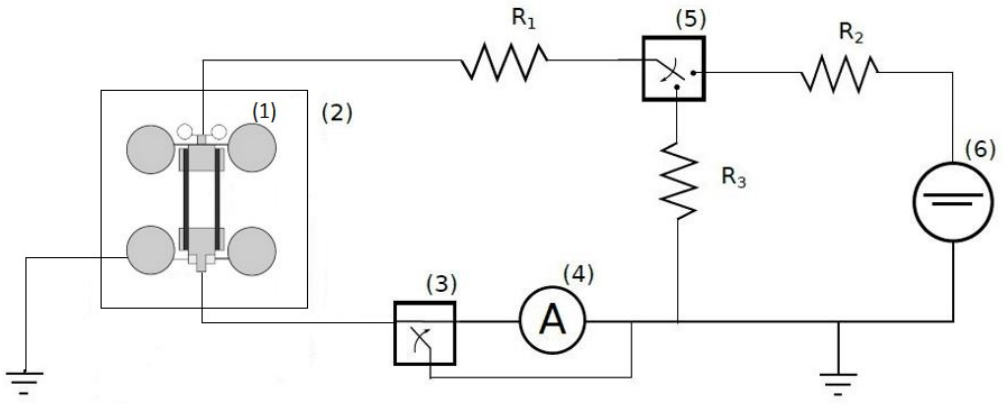

Figure 3.11: An equivalent circuit representing the dielectric response in time domain measurement setup: (1) test object, (2) Faraday cage and climate chamber, (3) low voltage short circuit relay, (4) picoamperemeter, (5) high voltage switch relay and (6) a stable HVDC source. $R1 = 50M\Omega$, $R2 = 50M\Omega$ and $R3 = 10M\Omega$.

The test procedure sequences used for dielectric response measurements are presented in Tables 3.3, 3.4 and 3.5.

Measurements for samples stated in Table 3.3 are performed at three temperature levels : 30°C (low load conditions), 90°C (high load conditions) and 150°C (failure mode). Test sequence is 30°C, 90°C, 150°C and then repeated at 30°C. The latter is done to show whether

the test has affected the electrical properties of the stress control tube due to high voltage and temperature application. Such a difference can be caused by a hysteresis effect or desorption of volatiles when a test sample is subjected to high temperature. The relative humidity in the climate chamber is kept at 0%.

A second sample, Test Sample 2 from the same type and aging conditions is subjected to dielectric response tests to confirm the validity of the initial results. Test voltage level is restricted to the highest one, in order to minimize the test period as dielectric response measurements used in this master project are sufficiently time consuming.

Test Sample 1			
Temperature, [°C]	Relative Humidity [%]	Test Voltage [kV]	Electric Field [V/mm]
30	0	1, 5, 10, 20	10, 50, 100, 200
90	0	1, 5, 10, 20	10, 50, 100, 200
150	0	1, 5, 10, 20	10, 50, 100, 200
30	0	1, 5, 10, 20	10, 50, 100, 200
Test Sample 2			
30	0	20	200

Table 3.3: Test procedure sequence for:1) unaged samples 2) samples, thermally aged for 50 days at 98°C and dry air conditions 3) samples, thermally aged for 50 days at 98°C and high humidity conditions 4) samples,thermally aged for 15 days at 150°C and dry air conditions.

Test Sample 1			
Temperature [°C]	Relative Humidity [%]	Test Voltage [kV]	Electric Field [V/mm]
30	0	1, 5, 10	10, 50, 100
90	0	1, 5, 10	10, 50, 100
150	0	1, 5, 10	10, 50, 100
30	0	1, 5, 10	10, 50, 100
Test Sample 2			
30	0	10	100

Table 3.4: Test procedure sequence for: 1) samples, thermally aged for 75 days at 98°C and dry air conditions 2) samples, thermally aged for 75 days at 98°C and high humidity conditions.

Test Sample 1			
Temperature [°C]	Relative Humidity [%]	Test Voltage [kV]	Electric Field [V/mm]
30	0	1, 1.5, 2	10, 15, 20
90	0	1, 1.5, 2	10, 15, 20
150	0	1, 1.5, 2	10, 15, 20
30	0	1, 1.5, 2	10, 15, 20
Test Sample 2			
30	0	2	20

Table 3.5: Test procedure sequence for samples, thermally aged for 50 days at 150° and dry air conditions.

Test samples, subjected to water absorption at 90°C for 30 days represent the state of a stress control tube in a cable joint, operating in high humidity surrounding (e.g. wet soil, typical for Norway) and at the top level of the normal operation temperature. The water conditioning was performed in a sealed polyethylene box, partially filled with water, as the samples were placed on a PTFE stands, just above the water level. The box was located inside a heat chamber, maintaining a stable temperature of 90°C. The period of 30 days was chosen, based on previous water uptake measurements, done for the same stress control tube material. The water uptake process consists of two different periods, the first following a typical saturation curve, while the second represents a linear increase with much lower water uptake rate [27]. The obtained results show that the linear increase starts after approximately 30 days [27].

The measurements are done at 30°C and 95% of relative humidity, which represents the real case scenario of measuring cables on-site. First, the supply to the cable section considered for testing is switched off and then it is waited a sufficient period before measurements, during which the cable/cable joint temperature decreases.

Test Sample with Water Conditioning			
Temperature [°C]	Relative Humidity [%]	Test Voltage [kV]	Electric Field [V/mm]
30	95	1, 5, 10, 20	10, 50, 100, 200
30	95	1, 5, 10, 20	10, 50, 100, 200

Table 3.6: Test procedure sequence for unaged samples, subjected to water conditioning for 30 days at 90°C and high humidity conditions.

Test Sample with Water Conditioning			
Temperature [°C]	Relative Humidity [%]	Test Voltage [kV]	Electric Field [V/mm]
30	95	1, 2.5, 5	10, 25, 50
30	95	1, 2.5, 5	10, 25, 50

Table 3.7: Test procedure sequence for samples,thermally aged for 15 days at 150°C and dry air conditions and afterwards subjected to water absorption for 30 days at 90°C and high humidity conditions.

Analysis of measured data

Measurements for polarization and depolarization currents were stored in text document files by LabView software. Those files were converted into Excel files and processed by MATLAB software for obtaining polarization and depolarization currents, conductivity, dielectric response function values and their graphical representation. Activation energy was calculated by means of Excel files.

Chapter 4

Results and Observations

4.1 Tensile Test

Tensile test is used to characterize the test samples degree of aging, as it was desirable to reach at least 50% decrease of the maximum extension before breaking compared to reference sample results. Additionally, it is examined how different parameters like temperature and presence of humidity affects the aging.

Three conditions of aging were chosen: 1) dry air at 98°C 2) wet air at 98°C and 3) dry air at 150°C. For conditions 1) and 2) tensile tests were conducted for samples aged for 12, 17, 24, 39, 50 and 75 days. For condition 3) measurements were done for samples aged for 5, 10, 15 and 50 days.

The parameters chosen to represent the level of aging are extension at break and percentage strain at break. The measurements for all three aging conditions are compiled and presented in one and the same graphs as this makes direct comparison easier. The results are presented in Figure 4.1 and Figure 4.2. Detailed tensile test results and data can be found in Appendix A.1.

As it was explained in Section 3.1, for various reasons the stress control tube thickness is not a uniform value. Therefore, five samples from one and the same test object are used. This gives a statistical scatter of measurement results, which is presented in the graphs.

The results for conditions 1) and 2) shows relatively gradual aging rate as at the most aged level (75 days), the test samples still didn't reach the 50% decrease of their mechanical properties. This shows that even during a relatively long and high loading cycle of the cable system, stress control tube can keep relatively high level of its physical properties. Additionally, no visible discoloration or forming of cracks was observed. This ensures extended life at operating conditions close to the nominal ones.

Conditions 1) and 2) have the same aging temperature of 98°C with the only difference that high level of humidity is included in condition 2). This is done to estimate the effect of water to the material properties.

As it was explained in Chapter 2.5, thermo-oxidation process inception involves the reaction between a free radical on a polymer chain and an oxygen molecule, which is followed by a chain reaction until inactive products are produced. On the other hand, presence of water can show hydrolysis effect on polymers. The split between the bounds of monomer units results to a decrease of molar mass and consequently lower mechanical properties [9]. Water usually acts as a plasticizer, leading to a decrease of the glass transition temperature (softening temperature) and yield strength of the polymer material [25]. Although thermo-oxidation and hydrolysis rely upon different reaction processes, they are closely related while both of them often act simultaneously and may reinforce each other [9].

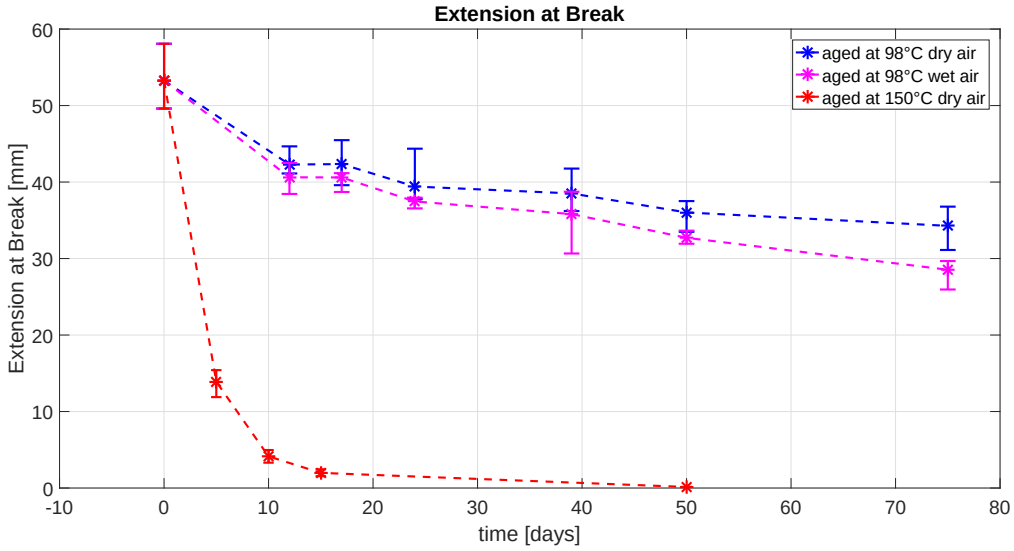

Figure 4.1: Extension at break in function of time for 1) SCT samples aged at 98°C dry air, 2) SCT samples aged at 98°C wet air, 3) SCT samples aged at 150°C dry air.

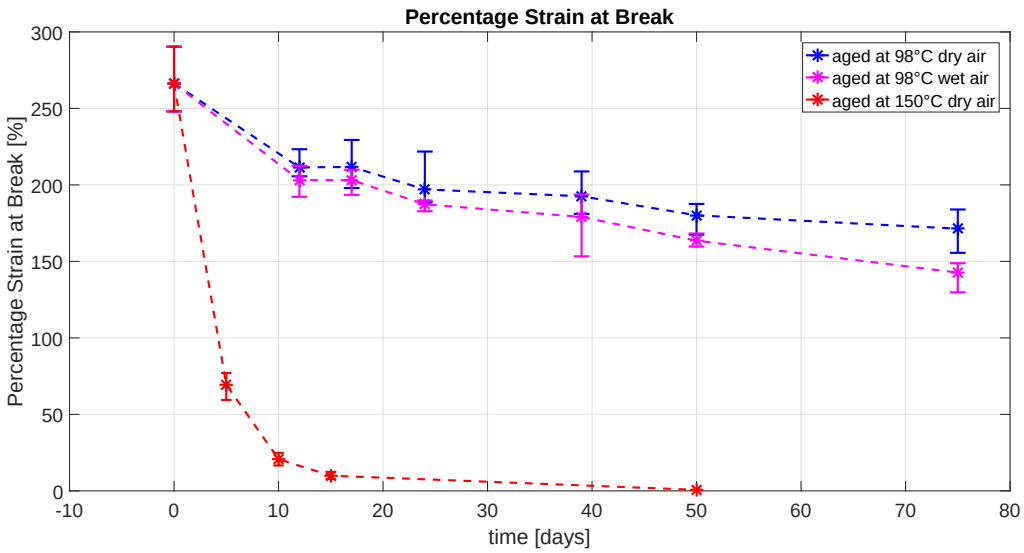

Figure 4.2: Percentage strain at break in function of time for 1) SCT samples aged at 98°C dry air, 2) SCT samples aged at 98°C wet air, 3) SCT samples aged at 150°C dry air.

As it can be seen in Figure 4.1 and Figure 4.2 the results for conditions 1) and 2) are very close to each other, as in most of the measurement points the minimum values of condition 1) overlap with the maximum values of condition 2). This shows that water had minimal effect on aging for these exact conditions and period of exposure. However, it should be mentioned that water absorption is a continuous process and it may take months before substantial amount of moisture has been absorbed by the material, and significantly longer periods before the material is saturated [22]. Additionally, the water uptake rate and material property degradation are accelerated at increased temperatures [22].

When the aging temperature is elevated above the melting one (104.8°C), as in this case it is 150°C, a very rapid aging rate is observed, represented by the mechanical properties decrease, shown by the red curve in Figure 4.1 and Figure 4.2. Already at day 5 of aging, it is obtained more than a 50% decrease for the parameters extension at break and percentage strain at break. For the sample aged for 50 days it was very difficult a dog bone test sample to be produced, due the high embrittlement of the stress control tube material, as only one of five kept its integrity and was subjected to test. Extension at break result is 0,13586 mm and percentage strain at break 0,67930 %, which clearly shows a total loss of mechanical properties. This can be explained by providing sufficient thermo-chemical driving energy by the elevated temperature conditions. The excessive energy supplied can depolymerize otherwise chemically stable long-chain single-bonded polymer molecules back to low-molecular

weight state, which causes degradation [25]. Even short periods of exposure to high temperatures can lead to irreversible chemical and physical changes, as the stiffness and strength decrease. Oxidation is considered to be the major degradation mechanism at elevated temperatures as degradation rate follows the amount of oxygen present [22]. Also at higher temperatures, oxygen diffusion increase, which further accelerates degradation (aging) process. This is very dangerous especially for cable joints, which has a composite design, consisting of materials with different thermal expansion abilities. That can lead to creation of mechanical forces which can be detrimental for a material with decreased mechanical properties.

As a general conclusion it can be said that temperature has much stronger effect on aging process and SCT mechanical properties than humidity presence. Cable joints design, installation and operating conditions should be performed in such way, that overheating is avoided.

4.2 Differential Scanning Calorimetry

Oxidation Induction Time

For a comparison of OIT measurements isothermal interval 3) depicted in the test programme was used.

In order to obtain a general idea how oxidation process affects the OIT measurement thermogram, two tests with the same temperature programme were done with the only difference that in one of them only nitrogen gas was used and in the second one the required switching to oxygen was added. As can be seen in Figure 4.3 an oxidation process is indicated in the second curve (red), compared to the clear baseline of the first when only nitrogen was used.

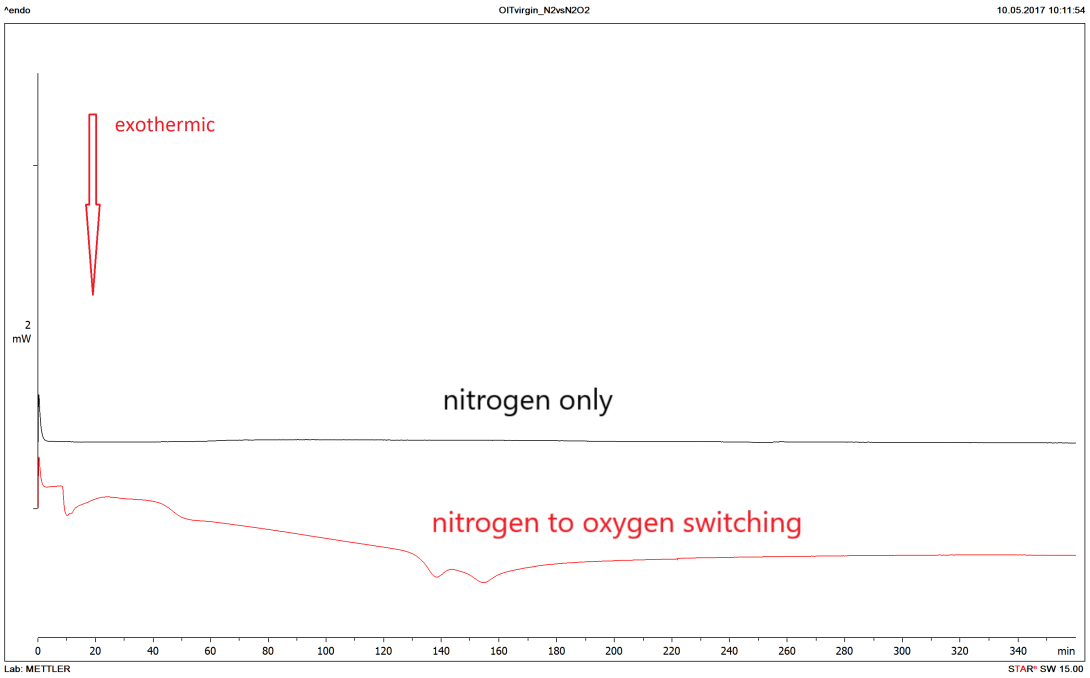

Figure 4.3: Effect of oxygen to a reference sample, subjected to an isothermal temperature of 210°C for 360 min.

A sequence of OIT measurements were done for a reference (not aged) samples, as explained in Chapter 3.4.2 in order to find a proper test temperature at which oxidation induction times will be long enough for comparison. Values longer than 15 minutes are required for better examining of results [24]. Unfortunately, all OIT results were in the range of 3-4 minutes. The results for the highest and the lowest test temperature are presented in Figure 4.4 and Figure 4.5 All measurements can be found in Appendix A.2.

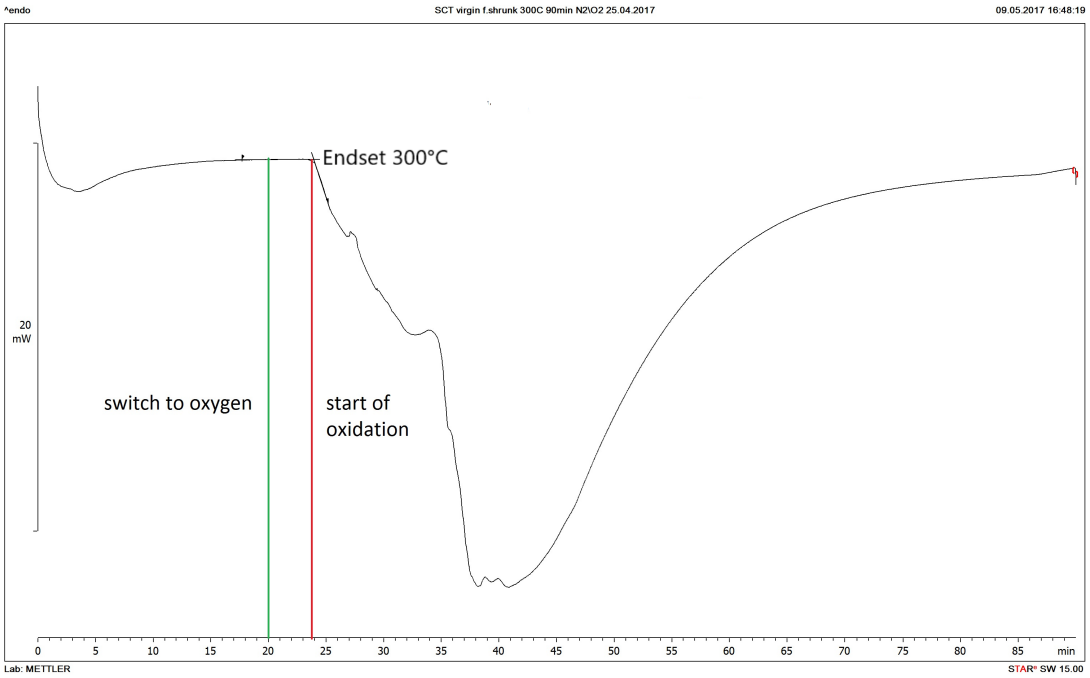

Figure 4.4: OIT measurement for a reference sample, tested at isothermal temperature of 300°C for 90 min.

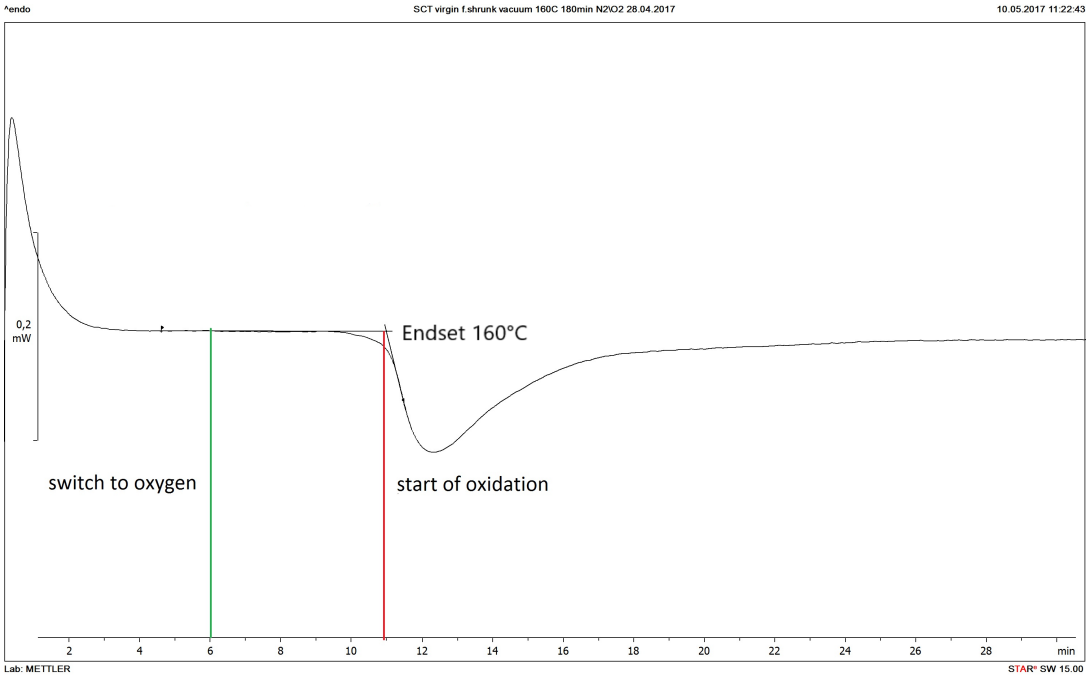

Figure 4.5: OIT measurement for a reference sample, tested at isothermal temperature of 160°C for 180 min.

In Figure 4.6 all measurements are compared. As can be seen at higher temperatures, the oxidative peak is much more bigger. With decreasing of the test temperature, the peak becomes significantly smaller, but this doesn't affect the OIT itself. Below temperatures of 160^oC the oxidation process becomes too small to be clearly detected.

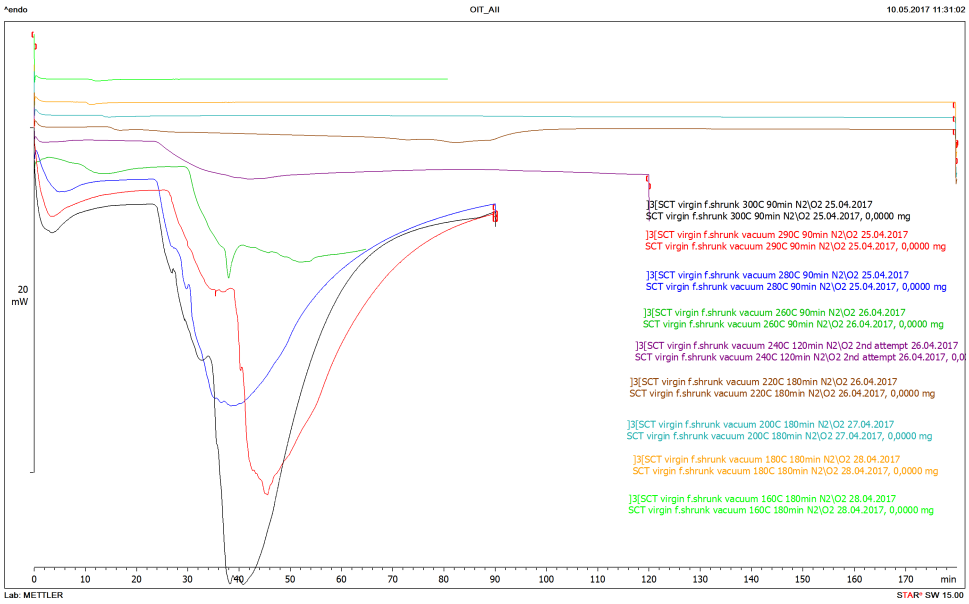

Figure 4.6: OIT measurements for test temperature range of 160-300°C.

The short OIT values obtained after the measurements were considered as not suitable for comparison. Therefore, it was continued with oxidation induction temperature estimation as an alternative DSC method.

Oxidation Induction Temperature

The stress control tube samples, subjected to T_{ind} measurement are presented in Table 4.1.

T_{ind} measurements	
Aging conditions	Days of aging
Reference sample	not aged
Dry air at 98°C	12, 17, 24, 39, 50, 75
Wet air at 98°C	12, 17, 24, 39, 50, 75
Dry air at 150°C	5, 10, 15, 50

Table 4.1: Test procedure sequence for T_{ind} measurements.

For stress control tube aged in dry air at 98°C, T_{ind} results varies between 276,72°C and 274,61°C, accordingly for the less aged (12days) and the most aged (75 days) test samples. The difference of 2,11°C is small, but still an expected relationship between T_{ind} and aging period is observed as can be seen in Figure 4.7. When a polymeric material is subjected to thermal aging, antioxidants are gradually consumed with time, resulting in less thermal resistivity of the material, which means that the oxidation process starts at lower temperature.

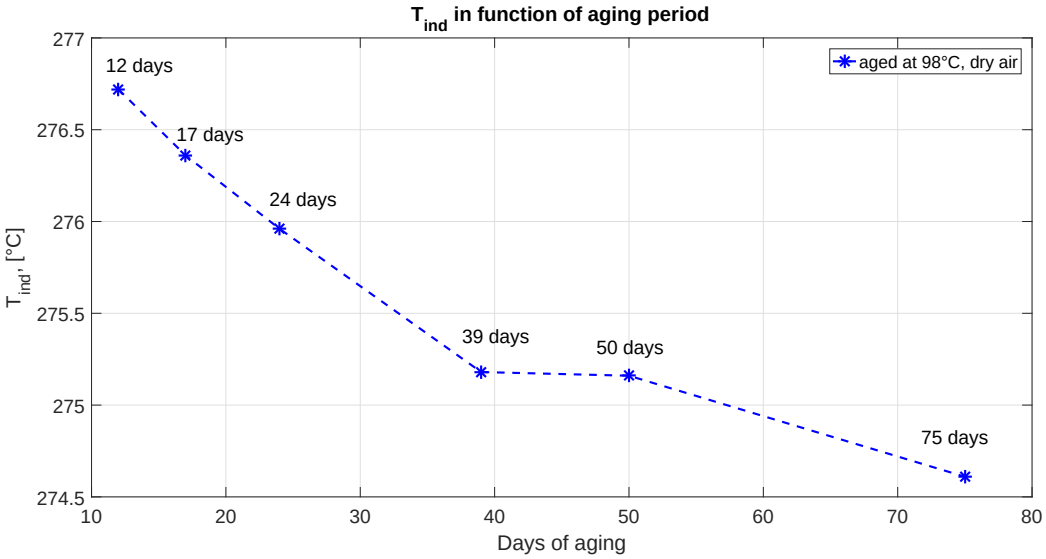

Figure 4.7: T_{ind} in function of time for SCT, aged in dry air at 98°C.

T_{ind} measurements for SCT, aged in wet air at 98°C are shown in Figure 4.8. They follow the same pattern and compared to the samples aged in dry air shows slightly lower oxidation induction temperatures as can be seen in Figure 4.9. This shows that presence of humidity has not very significant, but negative effect on the physical properties and thermal resistance of this type of SCT. Those measurements are confirmed by the tensile test results, where also a small difference between dry and wet aging conditions at the same temperature of 98°C is observed.

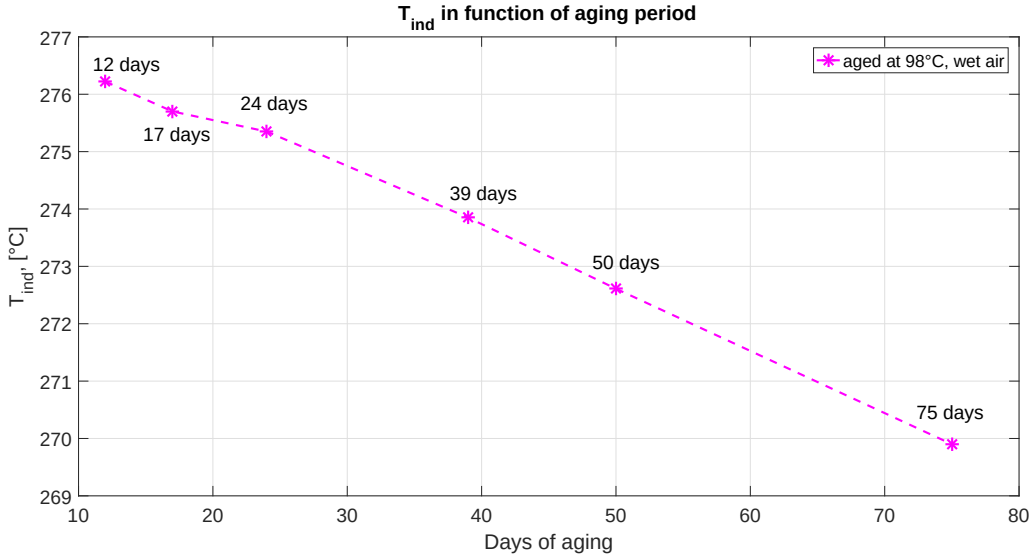

Figure 4.8: T_{ind} in function of time for SCT aged in wet air at 98°C.

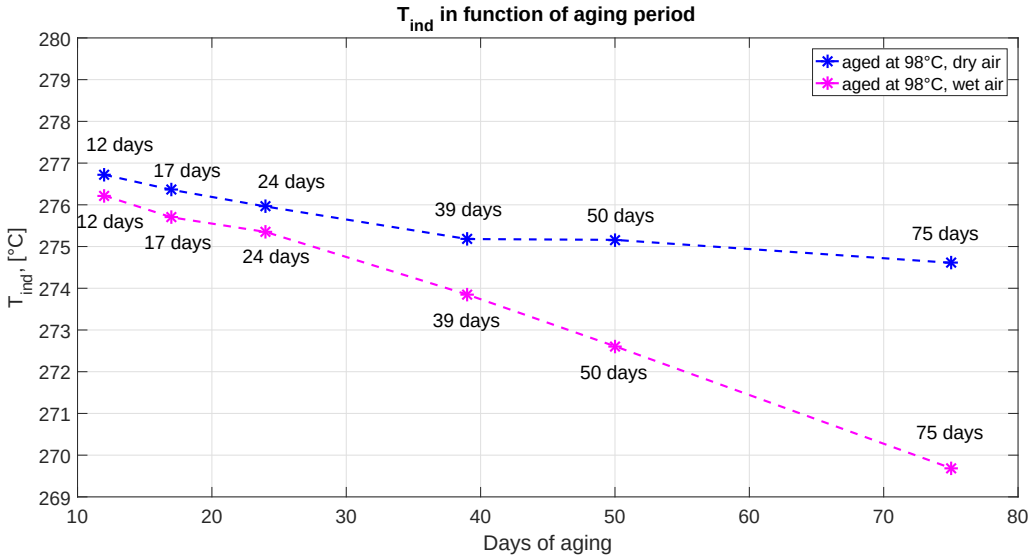

Figure 4.9: Comparison between T_{ind} for dry and wet aging conditions at 98°C.

As can be seen in Figure 4.10 and Figure 4.11 the results for SCT aged in dry air at 150°C show a significant decrease in T_{ind} of more than 35°C, compared to SCT aged at 98°C. This shows that aging at elevated temperatures above the melting point rapidly increase retarding mechanisms in material and antioxidant consumption. These results are in compliance with the tensile test measurements, which show a rapid decrease in mechanical properties of SCT aged at 150°C.

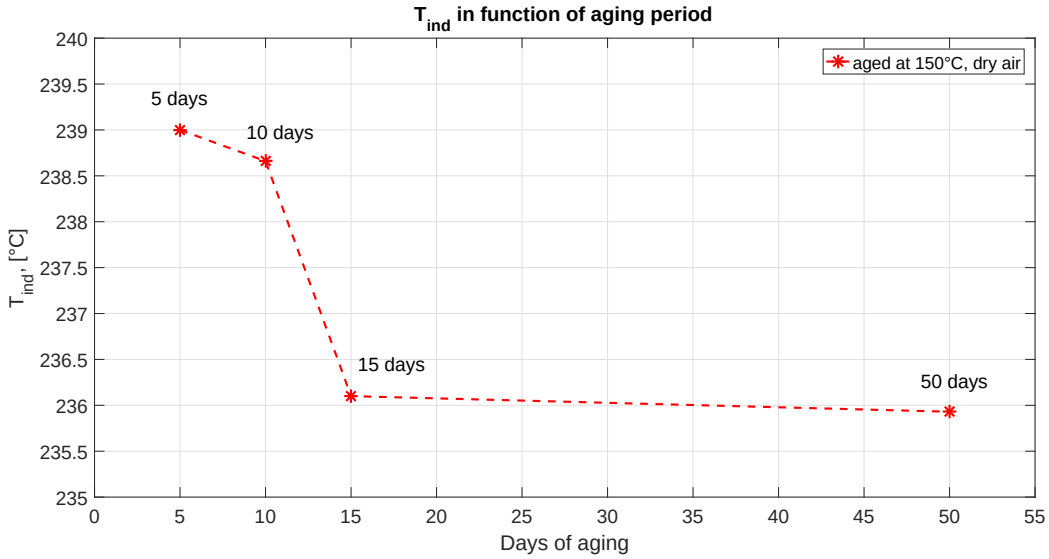

Figure 4.10: T_{ind} time dependency for SCT aged in dry air at 150°C.

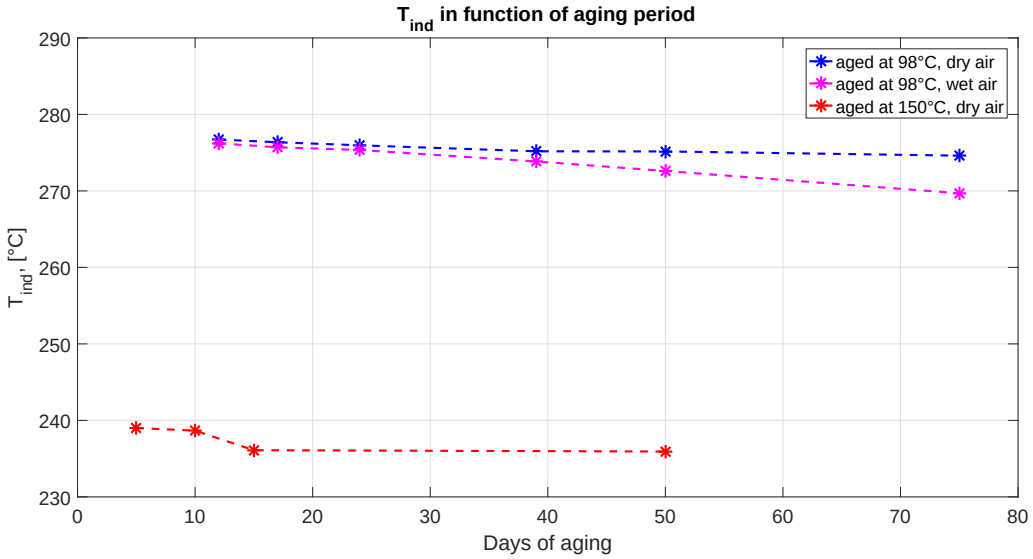

Figure 4.11: Comparison between T_{ind} for test objects aged in dry air at 98°C, wet air at 98°C and dry air at 150°C.

A direct comparison between extension at break and oxidation induction temperature is shown in Figure 4.12. Increased oxidation process (T_{ind} decreases) leads to deterioration of material mechanical properties as the effect rapidly increases when temperature is elevated to 150°C (above the melting point).

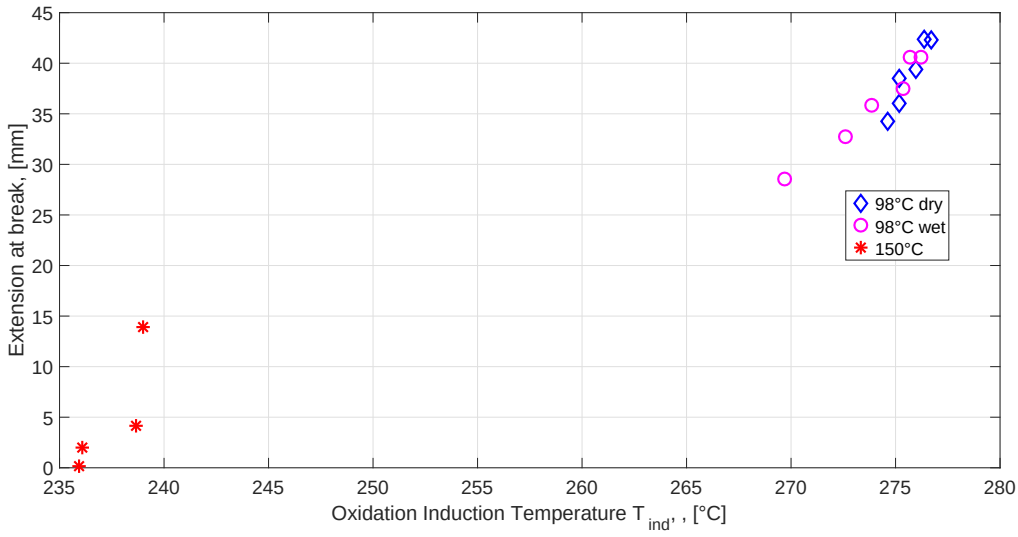

Figure 4.12: Extension at break in function of oxidation induction temperature T_{ind}.

4.3 Dielectric Response Measurements

4.3.1 Polarization and Depolarization Currents

Noise Measurements

Prior to each dielectric response test the noise was measured for a period of 900 seconds. The reason for doing that is the small magnitude of the measured values for polarization and depolarization currents in the range of 10^{-11} — 10^{-5}, which gives a high sensitivity to noise, especially for the lowest current measurements. A typical illustration for the noise amplitude is presented in Figure 4.13.

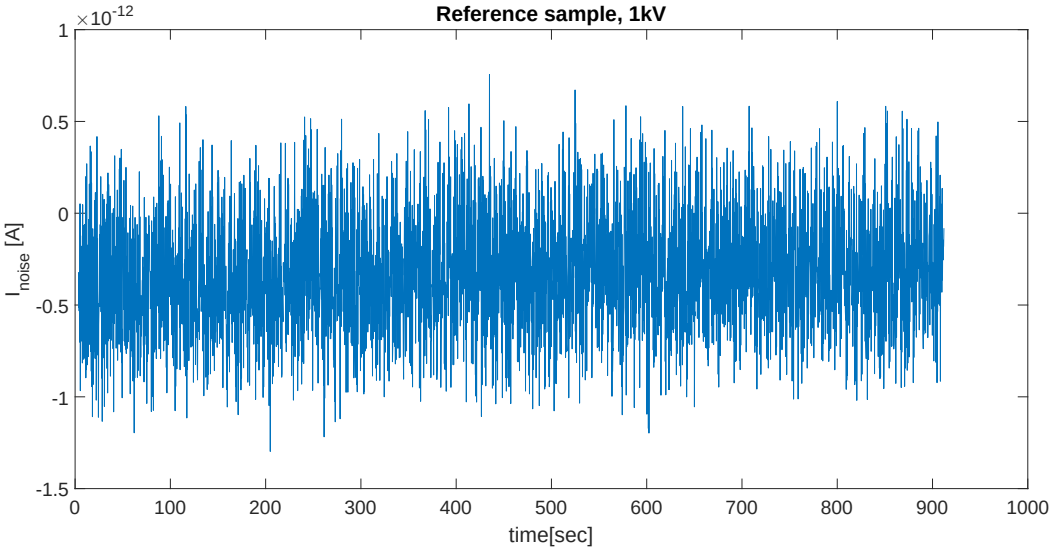

Figure 4.13: Noise measurement for a reference sample, tested at 1kV and 30°C.

The noise level is of magnitude less than $10^{-12}[A]$. Therefore, it is assumed that the noise impact on the dielectric response measurements can be neglected.

It is observed that polarization currents don't change significantly with time showing that the polarization is low compared to the conductive part of the currents.

Depolarization currents seems to follow Curie von Schweidler's law, $I_d \approx t^{-n}$ [18] and they are gradually decreasing. For a reference sample at lower test voltage and temperature after certain discharging time, depolarization currents became too low, challenging the measuring equipment and this resulted in an oscillating curve end, see Figure 4.14. With increased applied electric field and temperature, current values increases making measurement curves

more stable.

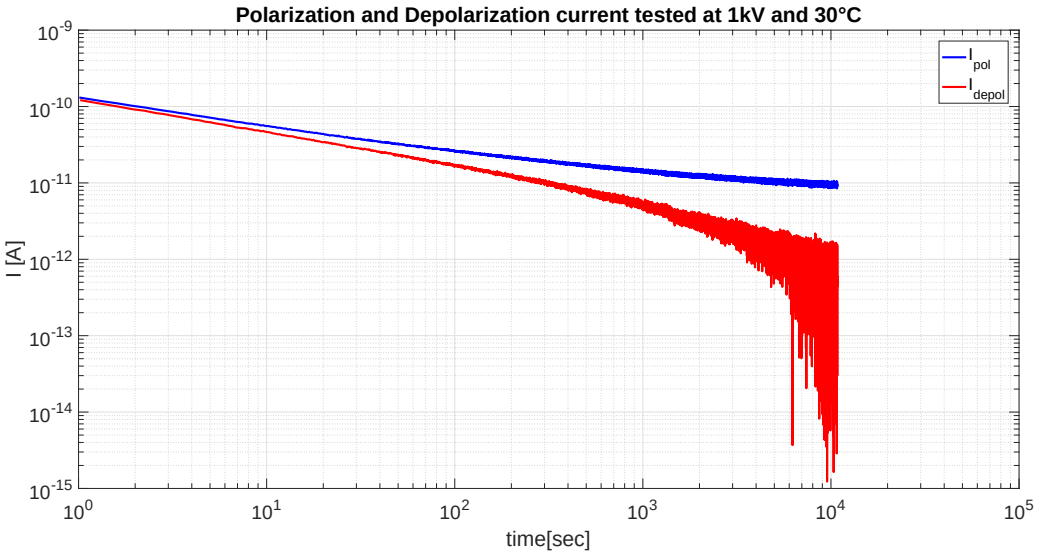

Figure 4.14: Polarization and depolarization current measurements done for a reference sample at 1 kV and 30°C.

Polarization and Depolarization Currents in function of applied electric field

As can be seen from the comparison between Figure 4.14 and Figure 4.15, when the test voltage is increased from 1kV to 20kV, the values of PDC also increase which shows a voltage dependency.

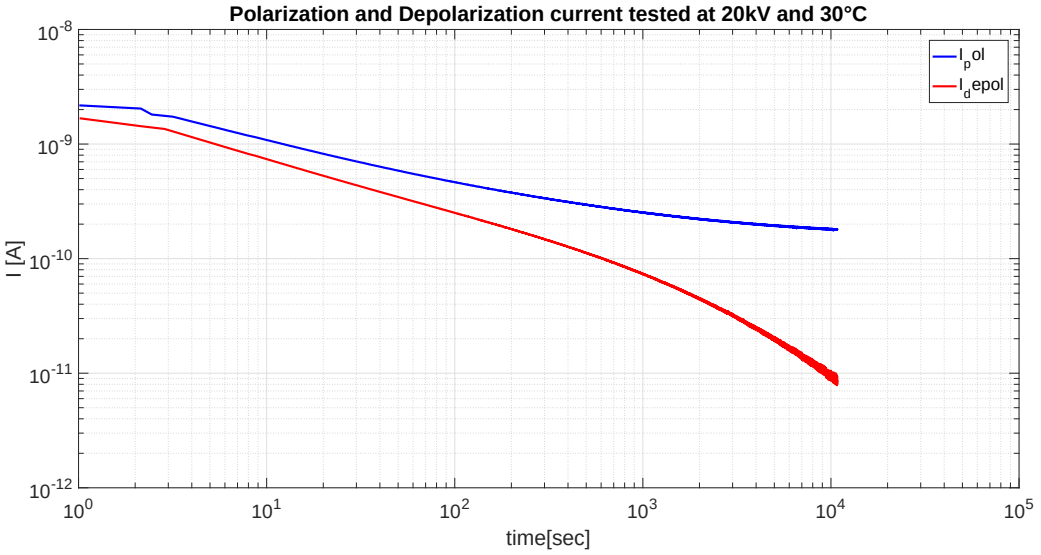

Figure 4.15: Polarization and depolarization current measurements done for a reference sample at 20 kV and 30°C.

Polarization and Depolarization Currents in function of test temperature

The results presented in Figure 4.14 and Figure 4.16 show that PDC are much more tempera-

ture than voltage dependent. When the test temperature is increased from 30°C to 150°C, the polarization current increases with approximately 3 decades. At this case, it is three times more than the case when the applied electric field is increased from the minimum to the maximum test level (from 0.01 kV/mm to 0.2 kV/mm). It is observed that at elevated temperature, the polarization currents reached a conductive steady state much earlier and even a slight increase at the end of the test period, Figure 4.16. This can be a result of a space charge build-up and material changes due to the high temperature and the relatively long testing time (3 hours). Tensile and DSC tests already confirmed that a temperature of 150°C can result in fast changes of the physical properties for SCT material.

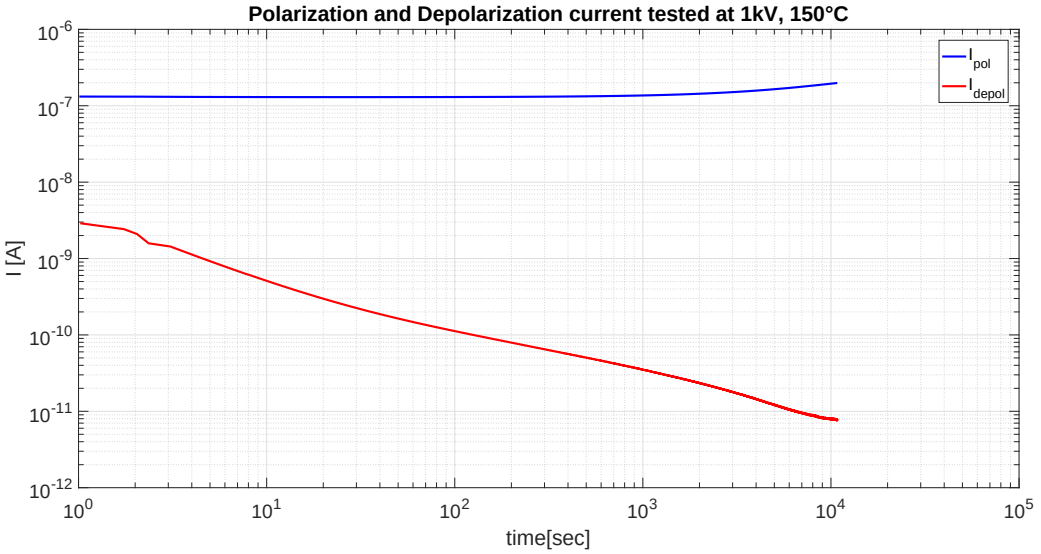

Figure 4.16: Polarization and depolarization current measurements done for a reference sample at 1 kV and 150°C.

Polarization and Depolarization Currents in function of aging degree

In Figure 4.17 and Figure 4.18, it is shown a comparison between PDC for a reference sample and one aged at 150°C for 15 days, as the tests were done at identical conditions. It can be observed that even for that short period of exposure to high temperature, an increase of one decade for currents is detected. Most likely, this increase is a result from overheating causing material oxidation.

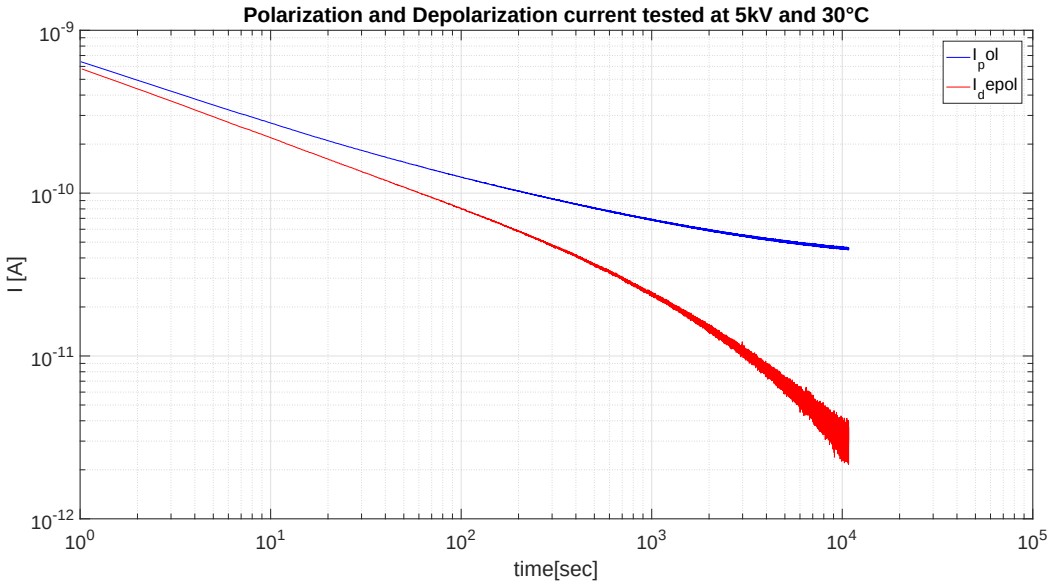

Figure 4.17: Polarization and depolarization current measurements done for a reference sample at 5 kV and 30°C.

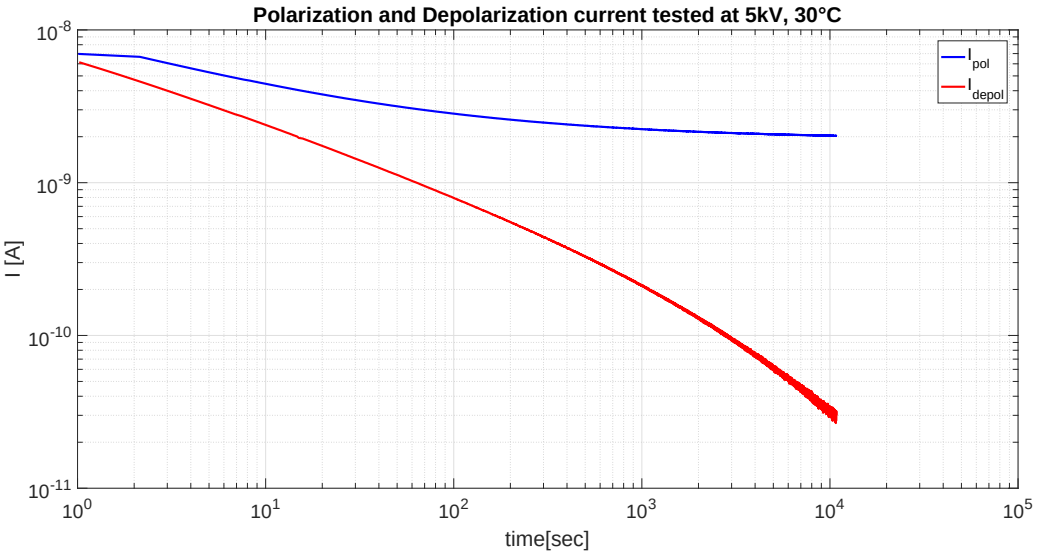

Figure 4.18: Polarization and depolarization current measurements done for a sample aged at 150°C for 15 days. Measurements done at 5 kV and 30°C.

Figure 4.19 shows that for an aged SCT material, depolarization currents are much less voltage dependent compared to polarization currents. This complies with the measurements done for real service aged cable joints, presented in [10]. A criterion for differentiating between service aged cable joint and heavily water tree degraded cables was proposed. It is based on nonlinear (voltage dependent) polarization currents and linear depolarization currents obtained for the cable joint, whereas the depolarization currents for water treed cables are expected to be much more voltage dependent.

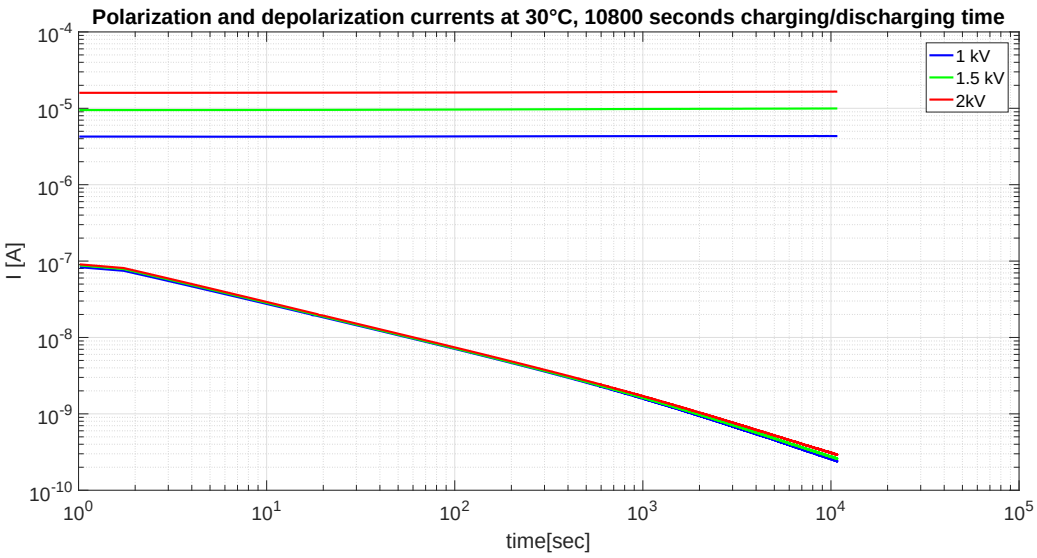

Figure 4.19: Polarization and depolarization current measurements done for a sample aged at 150°C for 50 days. Measurements are done at 30°C.

Additionally, it can be observed that polarization currents are much larger than the depolarization ones, even at low voltages and after short times of measurement. This is a sign for a large contribution from the stress control tube conductivity.

Polarization and Depolarization Currents in function of humidity

In Figure 4.20 measurement results for a reference sample and a sample subjected to water absorption are presented. It is observed that the moisture content in the SCT material gives an increase of more than a decade for the measured currents. That reveals that polarization and depolarization currents are strongly dependent on the humidity. It is also observed that depolarization currents for SCT with high moisture content has larger decay rate.

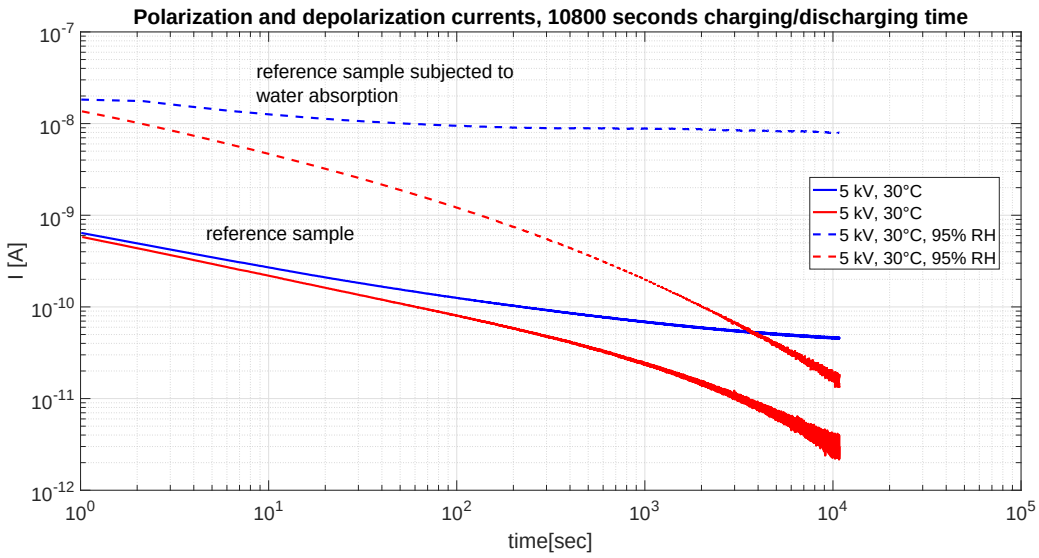

Figure 4.20: Polarization and depolarization currents for a reference sample (measurements done at 5 kV, 30°C and 0% of relative humidity) and a reference sample, subjected to water absorption at 90°C for 30 days (measurements done at 5 kV, 30°C and 95% of relative humidity) .

Polarization and Depolarization Currents in function of aging degree and humidity

Measurements show that the highest rise of polarization and depolarization current values is obtained when aging is combined with high moisture content in the SCT material. Results for a sample, which was thermally aged and then subjected to water absorption are shown in Figure 4.21. Here, a similar effect showing linearity of depolarization currents (currents are relatively independent of voltage) is observed, as for the highly thermally aged sample in Figure 4.19. Once again, the difference between polarization and depolarization currents is sufficient, showing high conductivity contribution. Low resistance (high conductivity) of SCT material is strongly dependent on moisture content, especially for aged material. Those results also complies with the observations done for real service aged cable joints in [10].

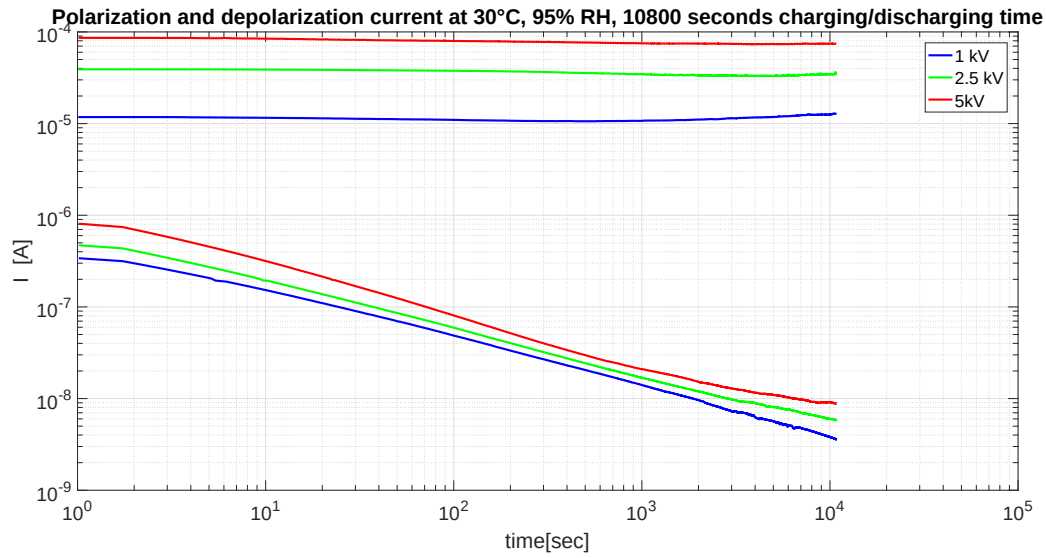

Figure 4.21: Polarization and depolarization current measurements done for a sample aged at 150°C for 15 days and additionally subjected to high humidity for 30 days at 90°C. Measurements done at 1, 2.5, 5 kV and 30°C.

Polarization Currents Hysteresis Effect

Dielectric response measurements were performed at 30°C, 90°C and 150°C and after that repeated at 30°C. As can be seen in Figure 4.22, the polarization current measured at the second time at 30°C is slightly higher than the first run of the test at the same temperature. A possible reason for that could be the desorption of volatiles from the stress control tube during the 150°C tests leading to increasing material conductivity. It could be also explained with a changed semi-crystalline content of the SCT material when cooled from 150°C to 30°C.

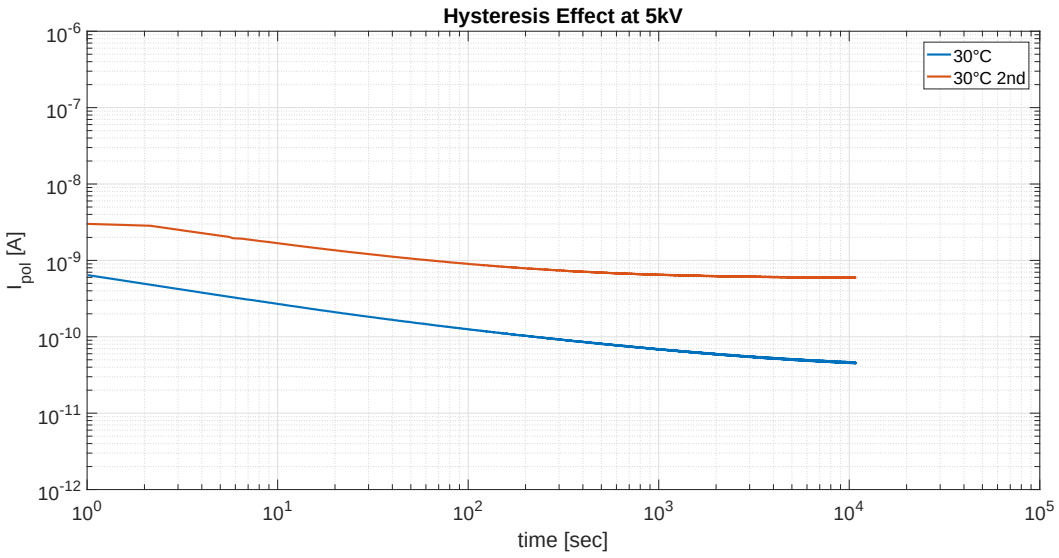

Figure 4.22: Hysteresis effect measurements done for a reference sample at 5 kV and 30°C.

4.3.2 Conductivity Results

Conductivity is relatively electric field independent up to 0,2 kV for a reference (unaged) stress control tube and low temperatures as can be seen in Figure 4.23.

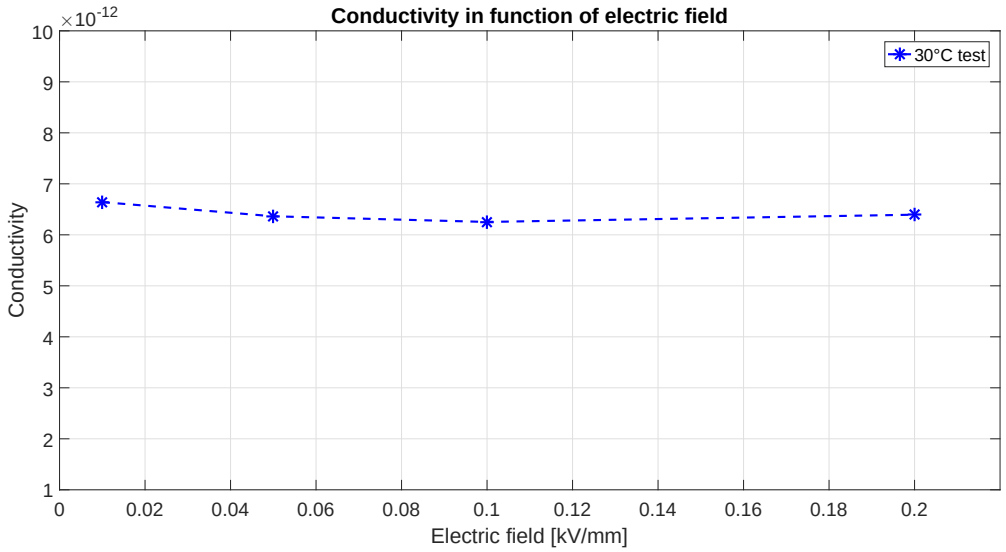

Figure 4.23: Conductivity measurements done for a reference sample at 30°C test temperature.

Conductivity Hysteresis Effect

After execution of measurements at 150°C and repeating them, when the test sample cools down to 30°C, a hysteresis effect of the conductivity is observed. Basically, this is the same hysteresis phenomena shown in Figure 4.22.

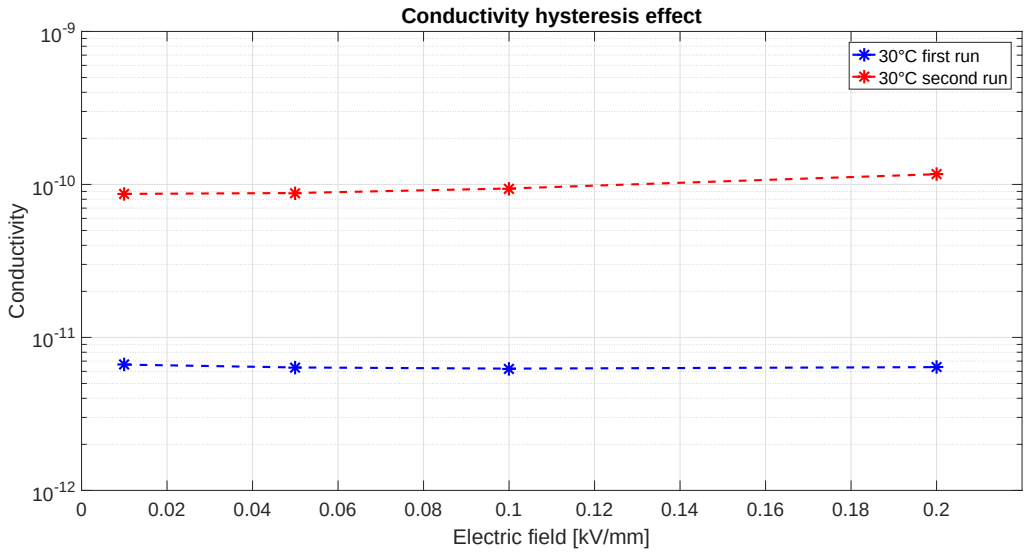

Figure 4.24: Conductivity hysteresis effect for a reference sample.

Conductivity in function of test temperature

The conductivity of a stress control tube should be at least 100 times higher than the cable and joint insulation in order local field enhancements to be prevented [8]. On the other hand, there is a limit for the highest conductivity value due to the fact that increased conductivity leads to bigger current flowing through the stress control tube to ground, resulting in increased ohmic losses.

The results in Figure 4.25, Figure 4.26 and Figure 4.27 show that conductivity clearly increases with increasing temperature. If conductivity values becomes too high, SCT will be subjected to substantial Joule heating. Additionally, high temperature exposure causes, with time, thermal aging represented by the oxidation of the SCT material. As can be seen in Figure 4.25, Figure 4.26 and Figure 4.27, higher aging degree of the material causes larger conductivity values.

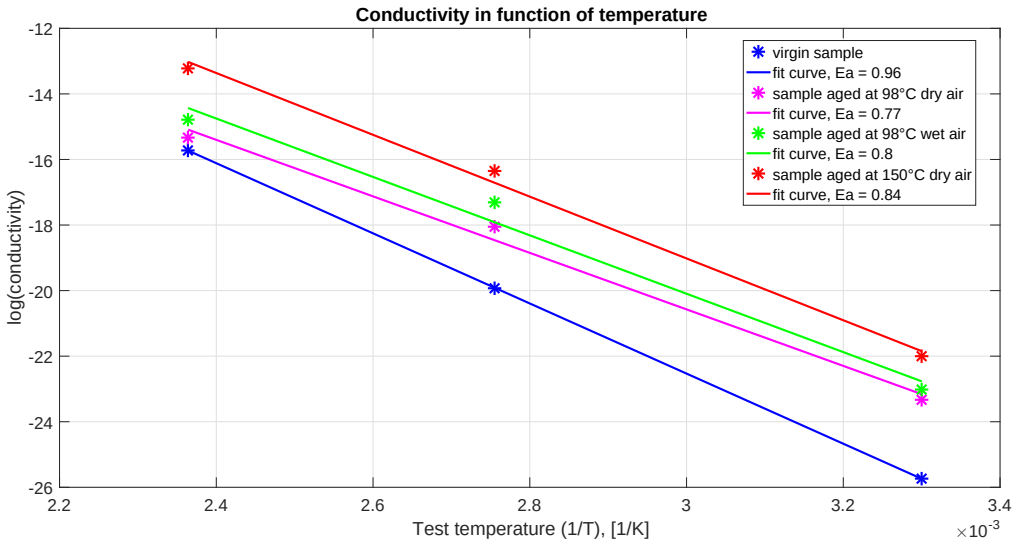

Figure 4.25: Conductivity in function of test temperature at 1 kV. Comparison is made for 1) reference sample 2) sample aged at 98°C dry air for 50 days 3) sample aged at 98°C wet air for 50 days and 4) sample aged at 150°C dry air for 15 days. Activation energy E_a [eV] results are presented.

With time, SCT material exposed to high temperatures experiences higher oxidation level, accelerating the aging. Higher aging makes the material conductivity less dependent on temperature, keeping relatively constant high values. An example is given with conductivity curves (red lines) for SCT sample aged at 150°C for 15 days (Figure 4.25) and 50 days (Figure 4.26).

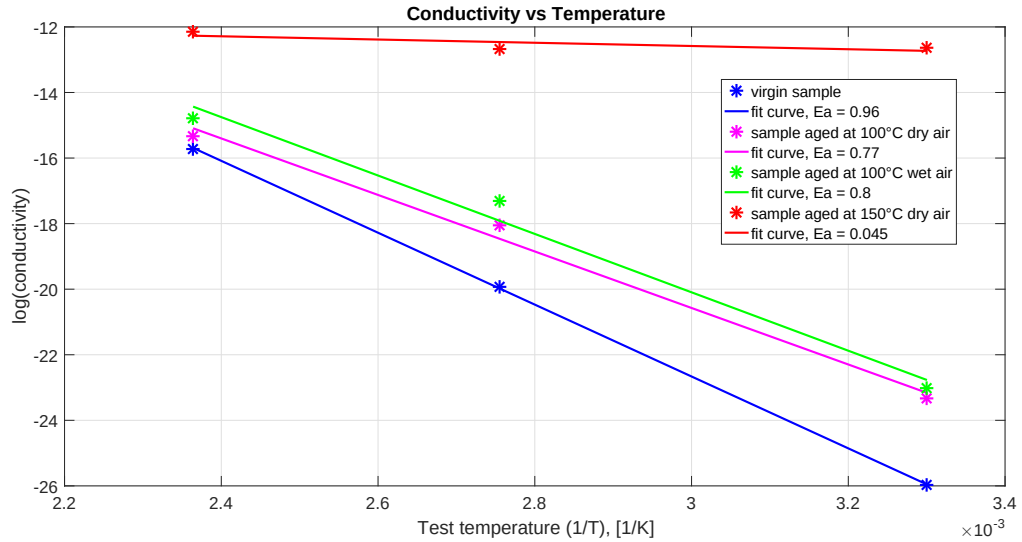

Figure 4.26: Conductivity in function of test temperature at 1 kV. Comparison is made for 1) reference sample 2) sample aged at 98°C dry air for 50 days 3) sample aged at 98°C wet air for 50 days and 4) sample aged at 150°C dry air for 50 days. Activation energy E_a [eV] results are presented.

Conductivity in function of aging conditions, test temperature and applied field

While both oxidation level and operating temperature significantly affects the conductivity, the latter stays relatively constant in function of applied electric field (up to 0,2 kV/mm) as it is shown in Figure 4.27.

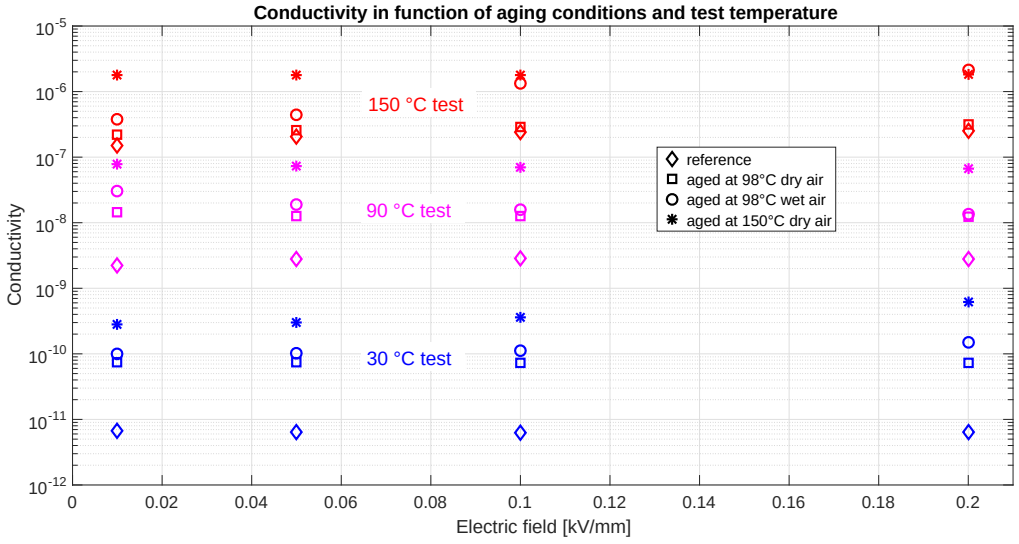

Figure 4.27: Conductivity in function of aging conditions and test temperature. Comparison is made for 1) reference sample 2) sample aged at 98°C dry air for 50 days 3) sample aged at 98°C wet air for 50 days and 4) sample aged at 150°C dry air for 15 days.

In Figure 4.28 conductivity results for samples exposed to all aging conditions are presented as they aged for one and the same period of 50 days. The test voltages for the sample aged

at 150°C dry air conditions were limited to 1, 1.5 and 2 kV due to high polarization currents at higher fields, reaching the limit of the measuring setup. Here, clearly can be seen that SCT aged at high temperatures of 150°C larger than the melting point has significantly higher conductivity than SCT exposed to temperature of 98°C below the melting point, even at lower electric fields. Also that higher conductivity values are found to be much less temperature dependent.

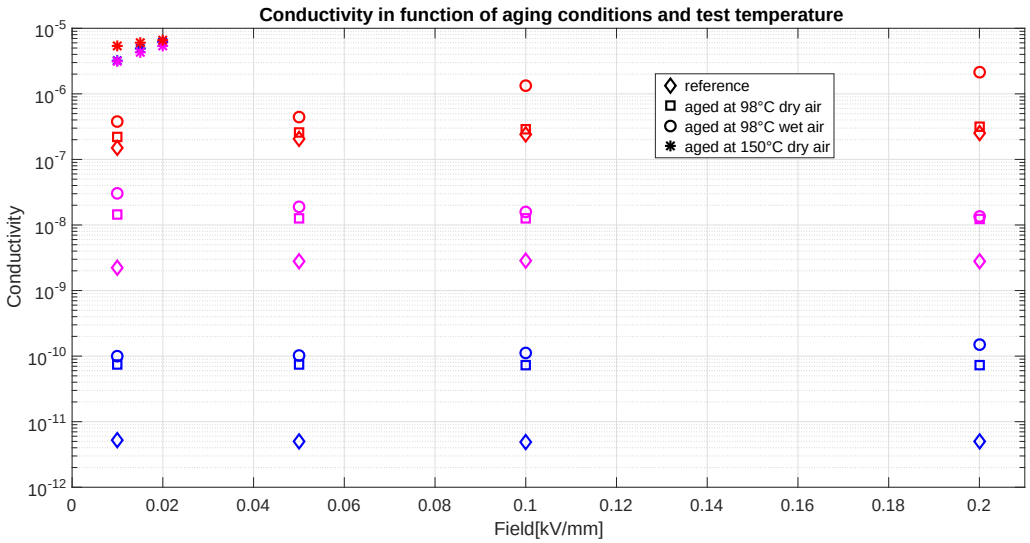

Figure 4.28: Conductivity in function of aging conditions and test temperature. Measurements done for test objects aged at 98°C dry air, 98°C wet air and 150°C dry air. All samples are aged for a period of 50 days.

In Figure 4.28 conductivity results for SCT aged at 98°C dry air and 98°C wet air for 50 days are very close. It is not the case when the aging period for that conditions is continued to 75 days, Figure 4.29. Samples aged in high humidity environment shows higher conductivity values with time.

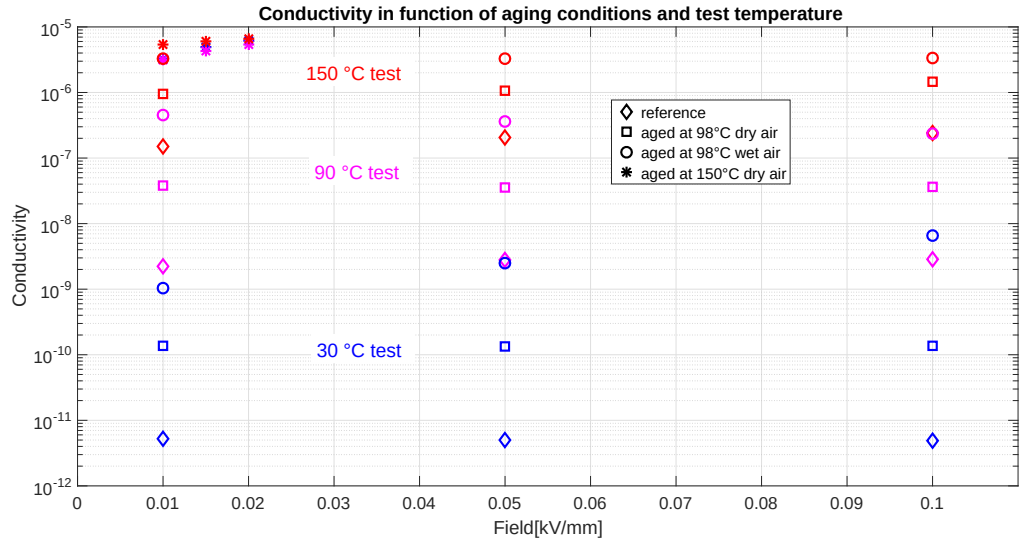

Figure 4.29: Conductivity in function of aging conditions and test temperature. Comparison is made for 1) reference sample 2) sample aged at 98°C dry air for 75 days 3) sample aged at 98°C wet air for 75 days and 4) sample aged at 150°C dry air for 50 days.

Conductivity in function of oxidation induction temperature

As presented in Figure 4.28, it was shown that aging conditions can have significant influence on SCT conductivity. Metallic connector faults, found in the medium voltage cable joints can increase the temperatures to 150°C. Exposed to such a temperature, SCT deteriorates faster and obtains a rapid increase in the conductivity. In Figure 4.30, it is shown that such SCT not only has much larger conductivity, but also much lower physical and mechanical properties, represented by the lower oxidation induction temperature of the material T_{ind}.

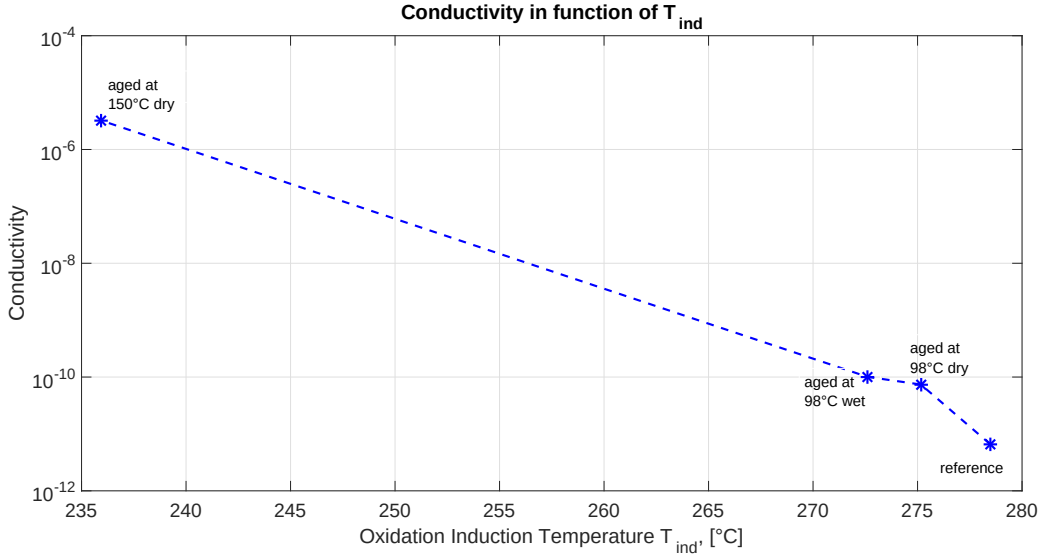

Figure 4.30: Conductivity in function of T_{ind} for test objects aged at 98°C dry air, 98°C wet air and 150°C dry air. All samples are aged for a period of 50 days. Dielectric response tests are performed at 1 kV and 30°C.

In addition to temperature and thermal aging, another factor that most likely can contribute to the conductivity increase is the absorbed by the SCT moisture. A reference sample and an aged one were subjected to moisture absorption at 90°C for 30 days and then tested in a climate chamber maintaining 30°C and 95% RH.

In Figure 4.31, conductivity results are presented in function of oxidation induction temperature for dry samples (blue line) and those subjected to water absorption (red line). As it was explained before lower T_{ind} represents higher aging degree. It is observed that absorbed moisture significantly increases conductivity. A special attention should be given to the case when water absorption is combined with thermal aging, which results in very rapid conductivity increase. In this case, values of 6 decades higher, compared to those of a dry reference sample are observed.

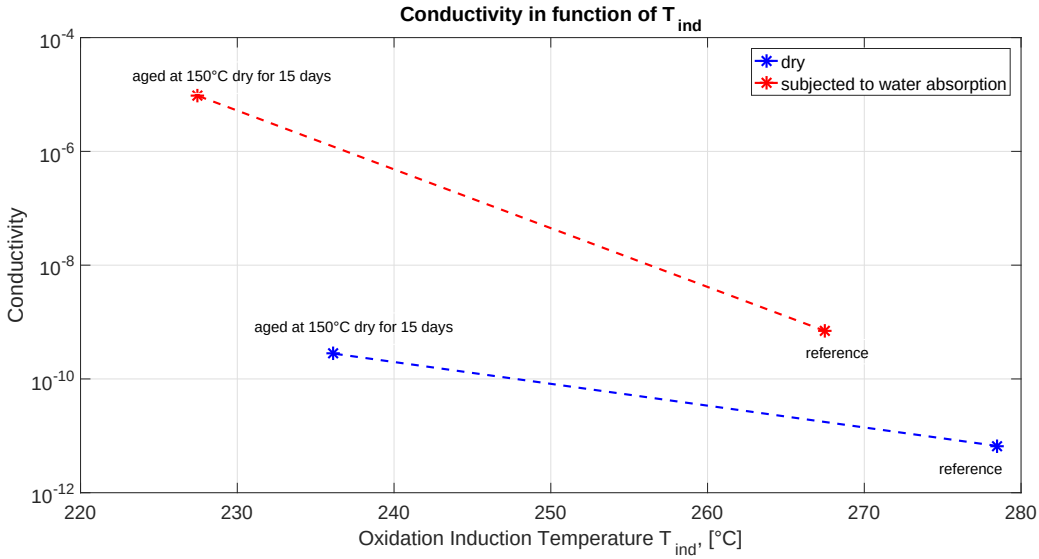

Figure 4.31: Conductivity in function of T_{ind}.

Figure 4.32 shows conductivity in function of oxidation induction temperature for different aging conditions and periods. As can be seen, when the temperature at which SCT is exposed increases, the oxidation of the material increases too (T_{ind} decreases) and correspondigly conductivity values are also rising. Moreover, the effect of humidity presence during aging is clearly visible as the resulting conductivity is significantly higher compared to a SCT which is thermally aged in dry environment.

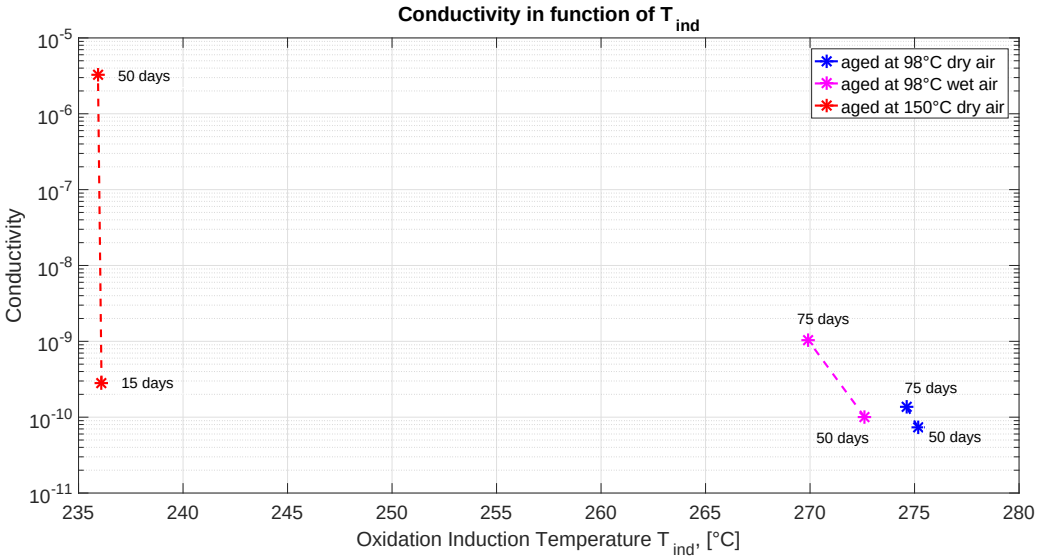

Figure 4.32: Conductivity in function of T_{ind} for 1) SCT aged at 98°C dry air for 50 and 75 days, 2) 98°C wet air for 50 and 75 days, 3) SCT aged at 150°C dry air for 15 and 50 days.

Dielectric Response Function Results

Dielectric response function is found to be temperature dependent as can be seen in Figure 4.33. Temperature dependency for a reference sample and a sample, aged at 150°C is slightly higher than those aged at 98°C.

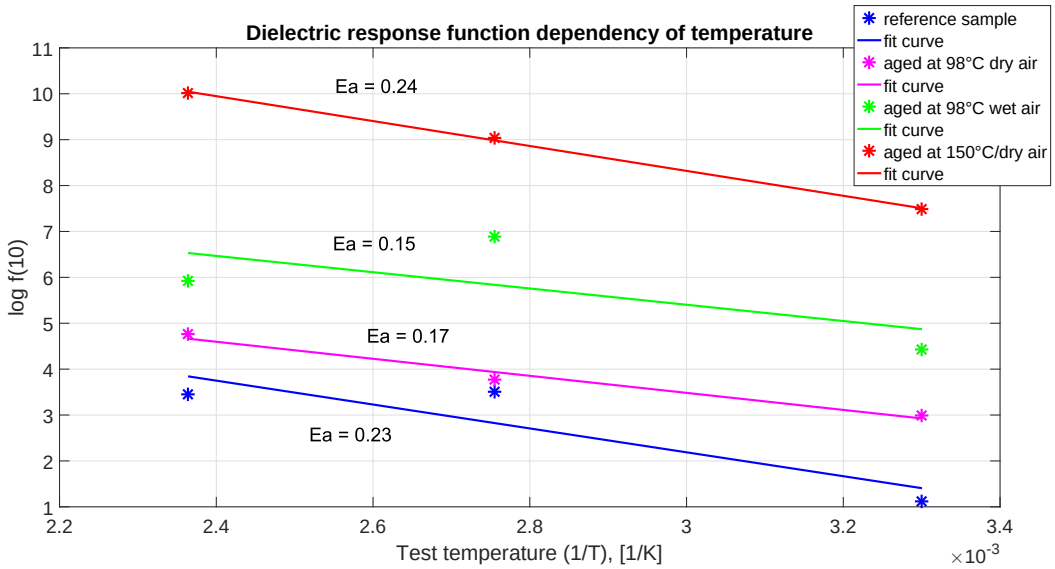

Figure 4.33: Response function and test temperature dependency. Tests are done at 1 kV and 30°C. Comparison is made for 1) reference sample 2) sample aged at 98°C dry air for 75 days 3) sample aged at 98°C wet air for 75 days and 4) sample aged at 150°C dry air for 50 days. Activation energy E_a [eV] results are presented.

When dielectric response function is presented in relation with oxidation induction temperature, a similar pattern observed in the conductivity is revealed, see Figure 4.34. Response

function is increasing with the material oxidation and maximum values are obtained, when further a moisture content is present in the already aged SCT.

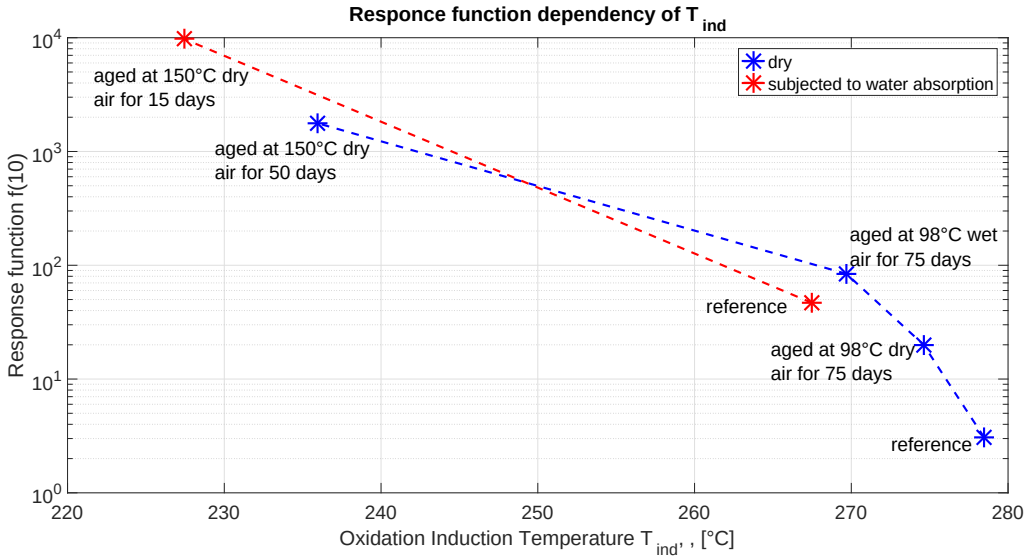

Figure 4.34: Dielectric response function dependency of T_{ind}. Comparison is made for 1) reference sample, 2) sample aged at 98°C dry air for 75 days, 3) sample aged at 98°C wet air for 75 days, 4) sample aged at 150°C dry air for 50 days, 5) reference sample subjected to water absorption, 6) sample aged at 150°C dry air for 15 days and after that subjected to water absorption.

Chapter 5

Conclusion

Measurement results show that polarization currents for stress control tube Raychem JSCR 42/16 strongly depend on temperature and oxidation degree (thermal aging level) of the material. An increase of 6 decades is observed for a material subjected to thermal aging and water absorption, compared to an unaged stress control tube.

Depolarization currents for highly aged stress control tube samples become voltage independent. This can be used as a criterion to differentiate service aged cable joint from a heavily water tree degraded cable insulation, as for the letter much more voltage dependency is expected for the depolarization currents.

From experimental work in the laboratory, it is found that the conductivity of the stress control tube is strongly temperature dependent, as the conductivity becomes larger when the temperature increases. For unaged SCT samples, the conductivity increases with around 4 decades when the temperature is elevated from 30°C to 150°C, while the rise for moderately aged samples (aged at 98°C dry and wet air for 50 days) is more than 3 decades for the same temperature interval. Heavily thermally aged SCT samples (aged at 150°C for 50 days), characterized by large embrittlement and total loss of mechanical properties (extension at break = 0.1 mm) show much less temperature dependency (less than an order for 30°C—150°C interval), but keep higher conductivity increase, which can reach more than 5 decades, compared to unaged SCT, measured at 30°C.

No significant field dependence is observed for up to 0.2 kV and all test temperatures.

The stress control tube does not experience complete reversible change from more conductive to resistive state. After being subjected to a temperature of 150°C, the conductivity of the tested material increases, which reveals that the electrical properties of the stress control tube are prone to changes after the field grading material is exposed to high temperatures for short times of around a day. For that time period the conductivity can obtain an increase of 1 decade.

Thermal aging degree of the stress control tube affects the conductivity proportionally. Elevating the temperature, at which the material ages, leads to increased oxidation, providing higher conductivity. A rapid increase is observed when temperatures are as high as 150°C. Measurements show a difference of 3 decades in conductivity results in favor of SCT samples aged at 150°C, compared to those aged at 98°C (wet and dry air), all of them aged for the same time period of 50 days.

Measurement results show that during aging, with time, the conductivity of the stress control tube increases. Conductivity and rate of aging are strongly dependent on the temperature at which the material is exposed. For SCT samples aged at 150°C (dry air), the conductivity increase rate is more than 3 times higher than for the SCT samples aged at 98°C (dry and wet air). Presence of humid environment during thermal aging also has significant impact on the conductivity rise. At the end of aging period (day 75) for SCT samples aged at 98°C, the conductivity for those objects, exposed to wet air show values higher with 1 decade, compared to those aged in dry air.

Test reveals that water content in SCT material leads to significant conductivity rise. Two decades higher values are observed for an unaged SCT sample subjected to water absorption, compared to a dry unaged one. Therefore, it can be concluded that conductivity is strongly dependent on humidity level of cable joint environment and moisture absorbed by SCT.

The highest conductivity increase of around six decades is observed when a significant level of thermal aging is combined with high humidity presence. Currents, corresponding to such a high magnitude of increase can cause critical changes, such as increased heat generation that can cause a thermal breakdown of the material. If the stress control tube has not sufficient contact or fails to cover parts of the cable system, the conductivity increase can lead to dangerous field concentration at the edge of the tube, which can result in a breakdown.

Experimental work done during this master thesis along with the obtained results show that there is a high probability that low resistance (high conductivity) of cable sections, detected during on-site test diagnostics is due to service aged cable joints, subjected to overheating and humidity. If this is the case, repairing of a cable joint is much cheaper than changing a cable, which will lead to a considerable cost and time reduction for maintenance activities.

Time based dielectric response analysis is proven as an easy to apply and reliable enough initial diagnostic method, which can be applied for on-site and laboratory testing of cable

sections which includes heat-shrink cable joints.

Results obtained during this master project will contribute to the data-base of SINTEF Energy Research and help in developing a relatively simple method for initial diagnostic testing of cable sections, involving a commercially available insulation tester and specialized software package for analysis.

Chapter 6

Further Work

This master thesis examined the physical, mechanical and electrical properties of stress control tube material aged at temperatures of 98°C and 150°C. Tests revealed large difference between the results for these two temperature levels. It will be feasible to investigate how physical and electrical properties changes at temperatures in between the range of 98°C—150°C.

The results shows that the conductivity is relatively independent of the applied electric field for values up to 0.2 kV/mm. Further investigation can be done at higher electrical fields. The dielectric response measurement setup can be modified to provide higher test voltage or a shorter test object can be used in order to increase the applied field.

Further investigation how humidity affects conductivity can be done. In this master project a reference (unaged) and a test sample aged at 150°C for 15 days were subjected to water absorption. It is of interest that test objects with different aging degree are exposed to high humidity, in order to investigate how conductivity changes at different aging degrees, combined with moisture presence in the stress control tube material.

Bibliography

[1] Cable accessories for up to 245 kv raychem technology brochure, te connectivity.

[2] Heat shrink raychem technology brochure, te connectivity.

[3] Iec 60811-1-1 common test methods for insulating and sheathing materials of electric cables and optical cables.2001-07.

[4] Low current measurements - application note series, number 1671. [online - accessed 05.05.2017].

[5] Modulated and pressure dsc services [online].

[6] *Compendium ELK-30 Condition Assessment of High Voltage Components*. NTNU, 2016.

[7] William Callister. *Fundamentals of Materials Science and Engineering, Fifth Edition*. John Wiley & Sons, Inc., 2001.

[8] T. Christen, L. Donzel, and F. Greuter. Nonlinear resistive electric field grading part 1: Theory and simulation. *IEEE Electrical Insulation Magazine*, 26(6):47–59, November 2010.

[9] Eric David. Aging of polymeric materials: principles. Technical report, Universite du Quebec, Mechanical engineering department.

[10] Henrik Enoksen, Espen Eberg, Sverre Hvidsten, Ole Hatlen, and Eva Rognsvaag. Condition assessment of xlpe mv cable joints by using an insulation tester. *23rd International Conference on Electricity Distribution*, 2015.

[11] Henrik Enoksen, Sverre Hvidsten, Mai-Linn Sanden, and Frank Mauseth. Temperature and electric field dependence of the time domain dielectric response of a medium voltage cable joint stress control sleeve. 2015.

[12] Wolfgang Grellman. *Polymer Testing*. Carl Hanser Verlag, 2007.

[13] S. Hvidsten, M. Vandbakk, and F. Mauseth. Dielectric properties of organic contaminations in xlpe cable insulation. *2012 Annual Report Conference on Electrical Insulation and Dielectric Phenomena*, 2012.

[14] Ontario Hydro, L.A. Gonzalez, E.M. Lehockey, and Canadian Electricity Association. Research & Development. *Long Term Reliability of Polymer Cables at High Temperatures*. Research report (Canadian Electricity Association). Canadian Electricity Association, 1997.

[15] Erlig Ildstad. Tet 4195 high voltage equipment - cable technology, ntnu.

[16] Erlig Ildstad. Tet 4160 insulating materials for high voltage applications, ntnu, 2016.

[17] Erling Ildstad. High voltage insulation materials. *TET4160, NTNU*, 2012.

[18] A. K. Jonscher. *Dielectric Relaxation in Solids*. Chelsea Dielectric Press, London, United Kingdom 46, 1983.

[19] Eva Mårtensson. *Modelling electrical properties of composite materials*. PhD thesis, KTH, Electrical Systems, 2003. NR 20140805.

[20] L. R. Mason and A. B. Reynolds. Comparison of oxidation induction time measurements with values derived from oxidation induction temperature measurements for epdm and xlpe polymers. *Polymer Engineering & Science*, 38(7):1149–1153, 1998.

[21] F. Mauseth, H. L. Halvorson, and S. Hvidsten. Diagnostic testing of thermally aged medium voltage xlpe cable joints. *2012 Annual Report Conference on Electrical Insulation and Dielectric Phenomena*, 2012.

[22] A. S. Maxwell, W.R. Broughton, G. Dean, and G. D. Sims. Npl report depc mpr 016, review of accelerated ageing methods and lifetime prediction techniques for polymeric materials. Technical report, National Physical Laboratory, United Kingdom, March 2005.

[23] Hans Kristian Hygen Meyer. Development of test methods for a combined dc power and fiber optic deep water subsea cable - effect of dc pre-stress on ac withstand strength. Master's thesis, Department of Electric Power Engineering, Norwegian University of Science and Technology, 2015.

[24] Alan T. Riga and Gerald H. Patterson, editors. *Oxidative Behavior of Materials by Thermal Analytical Techniques*. ASTM, 1997.

[25] Margaret Roylance and David Roylance. *ENVIRONMENTAL DEGRADATION OF ADVANCED AND TRADITIONAL ENGINEERING MATERIALS*, chapter Chapter 14. Forms of Polymer Degradation: Overview.

[26] M.D.A. Saldana and S.I. Martinez-Monteagudo. Oxidative stability of fats and oils measured by differential scanning calorimetry for food and industrial applications. In Amal Ali Elkordy, editor, *Applications of Calorimetry in a Wide Context - Differential Scanning Calorimetry, Isothermal Titration Calorimetry and Microcalorimetry*, chapter 19. InTech, Rijeka, 2013.

[27] Mai-Linn Sanden. Condition assessment of medium voltage cable joints - dielectric spectroscopy of field grading materials. Master's thesis, NTNU, 2015.

[28] C. Stancu, P. V. Notingher, and L. V. Badicu. Dielectric response function for nonhomogeneous insulations. *Electrical Insulation and Dielectric Phenomena (CEIDP), 2011 Annual Report Conference on 2011*, 2011.

[29] W. Steinmann, S. Walter, M. Beckers, G. Seide, and T. Gries. *Thermal Analysis of Phase Transitions and Crystallization in Polymeric Fibers, Applications of Calorimetry in a Wide Context - Differential Scanning Calorimetry, Isothermal Titration Calorimetry and Microcalorimetry*, chapter 12. InTech, 2013.

Appendix A

Results

A.1 Tensile Test

Detailed results from Tensile test are presented in Tables A.1, A.2, A.3, A.4.

Reference Sample			
Unaged	Maximum	Minimum	Mean
Extension at Break [mm]	58.075	49.609	53.266
Percentage Strain at Break [%]	290.37	248.05	266.33

Table A.1: Tensile test results for a reference SCT test object.

Sample aged at 98°C dry air			
aged for 12 days	Maximum	Minimum	Mean
Extension at Break [mm]	44.66	41.123	42.289
Percentage Strain at Break [%]	223.33	205.61	211.44
aged for 17 days	Maximum	Minimum	Mean
Extension at Break [mm]	45.478	39.592	42.348
Percentage Strain at Break [%]	227.39	197.96	211.74
aged for 24 days	Maximum	Minimum	Mean
Extension at Break [mm]	44.361	37.770	39.414
Percentage Strain at Break [%]	221.81	188.85	197.07
aged for 39 days	Maximum	Minimum	Mean
Extension at Break [mm]	41.762	36.211	38.512
Percentage Strain at Break [%]	208.81	181.06	192.56
aged for 50 days	Maximum	Minimum	Mean
Extension at Break [mm]	37.511	33.496	36.026
Percentage Strain at Break [%]	187.55	167.48	180.13
aged for 75 days	Maximum	Minimum	Mean

Extension at Break [mm]	36.786	31.121	34.274
Percentage Strain at Break [%]	183.93	155.60	171.37

Table A.2: Tensile test results for a SCT test object aged at 98°C dry air.

Sample aged at 98°C wet air			
aged for 12 days	Maximum	Minimum	Mean
Extension at Break [mm]	42.493	38.445	40.621
Percentage Strain at Break [%]	212.47	192.23	203.11
aged for 17 days	Maximum	Minimum	Mean
Extension at Break [mm]	41.987	38.702	40.602
Percentage Strain at Break [%]	209.94	193.51	203.01
aged for 24 days	Maximum	Minimum	Mean
Extension at Break [mm]	37.959	36.556	37.464
Percentage Strain at Break [%]	189.80	182.78	187.08
aged for 39 days	Maximum	Minimum	Mean
Extension at Break [mm]	38.736	30.662	35.810
Percentage Strain at Break [%]	193.68	153.31	179.05
aged for 50 days	Maximum	Minimum	Mean
Extension at Break [mm]	33.646	31.936	32.713
Percentage Strain at Break [%]	168.23	159.68	163.57
aged for 75 days	Maximum	Minimum	Mean
Extension at Break [mm]	29.765	25.953	28.537
Percentage Strain at Break [%]	148.83	129.77	142.68

Table A.3: Tensile test results for a SCT test object aged at 98°C wet air.

Sample aged at 150°C dry air			
aged for 5 days	Maximum	Minimum	Mean
Extension at Break [mm]	15.414	11.885	13.894
Percentage Strain at Break [%]	77.068	59.423	69.472
aged for 10 days	Maximum	Minimum	Mean
Extension at Break [mm]	4.9717	3.3185	4.1451

Percentage Strain at Break [%]	24.859	16.592	20.725
aged for 15 days	Maximum	Minimum	Mean
Extension at Break [mm]	2.4624	1.5549	1.9889
Percentage Strain at Break [%]	12.312	7.7743	9.9447
aged for 50 days	Maximum	Minimum	Mean
Extension at Break [mm]	0.13586	0.13586	0.13586
Percentage Strain at Break [%]	0.67930	0.67930	0.67930

Table A.4: Tensile test results for a SCT test object aged at 150°C dry air.

A.2 Differential Scanning Calorimetry

Oxidation Induction Time

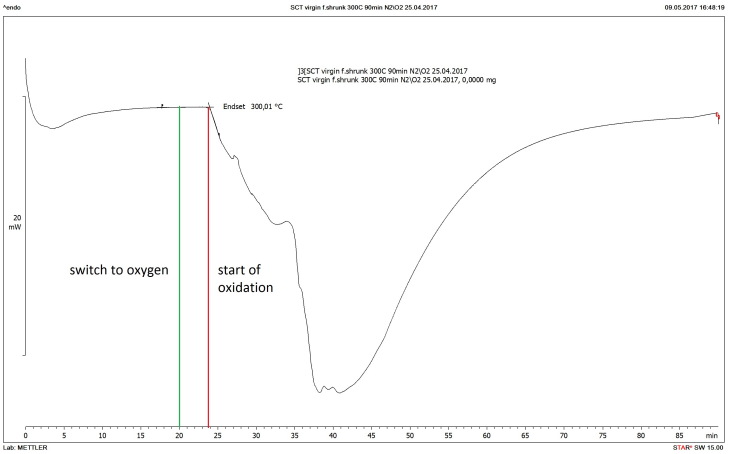

Figure A.1: Oxidation induction time thermogram for reference sample at isothermal temperature of 300°C for 90min.

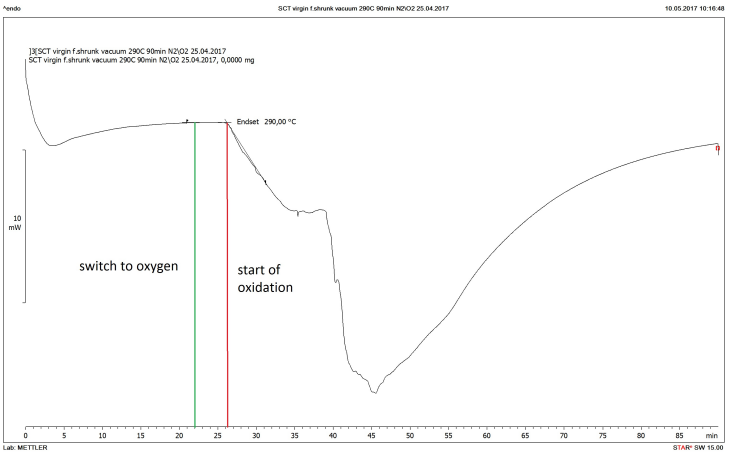

Figure A.2: Oxidation induction time thermogram for reference sample at isothermal temperature of $290^{o}C$ for $90min$.

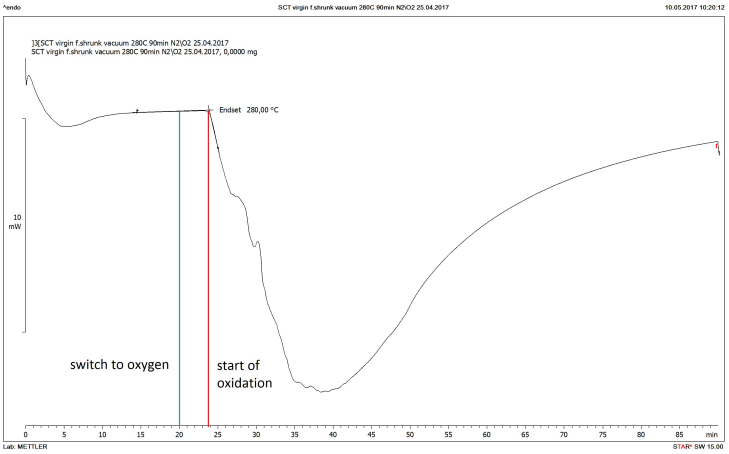

Figure A.3: Oxidation induction time thermogram for reference sample at isothermal temperature of 280°C for 90min.

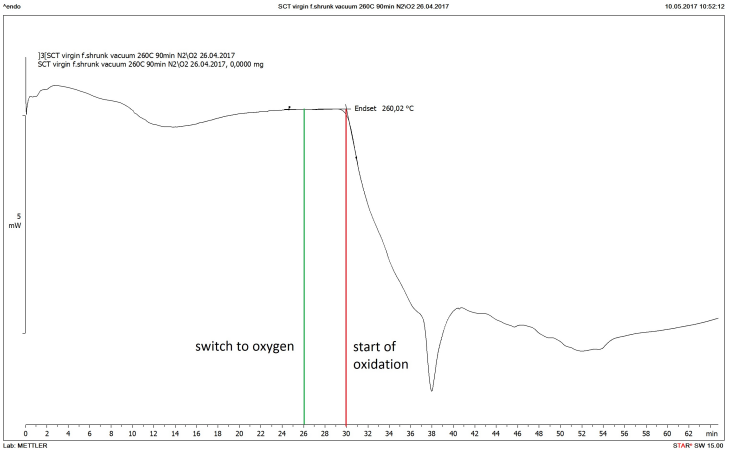

Figure A.4: Oxidation induction time thermogram for reference sample at isothermal temperature of 260°C for 90min.

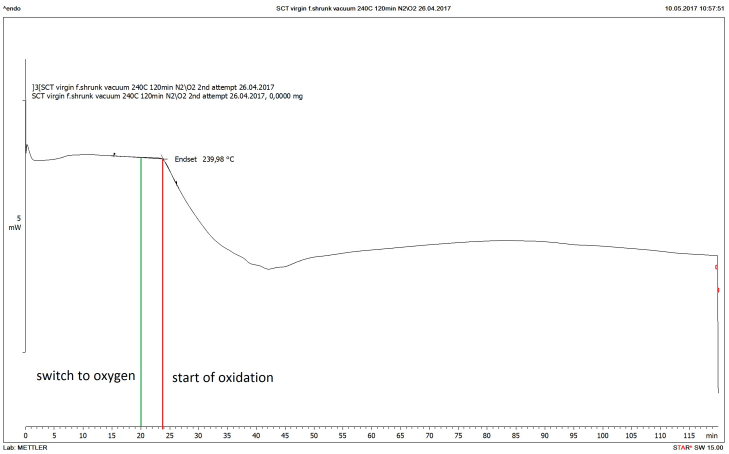

Figure A.5: Oxidation induction time thermogram for reference sample at isothermal temperature of 240°C for 120min.

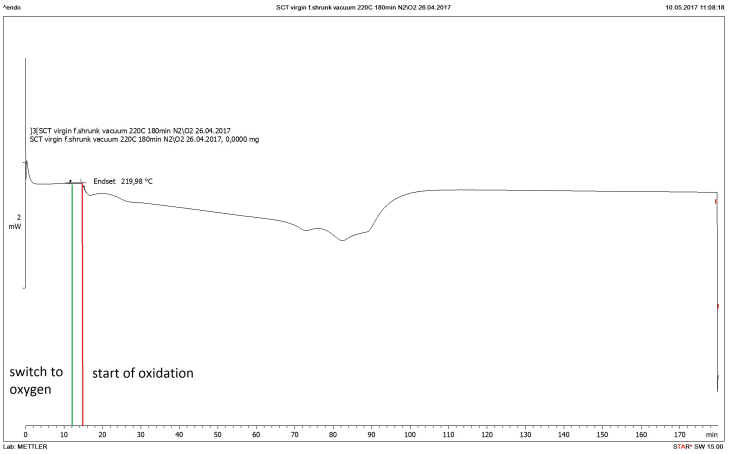

Figure A.6: Oxidation induction time thermogram for reference sample at isothermal temperature of 220°C for 180min.

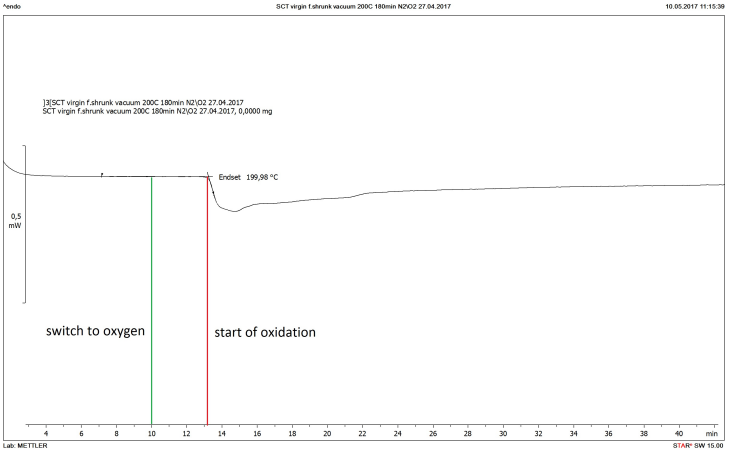

Figure A.7: Oxidation induction time thermogram for reference sample at isothermal temperature of 200°C for 180min.

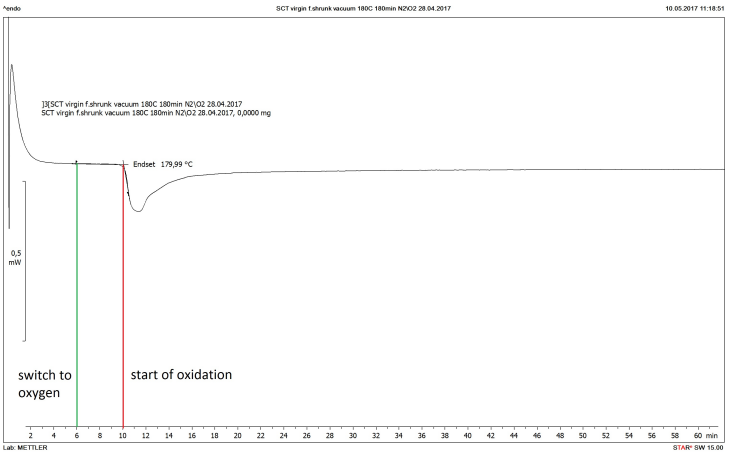

Figure A.8: Oxidation induction time thermogram for reference sample at isothermal temperature of 180°C for 180min.

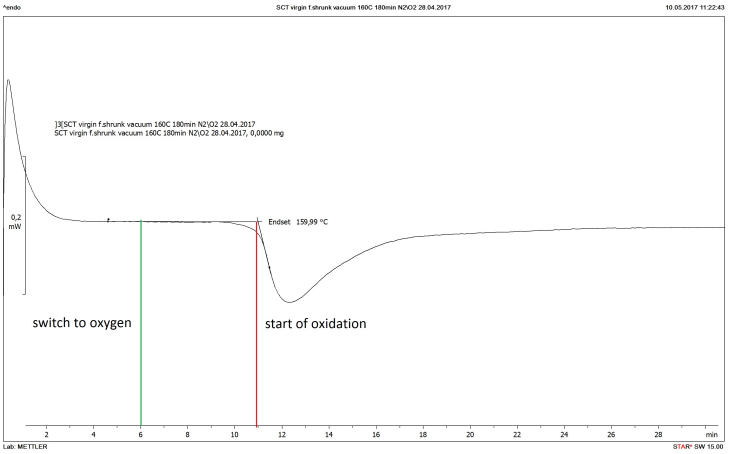

Figure A.9: Oxidation induction time thermogram for reference sample at isothermal temperature of 160°C for 180min.

Oxidation Induction Temperature

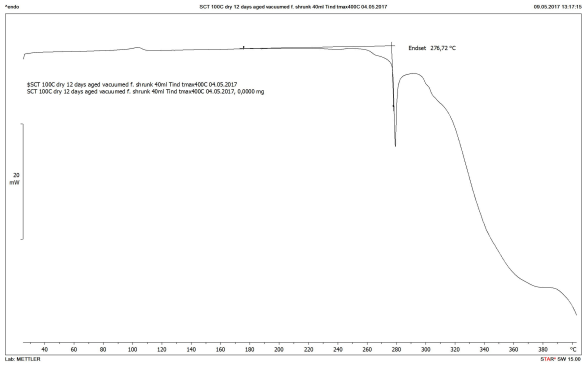

Figure A.10: Oxidation induction temperature for SCT sample aged at 98°C dry air for 12 days.

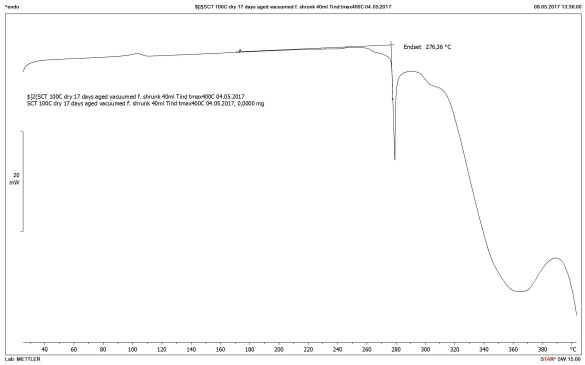

Figure A.11: Oxidation induction temperature for SCT sample aged at 98°C dry air for 17 days.

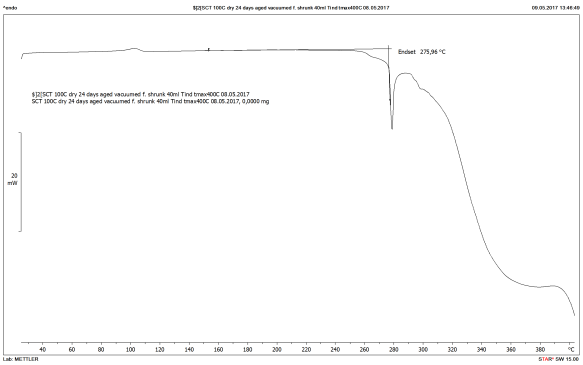

Figure A.12: Oxidation induction temperature for SCT sample aged at 98°C dry air for 24 days.

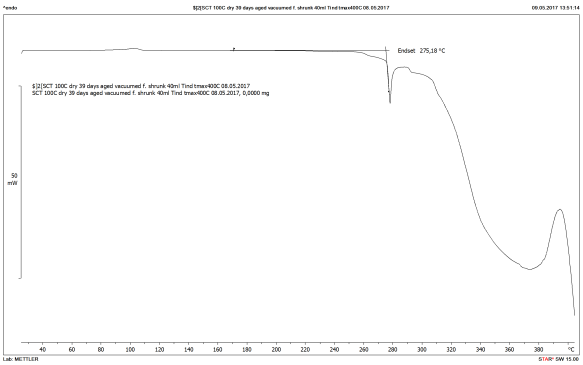

Figure A.13: Oxidation induction temperatur for SCT sample aged at 98°C dry air for 39 days.

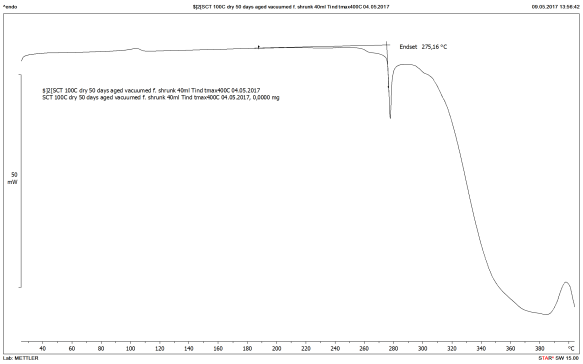

Figure A.14: Oxidation induction temperature for SCT sample aged at 98°C dry air for 50 days.

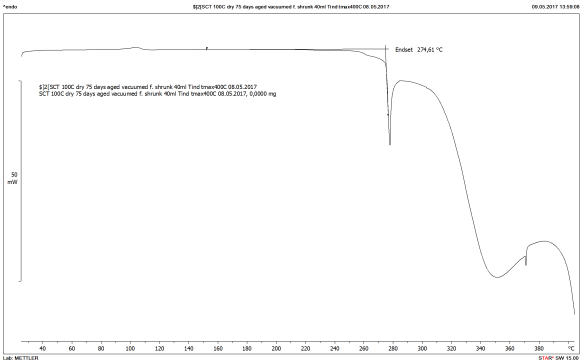

Figure A.15: Oxidation induction temperature for SCT sample aged at 98°C dry air for 75 days.

A.3 Time Domain Dielectric Response Measurements

Polarization Currents

Reference SCT test object

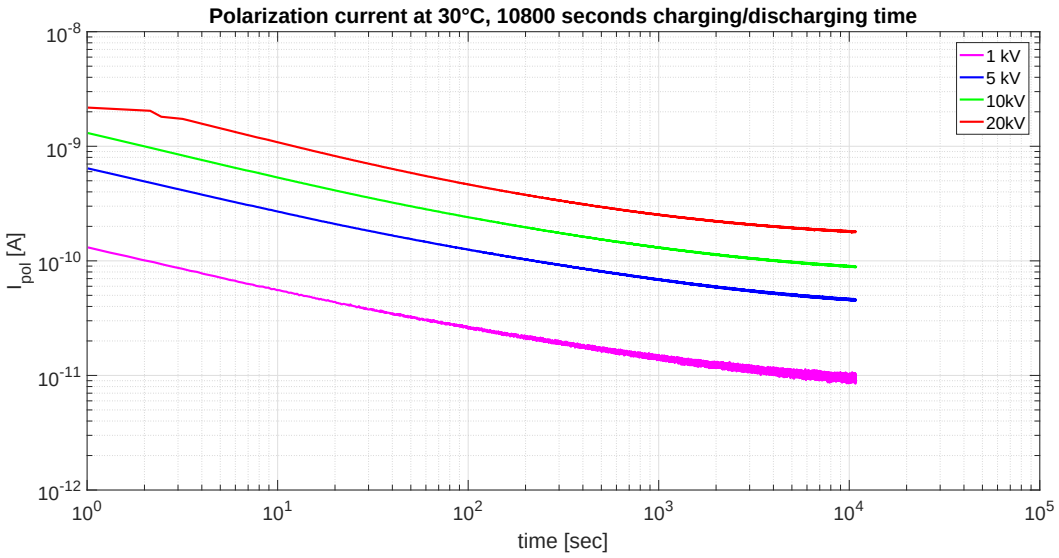

Figure A.16: Polarization currents for a reference SCT test object. Tests are done at 30°C, 1kV-5kV-10kV-20kV applied voltage and 10800 seconds of charging/discharging time.

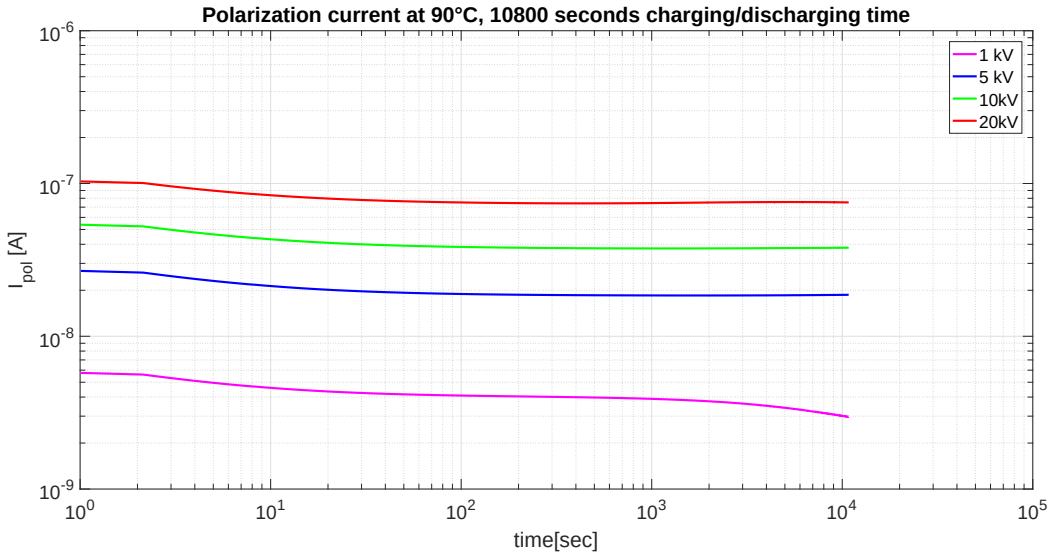

Figure A.17: Polarization currents for a reference SCT test object. Tests are done at 90°C, 1kV-5kV-10kV-20kV applied voltage and 10800 seconds of charging/discharging time.

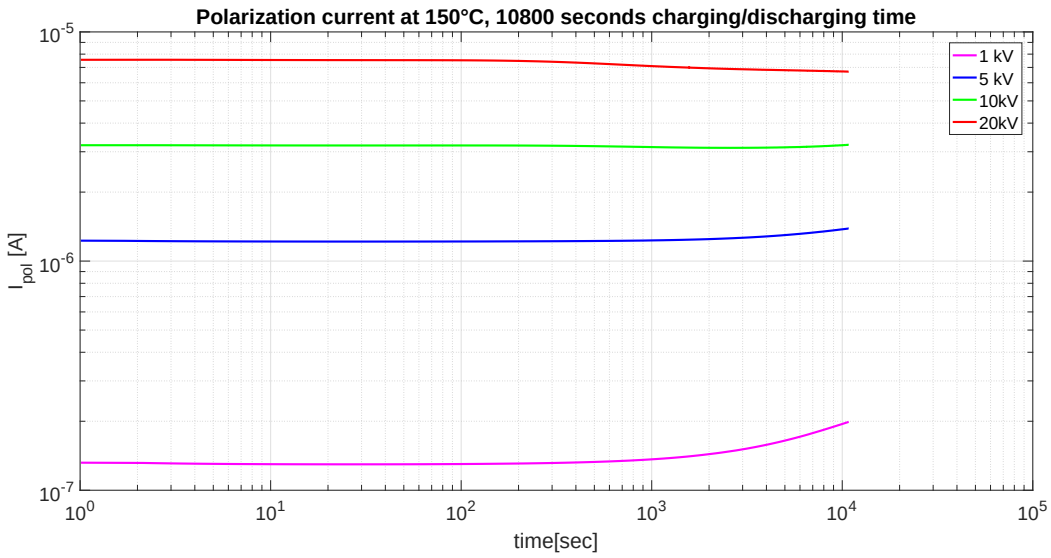

Figure A.18: Polarization currents for a reference SCT test object. Tests are done at 150°C, 1kV-5kV-10kV-20kV applied voltage and 10800 seconds of charging/discharging time.

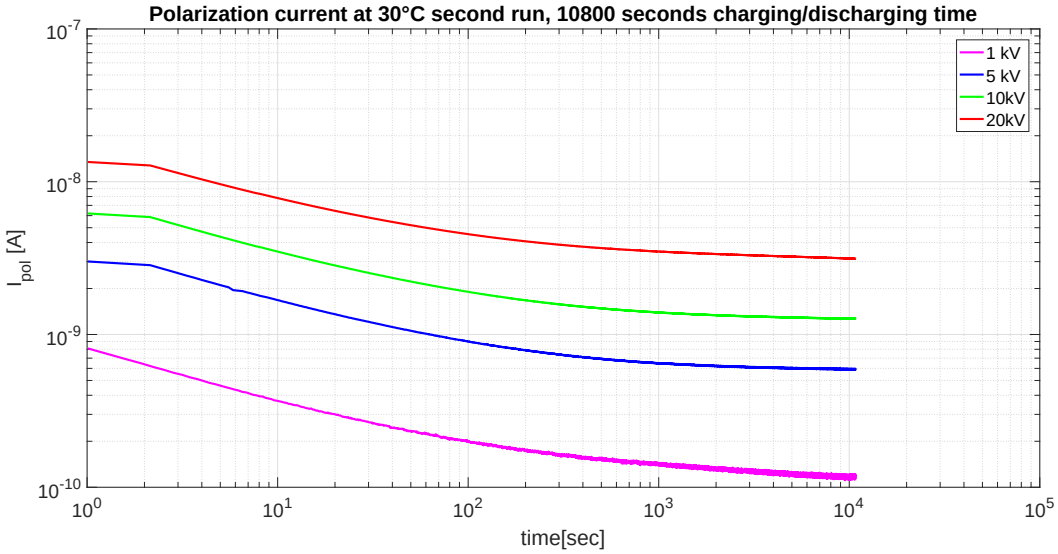

Figure A.19: Polarization currents for a reference SCT test object. Tests are done at 30°C (second run), 1kV-5kV-10kV-20kV applied voltage and 10800 seconds of charging/discharging time.

SCT test object aged at 98°C dry air for 50 days

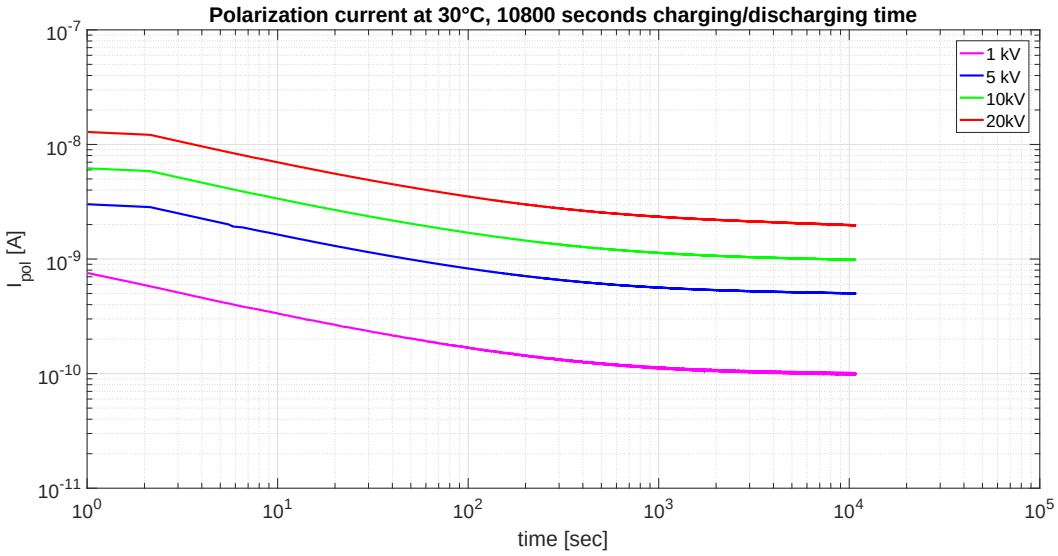

Figure A.20: Polarization currents for a SCT test object aged at 98°C dry air for 50 days. Tests are done at 30°C, 1kV-5kV-10kV-20kV applied voltage and 10800 seconds of charging/discharging time.

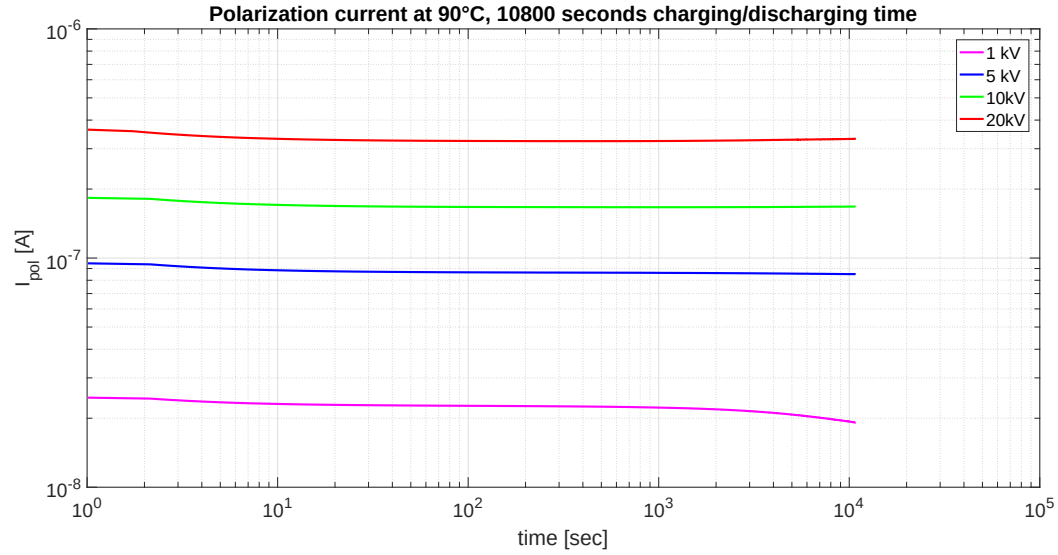

Figure A.21: Polarization currents for a SCT test object aged at 98°C dry air for 50 days. Tests are done at 90°C, 1kV-5kV-10kV-20kV applied voltage and 10800 seconds of charging/discharging time.

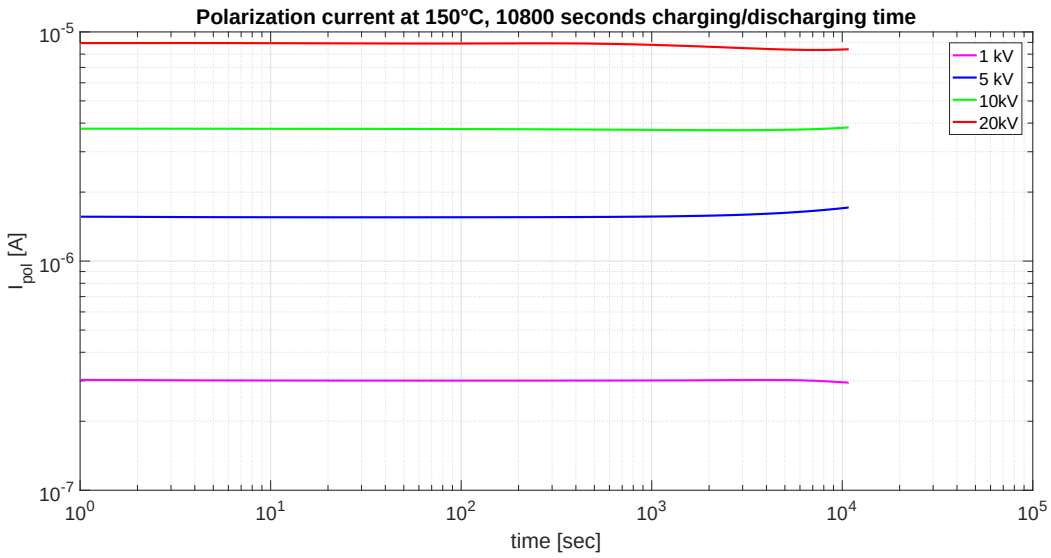

Figure A.22: Polarization currents for a SCT test object aged at 98°C dry air for 50 days. Tests are done at 150°C, 1kV-5kV-10kV-20kV applied voltage and 10800 seconds of charging/discharging time.

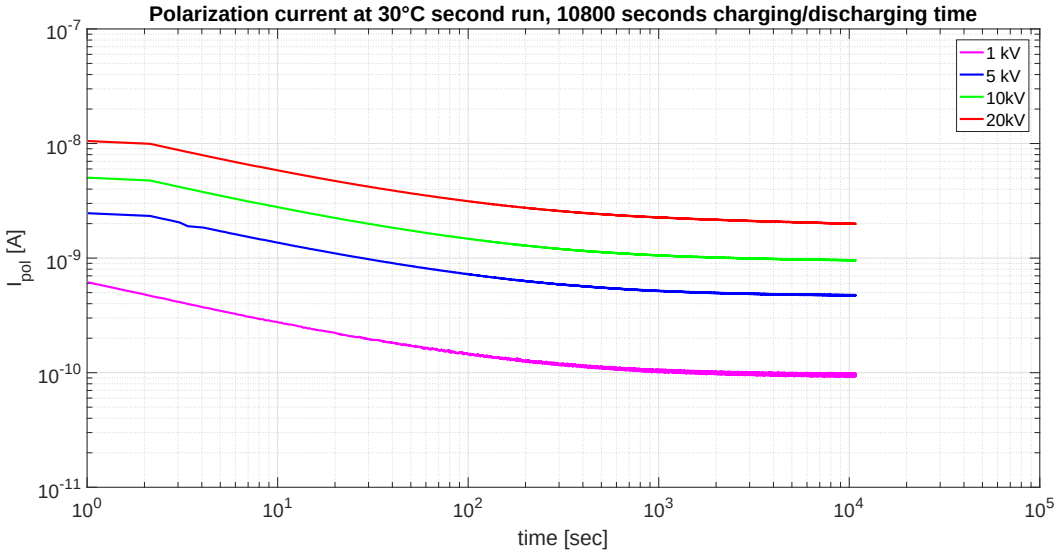

Figure A.23: Polarization currents for a SCT test object aged at 98°C dry air for 50 days. Tests are done at 30°C second run, 1kV-5kV-10kV-20kV applied voltage and 10800 seconds of charging/discharging time.

SCT test object aged at 98°C dry air for 75 days

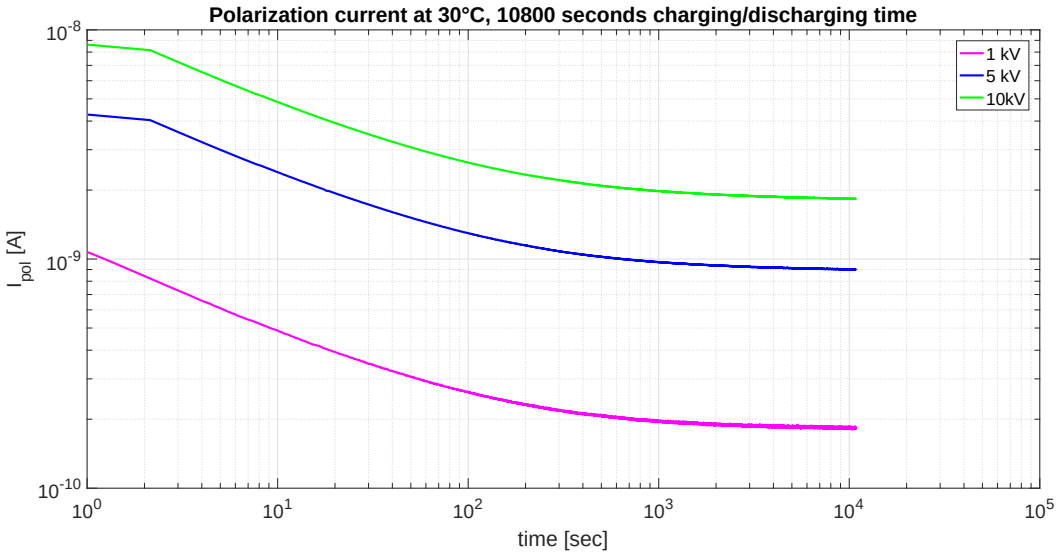

Figure A.24: Polarization currents for a SCT test object aged at 98°C dry air for 75 days. Tests are done at 30°C, 1kV-5kV-10kV applied voltage and 10800 seconds of charging/discharging time.

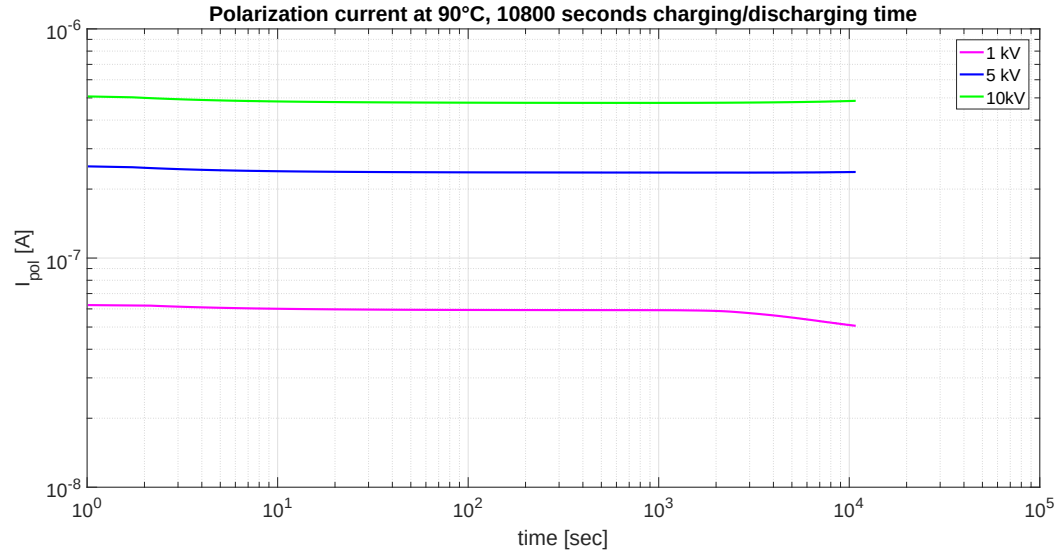

Figure A.25: Polarization currents for a SCT test object aged at 98°C dry air for 75 days. Tests are done at 90°C, 1kV-5kV-10kV applied voltage and 10800 seconds of charging/discharging time.

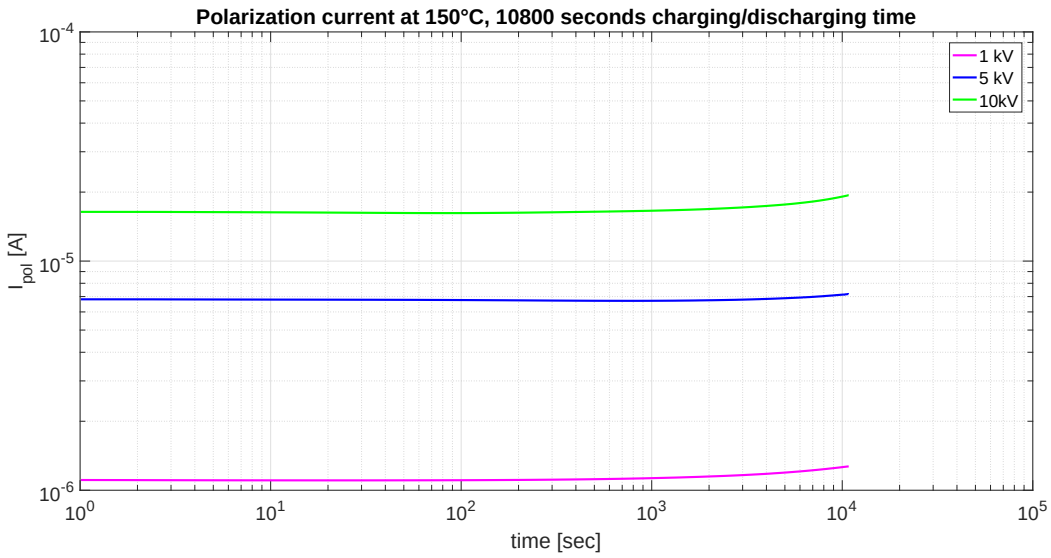

Figure A.26: Polarization currents for a SCT test object aged at 98°C dry air for 75 days. Tests are done at 150°C, 1kV-5kV-10kV applied voltage and 10800 seconds of charging/discharging time.

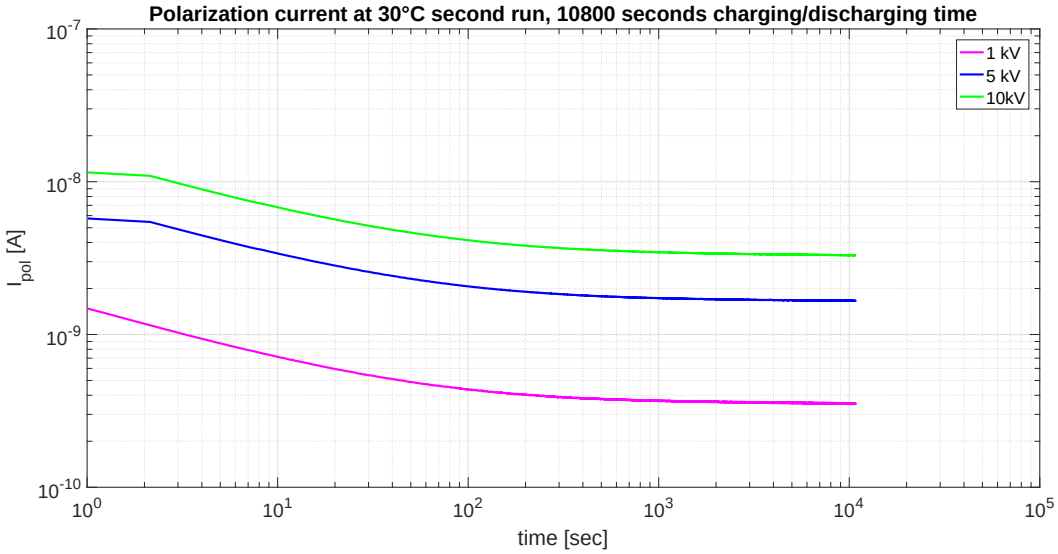

Figure A.27: Polarization currents for a SCT test object aged at 98°C dry air for 75 days. Tests are done at 30°C second run, 1kV-5kV-10kV applied voltage and 10800 seconds of charging/discharging time.

SCT test object aged at 98°C wet air for 50 days

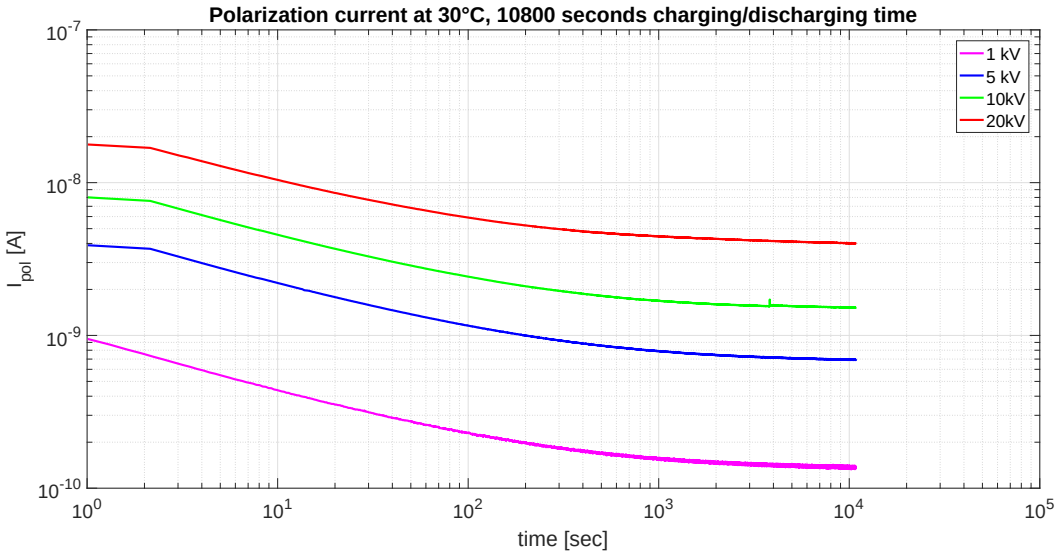

Figure A.28: Polarization currents for a SCT test object aged at 98^oC wet air. Tests are done at 30^oC, 1kV-5kV-10kV-20kV applied voltage and 10800 seconds of charging/discharging time.

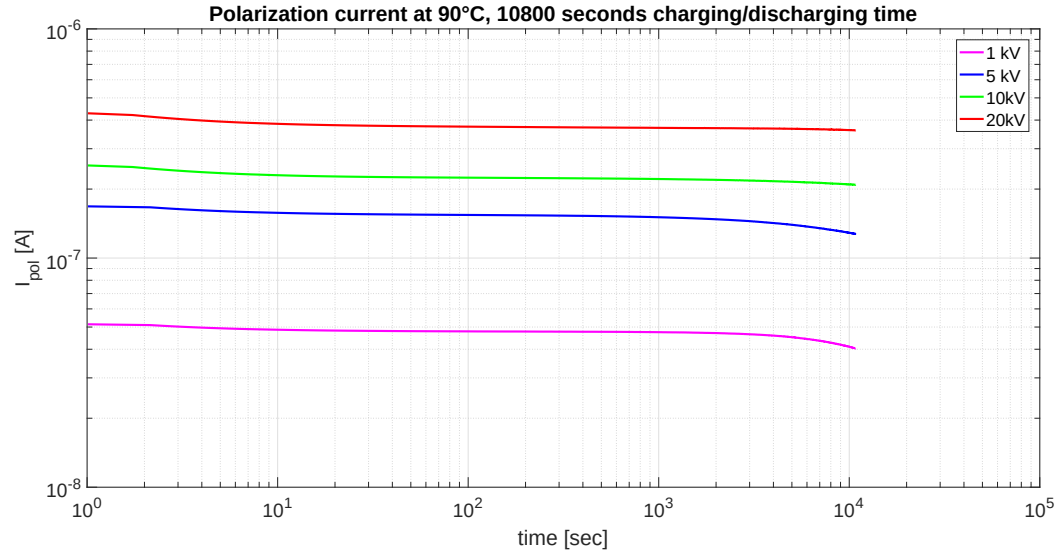

Figure A.29: Polarization currents for a SCT test object aged at 98°C wet air. Tests are done at 90°C, 1kV-5kV-10kV-20kV applied voltage and 10800 seconds of charging/discharging time.

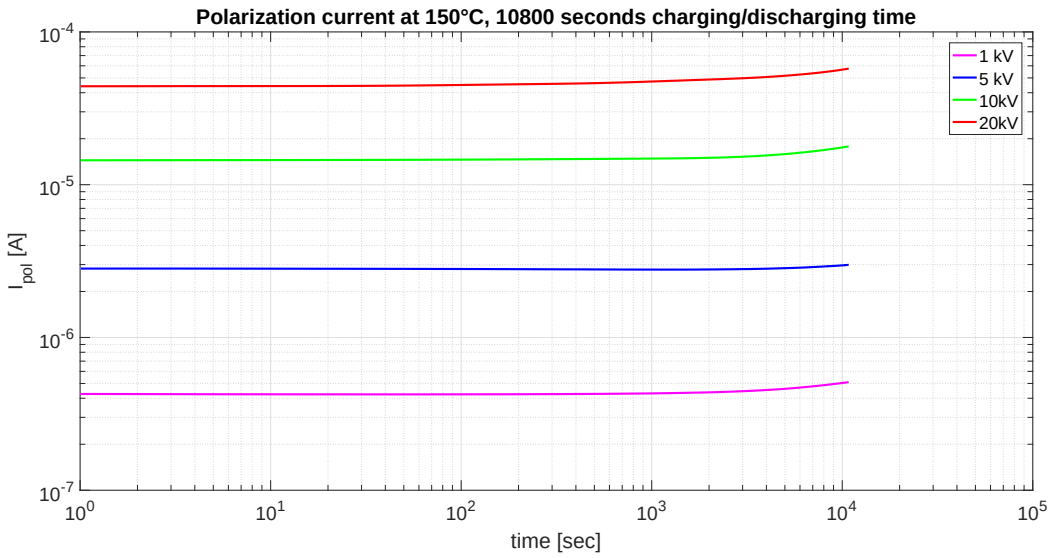

Figure A.30: Polarization currents for a SCT test object aged at 98°C wet air. Tests are done at 150°C, 1kV-5kV-10kV-20kV applied voltage and 10800 seconds of charging/discharging time.

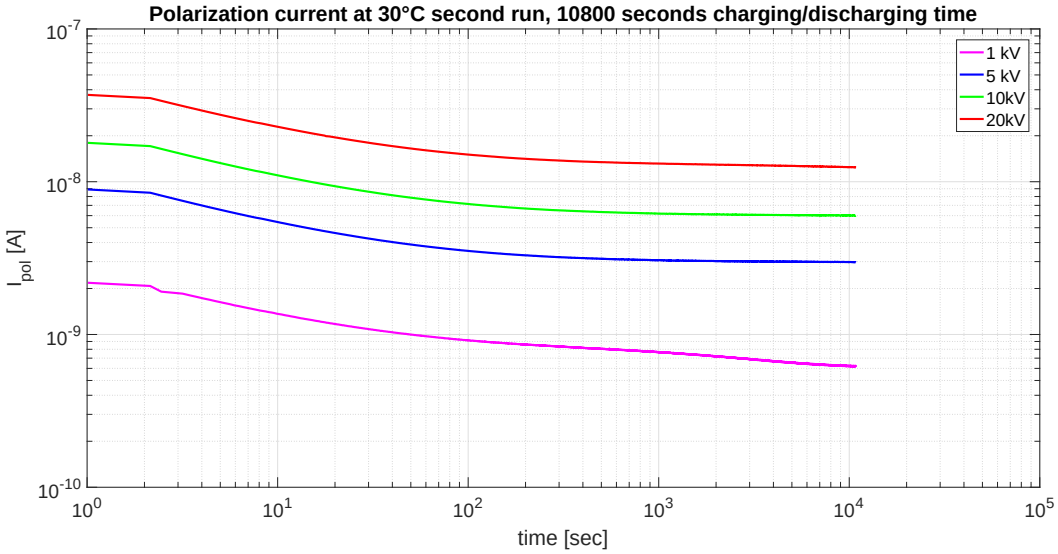

Figure A.31: Polarization currents for a SCT test object aged at 98°C wet air. Tests are done at 30°C second run, 1kV-5kV-10kV-20kV applied voltage and 10800 seconds of charging/discharging time.

SCT test object aged at 98°C wet air for 75 days

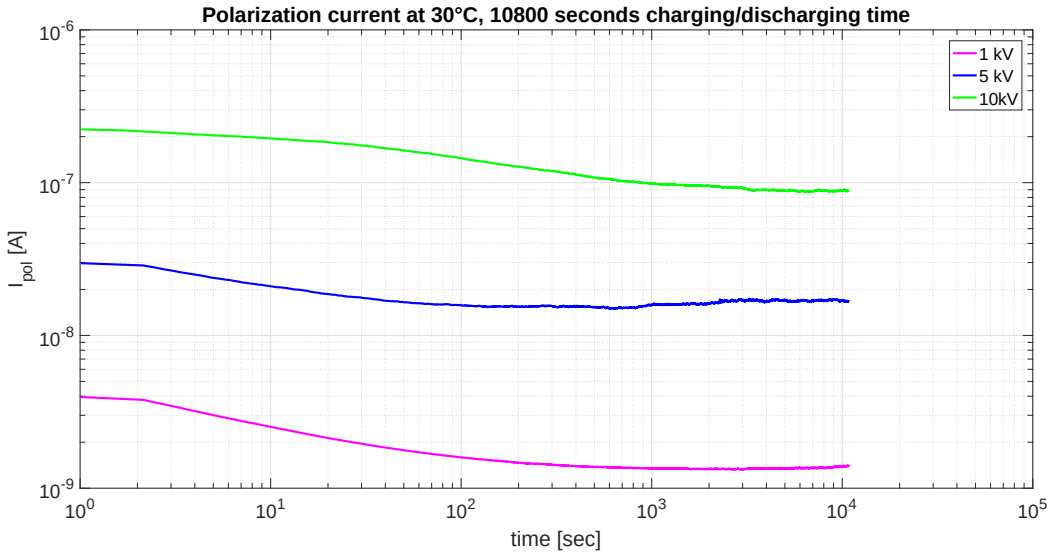

Figure A.32: Polarization currents for a SCT test object aged at 98°C wet air for 75 days. Tests are done at 30°C, 1kV-5kV-10kV applied voltage and 10800 seconds of charging/discharging time.

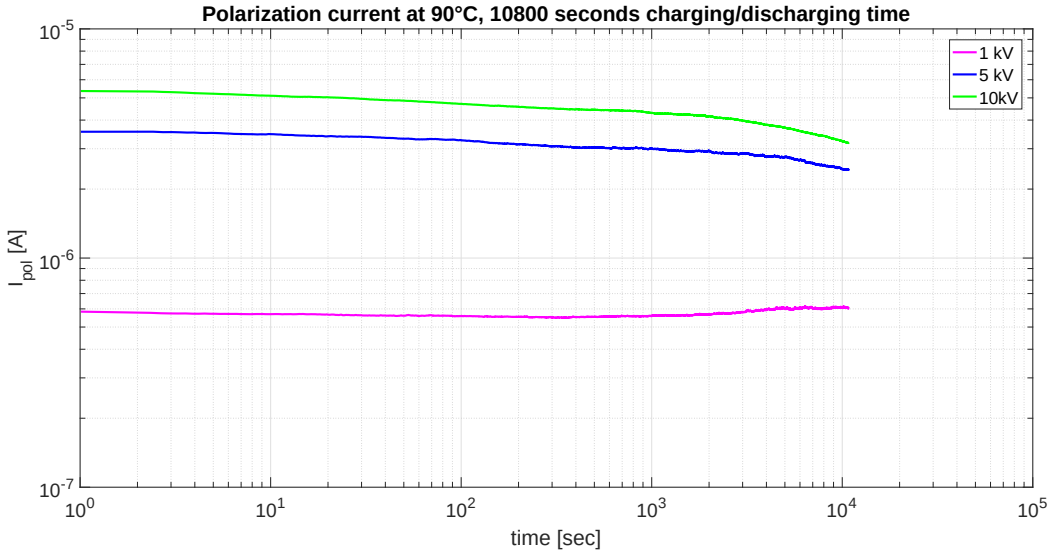

Figure A.33: Polarization currents for a SCT test object aged at 98°C wet air for 75 days. Tests are done at 90°C, 1kV-5kV-10kV-20kV applied voltage and 10800 seconds of charging/discharging time.

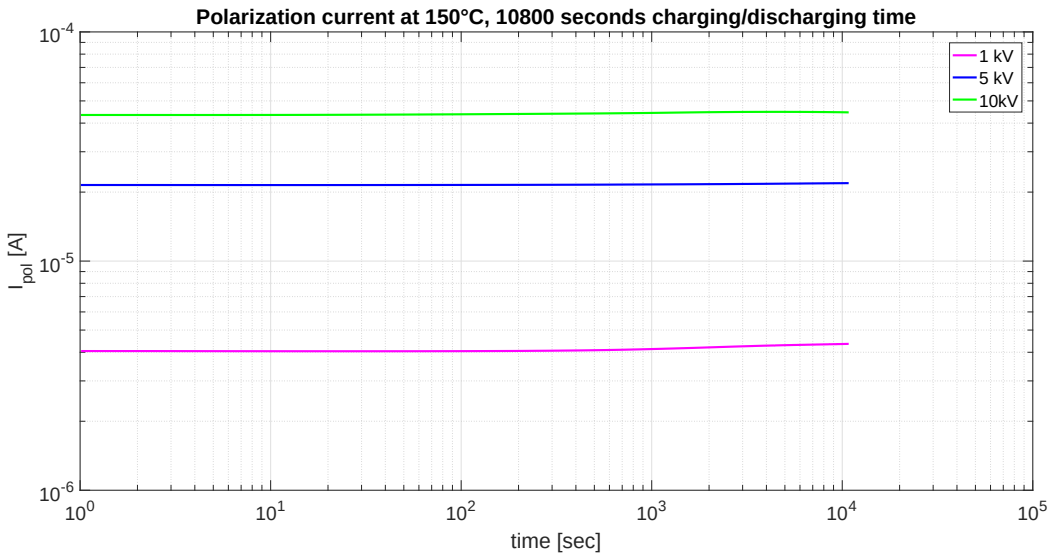

Figure A.34: Polarization currents for a SCT test object aged at 98°C wet air for 75 days. Tests are done at 150°C, 1kV-5kV-10kV applied voltage and 10800 seconds of charging/discharging time.

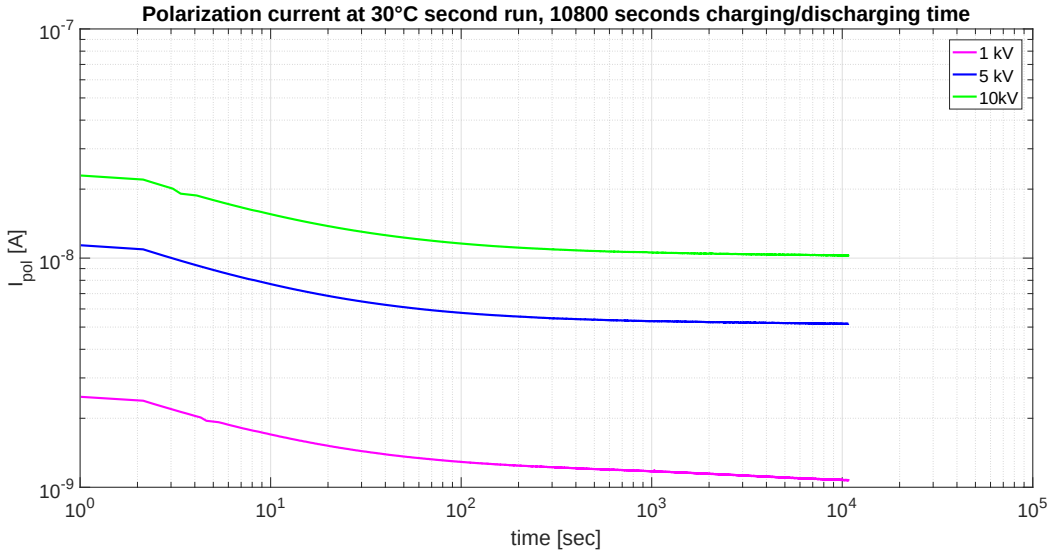

Figure A.35: Polarization currents for a SCT test object aged at 98°C wet air for 75 days. Tests are done at 30°C second run, 1kV-5kV-10kV applied voltage and 10800 seconds of charging/discharging time.

SCT test object aged at 150°C dry air for 15 days

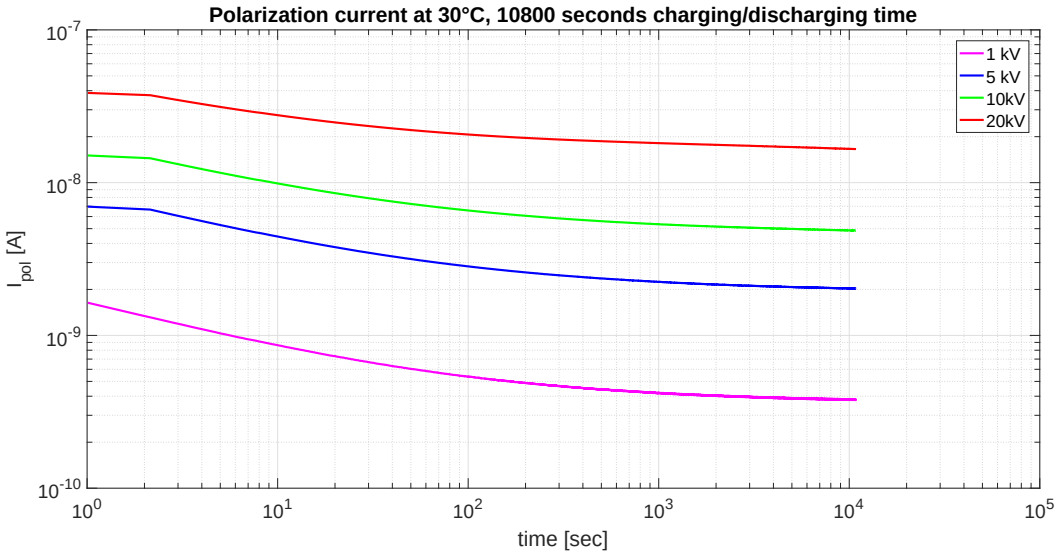

Figure A.36: Polarization currents for a SCT test object aged at 150°C dry air for 15 days. Tests are done at 30°C, 1kV-5kV-10kV-20kV applied voltage and 10800 seconds of charging/discharging time.

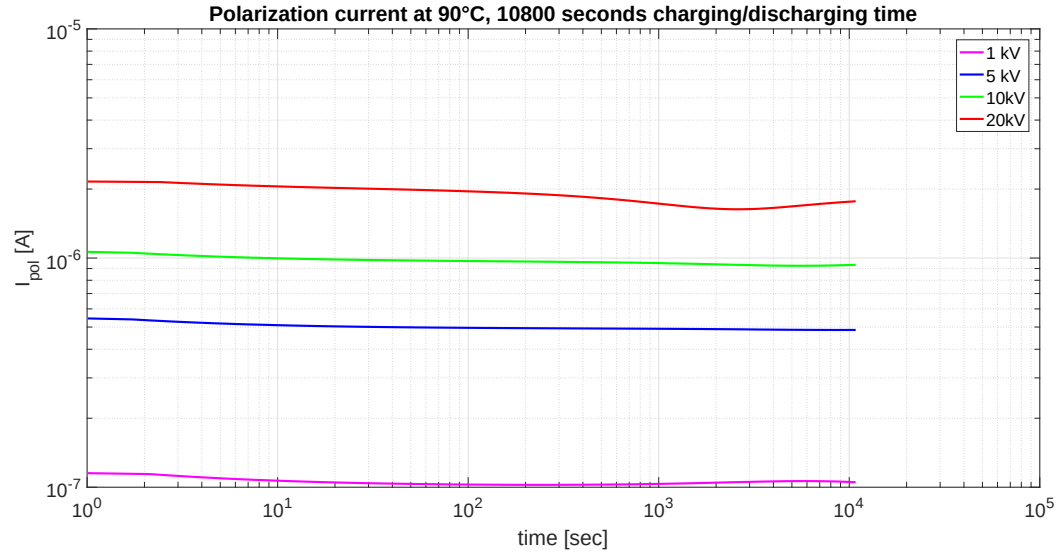

Figure A.37: Polarization currents for a SCT test object aged at 150°C dry air for 15 days. Tests are done at 90°C, 1kV-5kV-10kV-20kV applied voltage and 10800 seconds of charging/discharging time.

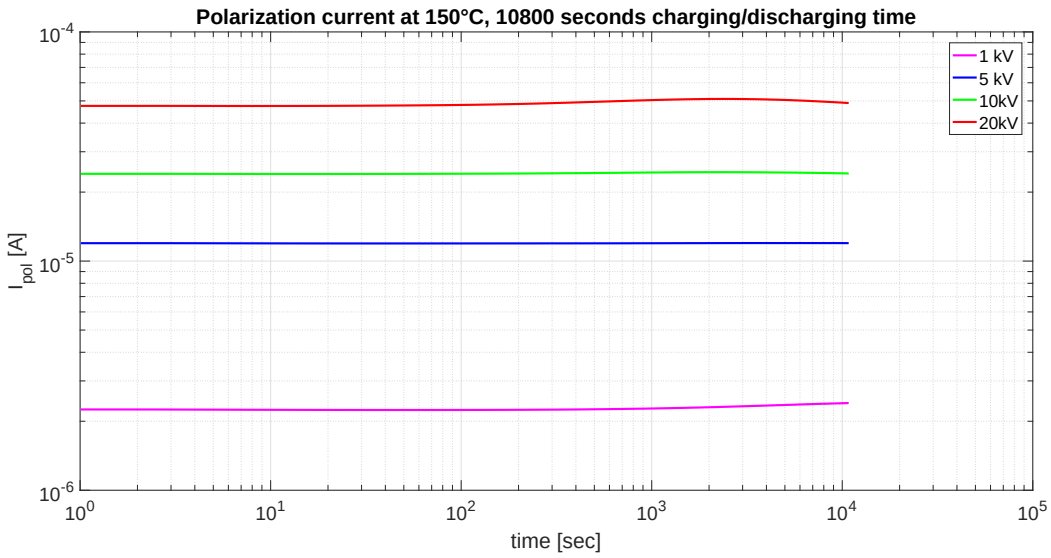

Figure A.38: Polarization currents for a SCT test object aged at 150°C dry air for 15 days. Tests are done at 150°C, 1kV-5kV-10kV-20kV applied voltage and 10800 seconds of charging/discharging time.

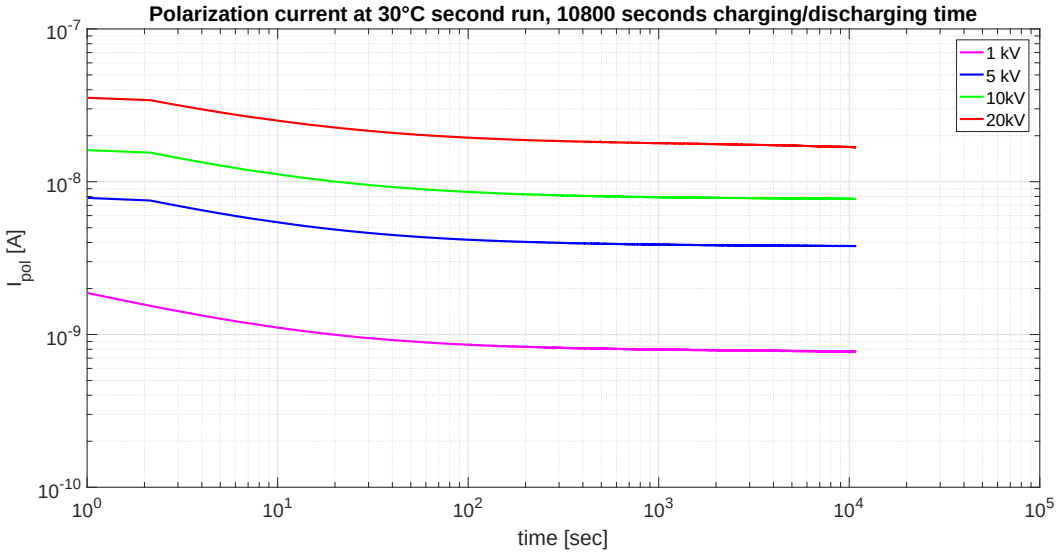

Figure A.39: Polarization currents for a SCT test object aged at 150°C dry air for 15 days. Tests are done at 30°C second run, 1kV-5kV-10kV-20kV applied voltage and 10800 seconds of charging/discharging time.

SCT test object aged at 150°C dry air for 50 days

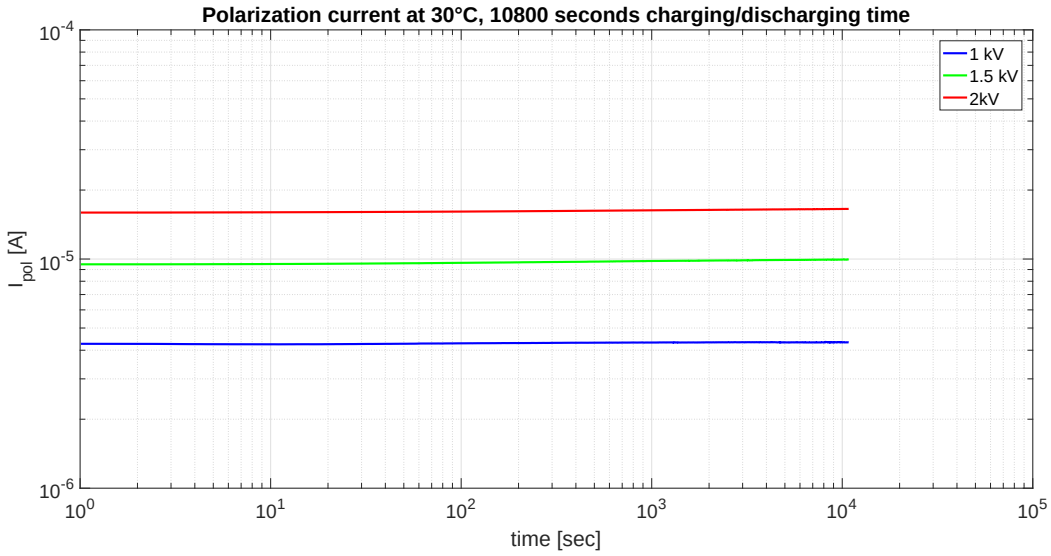

Figure A.40: Polarization currents for a SCT test object aged at 150°C dry air for 50 days. Tests are done at 30°C, 1kV-1.5kV-2kV applied voltage and 10800 seconds of charging/discharging time.

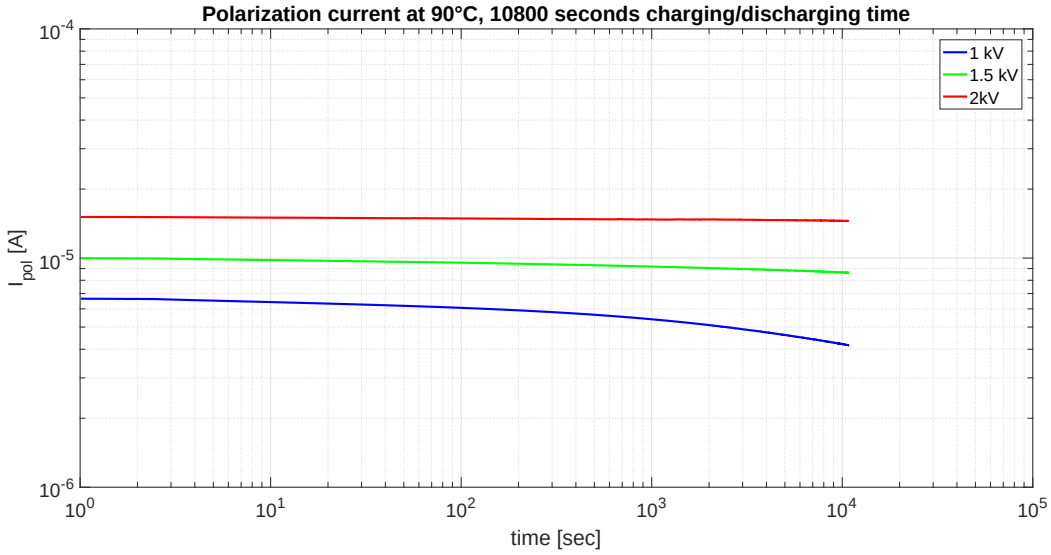

Figure A.41: Polarization currents for a SCT test object aged at 150°C dry air for 50 days. Tests are done at 90°C, 1kV-1.5kV-2kV applied voltage and 10800 seconds of charging/discharging time.

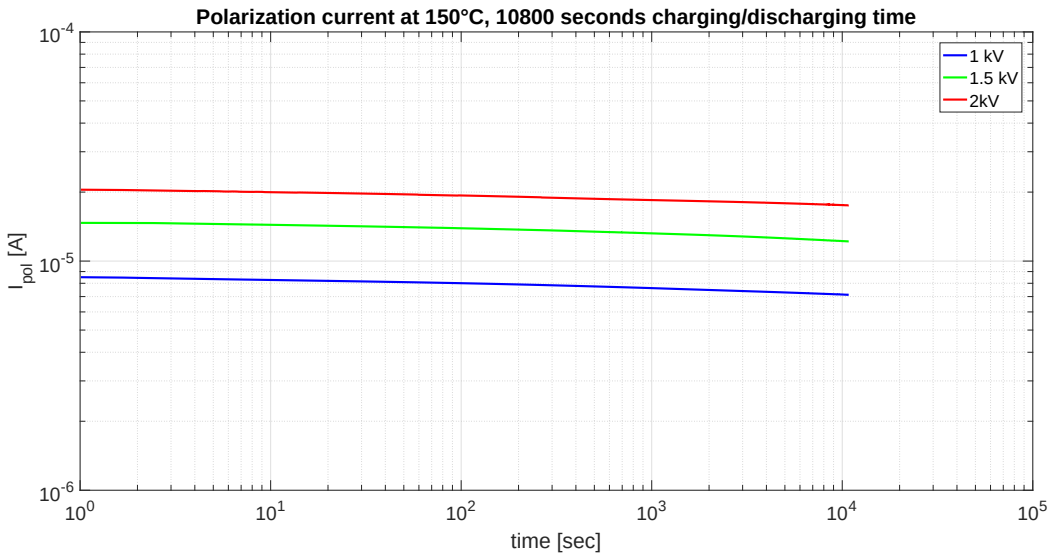

Figure A.42: Polarization currents for a SCT test object aged at 150°C dry air for 50 days. Tests are done at 150°C, 1kV-1.5kV-2kV applied voltage and 10800 seconds of charging/discharging time.

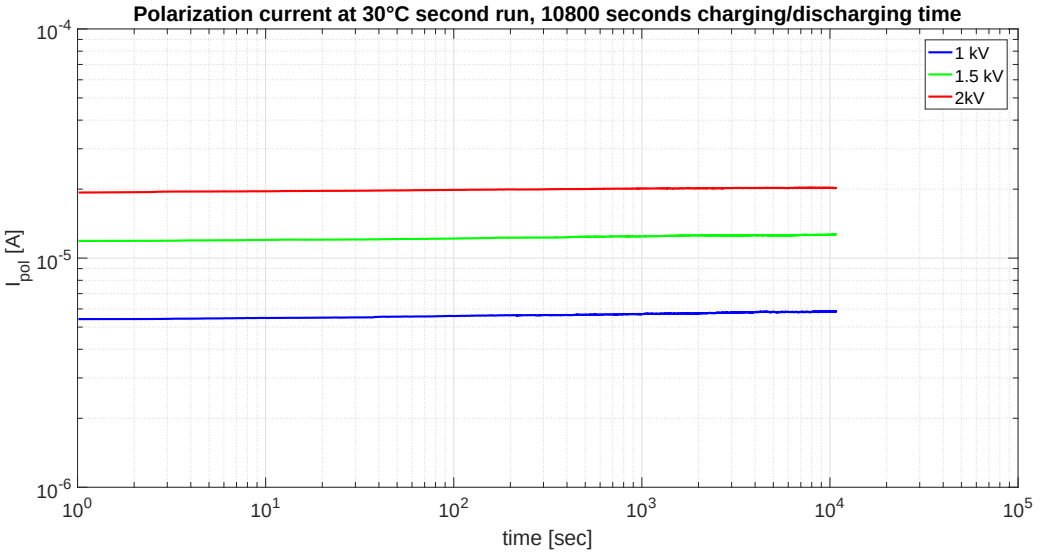

Figure A.43: Polarization currents for a SCT test object aged at 150°C dry air for 50 days. Tests are done at 30°C second run, 1kV-1.5kV-2kV applied voltage and 10800 seconds of charging/discharging time.

SCT reference test object subjected to water absorption at 90°C for 30 days

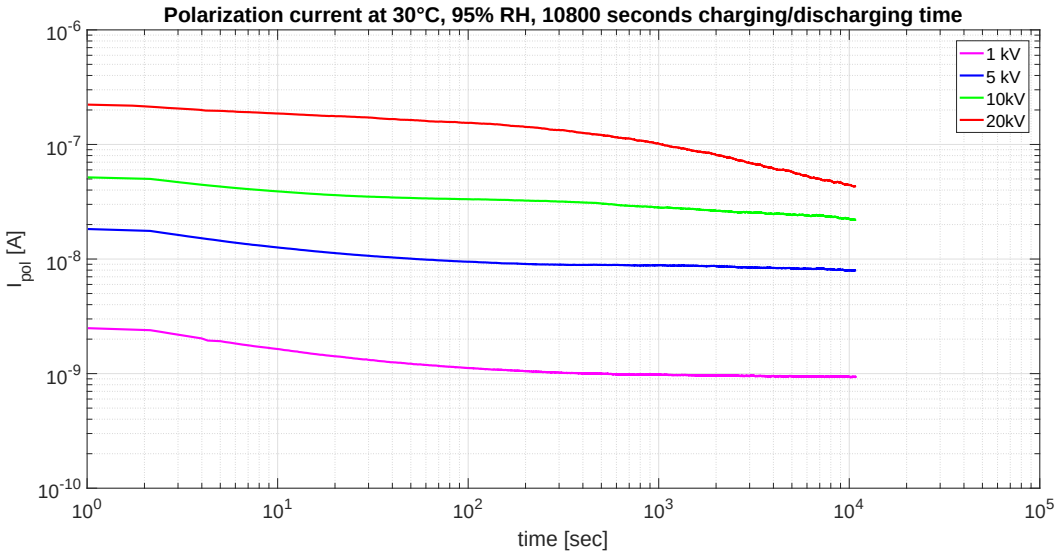

Figure A.44: Polarization currents for a reference SCT test object, subjected to water absorption at 90°C for 30 days. Tests are done at 30°C, 95% RH, 1kV-5kV-10kV-20kV applied voltage and 10800 seconds of charging/discharging time.

SCT test object aged at 150°C for 15 days and subjected to water absorption at 90°C for 30 days

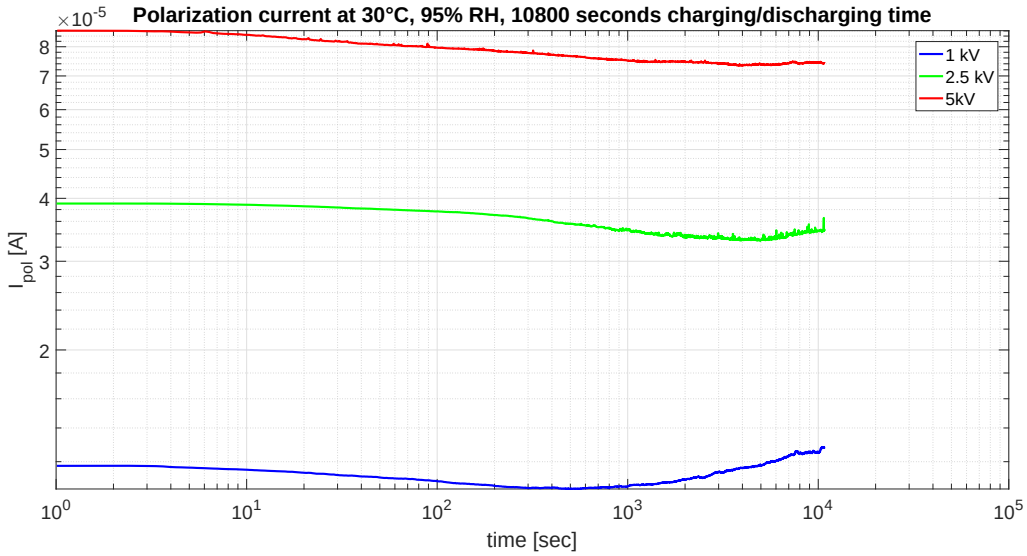

Figure A.45: Polarization currents for a SCT test object aged at 150°C for 15 days and subjected to water absorption at 90°C for 30 days. Tests are done at 30°C, 95% RH, 1kV-2.5kV-5kV applied voltage and 10800 seconds of charging/discharging time.

Depolarization Currents

Reference SCT test object

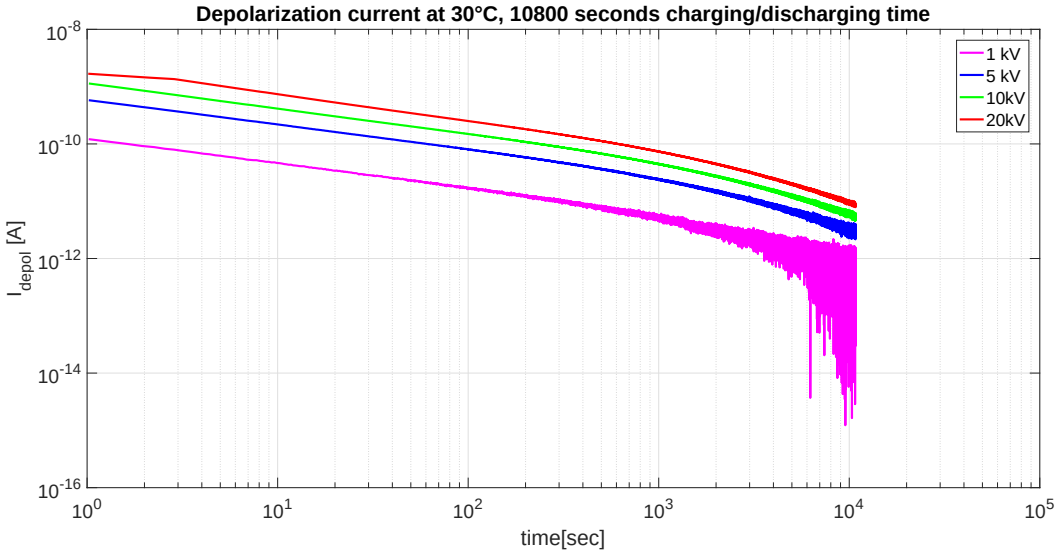

Figure A.46: Depolarization currents for a reference SCT test object. Tests are done at 30°C, 1kV-5kV-10kV-20kV applied voltage and 10800 seconds of charging/discharging time.

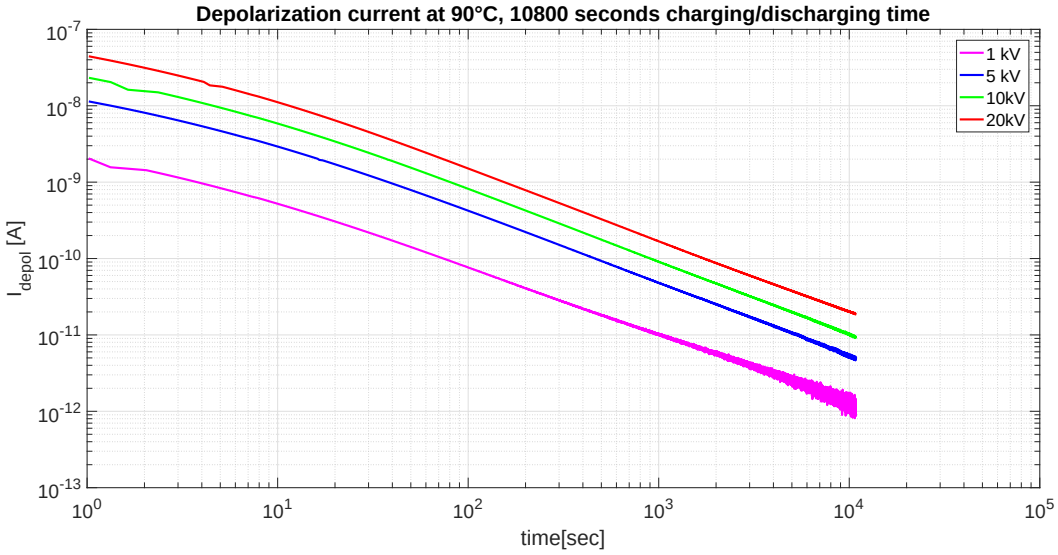

Figure A.47: Depolarization currents for a reference SCT test object. Tests are done at 90°C, 1kV-5kV-10kV-20kV applied voltage and 10800 seconds of charging/discharging time.

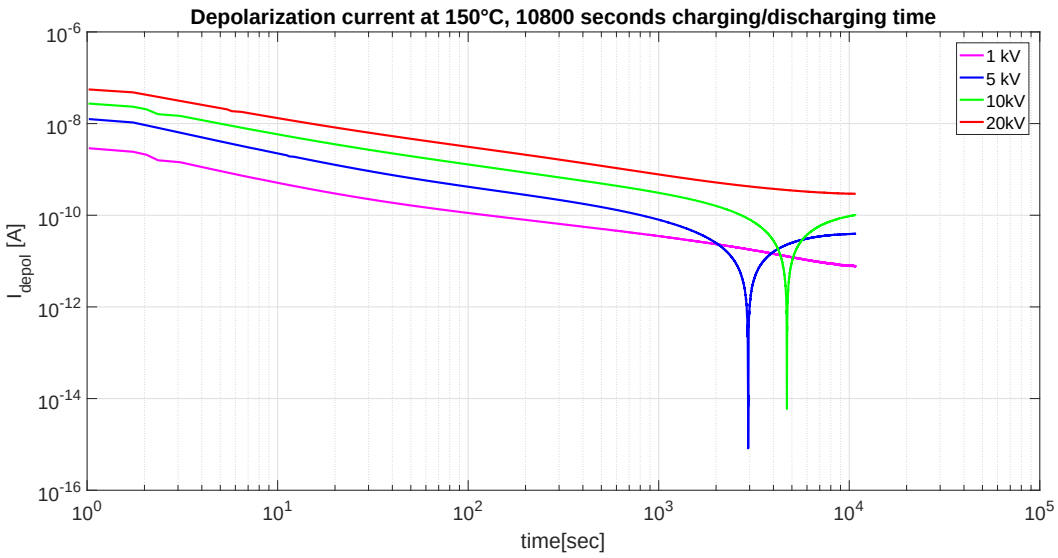

Figure A.48: Depolarization currents for a reference SCT test object. Tests are done at 150°C, 1kV-5kV-10kV-20kV applied voltage and 10800 seconds of charging/discharging time.

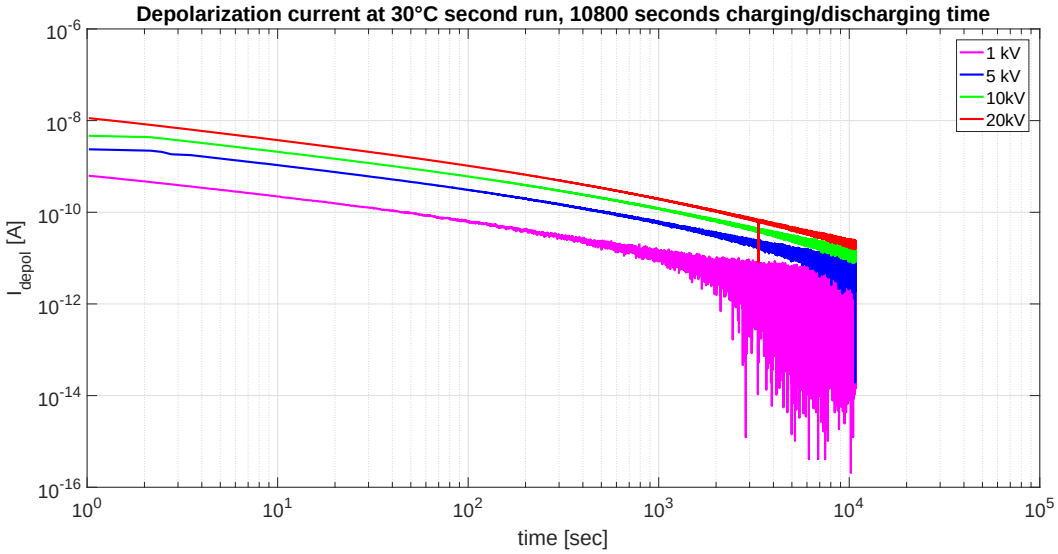

Figure A.49: Depolarization currents for a reference SCT test object. Tests are done at 30°C (second run), 1kV-5kV-10kV-20kV applied voltage and 10800 seconds of charging/discharging time.

SCT test object aged at 98°C dry air for 50 days

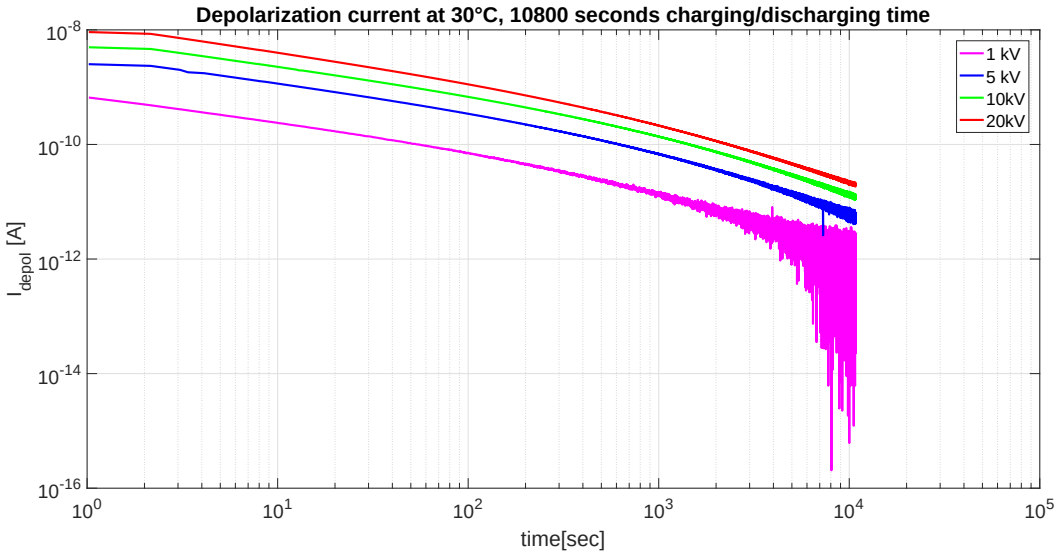

Figure A.50: Depolarization currents for a SCT test object aged at 98°C dry air for 50 days. Tests are done at 30°C, 1kV-5kV-10kV-20kV applied voltage and 10800 seconds of charging/discharging time.

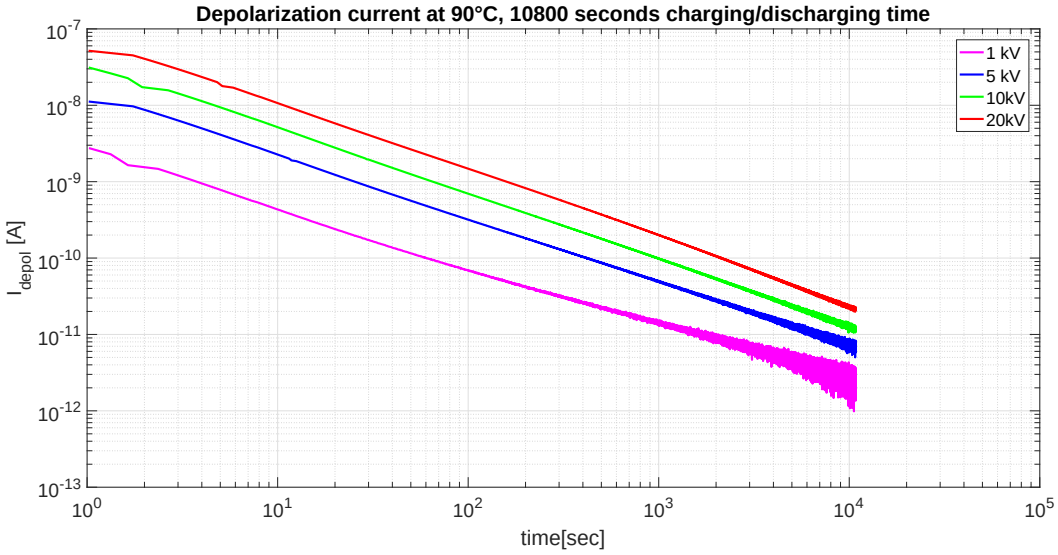

Figure A.51: Depolarization currents for a SCT test object aged at 98°C dry air for 50 days. Tests are done at 90°C, 1kV-5kV-10kV-20kV applied voltage and 10800 seconds of charging/discharging time.

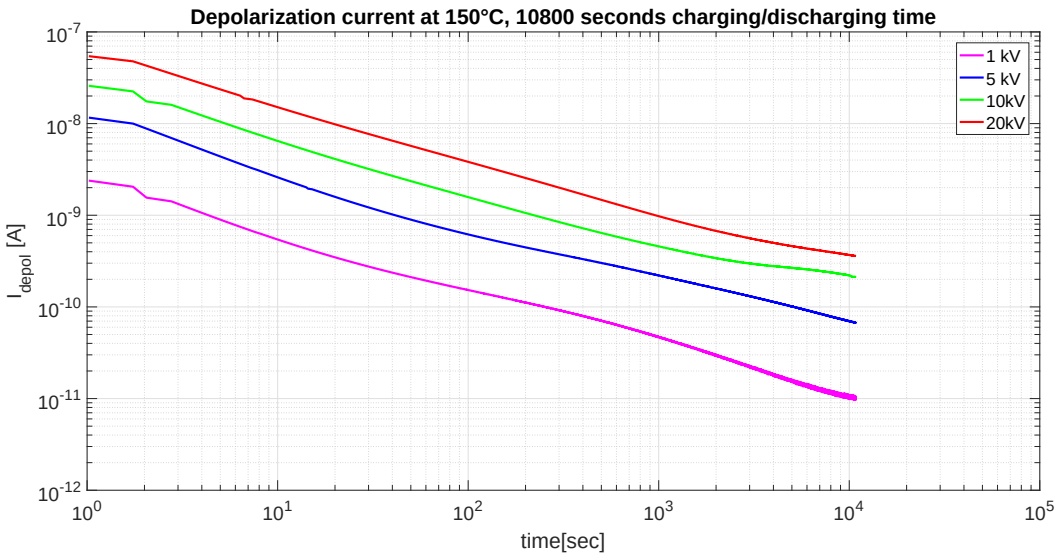

Figure A.52: Depolarization currents for a SCT test object aged at 98°C dry air for 50 days. Tests are done at 150°C, 1kV-5kV-10kV-20kV applied voltage and 10800 seconds of charging/discharging time.

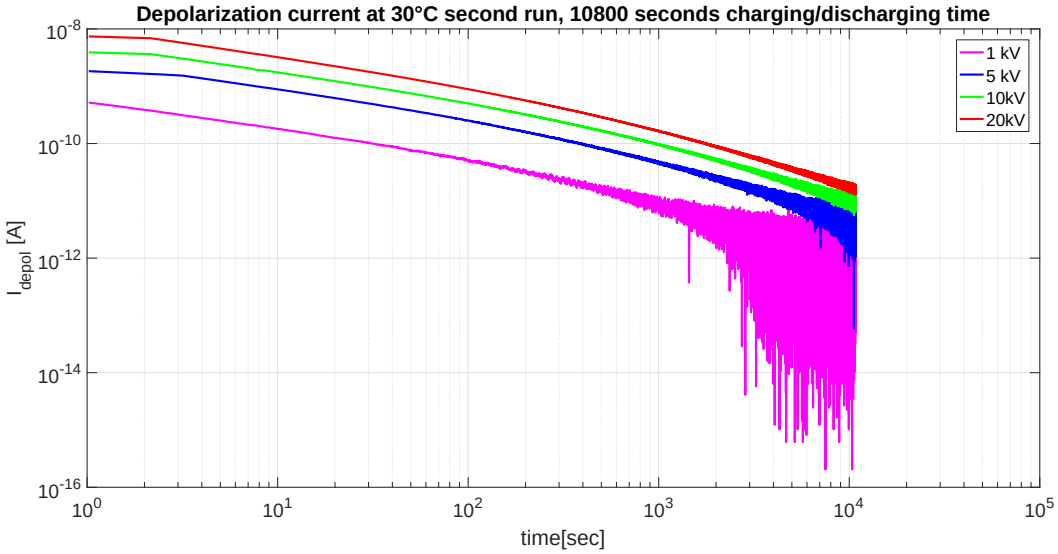

Figure A.53: Depolarization currents for a SCT test object aged at 98°C dry air for 50 days. Tests are done at 30°C second run, 1kV-5kV-10kV-20kV applied voltage and 10800 seconds of charging/discharging time.

SCT test object aged at 98°C dry air for 75 days

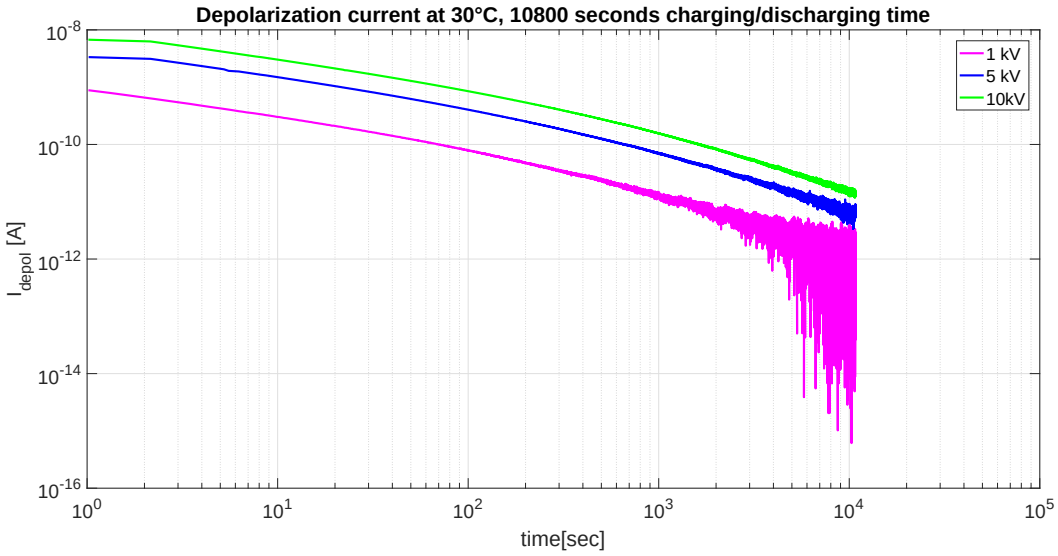

Figure A.54: Depolarization currents for a SCT test object aged at 98°C dry air for 75 days. Tests are done at 30°C, 1kV-5kV-10kV applied voltage and 10800 seconds of charging/discharging time.

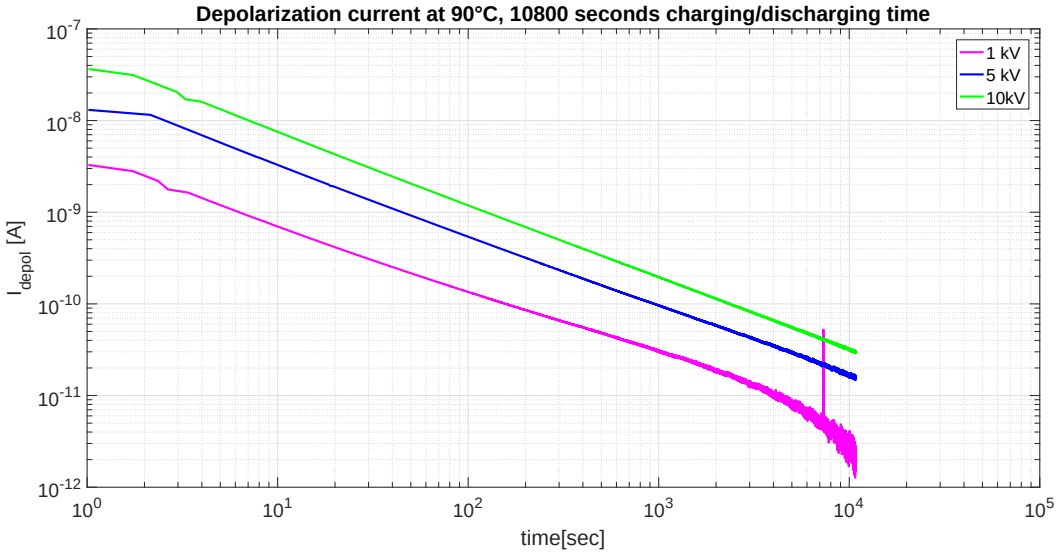

Figure A.55: Depolarization currents for a SCT test object aged at 98°C dry air. Tests are done at 90°C, 1kV-5kV-10kV applied voltage and 10800 seconds of charging/discharging time.

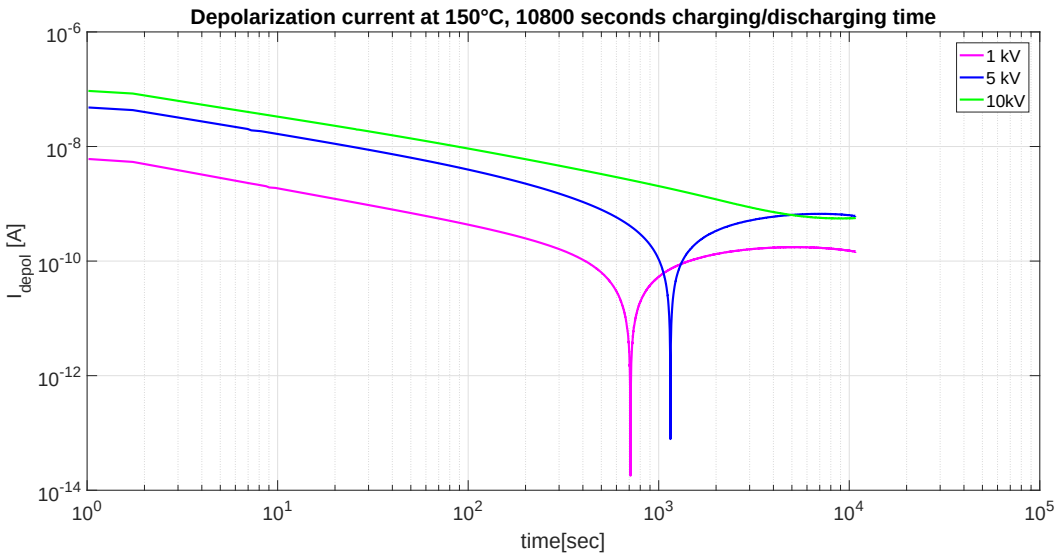

Figure A.56: Depolarization currents for a SCT test object aged at 98°C dry air. Tests are done at 150°C, 1kV-5kV-10kV applied voltage and 10800 seconds of charging/discharging time.

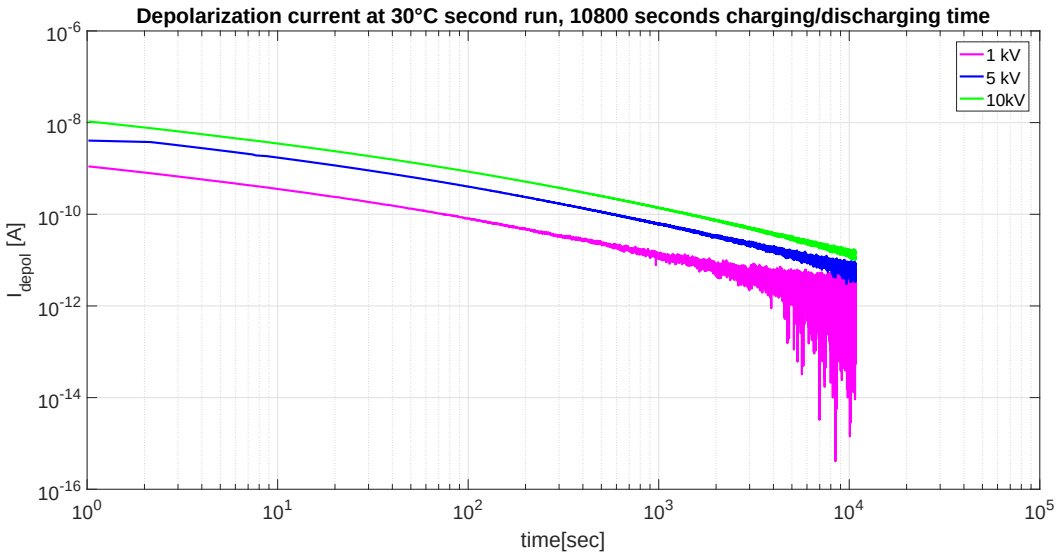

Figure A.57: Depolarization currents for a SCT test object aged at 98°C dry air. Tests are done at 30°C second run, 1kV-5kV-10kV applied voltage and 10800 seconds of charging/discharging time.

SCT test object aged at 98°C wet air for 50 days

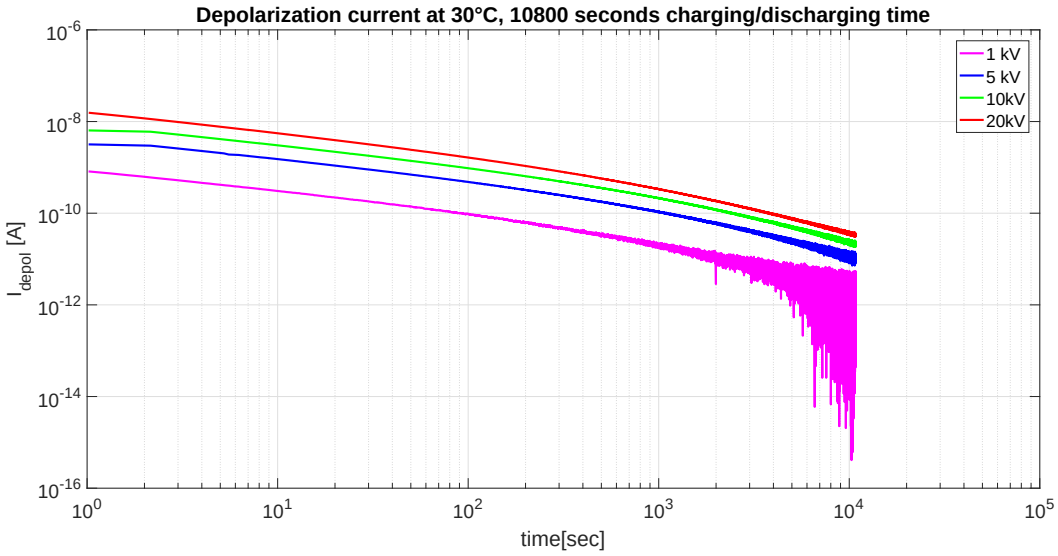

Figure A.58: Depolarization currents for a SCT test object aged at 98°C wet air for 50 days. Tests are done at 30°C, 1kV-5kV-10kV-20kV applied voltage and 10800 seconds of charging/discharging time.

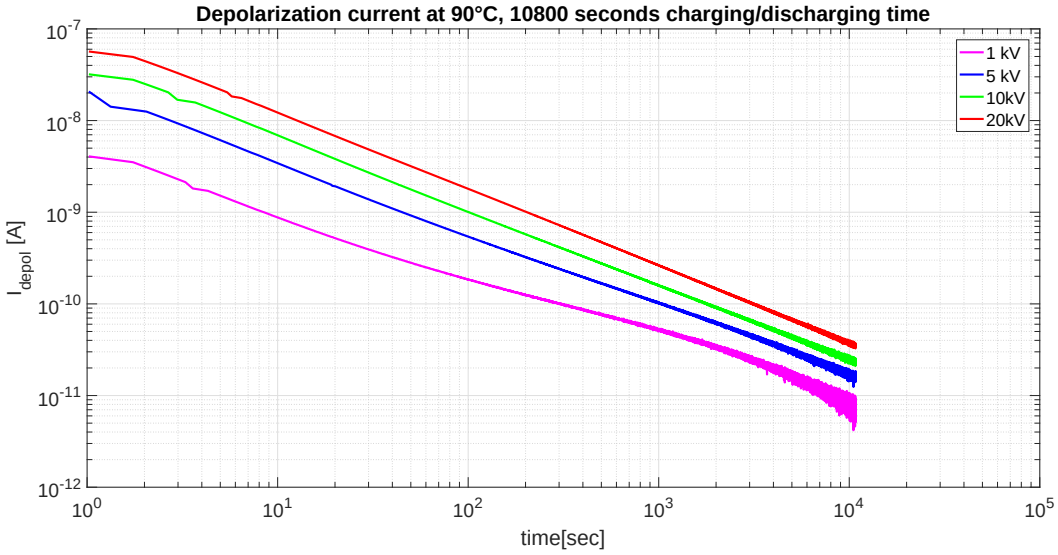

Figure A.59: Depolarization currents for a SCT test object aged at 98°C wet air for 50 days. Tests are done at 90°C, 1kV-5kV-10kV-20kV applied voltage and 10800 seconds of charging/discharging time.

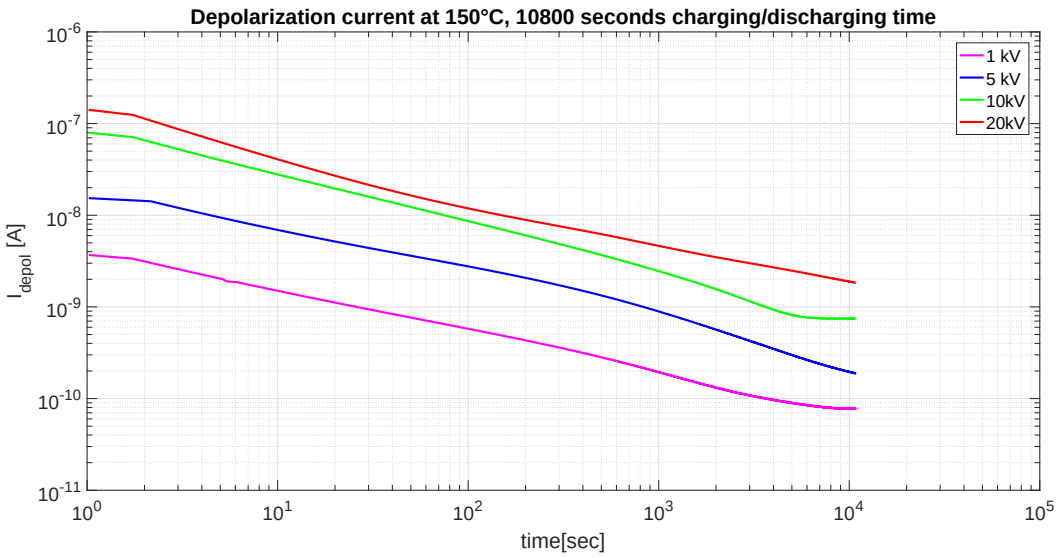

Figure A.60: Depolarization currents for a SCT test object aged at 98^oC wet air for 50 days. Tests are done at 150°C, 1kV-5kV-10kV-20kV applied voltage and 10800 seconds of charging/discharging time.

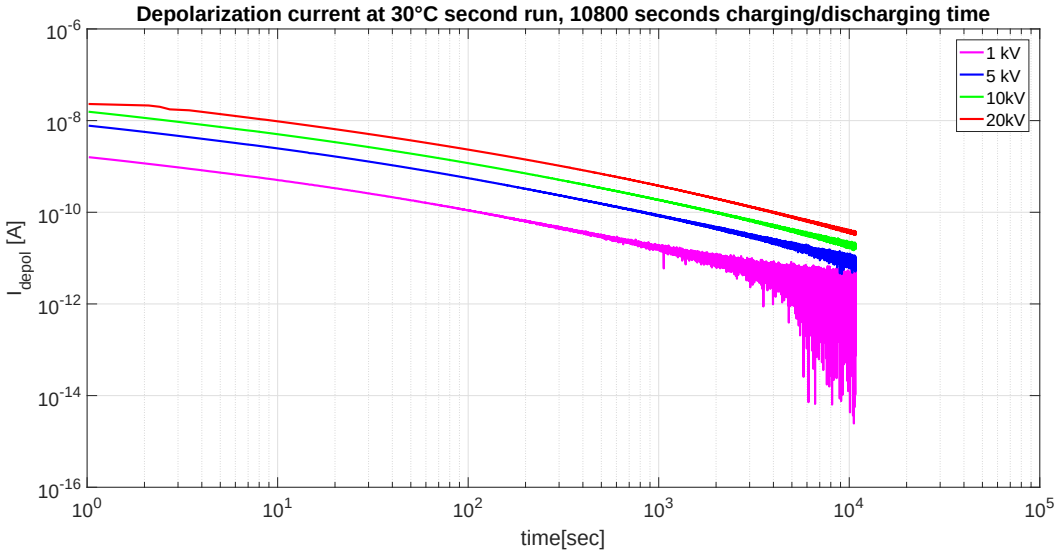

Figure A.61: Depolarization currents for a SCT test object aged at 98°C wet air for 50 days. Tests are done at 30°C second run, 1kV-5kV-10kV-20kV applied voltage and 10800 seconds of charging/discharging time.

SCT test object aged at 98°C wet air for 75 days

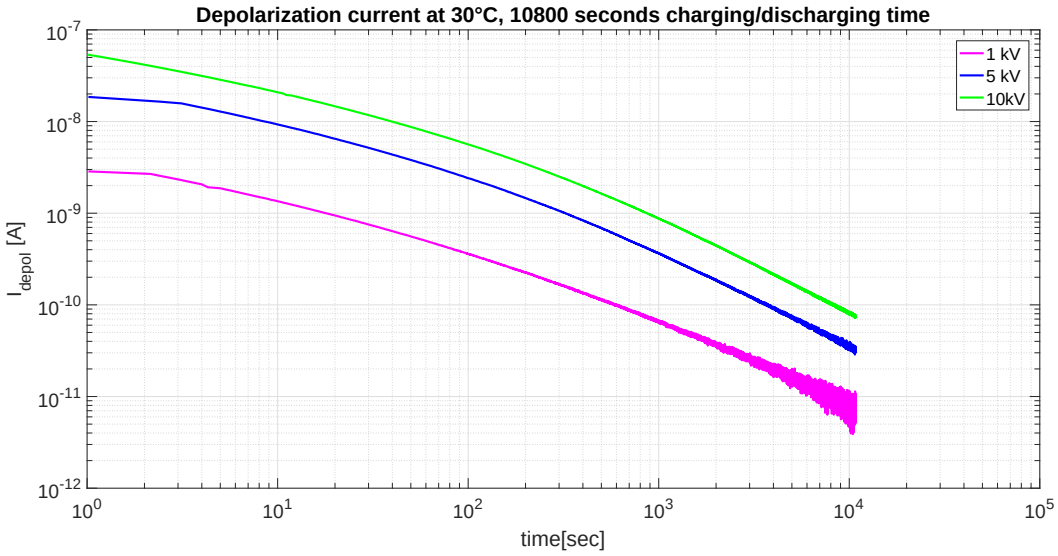

Figure A.62: Depolarization currents for a SCT test object aged at 98°C wet air for 75 days. Tests are done at 30°C, 1kV-5kV-10kV applied voltage and 10800 seconds of charging/discharging time.

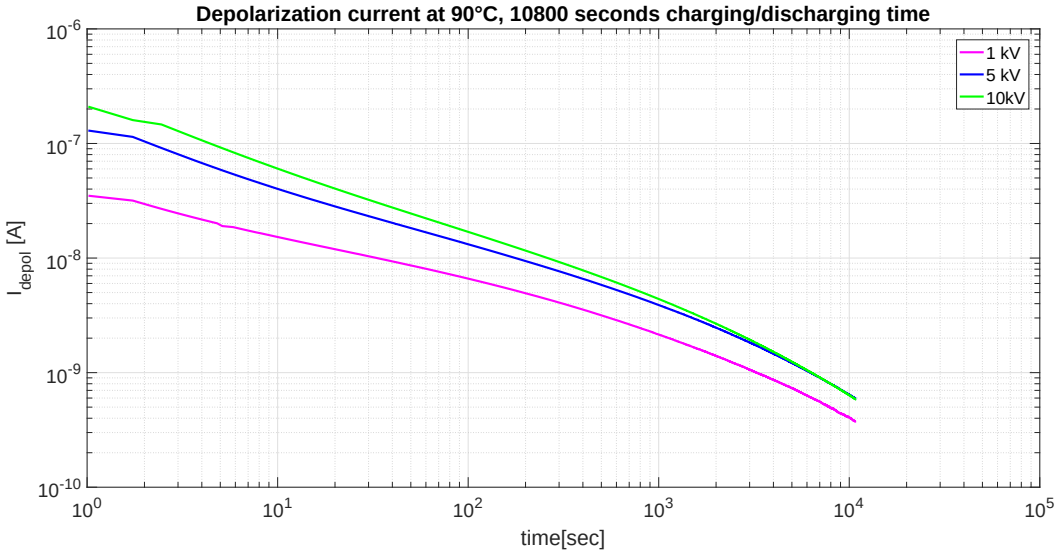

Figure A.63: Depolarization currents for a SCT test object aged at 98°C wet air for 75 days. Tests are done at 90°C, 1kV-5kV-10kV applied voltage and 10800 seconds of charging/discharging time.

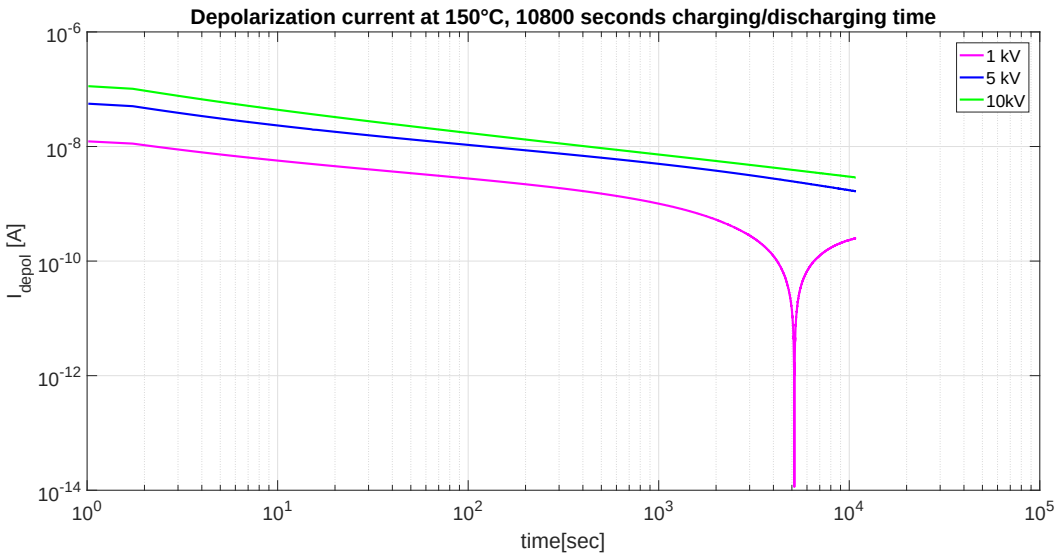

Figure A.64: Depolarization currents for a SCT test object aged at 98°C wet air for 75 days. Tests are done at 150°C, 1kV-5kV-10kV applied voltage and 10800 seconds of charging/discharging time.

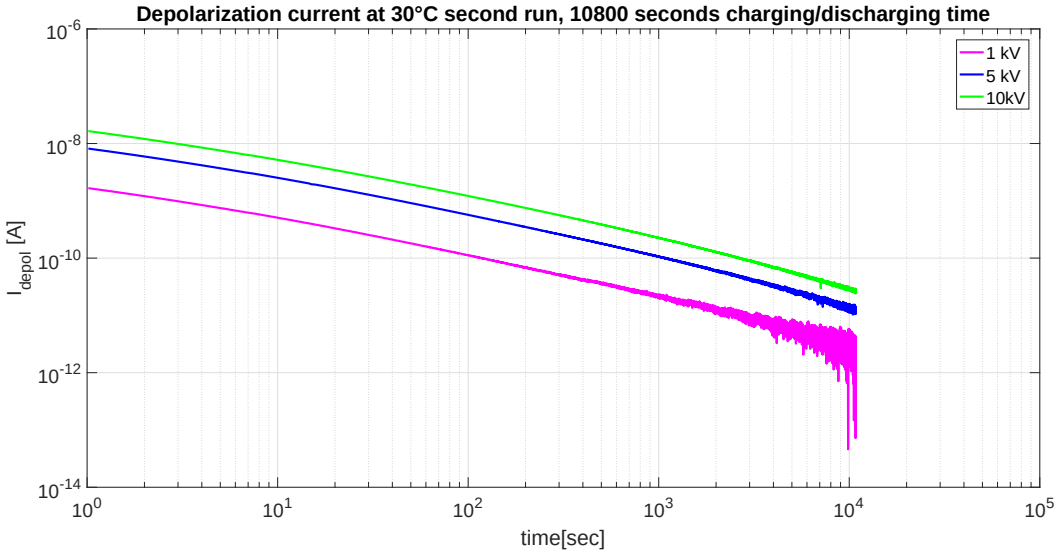

Figure A.65: Depolarization currents for a SCT test object aged at 98°C wet air for 75 days. Tests are done at 30°C second run, 1kV-5kV-10kV applied voltage and 10800 seconds of charging/discharging time.

SCT test object aged at 150°C dry air for 15 days

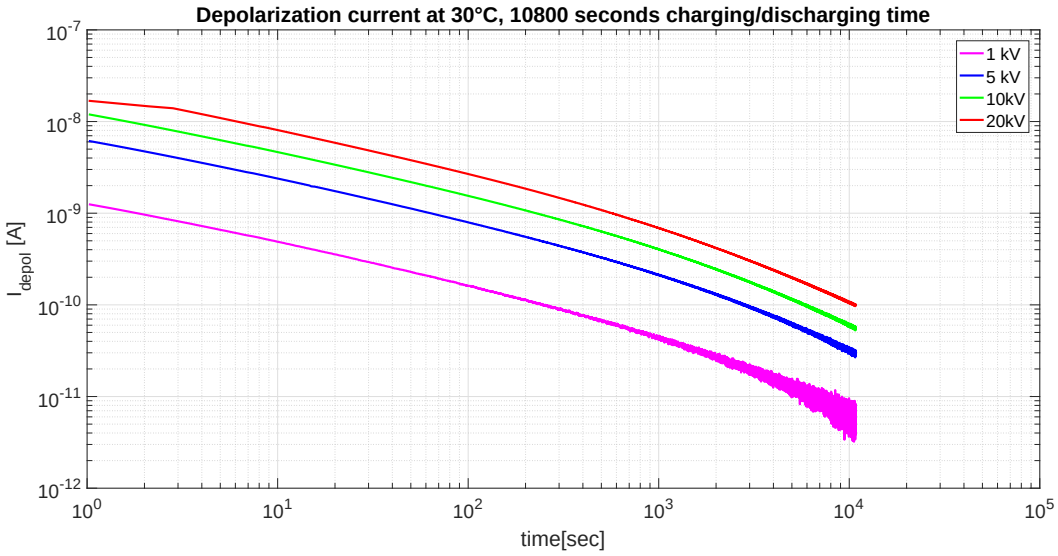

Figure A.66: Depolarization currents for a SCT test object aged at 150°C dry air for 15 days. Tests are done at 30°C, 1kV-5kV-10kV-20kV applied voltage and 10800 seconds of charging/discharging time.

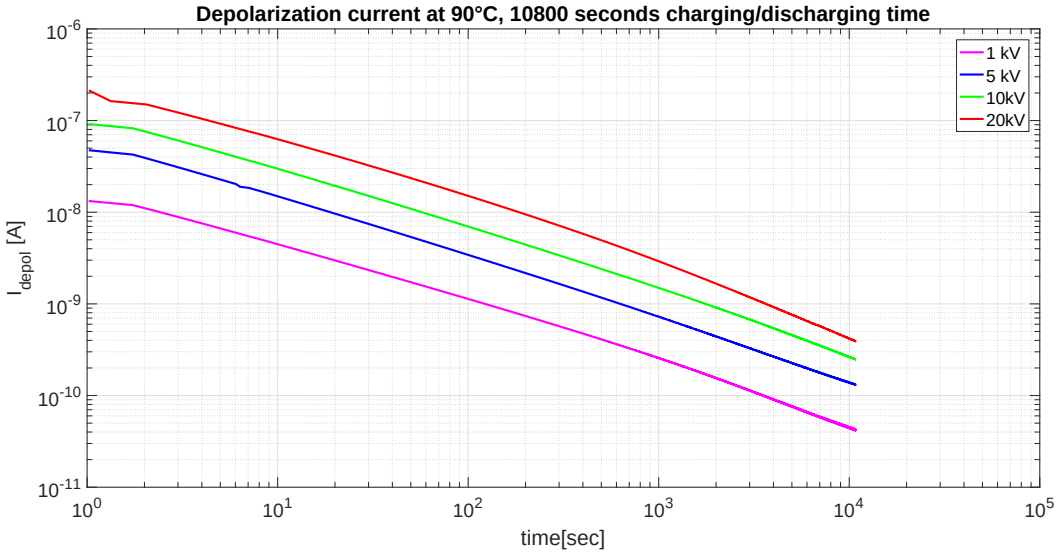

Figure A.67: Depolarization currents for a SCT test object aged at 150°C dry air for 15 days. Tests are done at 90°C, 1kV-5kV-10kV-20kV applied voltage and 10800 seconds of charging/discharging time.

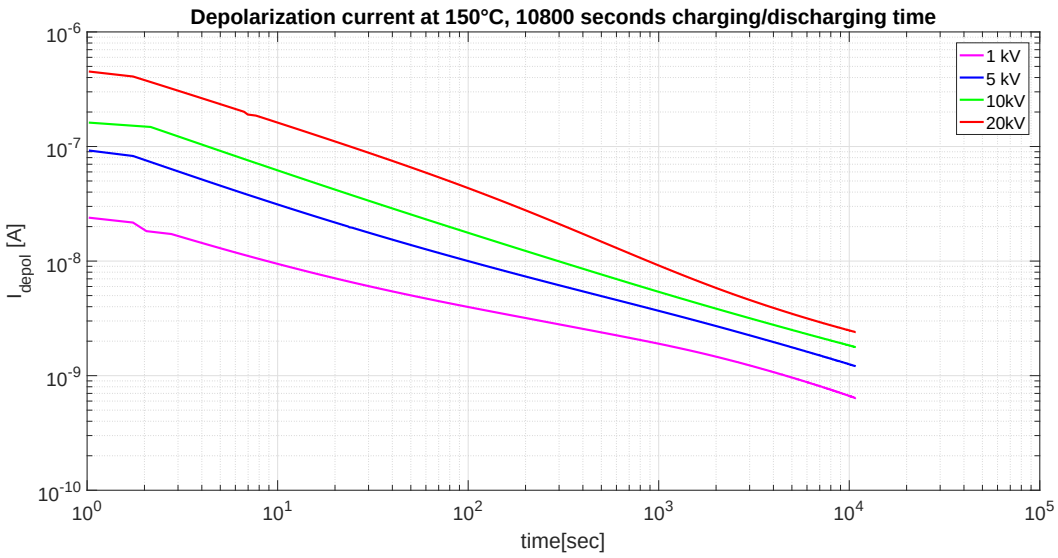

Figure A.68: Depolarization currents for a SCT test object aged at 150°C dry air for 15 days. Tests are done at 150°C, 1kV-5kV-10kV-20kV applied voltage and 10800 seconds of charging/discharging time.

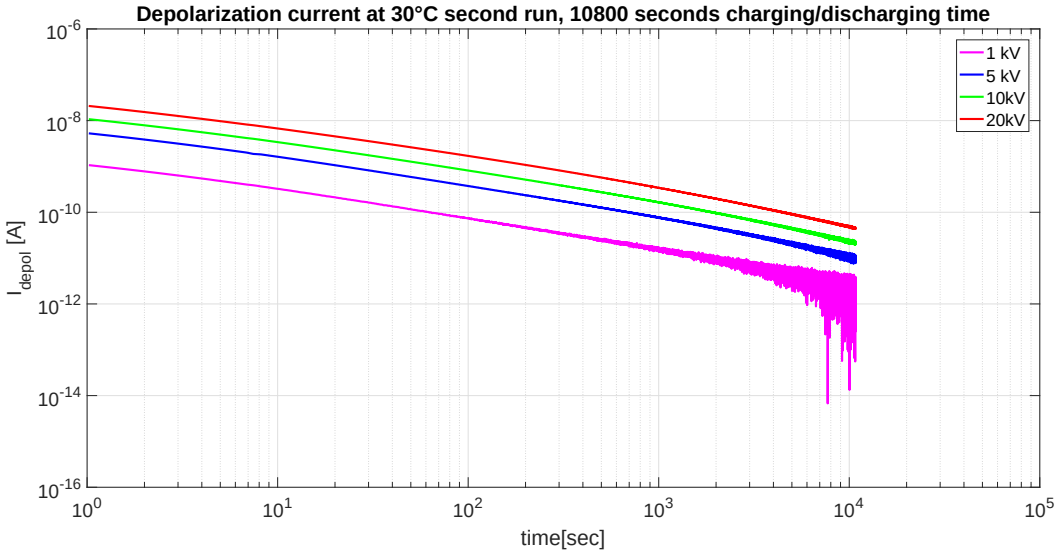

Figure A.69: Depolarization currents for a SCT test object aged at 150°C dry air for 15 days. Tests are done at 30°C second run, 1kV-5kV-10kV-20kV applied voltage and 10800 seconds of charging/discharging time.

SCT test object aged at 150°C dry air for 50 days

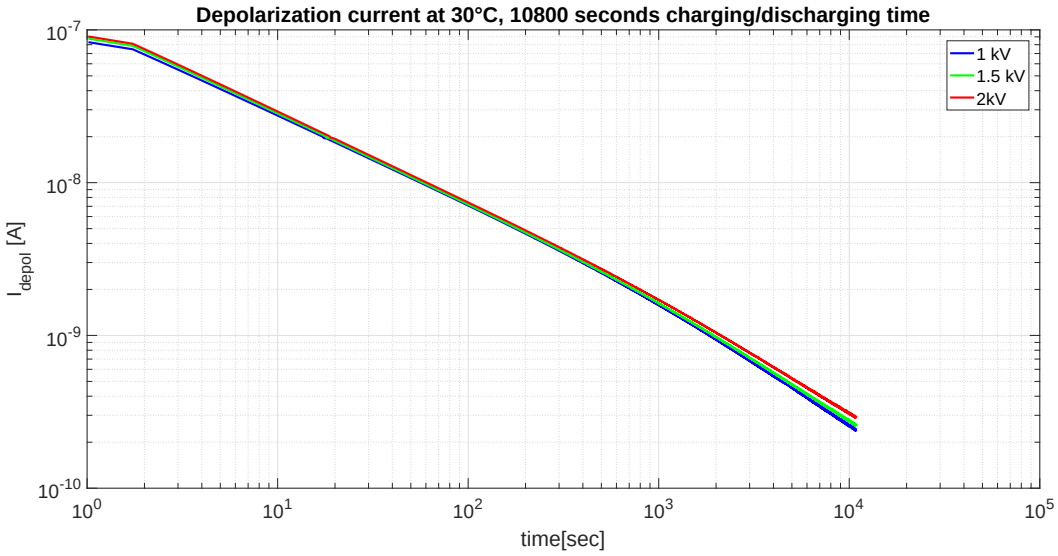

Figure A.70: Depolarization currents for a SCT test object aged at 150°C dry air for 50 days. Tests are done at 30°C, 1kV-1.5kV-2kV applied voltage and 10800 seconds of charging/discharging time.

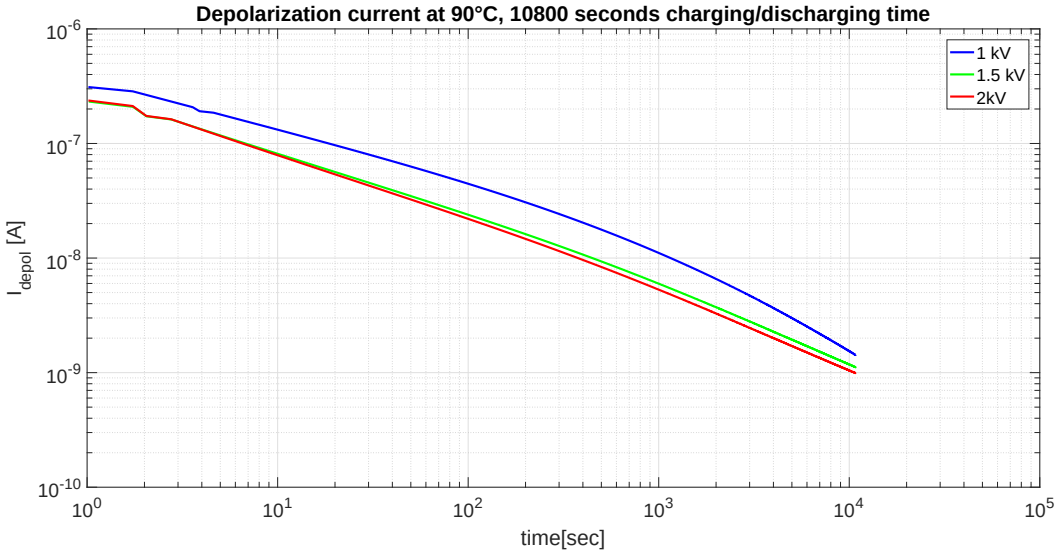

Figure A.71: Depolarization currents for a SCT test object aged at 150°C dry air for 50 days. Tests are done at 90°C, 1kV-1.5kV-2kV applied voltage and 10800 seconds of charging/discharging time.

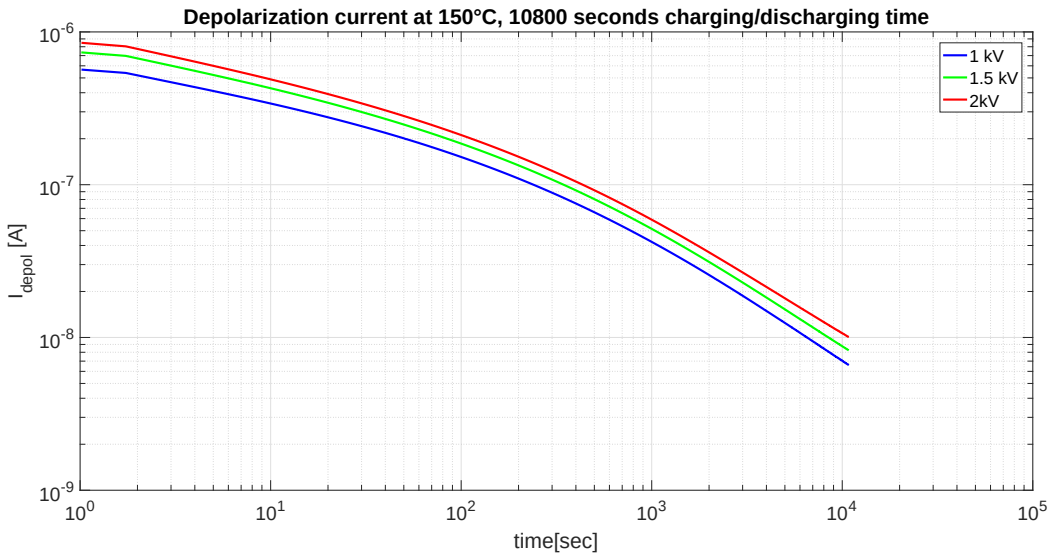

Figure A.72: Depolarization currents for a SCT test object aged at 150°C dry air for 50 days. Tests are done at 150°C, 1kV-1.5kV-2kV applied voltage and 10800 seconds of charging/discharging time.

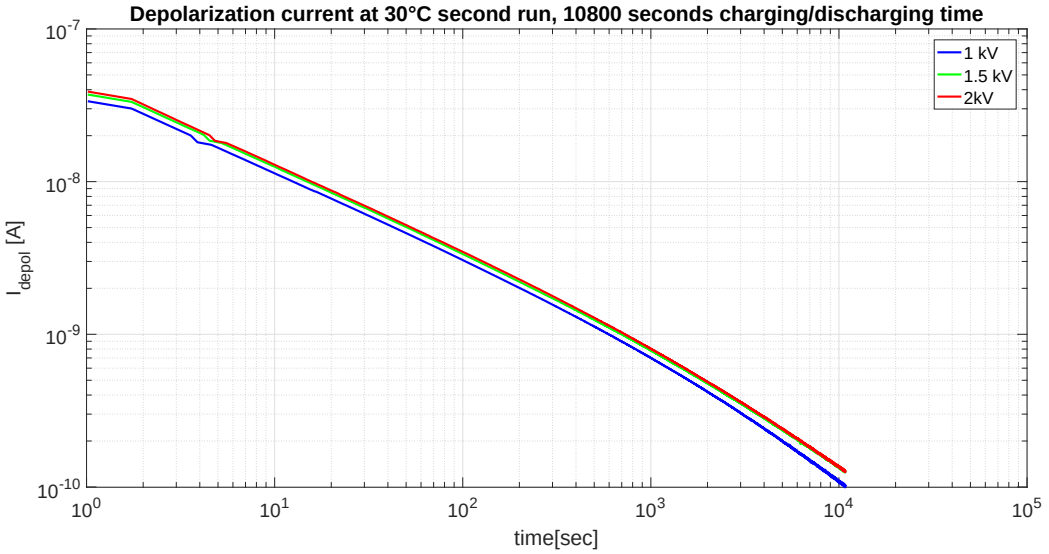

Figure A.73: Depolarization currents for a SCT test object aged at 150°C dry air for 50 days. Tests are done at 30°C second run, 1kV-1.5kV-2kV applied voltage and 10800 seconds of charging/discharging time.

SCT reference test object subjected to water absorption at 90°C for 30 days

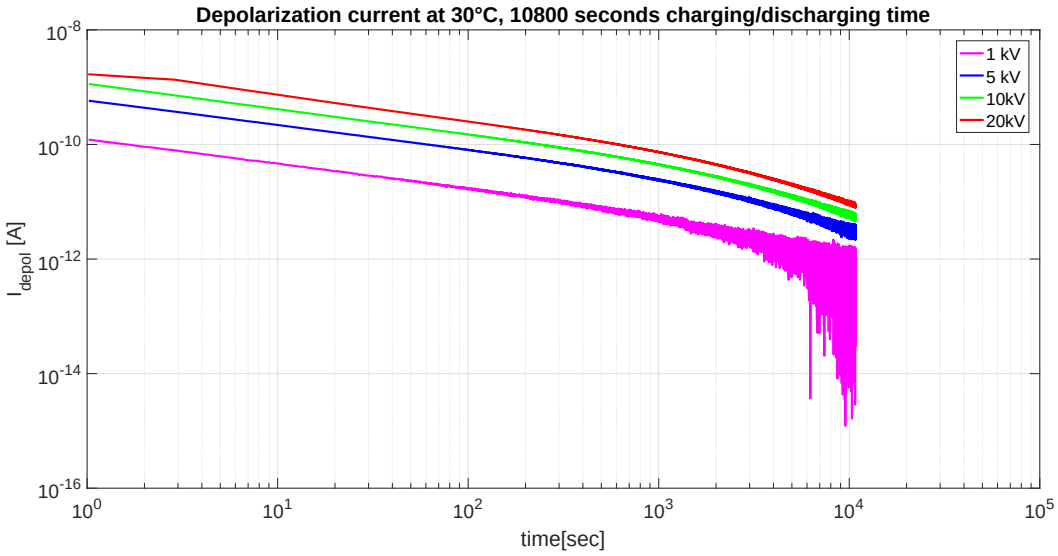

Figure A.74: Depolarization currents for a reference SCT test object, subjected to water absorption at 90°C for 30 days. Tests are done at 30°C, 95% RH, 1kV-5kV-10kV-20kV applied voltage and 10800 seconds of charging/discharging time.

SCT test object aged at 150°C for 15 days and subjected to water absorption at 90°C for 30 days

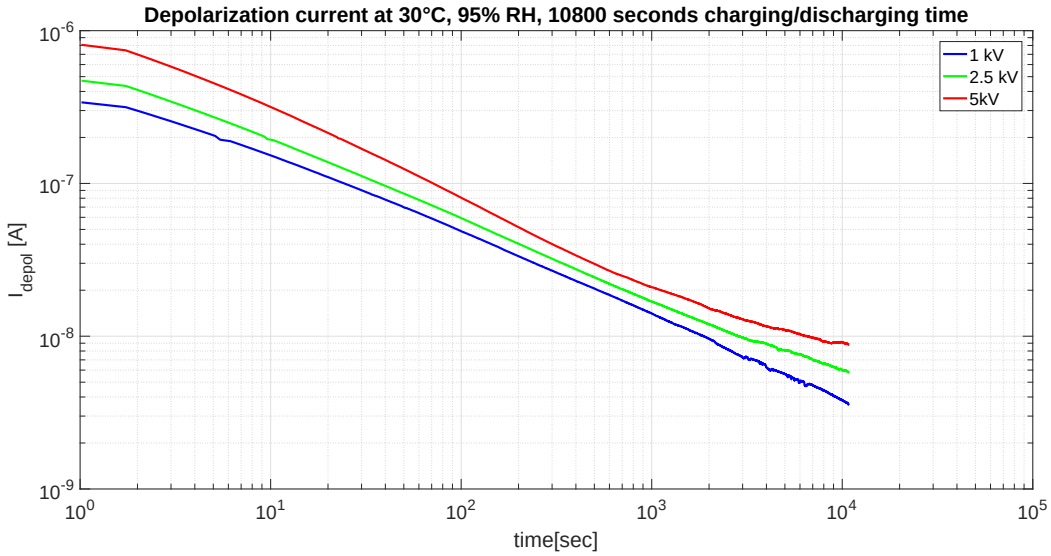

Figure A.75: Depolarization currents for a SCT test object aged at 150°C for 15 days and subjected to water absorption at 90°C for 30 days. Tests are done at 30°C, 95% RH, 1kV-2.5kV-5kV applied voltage and 10800 seconds of charging/discharging time.

Conductivity

Conductivity results for a reference SCT test object

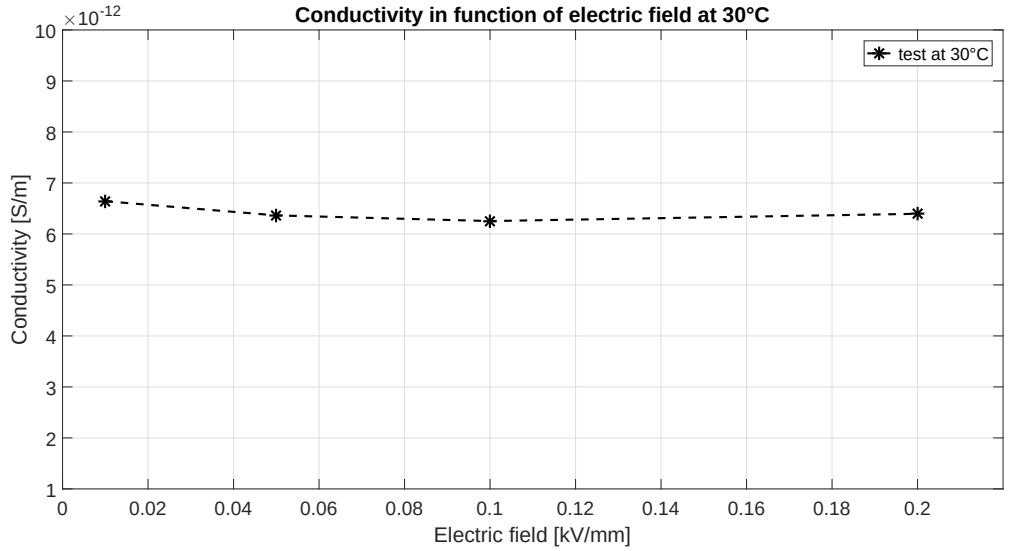

Figure A.76: Conductivity for a reference SCT test object. Tests are done at 30°C, 1kV-5kV-10kV-20kV applied voltage and 10800 seconds of charging/discharging time.

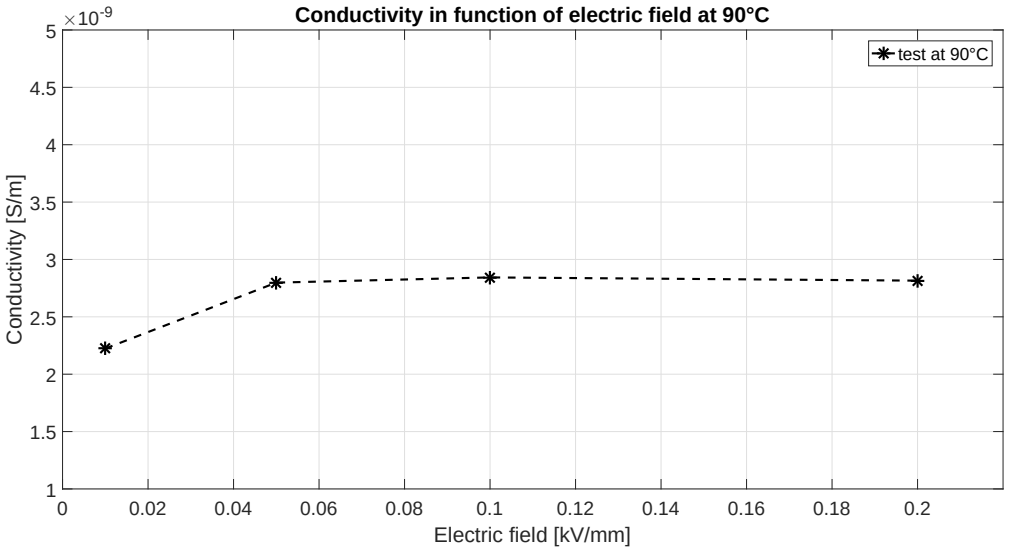

Figure A.77: Conductivity for a reference SCT test object. Tests are done at 90°C, 1kV-5kV-10kV-20kV applied voltage and 10800 seconds of charging/discharging time.

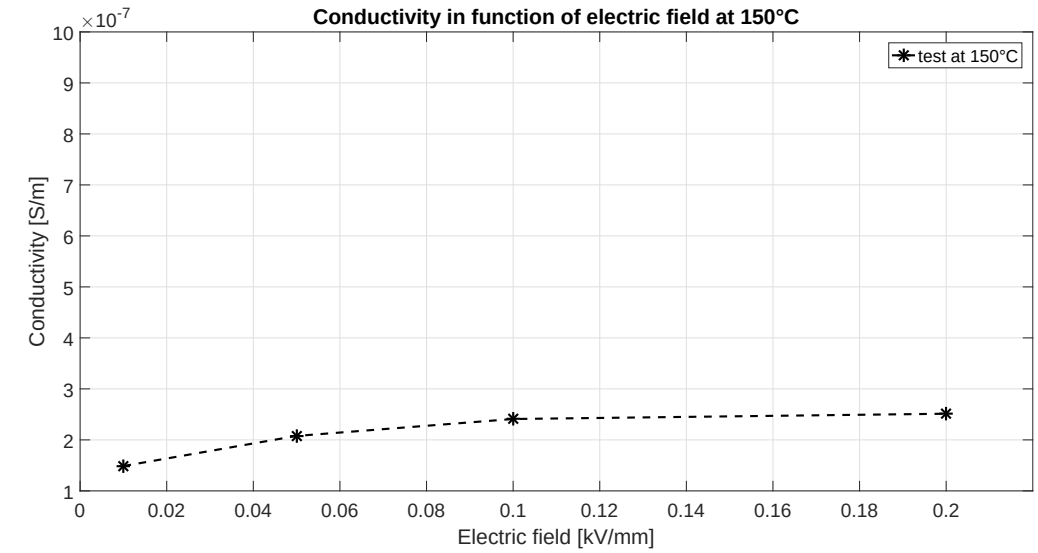

Figure A.78: Conductivity for a reference SCT test object. Tests are done at 150°C, 1kV-5kV-10kV-20kV applied voltage and 10800 seconds of charging/discharging time.

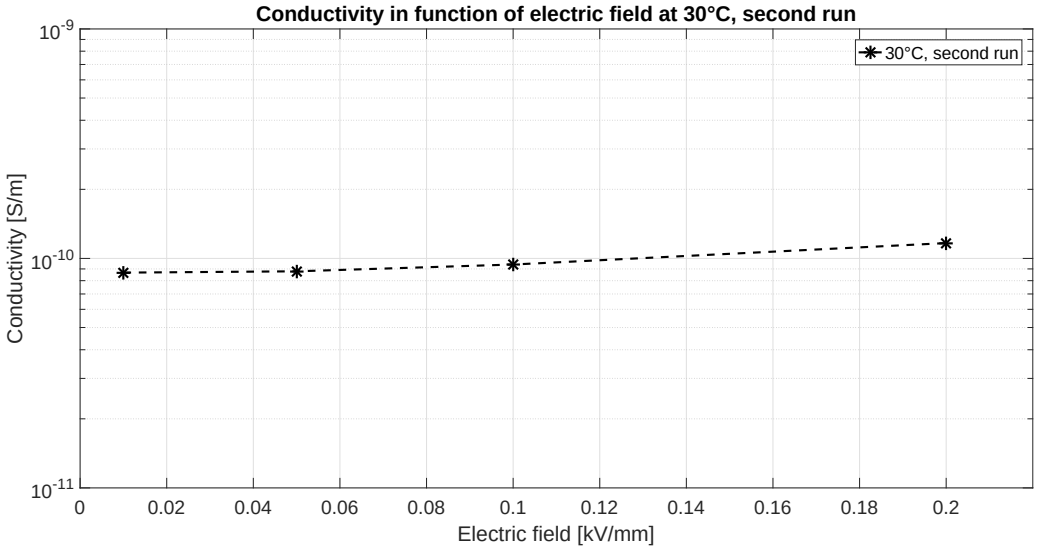

Figure A.79: Conductivity for a reference SCT test object. Tests are done at 30°C (second run), 1kV-5kV-10kV-20kV applied voltage and 10800 seconds of charging/discharging time.

Conductivity results for a SCT test object aged at 98°C dry air for 50 days

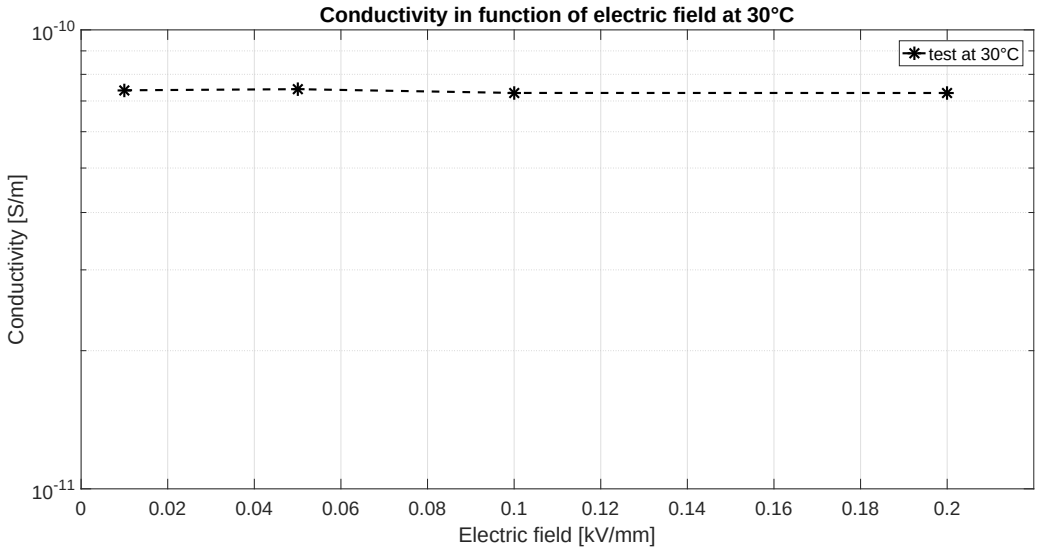

Figure A.80: Conductivity for a SCT test object aged at 98°C dry air for 50 days. Tests are done at 30°C, 1kV-5kV-10kV-20kV applied voltage and 10800 seconds of charging/discharging time.

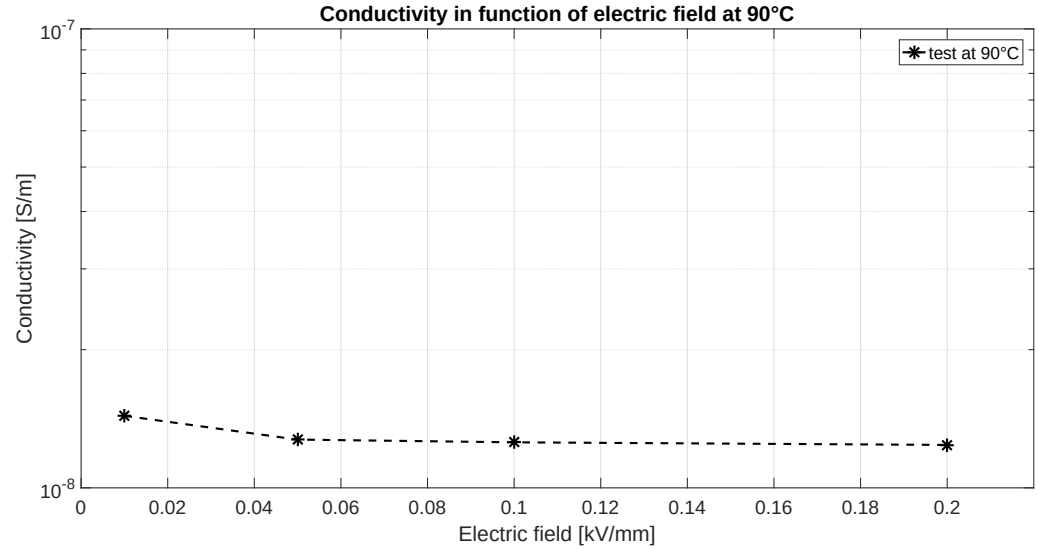

Figure A.81: Conductivity for a SCT test object aged at 98°C dry air for 50 days. Tests are done at 90°C, 1kV-5kV-10kV-20kV applied voltage and 10800 seconds of charging/discharging time.

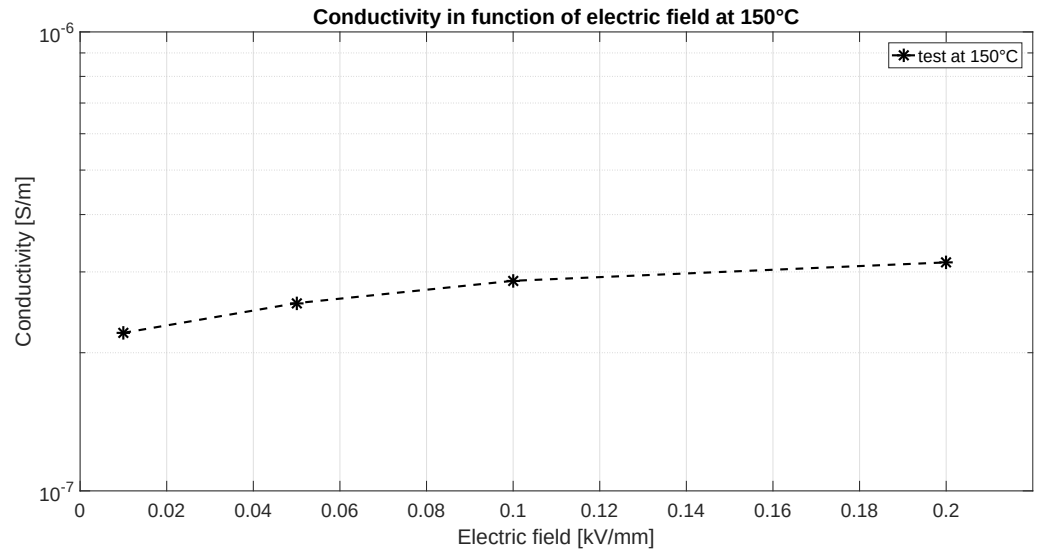

Figure A.82: Conductivity for a SCT test object aged at 98°C dry air for 50 days. Tests are done at 150°C, 1kV-5kV-10kV-20kV applied voltage and 10800 seconds of charging/discharging time.

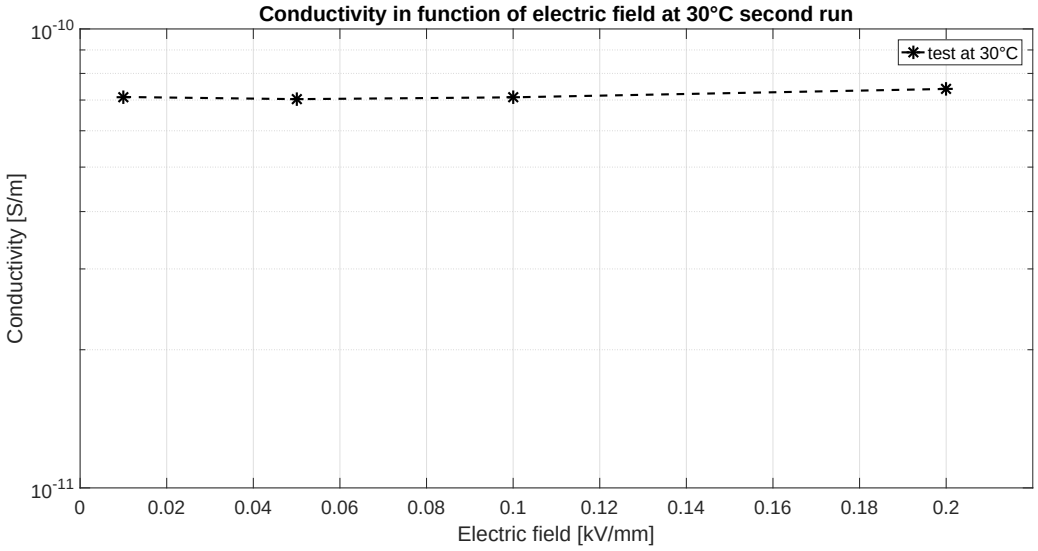

Figure A.83: Conductivity for a SCT test object aged at 98°C dry air for 50 days. Tests are done at 30°C second run, 1kV-5kV-10kV-20kV applied voltage and 10800 seconds of charging/discharging time.

Conductivity results for a SCT test object aged at 98°C dry air for 75 days

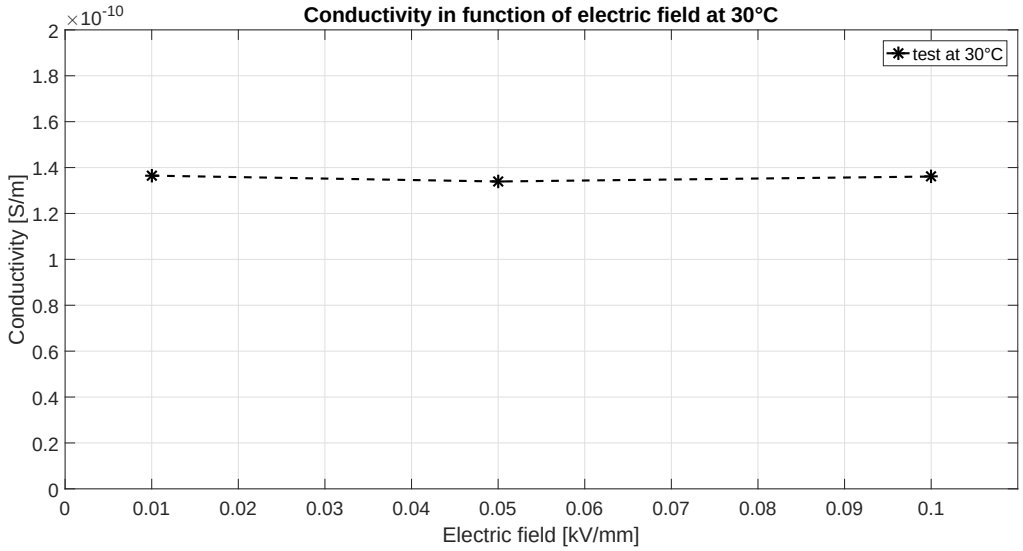

Figure A.84: Conductivity for a SCT test object aged at 98°C dry air for 75 days. Tests are done at 30°C, 1kV-5kV-10kV applied voltage and 10800 seconds of charging/discharging time.

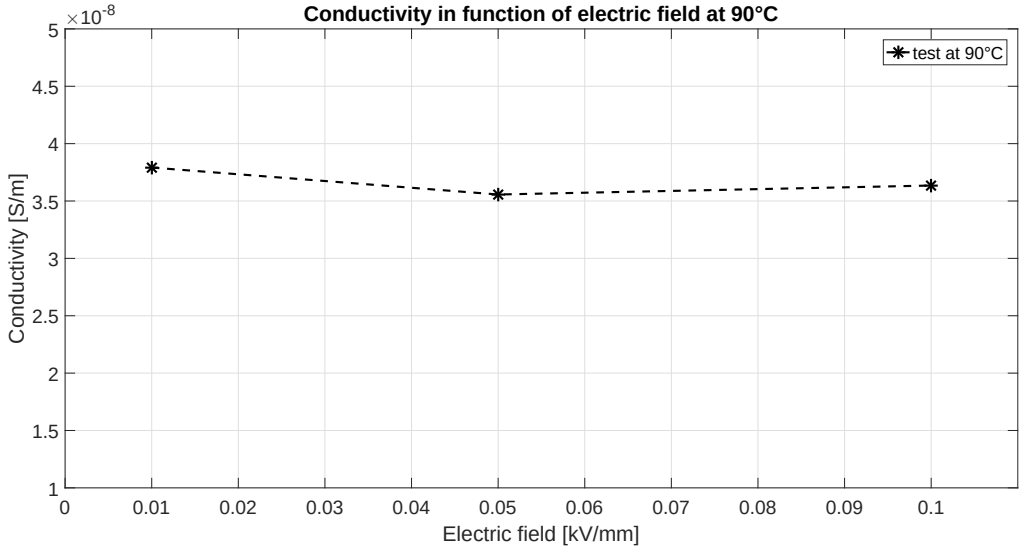

Figure A.85: Conductivity for a SCT test object aged at 98°C dry air for 75 days. Tests are done at 90°C, 1kV-5kV-10kV applied voltage and 10800 seconds of charging/discharging time.

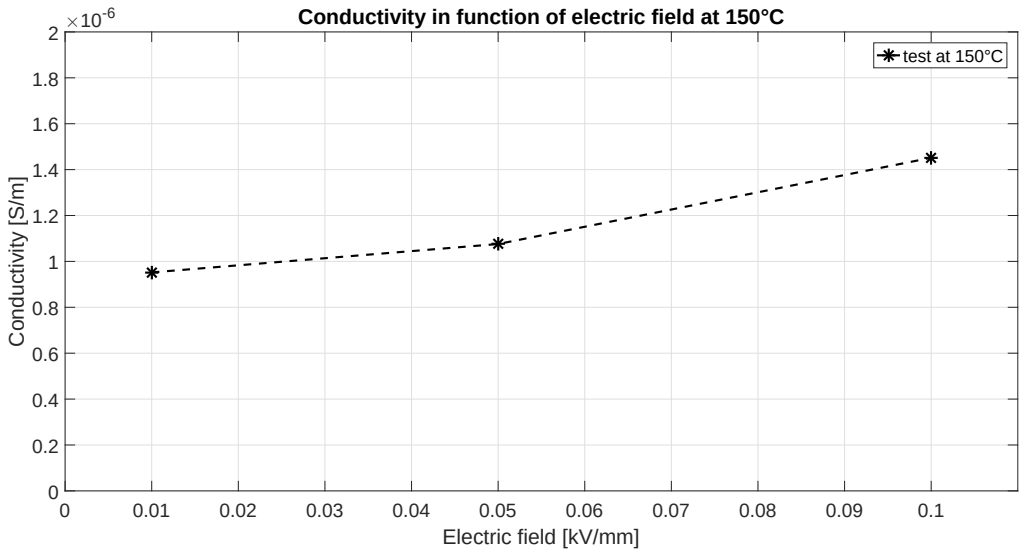

Figure A.86: Conductivity for a SCT test object aged at 98°C dry air for 75 days. Tests are done at 150°C, 1kV-5kV-10kV applied voltage and 10800 seconds of charging/discharging time.

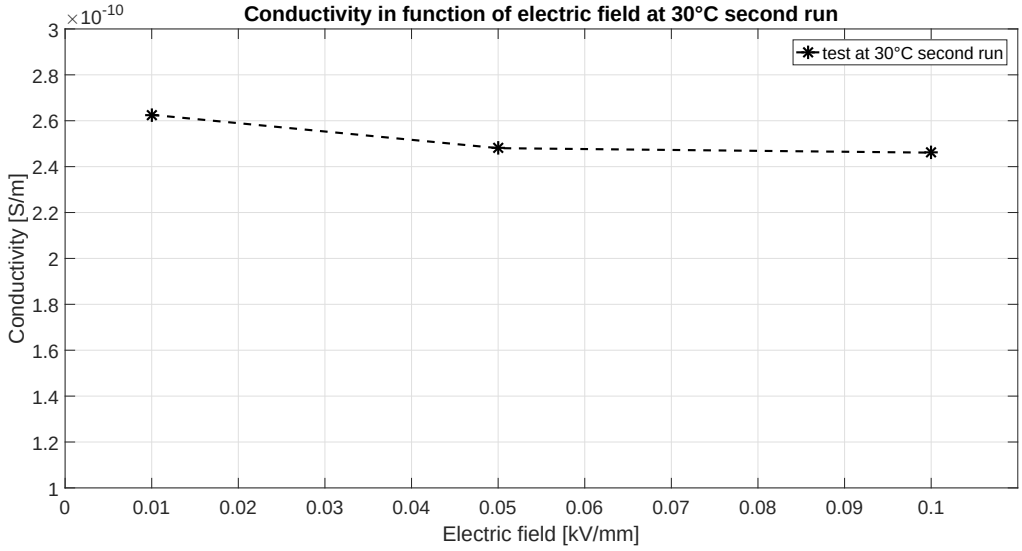

Figure A.87: Conductivity for a SCT test object aged at 98°C dry air for 75 days. Tests are done at 30°C second run, 1kV-5kV-10kV applied voltage and 10800 seconds of charging/discharging time.

SCT test object aged at 98°C wet air for 50 days

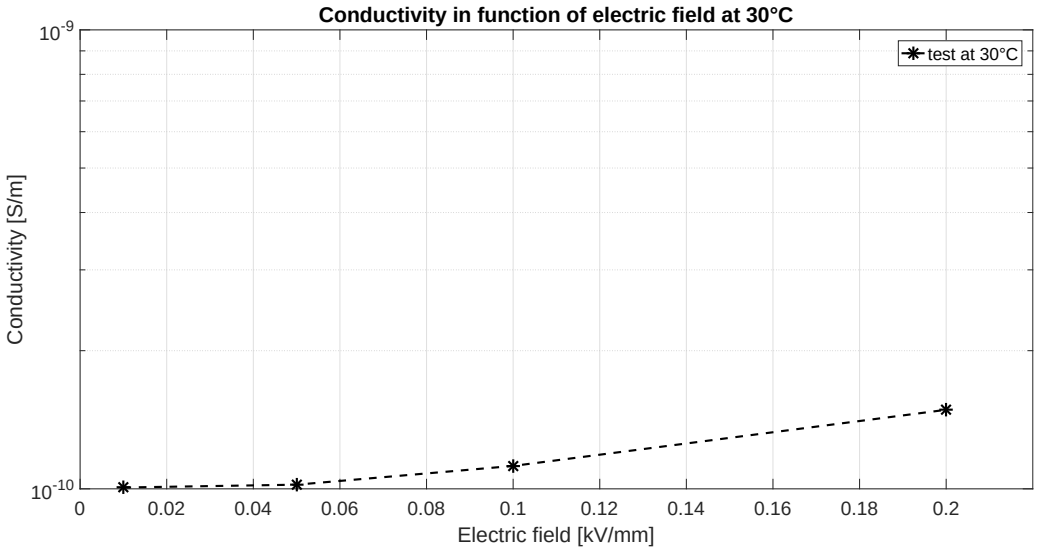

Figure A.88: Conductivity for a SCT test object aged at 98°C wet air for 50 days. Tests are done at 30°C, 1kV-5kV-10kV-20kV applied voltage and 10800 seconds of charging/discharging time.

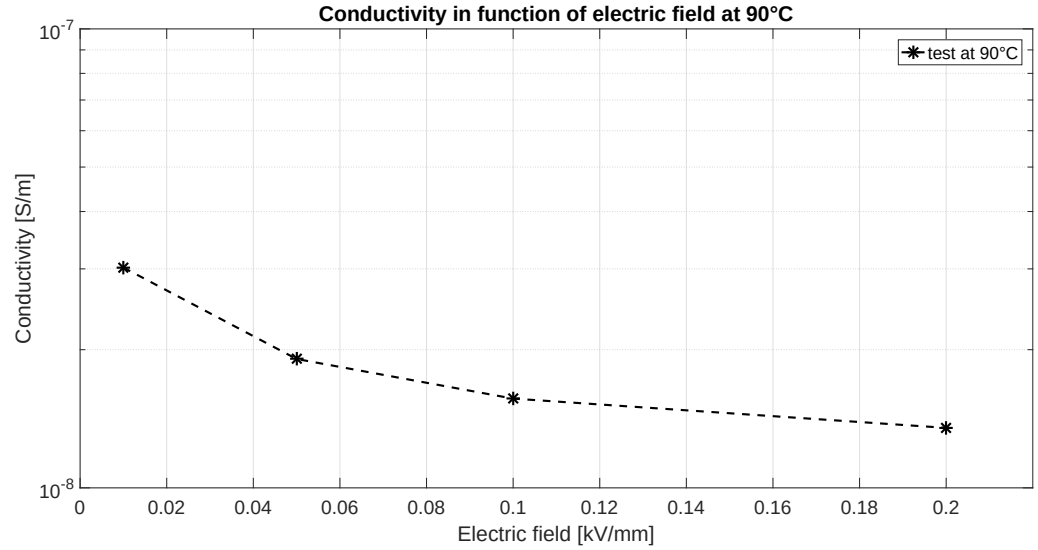

Figure A.89: Conductivity for a SCT test object aged at 98°C wet air for 50 days. Tests are done at 90°C, 1kV-5kV-10kV-20kV applied voltage and 10800 seconds of charging/discharging time.

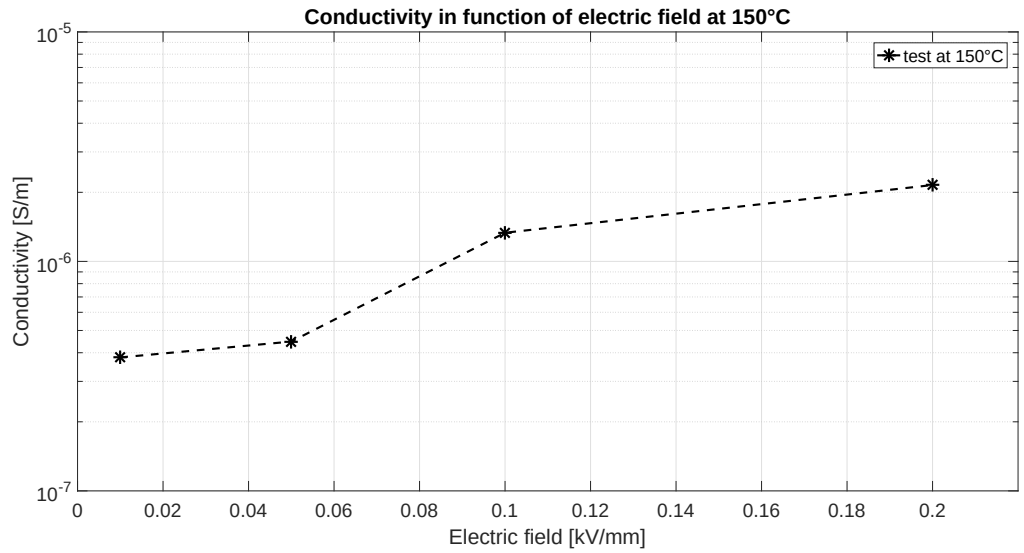

Figure A.90: Conductivity for a SCT test object aged at 98°C wet air for 50 days. Tests are done at 150°C, 1kV-5kV-10kV-20kV applied voltage and 10800 seconds of charging/discharging time.

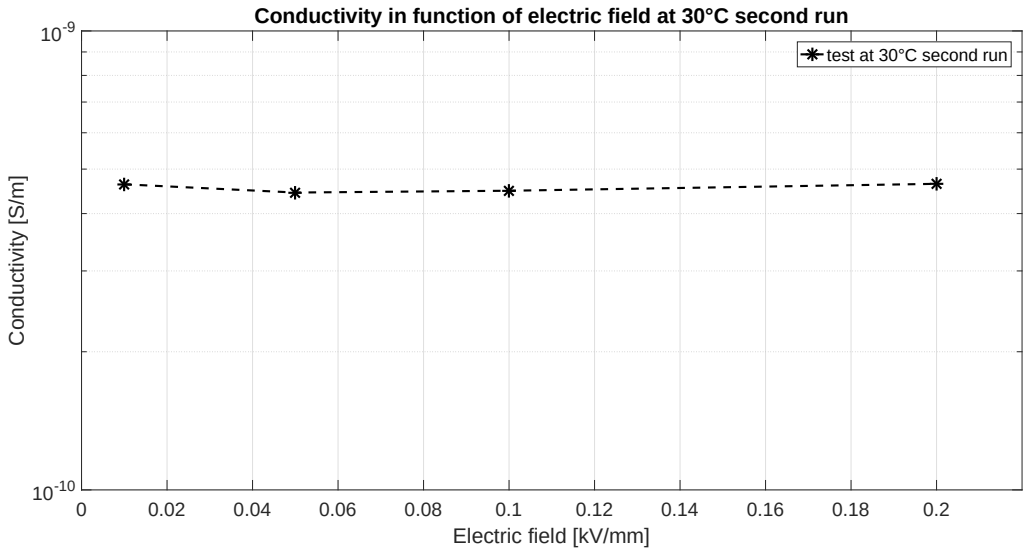

Figure A.91: Conductivity for a SCT test object aged at 98°C wet air for 50 days. Tests are done at 30°C second run, 1kV-5kV-10kV-20kV applied voltage and 10800 seconds of charging/discharging time.

SCT test object aged at 98°C wet air for 75 days

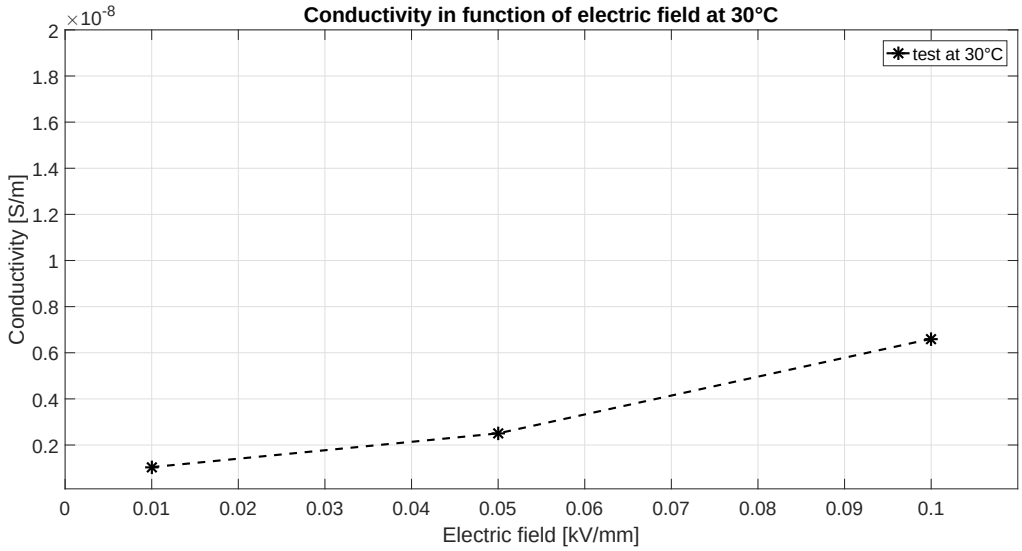

Figure A.92: Conductivity for a SCT test object aged at 98°C wet air for 75 days. Tests are done at 30°C, 1kV-5kV-10kV applied voltage and 10800 seconds of charging/discharging time.

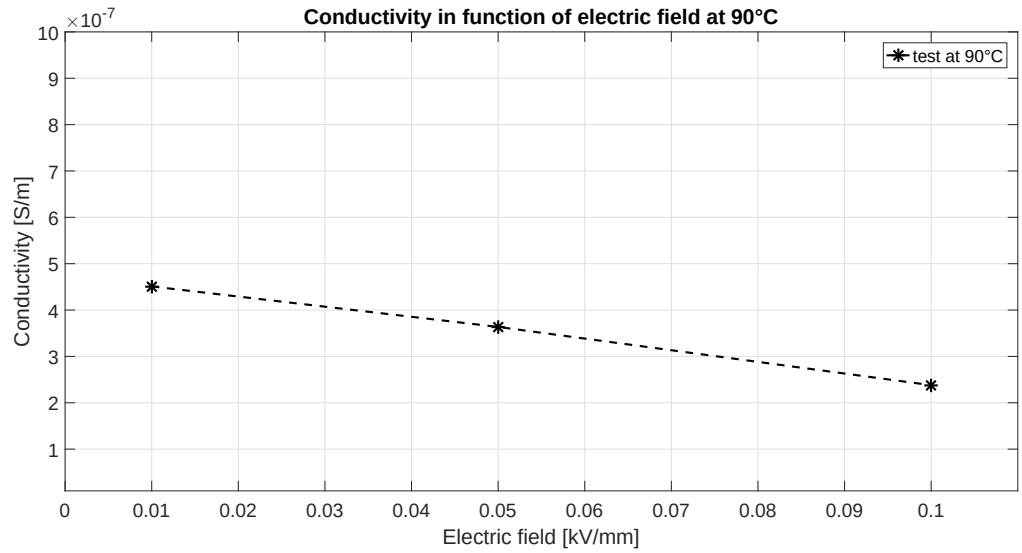

Figure A.93: Conductivity for a SCT test object aged at 98°C wet air for 75 days. Tests are done at 90°C, 1kV-5kV-10kV applied voltage and 10800 seconds of charging/discharging time.

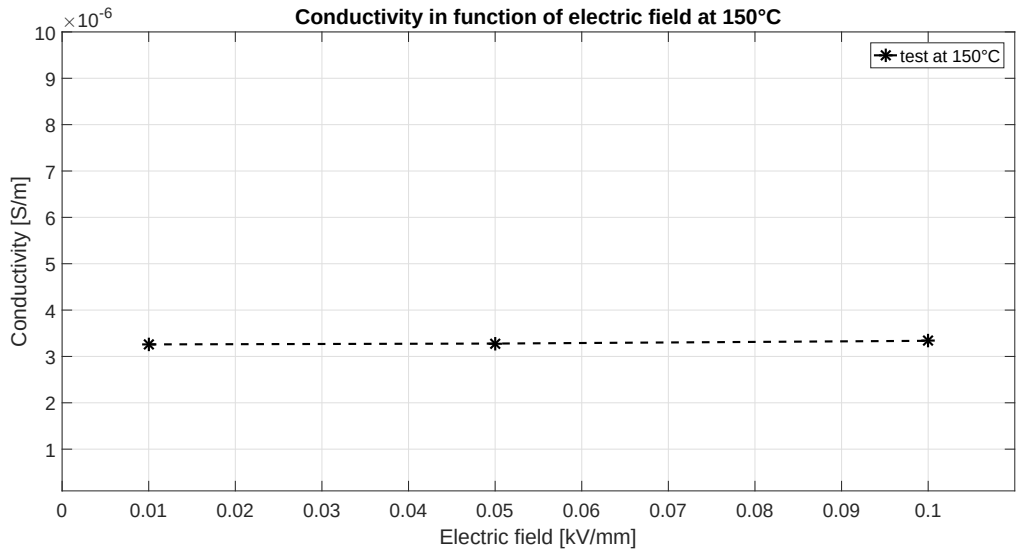

Figure A.94: Conductivity for a SCT test object aged at 98°C wet air for 75 days. Tests are done at 150°C, 1kV-5kV-10kV applied voltage and 10800 seconds of charging/discharging time.

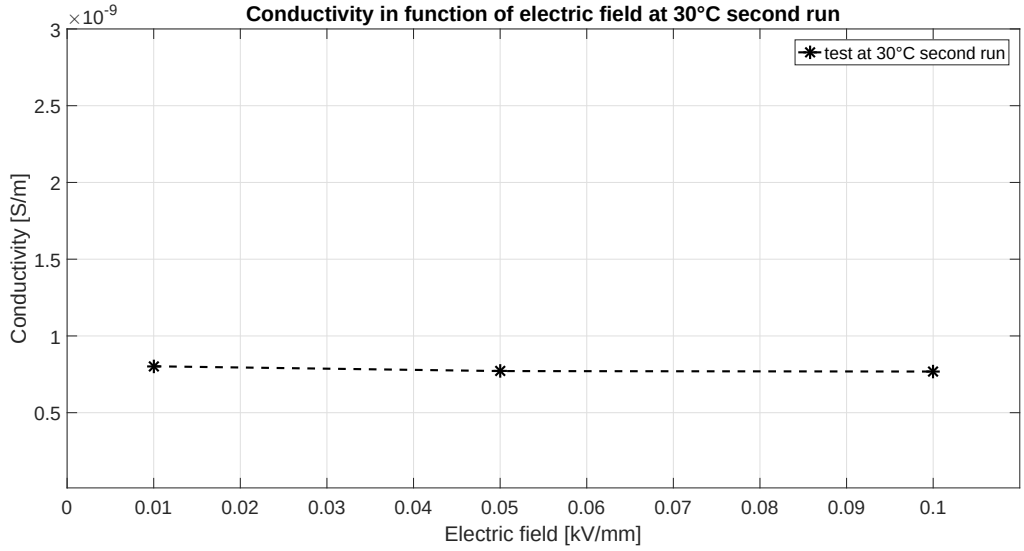

Figure A.95: Conductivity for a SCT test object aged at 98°C wet air for 75 days. Tests are done at 30°C second run, 1kV-5kV-10kV applied voltage and 10800 seconds of charging/discharging time.

Conductivity results for a SCT test object aged at 150°C dry air for 15 days

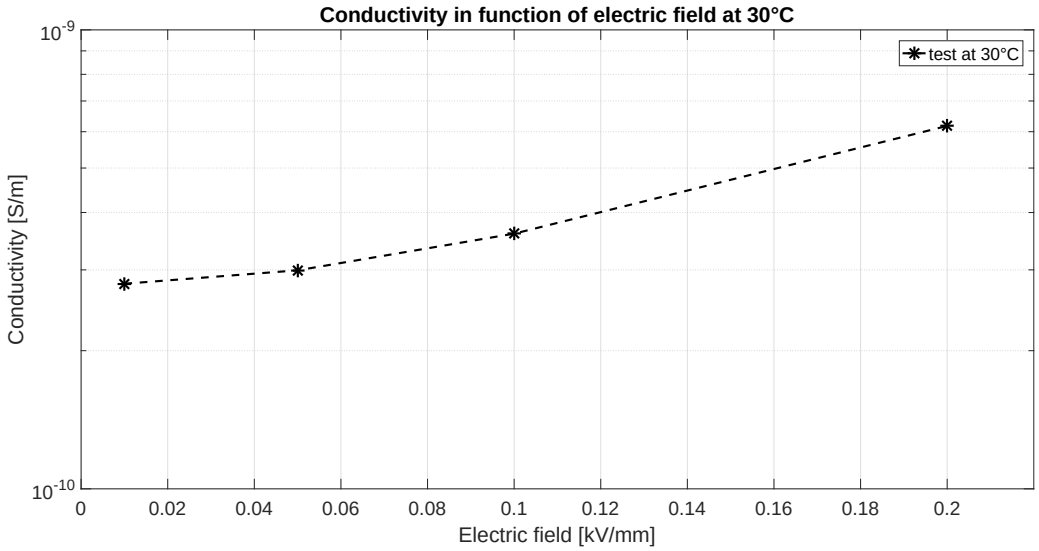

Figure A.96: Conductivity for a SCT test object aged at 150°C dry air for 15 days. Tests are done at 30°C, 1kV-5kV-10kV-20kV applied voltage and 10800 seconds of charging/discharging time.

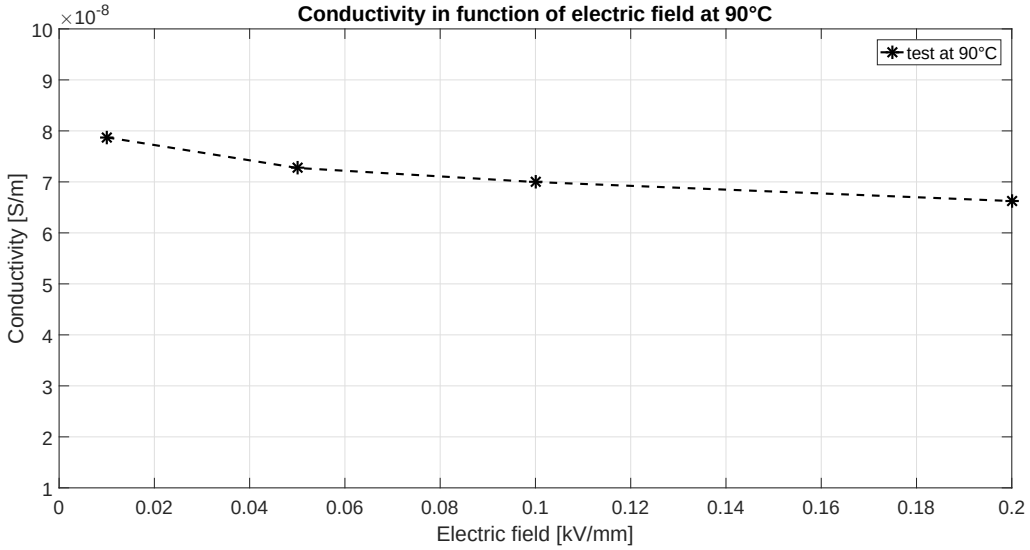

Figure A.97: Conductivity for a SCT test object aged at 150°C dry air for 15 days. Tests are done at 90°C, 1kV-5kV-10kV-20kV applied voltage and 10800 seconds of charging/discharging time.

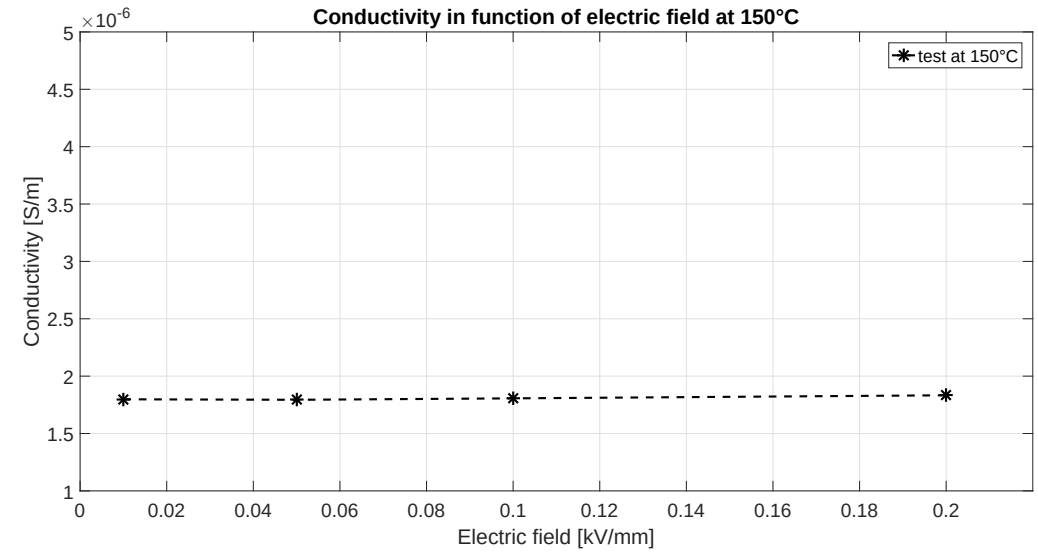

Figure A.98: Conductivity for a SCT test object aged at 150°C dry air for 15 days. Tests are done at 150°C, 1kV-5kV-10kV-20kV applied voltage and 10800 seconds of charging/discharging time.

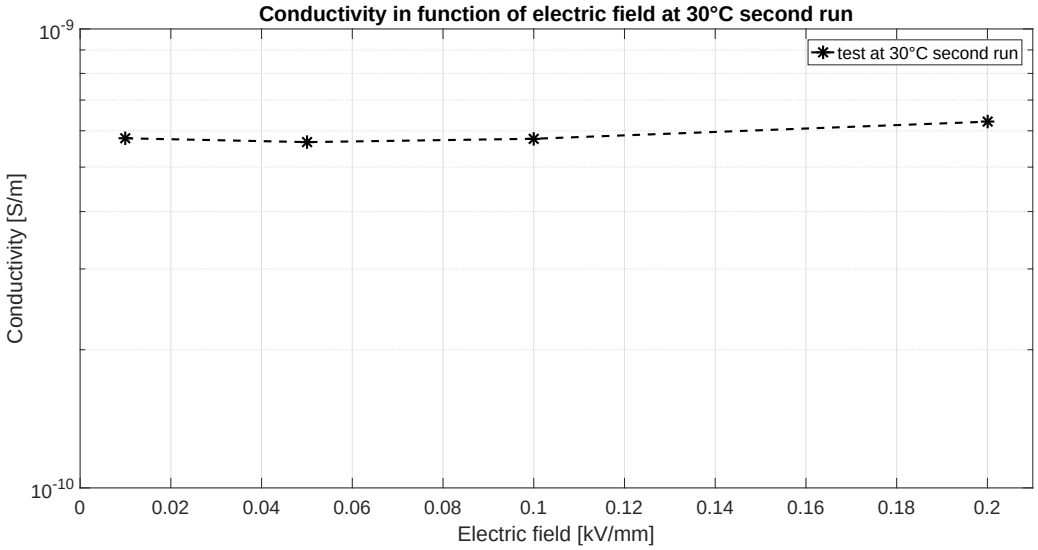

Figure A.99: Conductivity for a SCT test object aged at 150°C dry air for 15 days. Tests are done at 30°C second run, 1kV-5kV-10kV-20kV applied voltage and 10800 seconds of charging/discharging time.

Conductivity results for a SCT test object aged at 150°C dry air for 50 days

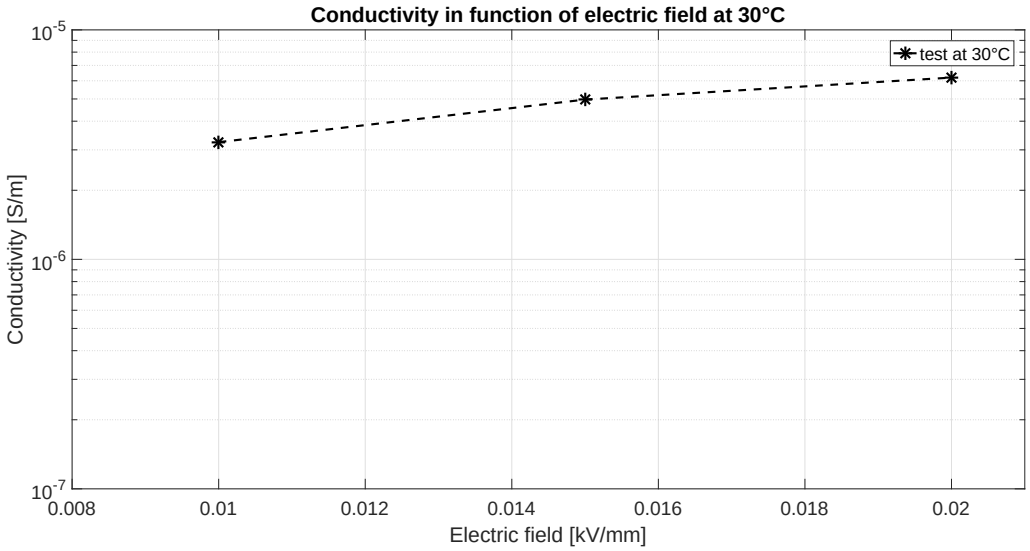

Figure A.100: Conductivity for a SCT test object aged at 150°C dry air for 50 days. Tests are done at 30°C, 1kV-1.5kV-2kV applied voltage and 10800 seconds of charging/discharging time.

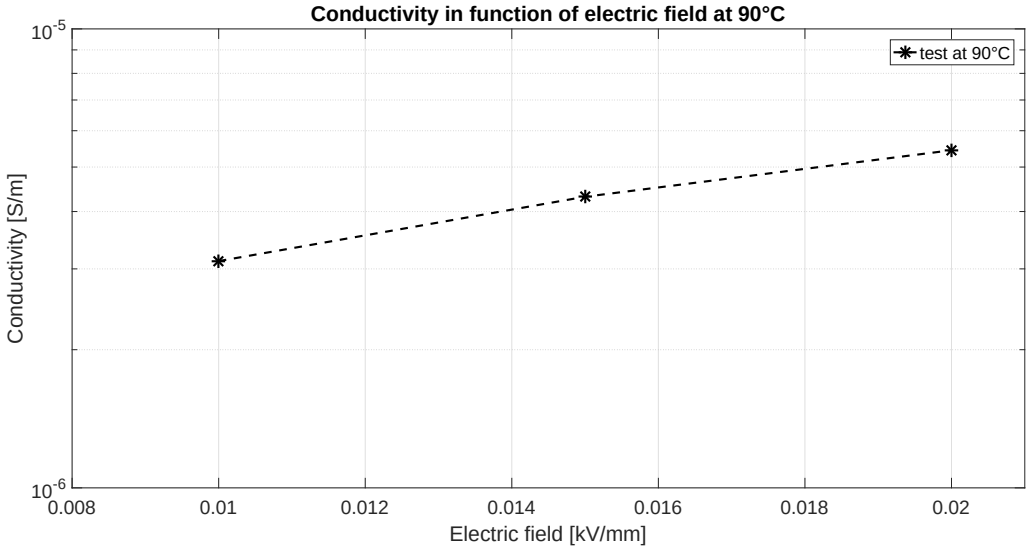

Figure A.101: Conductivity for a SCT test object aged at 150°C dry air for 50 days. Tests are done at 90°C, 1kV-1.5kV-2kV applied voltage and 10800 seconds of charging/discharging time.

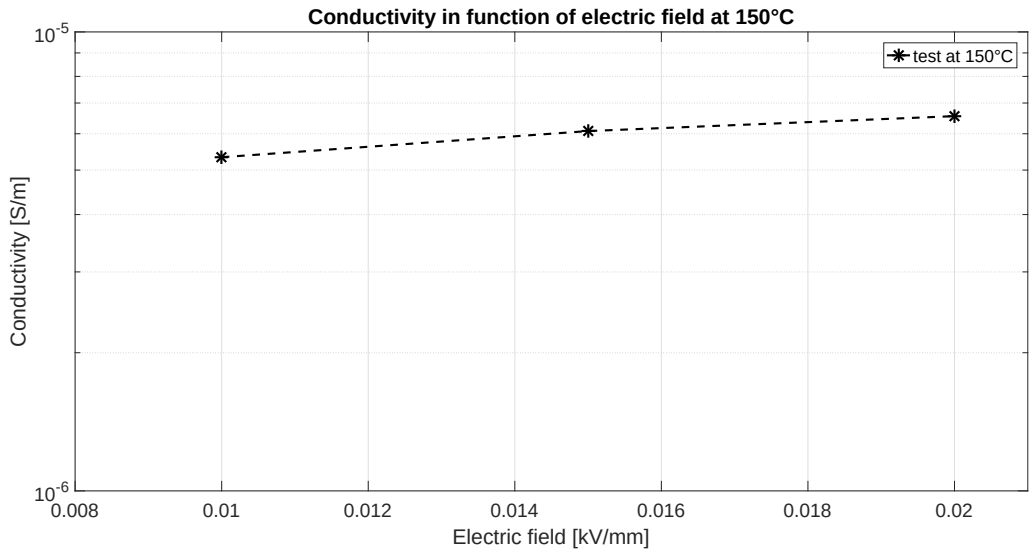

Figure A.102: Conductivity for a SCT test object aged at 150°C dry air for 50 days. Tests are done at 150°C, 1kV-1.5kV-2kV applied voltage and 10800 seconds of charging/discharging time.

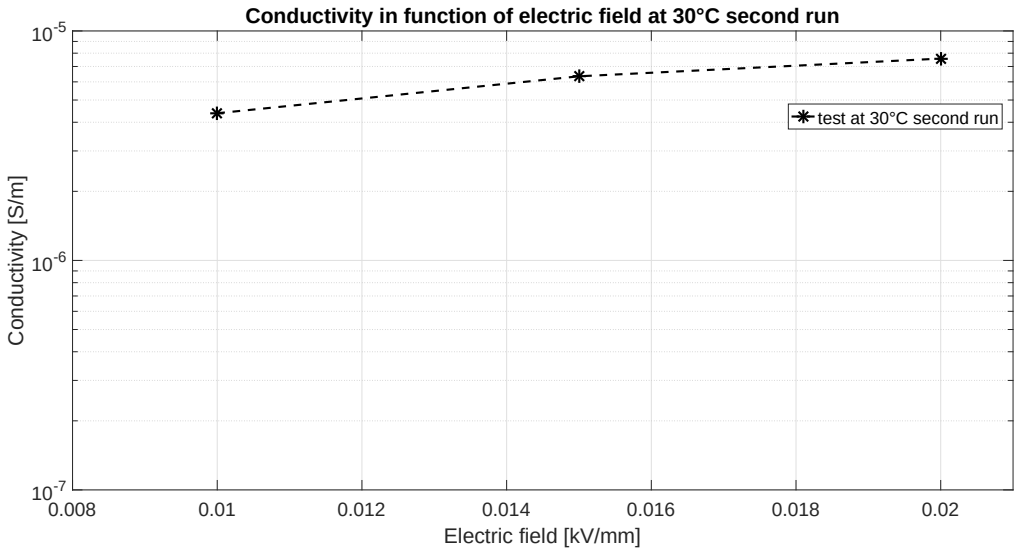

Figure A.103: Conductivity for a SCT test object aged at 150°C dry air for 50 days. Tests are done at 30°C second run, 1kV-1.5kV-2kV applied voltage and 10800 seconds of charging/discharging time.

Coductivity results for a SCT reference test object subjected to water absorption at 90°C for 30 days

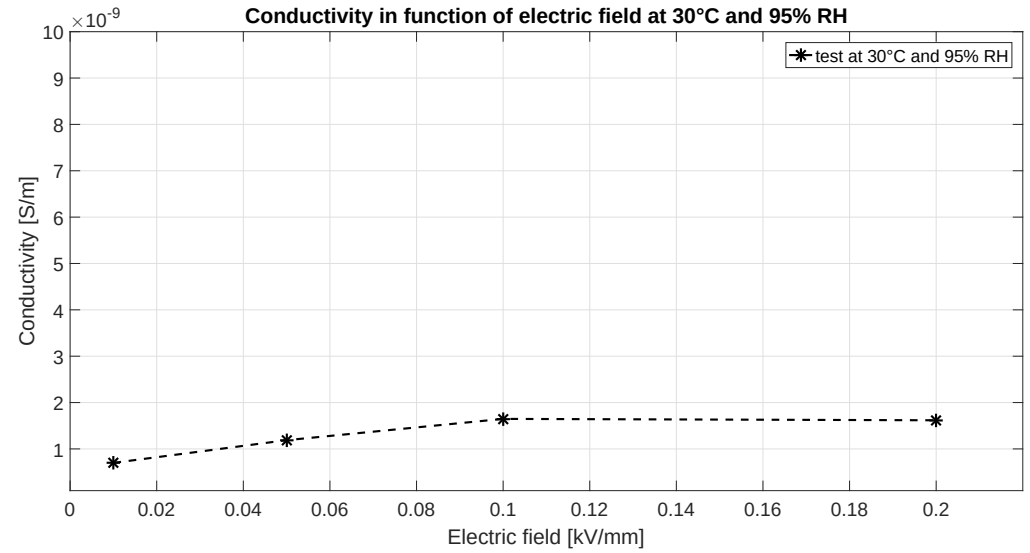

Figure A.104: Conductivity for a reference SCT test object, subjected to water absorption at 90°C for 30 days. Tests are done at 30°C, 95% RH, 1kV-5kV-10kV-20kV applied voltage and 10800 seconds of charging/discharging time.

Conductivity for a SCT test object aged at 150°C for 15 days and subjected to water absorption at 90°C for 30 days

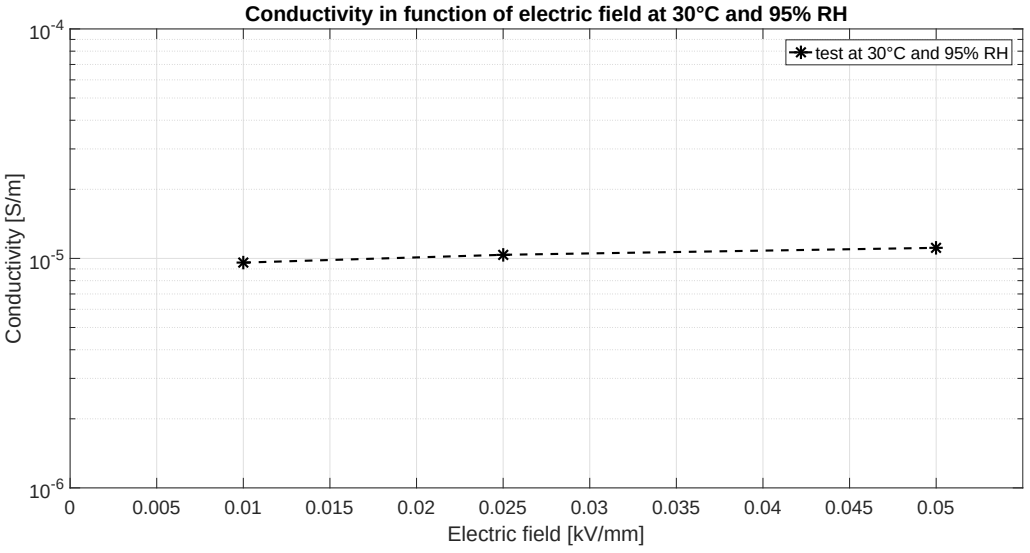

Figure A.105: Conductivity for a SCT test object aged at 150°C for 15 days and subjected to water absorption at 90°C for 30 days. Tests are done at 30°C, 95% RH, 1kV-2.5kV-5kV applied voltage and 10800 seconds of charging/discharging time.

Response Function f(10) Results

Dielectric response function results for a reference SCT test object

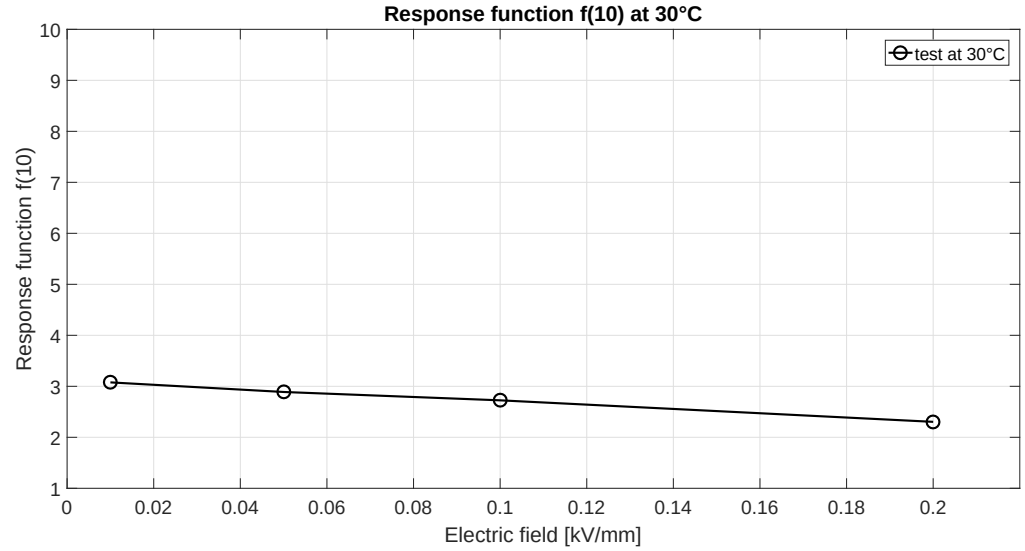

Figure A.106: Response function for a reference SCT test object. Tests are done at 30°C, 1kV-5kV-10kV-20kV applied voltage and 10800 seconds of charging/discharging time.

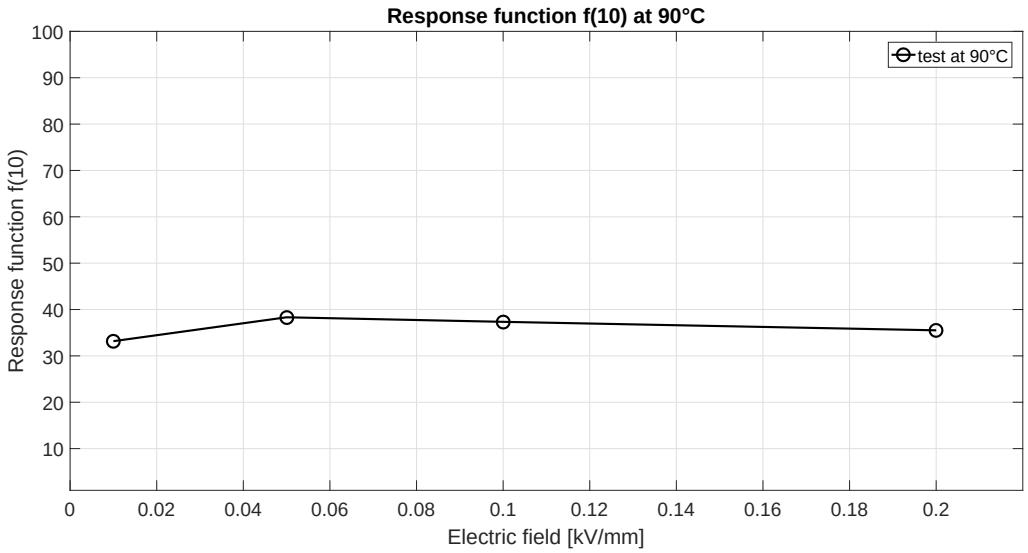

Figure A.107: Response function for a reference SCT test object. Tests are done at 90°C, 1kV-5kV-10kV-20kV applied voltage and 10800 seconds of charging/discharging time.

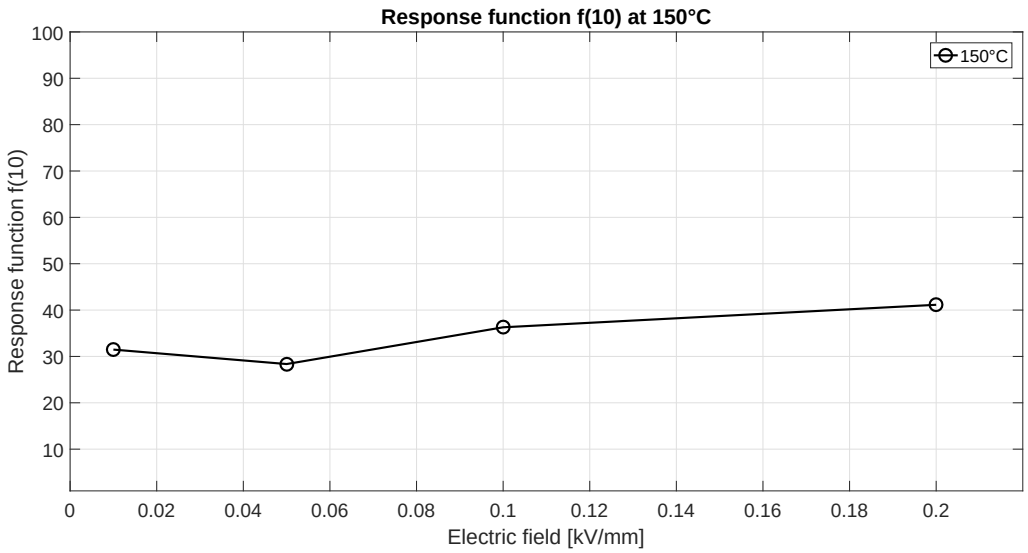

Figure A.108: Response function for a reference SCT test object. Tests are done at 150°C, 1kV-5kV-10kV-20kV applied voltage and 10800 seconds of charging/discharging time.

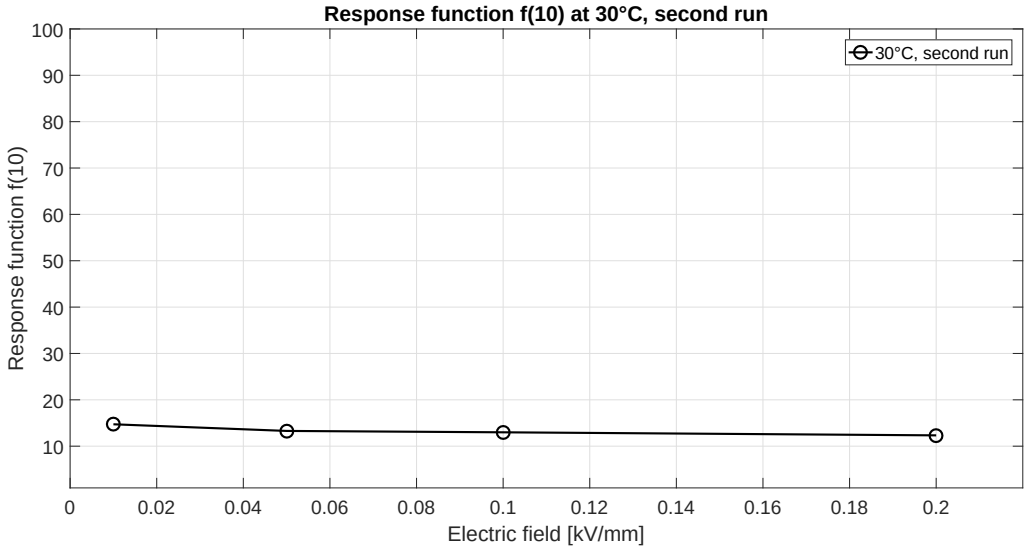

Figure A.109: Response function for a reference SCT test object. Tests are done at 30°C (second run), 1kV-5kV-10kV-20kV applied voltage and 10800 seconds of charging/discharging time.

Dielectric response function results for a SCT test object aged at 98°C dry air for 50 days

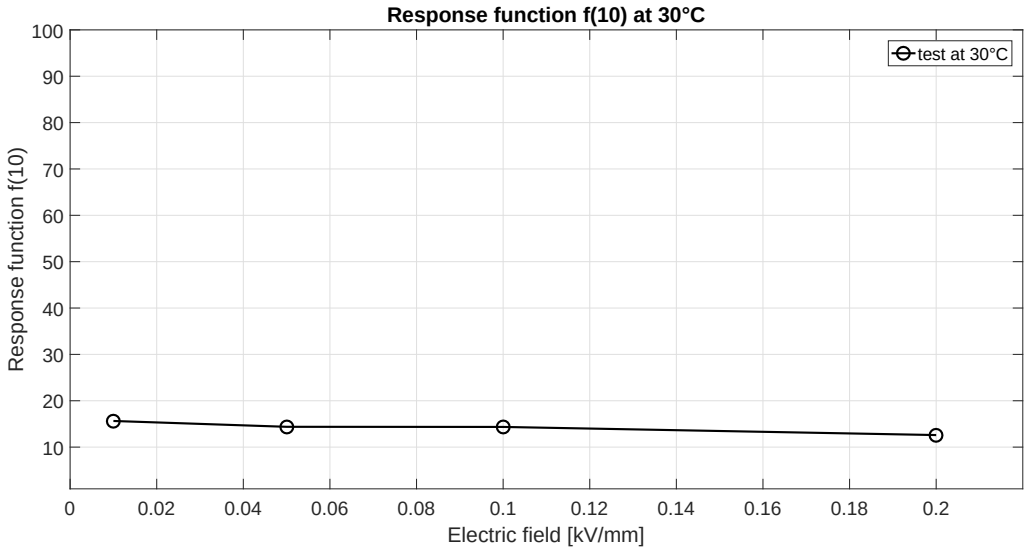

Figure A.110: Response function for a SCT test object aged at 98°C dry air for 50 days. Tests are done at 30°C, 1kV-5kV-10kV-20kV applied voltage and 10800 seconds of charging/discharging time.

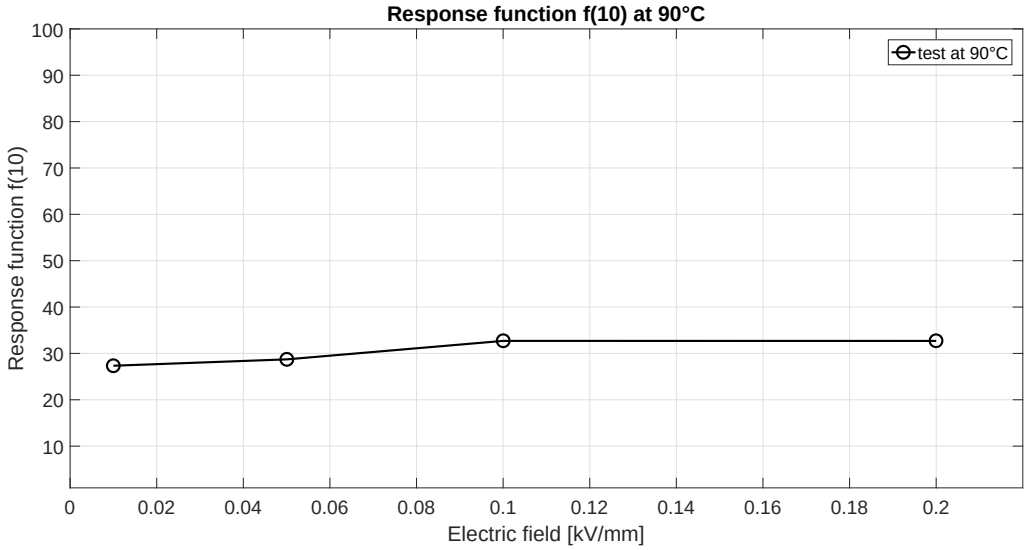

Figure A.111: Response function for a SCT test object aged at 98°C dry air for 50 days. Tests are done at 90°C, 1kV-5kV-10kV-20kV applied voltage and 10800 seconds of charging/discharging time.

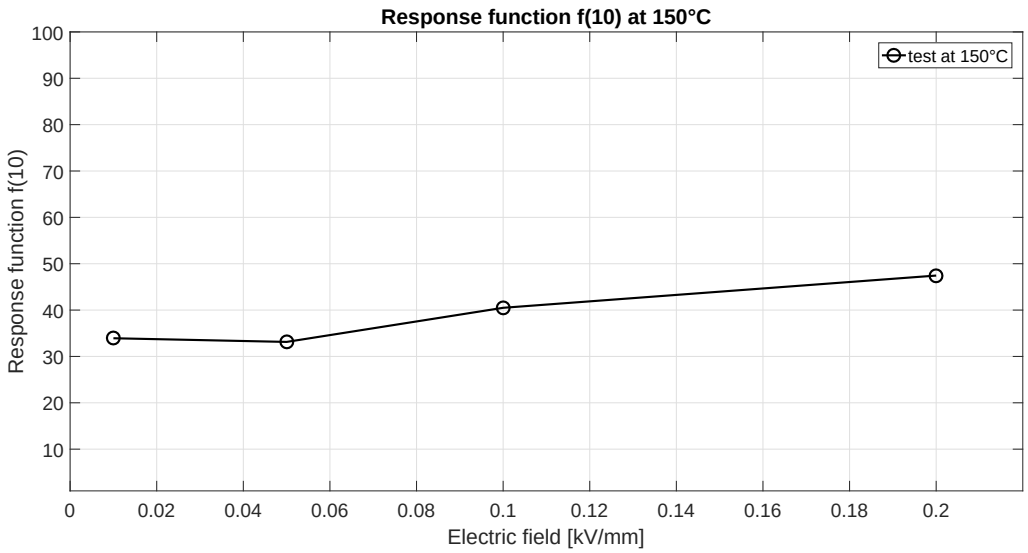

Figure A.112: Response function for a SCT test object aged at 98°C dry air for 50 days. Tests are done at 150°C, 1kV-5kV-10kV-20kV applied voltage and 10800 seconds of charging/discharging time.

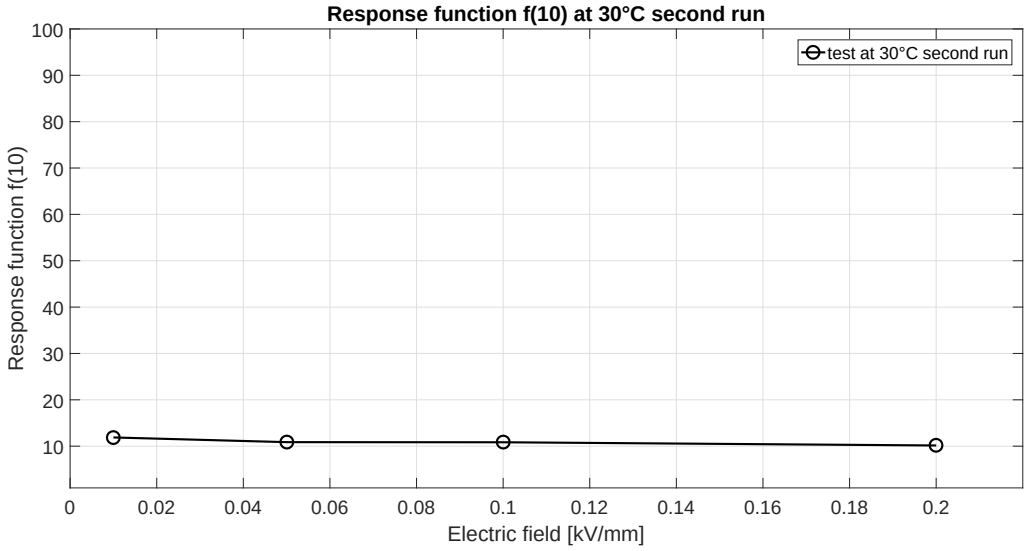

Figure A.113: Response function for a SCT test object aged at 98°C dry air for 50 days. Tests are done at 30°C second run, 1kV-5kV-10kV-20kV applied voltage and 10800 seconds of charging/discharging time.

Dielectric response function results for a SCT test object aged at 98°C dry air for 75 days

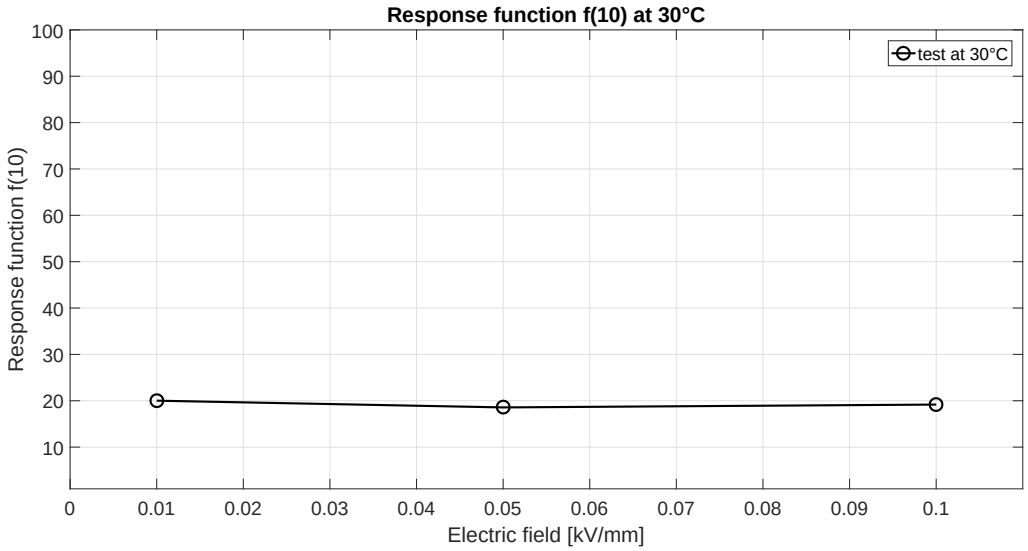

Figure A.114: Response function for a SCT test object aged at 98°C dry air for 75 days. Tests are done at 30°C, 1kV-5kV-10kV applied voltage and 10800 seconds of charging/discharging time.

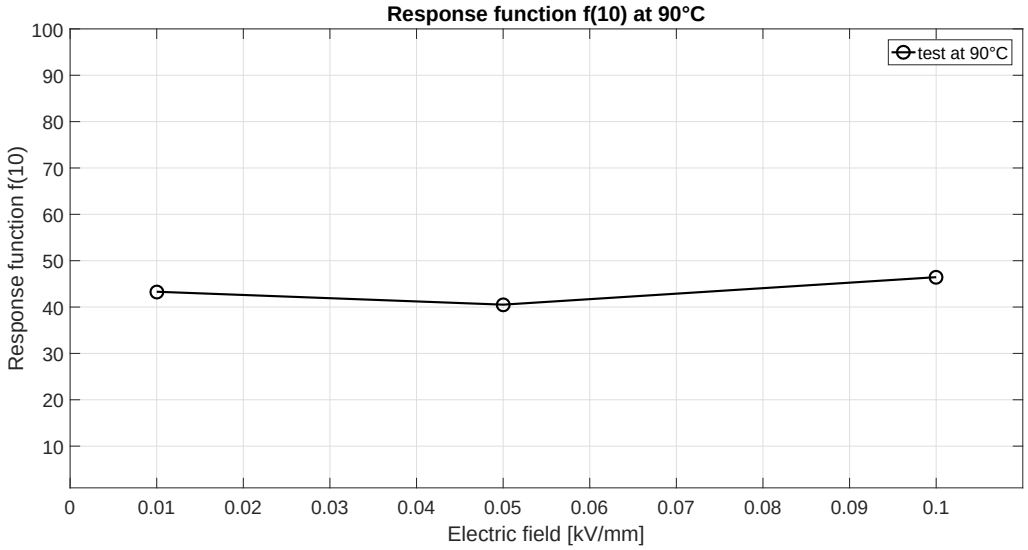

Figure A.115: Response function for a SCT test object aged at 98°C dry air for 75 days. Tests are done at 90°C, 1kV-5kV-10kV applied voltage and 10800 seconds of charging/discharging time.

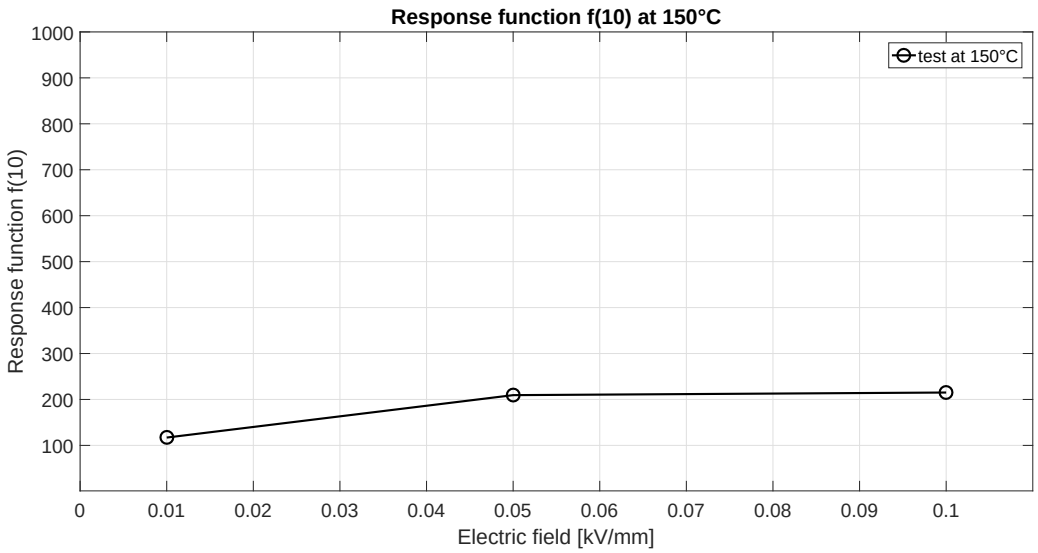

Figure A.116: Response function for a SCT test object aged at 98°C dry air for 75 days. Tests are done at 150°C, 1kV-5kV-10kV applied voltage and 10800 seconds of charging/discharging time.

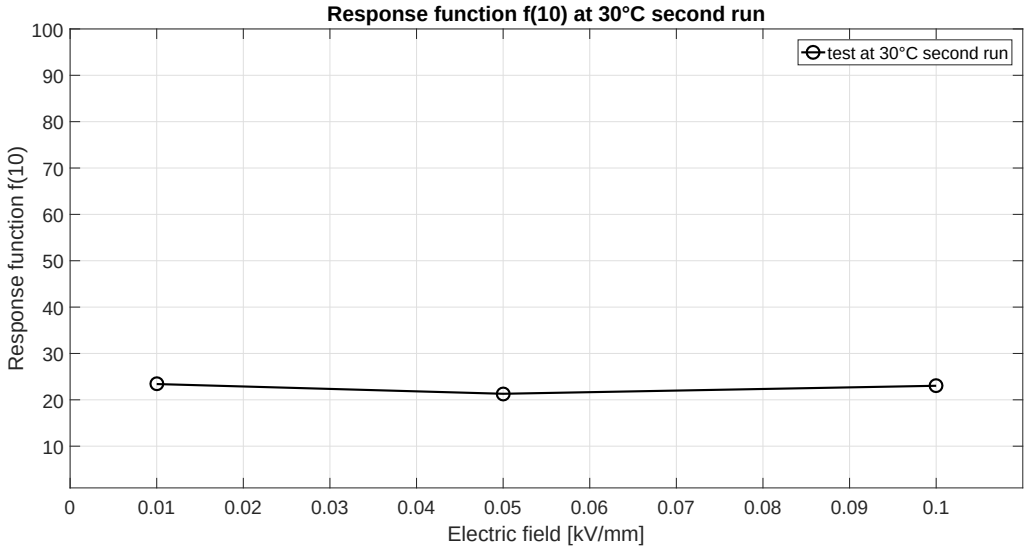

Figure A.117: Response function for a SCT test object aged at 98°C dry air for 75d days. Tests are done at 30°C second run, 1kV-5kV-10kV applied voltage and 10800 seconds of charging/discharging time.

Dielectric response function results for a SCT test object aged at 98°C wet air for 50 days

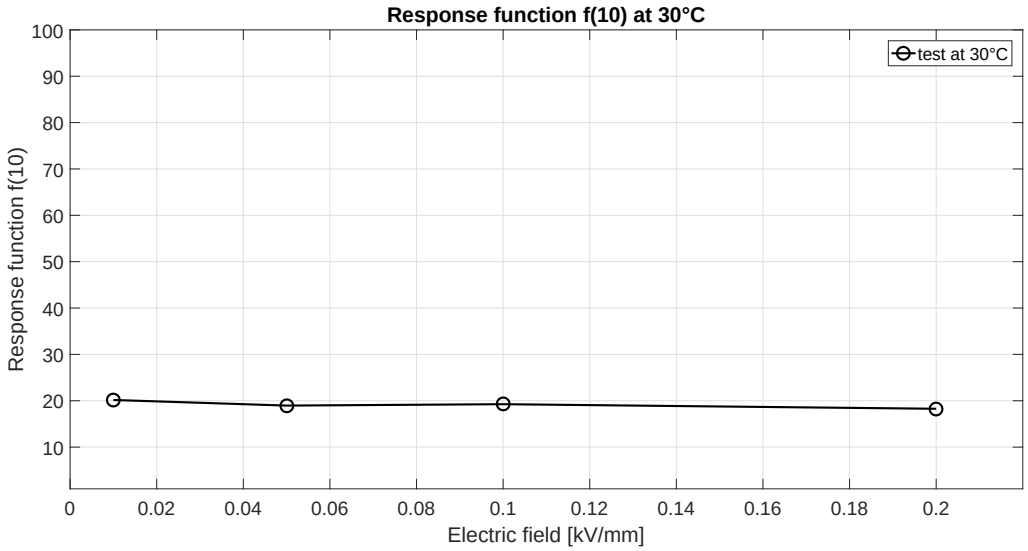

Figure A.118: Response function for a SCT test object aged at 98°C wet air for 50 days. Tests are done at 30°C, 1kV-5kV-10kV-20kV applied voltage and 10800 seconds of charging/discharging time.

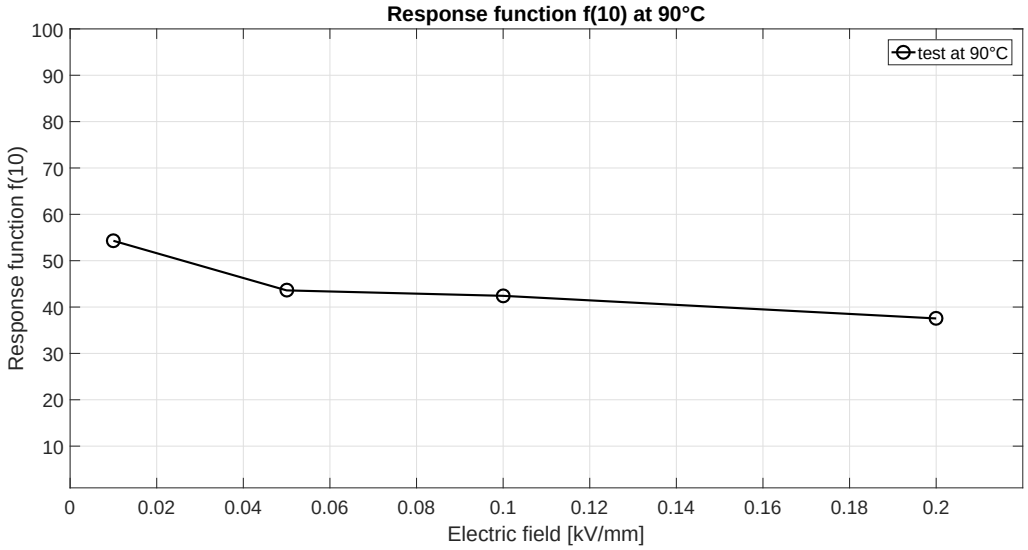

Figure A.119: Response function for a SCT test object aged at 98°C wet air for 50 days. Tests are done at 90°C, 1kV-5kV-10kV-20kV applied voltage and 10800 seconds of charging/discharging time.

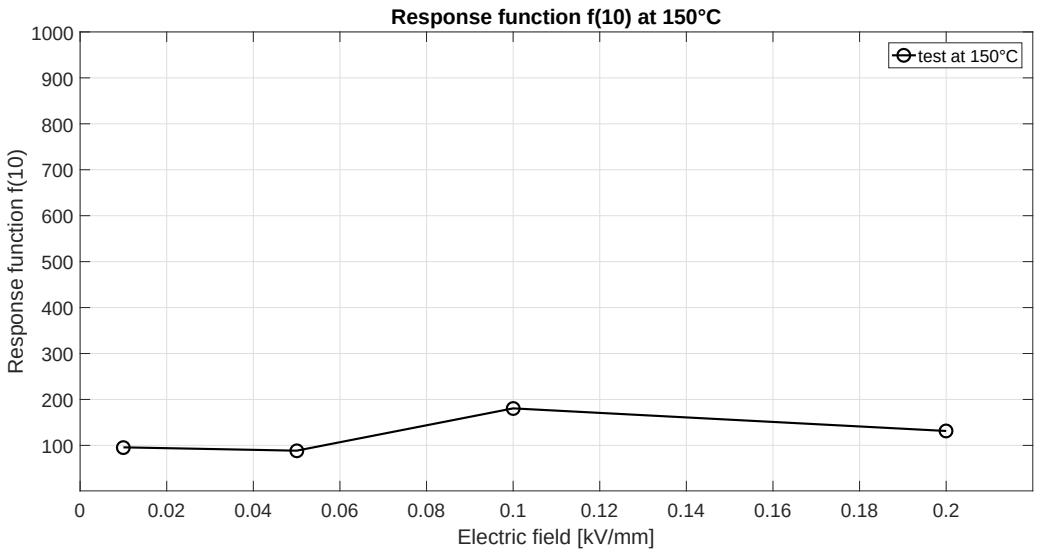

Figure A.120: Response function for a SCT test object aged at 98°C wet air for 50 days. Tests are done at 150°C, 1kV-5kV-10kV-20kV applied voltage and 10800 seconds of charging/discharging time.

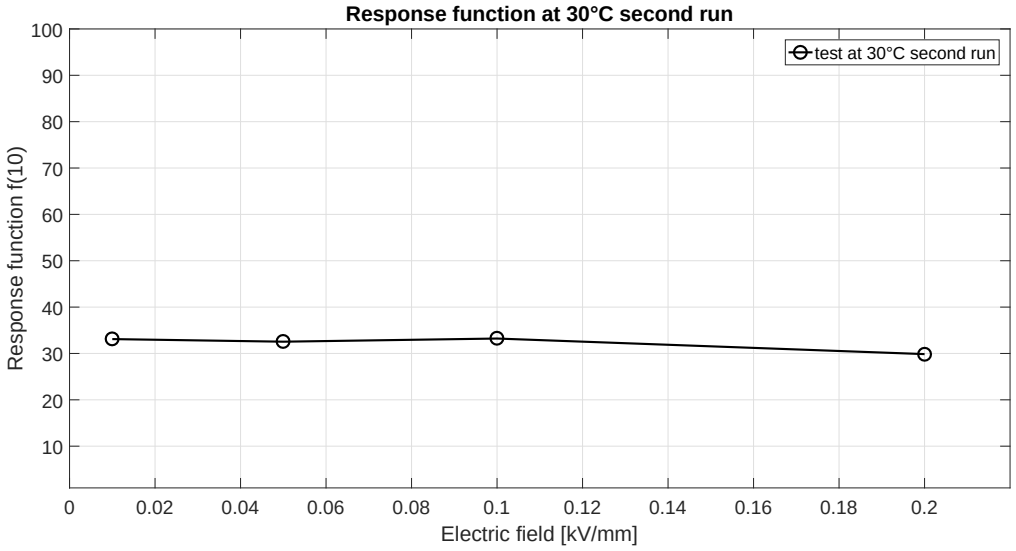

Figure A.121: Response function for a SCT test object aged at 98°C wet air for 50 days. Tests are done at 30°C second run, 1kV-5kV-10kV-20kV applied voltage and 10800 seconds of charging/discharging time.

Dielectric response function results for a SCT test object aged at 98°C dry air for 75 days

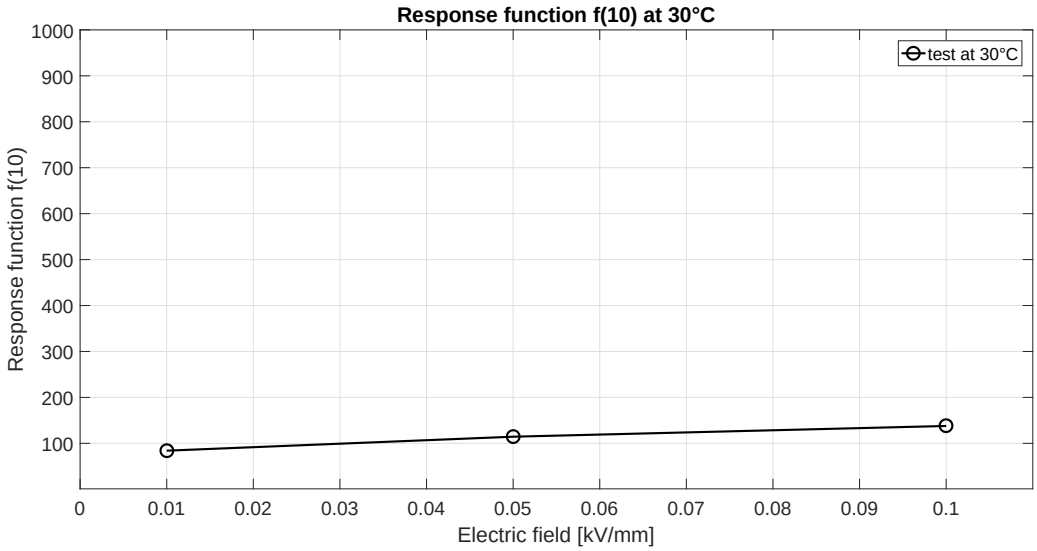

Figure A.122: Response function for a SCT test object aged at 98°C wet air for 75 days. Tests are done at 30°C, 1kV-5kV-10kV applied voltage and 10800 seconds of charging/discharging time.

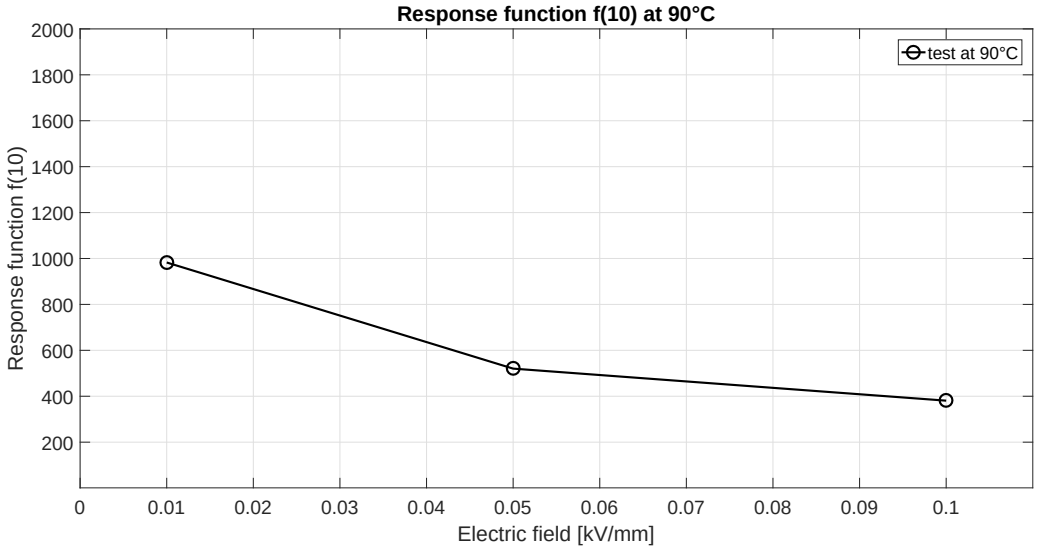

Figure A.123: Response function for a SCT test object aged at 98°C wet air for 75 days. Tests are done at 90°C, 1kV-5kV-10kV applied voltage and 10800 seconds of charging/discharging time.

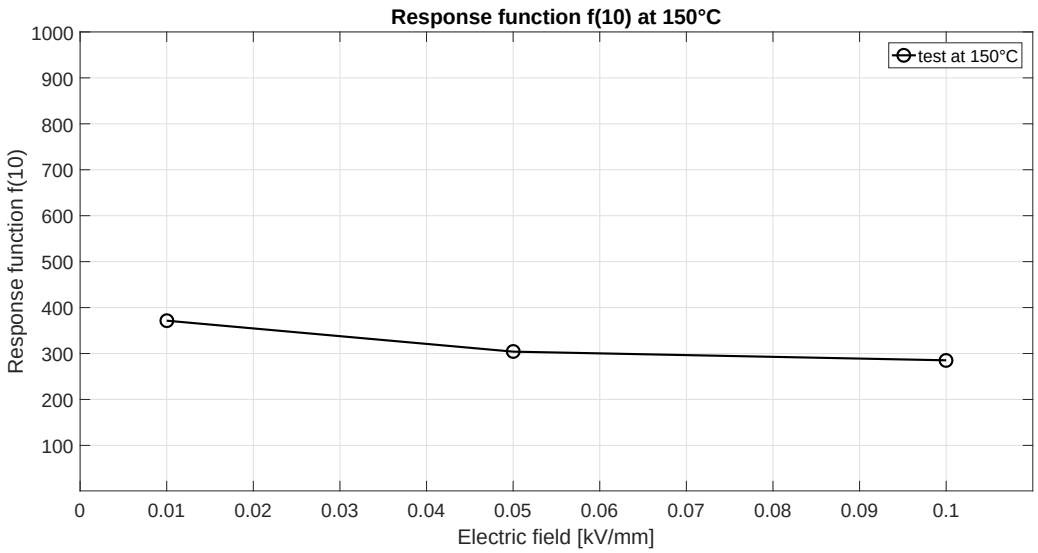

Figure A.124: Response function for a SCT test object aged at 98°C wet air for 75 days. Tests are done at 150°C, 1kV-5kV-10kV applied voltage and 10800 seconds of charging/discharging time.

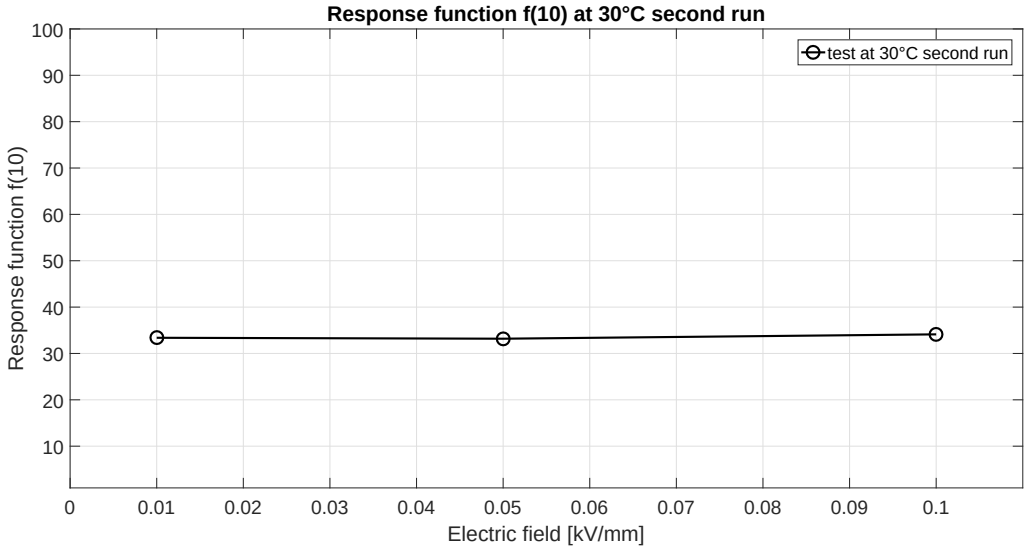

Figure A.125: Response function for a SCT test object aged at 98°C wet air for 75 days. Tests are done at 30°C second run, 1kV-5kV-10kV applied voltage and 10800 seconds of charging/discharging time.

Dielectric response function results for a SCT test object aged at 150°C dry air for 15 days

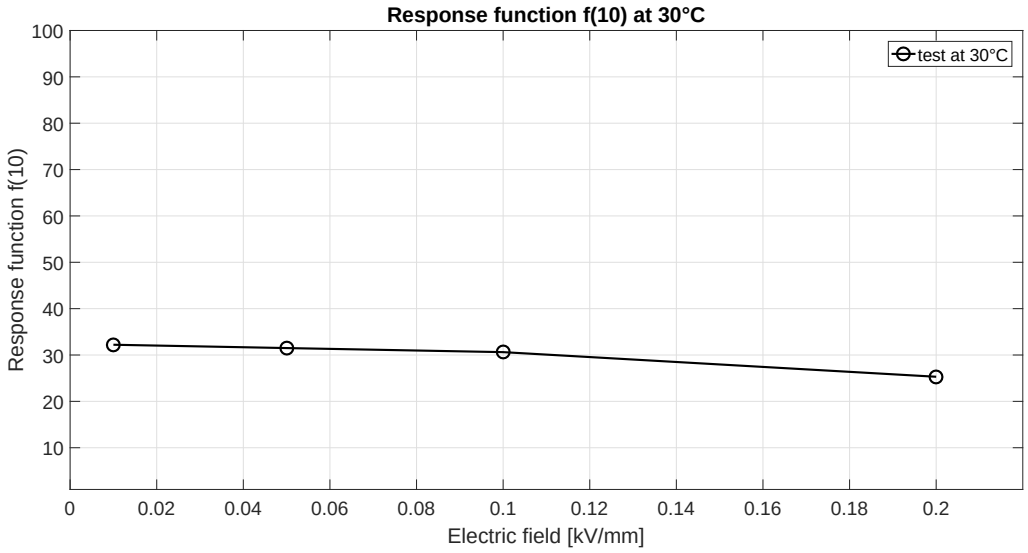

Figure A.126: Response function for a SCT test object aged at 150°C dry air for 15 days. Tests are done at 30°C, 1kV-5kV-10kV-20kV applied voltage and 10800 seconds of charging/discharging time.

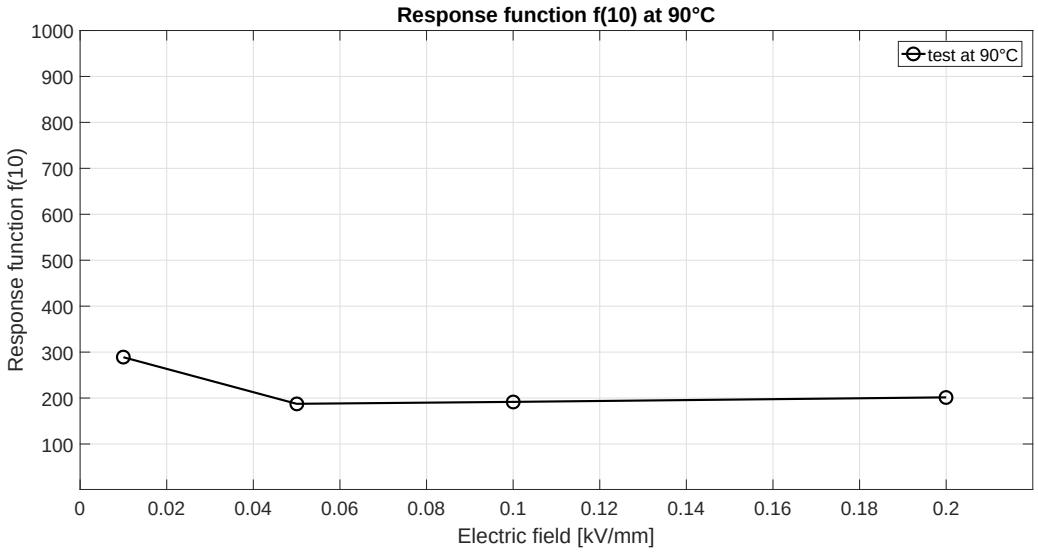

Figure A.127: Response function for a SCT test object aged at 150°C dry air for 15 days. Tests are done at 90°C, 1kV-5kV-10kV-20kV applied voltage and 10800 seconds of charging/discharging time.

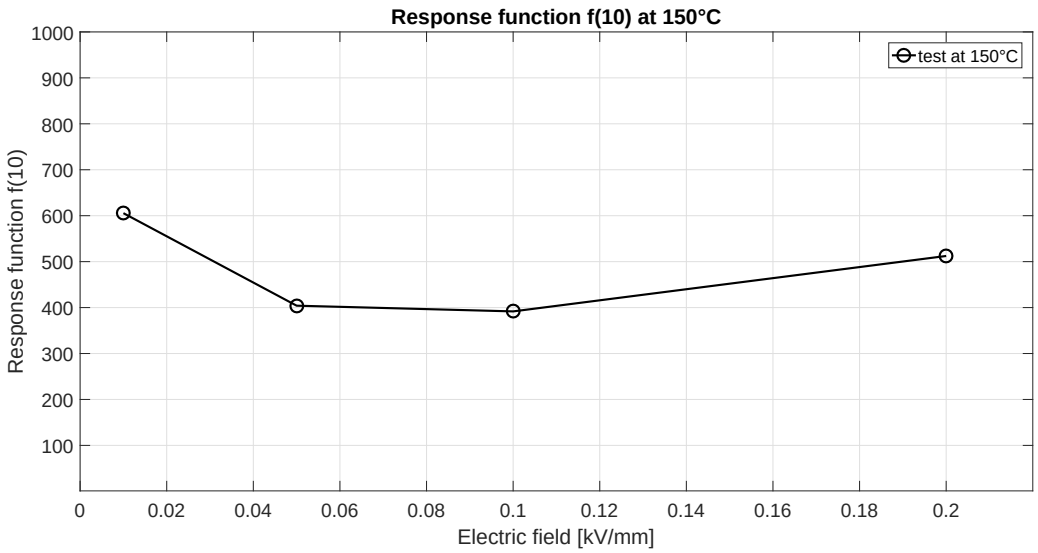

Figure A.128: Response function for a SCT test object aged at 150°C dry air for 15 days. Tests are done at 150°C, 1kV-5kV-10kV-20kV applied voltage and 10800 seconds of charging/discharging time.

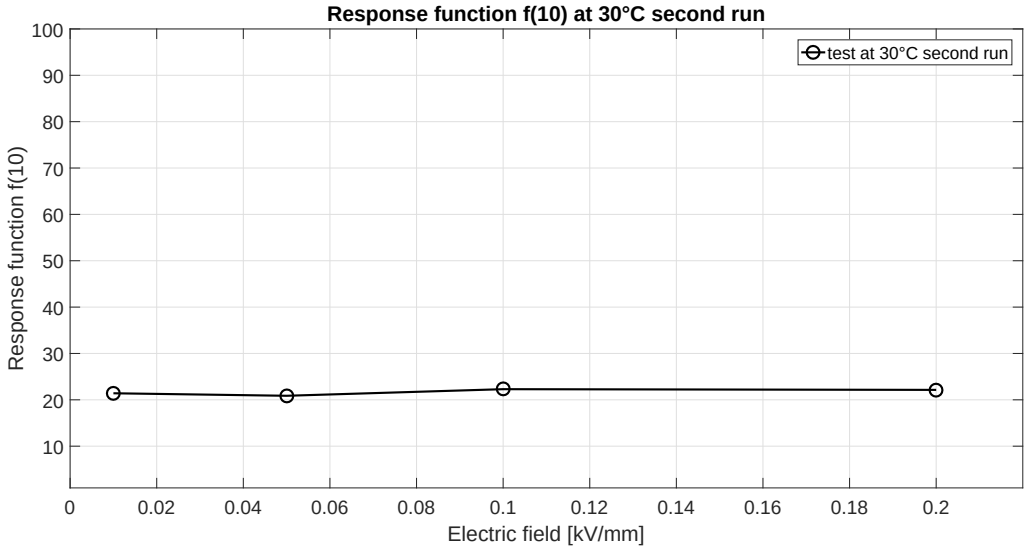

Figure A.129: Response function for a SCT test object aged at 150°C dry air for 15 days. Tests are done at 30°C second run, 1kV-5kV-10kV-20kV applied voltage and 10800 seconds of charging/discharging time.

Dielectric response function results for a SCT test object aged at 150°C dry air for 50 days

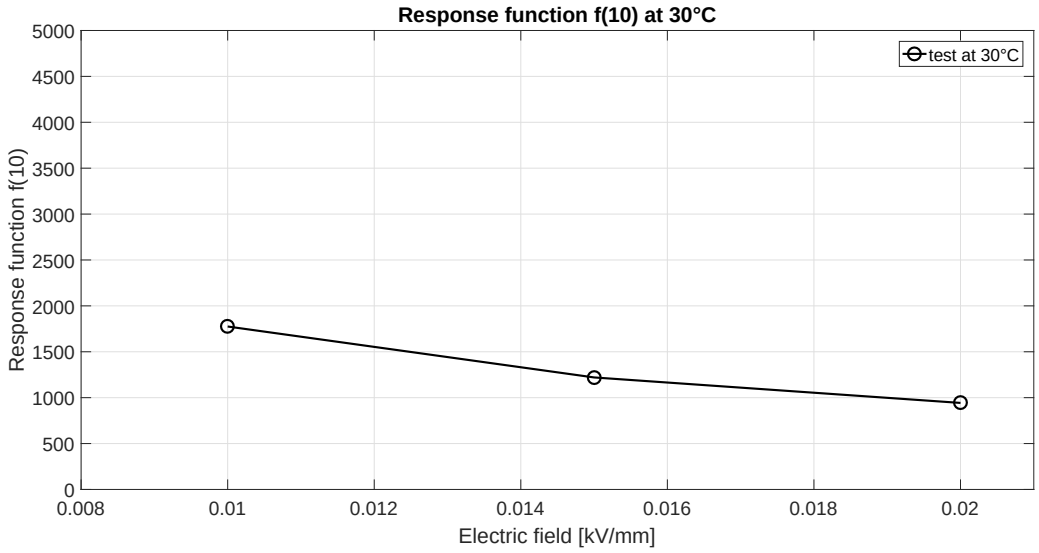

Figure A.130: Response function for a SCT test object aged at 150°C dry air for 50 days. Tests are done at 30°C, 1kV-1.5kV-2kV applied voltage and 10800 seconds of charging/discharging time.

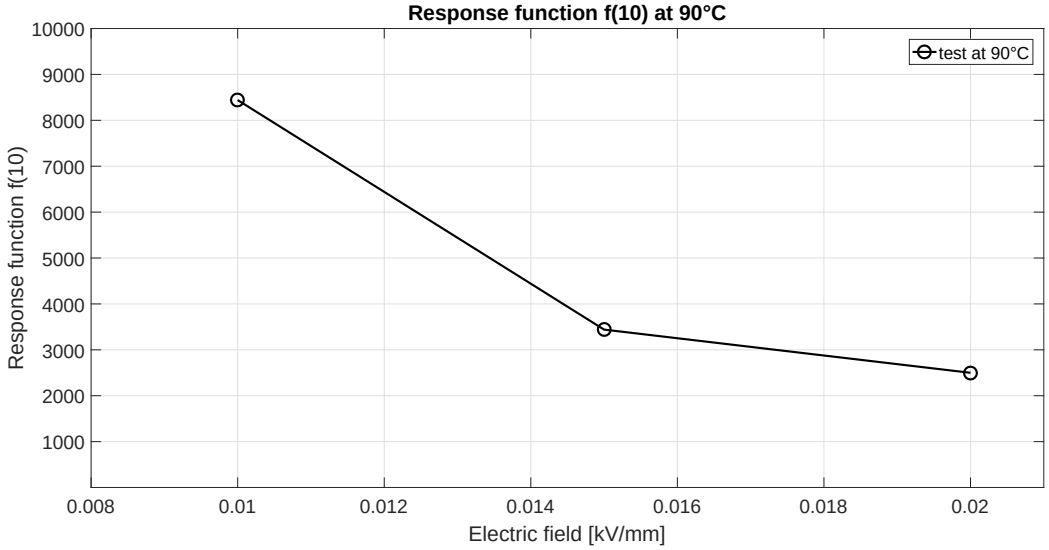

Figure A.131: Response function for a SCT test object aged at 150°C dry air for 50 days. Tests are done at 90°C, 1kV-1.5kV-2kV applied voltage and 10800 seconds of charging/discharging time.

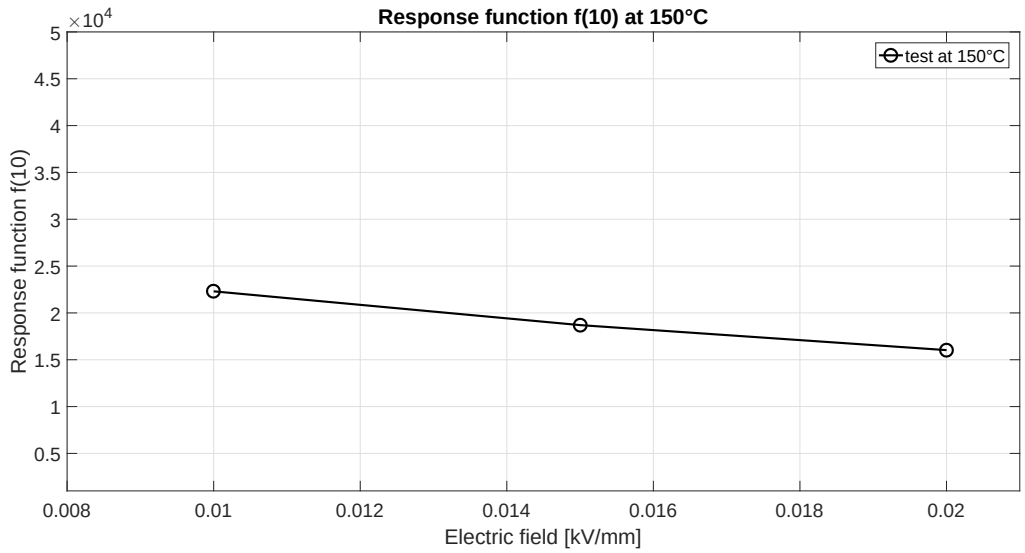

Figure A.132: Response function for a SCT test object aged at 150°C dry air for 50 days. Tests are done at 150°C, 1kV-1.5kV-2kV applied voltage and 10800 seconds of charging/discharging time.

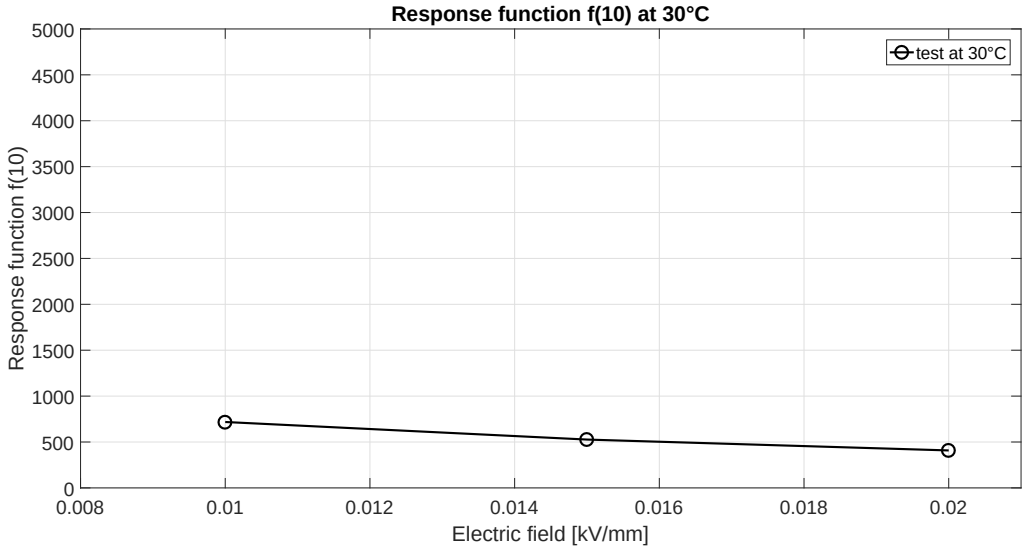

Figure A.133: Response function for a SCT test object aged at 150°C dry air for 50 days. Tests are done at 30°C second run, 1kV-1.5kV-2kV applied voltage and 10800 seconds of charging/discharging time.

DRF results for a SCT reference test object subjected to water absorption at 90°C for 30 days

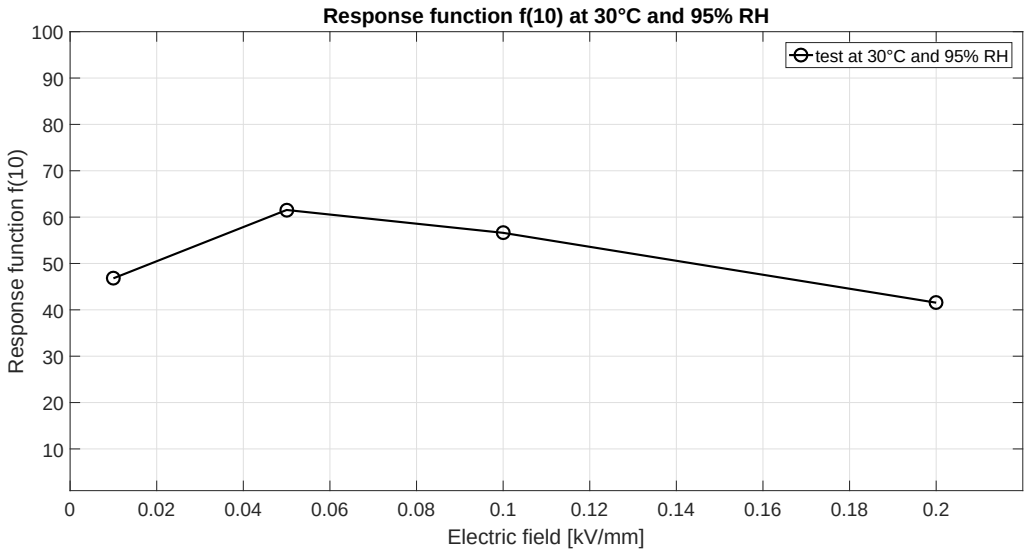

Figure A.134: Dielectric response function for a reference SCT test object, subjected to water absorption at 90°C for 30 days. Tests are done at 30°C, 95% RH, 1kV-5kV-10kV-20kV applied voltage and 10800 seconds of charging/discharging time.

Dielectric response function for a SCT test object aged at 150°C for 15 days and subjected to water absorption at 90°C for 30 days

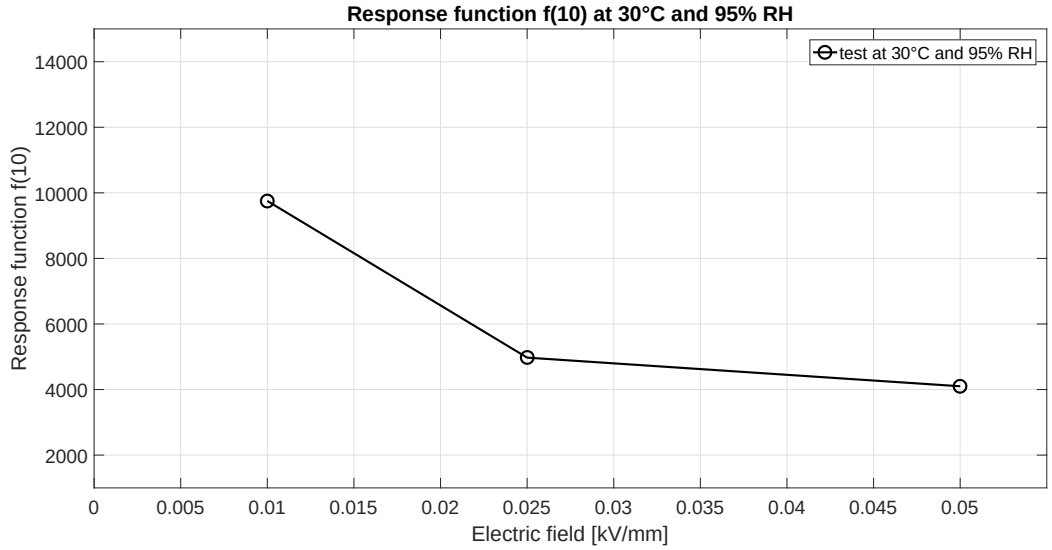

Figure A.135: Conductivity for a SCT test object aged at 150°C for 15 days and subjected to water absorption at 90°C for 30 days. Tests are done at 30°C, 95% RH, 1kV-2.5kV-5kV applied voltage and 10800 seconds of charging/discharging time.